IONIC RELATIONS OF *CHARA CORALLINA*: STUDIES ON THE TRANSPORT OF HCO_3^-, OH^- AND H^+ ACROSS THE PLASMA MEMBRANE

A Thesis submitted to the University of Adelaide
as a requirement for the degree of
Doctor of Philosophy

by

WILLIAM JOHN LUCAS, B.Sc. (Hons.)

Department of Botany
University of Adelaide.

January, 1975.

do not

I give consent to this copy of my thesis, when deposited in the University Library, being available for loan and photocopying.

Date 23/1/75 Signed ....

SUMMARY

The basic aim of the work presented in this thesis was to elucidate the operational characteristics of the HCO_3^-, OH^- and H^+ transport systems putatively located in the plasmalemma of *Chara corallina*. It was also hoped to determine the relative contributions, if any, that these three systems make towards the electrical characteristics of the plasmalemma.

Photosynthetic ^{14}C. assimilation was studied to obtain the relationship between HCO_3^- influx and total CO_2 fixation capacity. It was found that HCO_3^- transport, at the plasmalemma, was capable of extremely high fluxes. Maximum fixation rates in the presence of exogenous $^{14}CO_2$ and $H^{14}CO_3^-$ were considerably higher than previously reported values. Reasons are proposed for this discrepancy.

Experiments conducted over the pH range 4.8 - 11.0 demonstrated that photosynthetic carbon could be supplied simultaneously by CO_2 diffusion and HCO_3^- transport.

Mathematical analysis of the chemical diffusion system established by individual alkaline bands indicated that they do not develop from point efflux sources; band sources appeared to be operating. Individual OH^- band efflux values were calculated by fitting their established spherical diffusion patterns to the equation of a continuous spherical surface source. Close correlation was obtained between $H^{14}CO_3^-$ influx and total OH^- efflux calculated by this method.

A similar diffusion study was performed on the acid banding system; a cylindical coordinate diffusion pattern was observed. Net H^+ efflux was estimated using the continuous cylindrical surface source equation. This value was compared with other estimates of H^+ fluxes associated with Characean cells (Kitasato,1968; Spear,

Barr and Barr,1969; Richards and Hope,1974). It was considered that experimental support was not obtained for the model proposed by Spanswick (1972).

An experimental system was designed to test the obligate coupling between HCO_3^- and OH^- fluxes (i.e. a Mitchell-type anti-porter) proposed by Lucas and Smith (1973). The results of these experiments demonstrated categorically that the OH^- efflux process could function in the absence of exogenous HCO_3^- at the actual OH^- efflux site. Hence, the obligate coupling hypothesis was invalidated.

The inter-relationships between light intensity and activation of the OH^- and H^+ bands were investigated. The most significant feature of these results was that all OH^- bands are not of equal status; there was an apparent hierarchy of OH^- efflux bands. (A similar situtation was not observed for the acid efflux system). An hypothesis is presented to account for these results in terms of total cell OH^- band activation and regulation of the HCO_3^- and OH^- transport systems.

It is suggested that when HCO_3^- is present in the bathing solution, the HCO_3^- and OH^- systems, along with the H^+ system, may be involved in determining the electrical properties of the plasmalemma. The influence of various "cationic treatments" on the HCO_3^- influx capacity supported this proposal.

Spear et al. (1969) and Smith (1970) proposed two quite diffferent hypotheses relating Cl^- transport to H^+ movement across the plasmalemma. Parallel studies on the influence of light intensity on net H^+ efflux and Cl^- uptake were conducted to test these hypotheses; their apparent invalidation is discussed.

The effect of $(NH_4)_2SO_4$ on ^{14}C. fixation under both CO_2 and HCO_3^- assimilating conditions was studied with a view to clarifying its effects of Cl^- uptake. It was found that $(NH_4)_2SO_4$ interfered

with OH^- efflux, and at higher pH values the transport of HCO_3^- was inhibited. Possible inhibitory mechanisms are discussed.

Preliminary biophysical measurement were made on typical cells used in experiments detailed in this thesis. These values are compared with those obtained by other workers using this species.

DECLARATION

This thesis contains no material that has been accepted for the award of any other degree or diploma in any University and, to the best of my knowledge and belief, it contains no material previously published or written by any other person, except where due reference is made in the text.

W.J. Lucas

22/1/75

ACKNOWLEDGEMENTS

I am greatly indebted to Dr. F.A. Smith for his supervision and guidance throughout the course of this work. I would like to thank Dr. J.T. Wiskich, Dr. B.J. Steel and Professor J.C. Jaeger for advice and helpful discussion.

Thanks are also due to Professor N.A. Walker and Dr. F.A. Smith for making available their paper, before publication.

I would also like to thank Dr. R.T. Lange, Chairman of the Department of Botany, for use of laboratory facilities and also Professor A.B. Hope for the use of laboratory facilities in the School of Biological Sciences, Flinders University, Adelaide, South Australia. My thanks also go to all the members of the Botany Department for their help, and especially to Dr. G.G. Ganf, Mr. D.A. Day, Mr. S.P. Robinson and Mr. A.L. Fox for their help and willingness to discuss aspects of this work.

This work was carried out during the tenure of a Commonwealth Postgraduate Award.

The manuscript was most competently typed by Miss C. Wilkins, to whom I am extremely grateful.

ABBREVIATIONS

ATP	adenosine triphosphate
CCCP	carbonyl cyanide m-chloro-phenylhydrazone
CMU	3'-(p-chlorophenyl)-1;1-dimethylurea
DCMU	3'-(3,4-dichlorophenyl)-1',1'-dimethylurea
DNP	2,4-dinitrophenol
HEPES	N-2-hydroxy ethylpiperazine-N'-2-ethanesulfonic acid
MES	2-(N-morpholino) ethanesulfonic acid
mM	millimolar : 10^{-3} molar
mV	millivolt : 10^{-3} volt
$NADPH_2$	reduced nicotinamide adenine dinucleotide phosphate
nMol	nano moles : 10^{-9} moles
pmol	picomoles : 10^{-12} moles
TES	N-tris (hydroxymethyl) methyl-2-aminoethanesulfonic acid
Tricine	N-tris (hydroxymethyl) methyl glycine
Tris	tris (hydroxymethyl) amenomethane
Wm^{-2}	Watts per square metre
µM	micromolar : 10^{-6} molar

TABLE OF CONTENTS

CHAPTER ONE

INTRODUCTION

Assimilation of Bicarbonate Ions

The topic of photosynthetic assimilation of HCO_3^- by aquatic plants has indeed been controversial. The controversy stems from a lack of information and understanding of the equilibria involved when inorganic carbon is used in experiments relating to photosynthesis. Many of the early reports on this subject were inconclusive (Draper, 1844; Grischow, 1845; and Hassack, 1888) and unfortunately this is true of some present day work (Rybova and Slavikova, 1974).

In much of the early work it was assumed that the presence of $CaCO_3$ incrustations provided evidence that incrusting plants could utilize HCO_3^- (Cohn, 1862; Hanstein, 1873; and Hassack, 1888). This assumption was criticized, in principle, by Arens (1933) and will be detailed later. Lewin (1962), in her review on calcification, also pointed out that there are many aquatic plants which can utilize HCO_3^- but do not form incrustations of $CaCO_3$.

Moore, Whitley and Webster (1921) were the first authors to use the ability of plants to increase the pH of the bathing solution to high values, as an indication of HCO_3^- assimilation. In the same year Ruttner (1921) used electrical conductivity measurements to demonstrate that leaves of *Elodea* could utilize HCO_3^-. He showed that *Elodea* could decrease the CO_2 and HCO_3^- content of a $Ca(HCO_3)_2$ solution to a level in which only carbonate and hydroxide remained. Ruttner's interpretation was criticized by Arens (1933), who pointed out that if plants, bathed in a $Ca(HCO_3)_2$ solution, used only CO_2 they could still raise the pH of the solution. He pointed out that if the plants could remove all the CO_2 from the HCO_3^- solution, eventually only OH^- would remain. This criticism is valid. Theoret-

ically all the CO_2 could be removed from the solution, but in fact the respiratory generation of cytoplasmic CO_2 prevents this from occurring. This concept of CO_2 compensation will be discussed presently. Based on this CO_2 mediated pH rise, Arens suggested that if Ca^{++} solutions were present, $CaCO_3$ could be precipitated without HCO_3^- being utilized. Therefore he proposed that incrustations on photosynthetic tissue could not, by themselves, be used as a rigorous indicator of HCO_3^- assimilation. This point has been accepted and continually stressed in the literature (Steemann Nielsen, 1963; Watt and Paasche, 1963; and Raven, 1970).

In answer to the above criticism Ruttner (1947, 1948) demonstrated that the rate of HCO_3^- assimilation, by *Elodea*, was considerably faster than the rate at which CO_2 could be scrubbed from the HCO_3^- solution, either by boiling or aerating with CO_2-free air. Steemann Nielsen (1947), using parallel pH and photosynthetic O_2 evolution studies, showed that *Myriophyllum spicatum* could assimilate HCO_3^- but that the water moss *Fontinalis antipyretica* could use only CO_2. The results of these two workers are the first to show conclusively that some aquatic plants can photosynthetically assimilate HCO_3^-.

Plants not able to utilize HCO_3^- cannot, in general, raise the bathing solution pH value above 9.0; it appears that at this pH value assimilation stops. This maximum pH value can be termed the "compensation pH" (Raven, 1970), and the CO_2 concentration at this value depends upon the concentration of total inorganic carbon present in the system. In the experiments of Ruttner (1948) the CO_2 concentration would have been approximately 4μM which is very close to the compensation point CO_2 concentration of 3.2μM (land plants) quoted by Verduin (1954).

Criteria for Bicarbonate Assimilation

From the above discussion it is clear that a criterion can be proposed, by which it can be determined whether HCO_3^- is actually being assimilated. Using the known equilibrium constants, it is possible to calculate the concentration of free CO_2 in the bathing solution at the "compensation pH". Provided light is non-limiting, this concentration corresponds to the CO_2 compensation point. Now, if the "compensation pH" exceeds the calculated "compensation pH" (determined using the CO_2 compensation concentration obtained, by experimentation, at a lower pH where only CO_2 existed in solution) it is proposed that the discrepancy can be taken as an indication that the plant is assimilating HCO_3^- (Raven, 1970). The "compensation pH", of cells which can apparently utilize HCO_3^-, ranges from 9.2 to a maximum recorded value of 11.8 (*Spirogyra*, see Schutow, 1926). A large number of "compensation pH" values for marine algae have been reported by Blinks (1963), and the species which can assimilate HCO_3^- had compensation pH values ranging from 9.5 to 10.0.

The most serious source of error, when applying this criterion, is that other cellular processes exist which can alter the pH of the bathing solution. For example, there may exist a proton efflux system which may be related to the imbalance between cation and anion fluxes (see Raven, 1970; and Raven and Smith, 1974, for references). It is also difficult to assign a reasonable "compensation pH" value from the carbon dioxide compensation point at low pH. The assumption must be made that the range of bathing solution pH values employed does not affect cellular photosynthetic fixation reactions (Raven, 1970).

A more rigorous method by which HCO_3^- assimilation can be identified has been detailed by Raven (1970). This involves the investigation of the relationship between the concentration of unhydrated

CO_2 and the photosynthetic rate at low and high pH values. In the experimental procedure the low pH value should be such that > 90% of the total carbon exists as CO_2 and the high pH value such that > 95% of the total carbon exists as HCO_3^- or CO_3^{2-}. If the photosynthetic fixation rate is significantly greater, at the high pH, than would be predicted from the level of CO_2 present, then it can be concluded that HCO_3^- is entering the cell and contributing carbon for photosynthesis.

The main difficulty in the interpretation of the results pertaining to HCO_3^- assimilation is the fact that HCO_3^- may be acting as a reservoir of extracellular CO_2. Hood and Park (1962) attempted to remove the CO_2 from the HCO_3^- solution and hence determine whether photosynthetic fixation still proceeded. Their technique, results and conclusions were justifiably criticized by Watt and Paasche (1963) and also by Steemann Nielsen (1963). Although it has since been shown that the CO_2-reservoir-effect does not invalidate this criterion (Raven, 1968a) it is essential, in any new study, to establish this fact (see Appendix D in relation to Chapter 3).

This second criterion for assimilation of HCO_3^- was applied to the studies reported in this dissertation.

Characean Assimilation of HCO_3^-

Hanstein (1873) proposed that the *Chara* species he was studying could assimilate HCO_3^-. However, like many of the early workers he based his conclusion on the presence of $CaCO_3$ incrustations. He considered that HCO_3^- entered the cell as $Ca(HCO_3)_2$ and that for each $Ca(HCO_3)_2$, one molecule of CO_2 was fixed photosynthetically and a molecule of $CaCO_3$ was excreted. When the solubility product was exceeded, $CaCO_3$ was precipitated in and on the cell wall. This hypothesis of HCO_3^- transport has not received experimental verification.

Arens (1939) also proposed an hypothesis which attempted to explain the $CaCO_3$ banding pattern observed in numerous Characean species. He considered that the bare (non-incrusted) zones were equivalent to the lower leaf surface of *Elodea*, namely that HCO_3^- was absorbed through these regions. The encrusted zones were assumed equivalent to the upper leaf surface of *Elodea*, i.e. through this surface Arens suggested OH^- and CO_3^{2-} were excreted. This hypothesis was also entirely hypothetical and again no supporting evidence has been forthcoming.

Actually experimental evidence relating to HCO_3^- assimilation within the Characeae is sparse. Hassack (1888) reported that cells of *Nitella gracilis* and *Chara foetida* could synthesize starch when the bathing solution contained 0.05% (6.02mM) or 0.1% (12.05mM) $NaHCO_3$. The pH values were not specified, but are unlikely to have been higher than 8.3, assuming the solutions were freshly prepared. Therefore starch synthesis could have resulted from fixation of CO_2 supplied by diffusion of CO_2. Dahm (1926), using *Chara fragilis*, found that this species could raise the bathing solution pH to 9.7 after 8 hours illumination. On the basis of the results reported by Smith (1968a) it would appear that this species can utilize exogenous HCO_3^-.

However, it was not until the work of Smith (1967a, 1968a) that it was conclusively shown that Characean cells could photosynthetically utilize exogenous HCO_3^-. This work will be dealt with in detail in Chapter 3, in relation to the photosynthetic capacity of these cells.

Bicarbonate Influx and Hydroxyl Efflux

It is generally accepted that HCO_3^-, once it has entered the cell, supplies carbon to the chloroplasts via the equilibrium reaction $HCO_3^- + H^+ \rightleftharpoons H_2O + CO_2$, i.e. it is CO_2 which is utilized by the ribulose diphosphate carboxylase reaction (Cooper, Filmer,

Wishnick and Lane, 1969). Hence for each mole of carbon fixed, a mole of OH^- is generated in the cytoplasm.

The photosynthetic rate under exogenous HCO_3^- and the characteristic of photosynthesis in this experimental situation have been studied by numerous workers, using a variety of aquatic plants. However, the actual mechanism of HCO_3^- influx and OH^- efflux has received very little attention. Steemann Nielsen (1947) showed that HCO_3^- assimilation in *Myriophyllum* had a lower quantum yield than was observed when CO_2 was the exogenous carbon source. This suggested that there was an extra light-dependent reaction involved in the cellular utilization of HCO_3^- compared with CO_2. Steemann Nielsen (1951) proposed that HCO_3^- entry was passive, he considered that it was the excretion of OH^- which required the light energy. The cations which were observed to move during photosynthetic HCO_3^- utilization (Arens, 1936a,b; and Steemann Nielsen, 1947) were assumed to move passively (cf. Lowenhaupt, 1958).

It has been observed that when exogenous HCO_3^- is employed, not only does photosynthesis have a lower quantum yield, but that under light limiting and saturating conditions the rate is always lower compared with that which is obtained using exogenous CO_2. Steemann Nielsen (1947) attempted to explain these observations on the basis of the OH^- efflux requirements. He suggested that under light limiting conditions a photochemical reaction associated with OH^- efflux acted as the limiting factor. Under saturating light intensities he proposed that an enzyme, specifically connected with OH^- transport, acted as the limiting factor. Steemann Nielsen's proposals are weakened by his treatment of the entry of HCO_3^-. This he considered to be a passive process and his argument based on the stoichiometry of anion influx with respiration (Lundegårdh, 1949), was criticized by Österlind (1951). Österlind pointed out that

photosynthesizing cells possess an energy source other than respiration, and it is difficult to see why Steemann Nielsen could consider OH^- efflux to be closely connected with a "photochemical reaction" and yet discard this possibility for HCO_3^-. The HCO_3^- entry has been considered by other workers, to be associated with a photochemical reaction (see Raven, 1968a).

The hypothesis developed by Lowenhaupt (1956) is worth discussing, for he proposed an active cation pump to explain the HCO_3^- results of Arens (1930, 1933, 1936a,b) and Steemann Nielsen (1947). He proposed that "the concept of active transport of anions in the leaf (OH^-, HCO_3^- or others) would appear to involve several theoretical contradictions", unfortunately the nature of these "contradictions" was not detailed. Lowenhaupt's hypothesis was that active transport of cations occurred in three steps, the entire process was assumed to be light stimulated. The steps were:

(a) cation attachment to a binding group,

(b) reorientation of the group towards the other surface of the active membrane, and

(c) release of the cation.

There was considered to be a requirement for photosynthetic energy in that it facilitated the cation release step. In response to steps (a) - (c), synthesis of a bicarbonate-accepting compound was considered to occur in the plasmalemma. Lowenhaupt proposed that the transport of HCO_3^- was facilitated via this "compound".

It should be emphasized that this hypothesis was proposed for the rather unusual HCO_3^- and cation system observed in the leaves of *Myriophyllum* and *Elodea*. It is unlikely that this hypothesis would be applicable to HCO_3^- transport in Characean cells for large cation fluxes, associated with HCO_3^- assimilation, have not been observed (Raven, 1970, p. 203-4 where reference is made to unpublished results).

To date, the most complete analysis of HCO_3^- assimilation by an organism is that presented for *Hydrodictyon africanum* by Raven (1968). After demonstrating that *H. africanum* could utilize exogenous HCO_3^- as a photosynthetic substrate and that it was not simply acting as a reservoir for CO_2, Raven went on to show that the photosynthetic rate was always lower with exogenous HCO_3^- as the carbon source. This supported the results of Steemann Nielsen (1947) and Raven also interpreted his results as indicating that the light requirement to fix a mole of carbon, supplied exogenously as HCO_3^-, was greater than was required to fix a mole, supplied exogenously as CO_2.

By the use of photosynthetic light filters, Raven showed that a parallel "red drop" occurred for fixation from both exogenous CO_2 and HCO_3^- solutions. This parallel in response was also observed in the presence of an increasing DCMU concentration, i.e. the requirement of a higher quantum input for HCO_3^- persisted as photosynthetic fixation was inhibited. This type of response was not observed when the uncoupler CCCP was employed. Under its influence, fixation was inhibited to the same absolute level, whether the exogenous form of carbon was HCO_3^- or CO_2. Raven inferred from the CCCP results that ATP *per se* was not required for the actual transport of HCO_3^-. Following the earlier hypothesis of Steemann Nielsen, Raven proposed that his HCO_3^- results indicated that there was an extra light-dependent step in carbon fixation, when HCO_3^- was the exogenous carbon source. In contrast to Steemann Nielsen, he favoured the hypothesis that this step was associated with the active transport of HCO_3^- into the cell. The concept of active transport and the conclusions drawn by Raven concerning HCO_3^- transport will be discussed in a later section. However, it is worth mentioning at this point that Raven (1970) has extended the active transporters required, under $HCO3^-$ assimilating conditions, to include an active OH^- efflux process.

The pH Banding Phenomenon and its Relationship to HCO_3^- Assimilation

Several hypotheses which have attempted to relate the process of precipitation of $CaCO_3$ to HCO_3^- assimilation have already been mentioned. One hypothesis which has not been considered is that proposed by Spear, Barr and Barr (1969). These workers placed cells of *Nitella clavata* in a bathing solution which contained 0.1mM phenol red (an acid-base indicator). They observed that, in the light, the cell surface of *N. clavata* was divided into alternating acid and alkaline bands. Spear et al. (1969) proposed that the acid regions resulted from an active H^+ efflux system and they claimed that this offered experimental support for the electrogenic proton pump postulated by Kitasato (1968).

The alkaline regions were attributed to "a net passive H^+ influx". This hypothesis was rejected by Smith (1970) who suggested, since the alkaline bands increased in intensity in the presence of $NaHCO_3$, that they were formed by the efflux of OH^- resultant from HCO_3^- influx and CO_2 fixation. It is noteworthy that Smith (1970) used *Chara corallina* for his studies, and that this species also developed acid and alkaline bands, with the acid regions being dominant in terms of coverage of cell surface area.

MacRobbie (1970) suggested that the HCO_3^--OH^- hypothesis of Smith (1970) needed experimental confirmation. This stipulation should also have been applied to all the earlier hypotheses proposed to account for this alkalinization phenomenon. Lucas and Smith (1973) demonstrated conclusively that the alkaline bands, which developed on the cell surface of *C. corallina*, were dependent upon the presence of HCO_3^- in the bathing solution. The pH measurements along the *Chara* cell wall indicated that the alkaline bands had pronounced peaks whereas the acid regions were broader and more uniform. This alkaline and acid pattern was assumed to support the

concept of localized OH^- efflux, superimposed on an apparently uniform H^+ efflux system, but the two processes may be related to entirely separate cellular processes. These authors also suggested that the HCO_3^- influx system was not electrogenic (see later section for full definition). They based this conclusion on the fact that whereas the basic electrical characteristics of the various Characean species were similar, the species had very different abilities to utilize HCO_3^- (Smith, 1968). To establish a non-electrogenic system, it was proposed that HCO_3^- influx and OH^- efflux were coupled in an obligate manner such that an electrically neutral carrier system resulted. It should be stressed that there is no experimental support for this obligate HCO_3^-/OH^- coupled system. It is extremely important that this be realized because such a system is of considerable importance when the electrical properties of the plasmalemma are being considered. It is unfortunate that some workers in this field have assumed the obligate coupling proposed by Lucas and Smith to be valid without experimental confirmation (Richards and Hope, 1974). This hypothesis will be examined in detail in Chapters 5 and 7.

The proposal by Spear et al. that the acid regions convert HCO_3^- to H_2CO_3, which then enters the cell, must be incorrect since a process of this nature could not result in a localized concentration of OH^-. Quantitative evaluation of the OH^- efflux associated with $HCO3^-$ transport has received very little attention indeed, the only study being that performed by Lindahl (1963) on *Enteromorpha linza*. He determined that this species gave off as many equivalents of OH^- as it took up HCO_3^-. A complete quantitative analysis of the OH^- efflux and HCO_3^- influx associated with HCO_3^- assimilation, will be presented in Chapter 4.

Active Transport Systems in "Giant" Algal Cells

Definition of Active Transport

Before discussing the active transport systems which have been identified in the algal cells of the Characeae and Chlorococcales, the concept of active transport will be briefly reviewed. The first rigorous definition of active transport was proposed by Ussing (1949a). He defined it as the process by which an ion is moved against its electrochemical potential gradient. For this to occur, Ussing proposed that the transported ion was coupled to a decrease in free energy of some other cellular (metabolic) process. In a later paper (Ussing, 1949b) he derived the now very familiar Ussing flux ratio equation,

$$\frac{J_{in}}{J_{out}} = \frac{C^{o}_{j}}{C^{i}_{j} \exp\ (z_j F \Psi / RT)} \qquad \ldots\ldots\ldots (1.1)$$

where J_{in}, J_{out} are the influx and efflux respectively of the j^{th} ion, C^{o}_{j} and C^{i}_{j} are the concentrations of the j^{th} ion on the two sides of the membrane, the superscripts o and i refer to the outside and inside respectively, z_j is the algebraic valence of the j^{th} ion, Ψ is the electrical potential across the membrane, F is the Faraday Constant, R is the gas constant and T is the absolute temperature. This relationship was also derived independently by Teorell (1949).

Equation (1.1) has been used by both plant and animal physiologists to determine whether the ionic (net) flux is passive. The expression is quite general for passive, independent movement of ions and relates the fact that ionic movement is proportional to its electrochemical potential difference. The derivation assumed ideality of the solutions, which may not hold for some biological systems. Hence it should be remembered that it may be necessary to determine ionic activities rather than concentrations. The other

limitation, as pointed out by MacRobbie (1970), is that non-independence and interaction of ions in the membrane may influence the magnitude of the flux ratio. It is consequently more suitable to identify active transport by a flux ratio which has the incorrect sign on the logarithm of that ratio (MacRobbie, 1970). Other workers have attempted to apply the principles of irreversible or non-equilibrium thermodynamics to solve this problem (see Simons, 1969; and Thain, 1973). To use equation (1.1.) J_{in}, J_{out} C^{o}_{j}, C^{i}_{j} and Ψ must all be determined experimentally and this has at times proved to be difficult. This difficulty becomes acute when dealing with ions like HCO_3^- which can be converted to other chemical forms via various equilibrium reactions.

In mature cells it has often been observed that $J_{in} = J_{out}$ and hence under these conditions, equation (1.1) reduces to

$$\Psi = \frac{RT}{Z_j F} \quad \frac{C^{o}_{j}}{C^{i}_{j}} \qquad \text{.....(1.2)}$$

which is the well known Nernst equation. Equation (1.2) has also been used widely by plant physiologists to determine whether an ion is in thermodynamic equilibrium. It should be stressed that application of this equation is strictly valid only when influx and efflux are equal, activities are equal to concentrations and the ionic movements are independent.

Kedem (1961), using the principles of irreversible thermodynamics (see Katchalsky, 1961), extended the Ussing definition of active transport. She developed equations relating the flow of each component to its various driving forces of chemical potential, solvent drag and ion-ion interaction. If there was an active component of flow present, then a term which coupled the rate of a specific metabolic reaction to the active transport of that ion, was included in the flow equation. Until experimental results indicated otherwise,

Kedem proposed that all flows should be assumed inter-dependent, especially the chemical or metabolic reaction. Active transport was considered to be operating when there was a non-zero coupling coefficient between the flow of a particular ion and the chemical (metabolic) reaction.

MacRobbie (1970) criticized Kedem's description of active transport, levelling her criticism at the indirectness of the coupling between the specific process of active flow and the driving reaction(s) of metabolism. A further limitation is that, for plants in particular, it is difficult to ascertain the exact contribution, of the total metabolic rate, that is coupled to the active process. This is particularly true for photosynthetic tissue where, in the light, both respiration and photosynthesis could act as energy sources. This difficulty has meant that, as yet, the irreversible thermodynamic treatment has rarely been employed in ion transport studies related to plants.

Active Fluxes of K^+, Na^+ and Cl^-

In the work described in the following discussion the active nature of the ionic flux was determined, by the various workers, by employing either equation (1.1) or (1.2). Of the ionic fluxes studied, K^+, Na^+ and Cl^- have received the greater attention (an extensive list of references to this work is given in the review by MacRobbie, 1970, p. 259). In general it has been found that in all giant algal species studied, Na^+ is actively extruded whilst Cl^- is actively accumulated. The situation with respect to K^+ is not as uniform, *Nitella translucens* (MacRobbie, 1962), *Nitella clavata* (Barr and Broyer, 1964) and *Hydrodictyon africanum* (Raven, 1967) possess an active K^+ uptake mechanism while in *Chara corallina* K^+ appears to be in passive equilibrium and the fluxes have therefore been assumed to be passive.

Apparently in *N. translucens* and *H. africanum* the active transport of Na^+, K^+ and Cl^- is controlled by two independent systems; both systems are light stimulated. One is a coupled K^+/Na^+ system which is Ouabain-sensitive (Raven, 1967) and its coupling ratio is also light dependent. Under dark conditions the Na^+ efflux is reduced to approximately 50% of its value in the light, but K^+ influx in the dark is reduced to a very low level. A small passive contribution to the total cation fluxes is also present when the cell is illuminated, the passive cation permeability being considerably reduced in the dark.

The second system involves the coupling of cation fluxes to active chloride transport. The cation associated with this Cl^- influx varies from species to species, e.g. Na^+ is the cation involved in *N. translucens* (Smith, 1967b), K^+ for *Tolypella intricata* (Smith, 1968b) and Raven (1968b) showed that the cations K^+ and Na^+ could contribute to this flux in *H. africanum*. A reduction in Cl^- influx occurs when monovalent cations are excluded from the bathing solution. It has been suggested that this Cl^- stimulation is correlated with the relative passive permeabilities of these cations (Raven, 1968b). MacRobbie (1970) suggested that this apparently implied that Cl^- influx was electrogenic (this term will be defined in the section relating to membrane potentials). However, since limited experimental support has been obtained for this hypothesis, MacRobbie favoured the alternative explanation of these results, namely that the Cl^- pump transferred neutral salt. Work with *C. corallina* (Findlay, Hope, Pitman, Smith and Walker, 1969) suggested that part of the K^+ influx may be due to Cl^- transport which "alters the effective membrane potential difference". However this contribution to the potential was small, the mean value observed when cells were transferred from a Cl^- to a $SO_4^=$ solution was + 14mV. Pickard (1973)

also showed that replacing Cl^- by $SO_4^=$ had very little effect on the resting potential, in this case the potential became more negative by 5 to 10mV. At this point it is probably worth pointing out that this observed cation/cation and anion/cation coupling demonstrates the restriction which must be placed on the use of the Ussing flux ratio equation, since this expression requires independent ion movement.

For these specific cells (*N. translucens* and *H. africanum*), the energy for the K^+/Na^+ system has been demonstrated to be ATP, produced by photophosphorylation. The Cl^- system does not appear to require photosynthetically generated ATP; the nature of the coupling between the photosynthetic light reactions and this Cl^- transport system has not been fully elucidated. MacRobbie (1965, 1966) suggested that the Cl^- system was linked to a non-cyclic electron transfer reaction, however the nature of this linkage remains obscure. Spear et al. (1969) and Raven (1969b) proposed that the triose phosphate/phosphoglycerate shuttle (Latzko and Gibbs, 1969), across the chloroplast membrane, provided $NADH_2$ and ATP in the cytoplasm and that one (or both) of these high energy compounds was involved in the transport of Cl^- across the plasmalemma.

Chara corallina does not have a K^+/Na^+ linked transport system, as mentioned previously, K^+ appears to be in passive flux equilibrium (Hope, 1962). However, there is an active Na^+ efflux system present, but this is not light stimulated (Findlay et al., 1969). The Cl^- influx can be light stimulated, and if so, is sensitive to DCMU or CMU (Coster and Hope, 1968; and Smith and Raven, 1974). It is important to note that the extensive experiments of Findlay et al. (1969) demonstrated that *C. corallina* can exist in various "states" and that the Cl^- influx may not always be light stimulated nor respond to the removal of "counterions". The "State A" of Findlay et al. corresponds to the response observed in *N. translucens* and *H. africanum*, but in "states B-D" the K^+ and Cl^- fluxes are apparently independent. The nature and reason for these states remains

unknown and must surely serve as a warning that at least this cell is physiologically different from the other Characean species.

The energy source for Cl^- influx into *C. corallina* appears to be different from that present in *N. translucens* and *H. africanum*. Coster and Hope (1968) showed that low concentrations of DCMU lowered Cl^- influx in the light and Smith and West (1969) demonstrated that CCCP also reduced the light stimulated Cl^- influx. The work of Smith and West provided no evidence which supported the hypothesis that Cl^- influx was directly linked to non-cyclic photosynthetic electron flow reactions rather than photophosphorylation. The energetics of Cl^- transport in this cell was extended by Smith and Raven (1974), who proposed that cyclic phosphorylation cannot supply ATP for Cl^- transport in the absence of photosystem II. Even so the Cl^- situation does not seem to have been resolved completely, for example the competitive inhibition of Cl^- influx by HCO_3^- has not been successfully explained.

HCO_3^- and OH^- Fluxes: Active or Facilitated Transport.

It has already been mentioned that Steemann Nielsen (1947) and Raven (1968a) demonstrated that assimilation of exogenous HCO_3^- required more energy per mole of carbon fixed than when CO_2 entered by diffusion. Both authors considered that the extra energy was required by the cell for transport of either HCO_3^- or OH^-. However, to determine whether these fluxes are active or passive it is necessary to obtain experimentally accurate values of all the parameters associated with equation (1.1). To date this has not been accomplished, the values which have not been determined are the cytoplasmic concentrations of HCO_3^- and OH^-.

Raven (1968a) and Smith (1968a) did not use equation (1.1), instead they assumed that the cytoplasmic HCO_3^- level was zero and that the Goldman (1943) equation could be applied. (The limited

use of this equation will be discussed in the following section on membrane potentials). These workers calculated HCO_3^- permeability coefficient ($P_{HCO_3^-}$) values of 10^{-4} cm s^{-1} (*H. africanum*) and 5×10^{-4} to 5×10^{-5} cm s^{-1} (several Characeae). Raven (1970) concluded that since $P_{HCO_3^-}$ was approximately 10^5 times greater than P_{Cl^-}, the entry of HCO_3^- into the cell was not passive but occurred via "some chemical interaction of bicarbonate with the membrane". However, HCO_3^- entry may not be active, but could still occur via facilitated diffusion, i.e. passive entry of HCO_3^- mediated by a membrane bound carrier. If this was so, the facilitated diffusion mechanism would explain the high calculated "permeability coefficient."

The same conclusion, concerning the nature of HCO_3^- entry, could have been obtained using equation (1.1). Again an assumption of the cytoplasmic HCO_3^- concentration is necessary. Since $C^o_{HCO_3^-}$ was usually 1mM (see Smith, 1968a), $C^i_{HCO_3^-}$ was assumed to be non-zero and 10μM was used as a "working" concentration. It is also necessary to make an estimate of the membrane potential (Ψ_{co}) under HCO_3^- assimilating conditions, this is complicated by the sensitivity of Ψ_{co} to pH. The bathing solution pH value for HCO_3^- experiments was usually between 9 and 10. It is unfortunate that data for Ψ_{co} is sparse in this pH range and also the few reported values seem to vary for each species (cf. Spanswick, 1972; Volkov, 1973; and Richards and Hope, 1974). Using the data of Richards and Hope (1974), Ψ_{co} for *C. corallina* would be approximately 170 to 180mV. The flux ratio $\frac{J_{in}}{J_{out}}$ is > 1 because there was net transport of HCO_3^- into the cell, hence $\log \frac{J_{in}}{J_{out}}$ must be positive. However, employing the above estimates of $C^i_{HCO_3^-}$ and Ψ_{co} in equation (1.1), it was found that the logarithm of the equation was equal to -1.044. According to MacRobbie this would indicate that $HCO3^-$ transport is not passive.

It is possible, by holding $C^{o}_{HCO_3^-}$ and Ψ_{co} constant, to estimate the maximum concentration which could be established by facilitated diffusion. This was obtained by increasing $C^{i}_{HCO_3^-}$ until the sign of the logarithm became positive, the value at which this occurred was 0.9μM. Hence the supply of HCO_3^-, via facilitated diffusion, must remain as a possibility, but the internal HCO_3^- concentration would be very low. In consequence there would be the requirement of a very low Km for the photosynthetic fixation reaction. Raven (1970) stated that, at least for *H. africanum*, the experimental data did not support this low Km hypothesis and he concluded that it was more likely that HCO_3^- transport was active. Raven's argument was supported by the work of Werdan and Heldt (1972). These workers considered that inorganic carbon crossed the chloroplast outer membrane by diffusion of CO_2. (If there had been an active HCO_3^- transport system in the chloroplast membrane its Km may have been low).

The data available for *C. corallina* is insufficient to enable a definite conclusion on whether HCO_3^- transport is active. This is because the kinetic data for CO_2 fixation is incomplete and secondly it is not yet clear whether HCO_3^- can be assumed to move independently. Lucas and Smith (1973) considered HCO_3^- movement to be obligately coupled to OH^- efflux. If the transport is coupled, equation (1.1) cannot be used to determined whether the movement is passive or active. Hence, although the literature almost always refers to HCO_3^- influx as active, it can be seen that there must still be some doubt concerning the acceptance of this status.

There is also some doubt concerning the OH^- efflux situation in *C. corallina*. The cytoplasmic pH of plants can be assumed to lie between 6.5 and 7.5 (Waddell and Bates, 1969; Shieh and Barber, 1971; and Raven and Smith, 1974 for a review of this literature). However this is the average value of the cytoplasm and for

C. corallina this may not be equivalent to the pH value at the OH^- efflux sites. Nevertheless using 0.1μM for $C^i_{OH^-}$, 10μM for $C^o_{OH^-}$ (experimental pH of the bathing solution generally > 9.0) and 180mV for Ψ_{co} in equation (1.1) gave a negative logarithm. The net OH^- movement is out of the cell, therefore $\log \frac{J_{in}}{J_{out}}$ must also be negative, which would suggest that the observed OH^- efflux could be passive.

For *Chara corallina* the cytoplasmic pH may not be 7.0, especially during HCO_3^- assimilation, and also the localized OH^- efflux pattern (see Lucas and Smith, 1973) may establish a situation which can only be explained by invoking active OH^- efflux. Further experimentation is required before the status of either the HCO_3^- or OH^- system can be completely defined. It is also important to note that since, for the OH^- ion, the influx and efflux rates are not likely to be equal, equation (1.2) cannot be applied to determine the status of this ion.

There is one other extremely important ion which has not been discussed, this ion is of course the proton. The discussion relating to this ion will be deferred at this stage because it will be considered in the section on electrogenic membrane components in the Characeae. The other minor ions, which include sulphate, phosphate and acetate, will not be discussed since they have little or no bearing on the subject matter presented in this dissertation.

The Membrane Potential

Passive Diffusion Potentials

During the early electrical studies on the Characean membrane, it was generally thought that the electrical potential observed across the plasmalemma was developed by passive ionic fluxes, i.e. it was considered to result from an asymmetric distribution of ions across the membrane and the fact that ions of the salts involved had different ionic mobilities. The asymmetry in concentration was considered to result from neutral active transport systems (Dainty, 1962). Excellent reviews of this early work have been presented by Dainty (1962), MacRobbie (1970) and Higinbotham (1973).

In general equation (1.2) was employed when only one ion was involved. Hodgkin and Katz (1949) developed the expression for the situation where more than one ion was involved. They used the Goldman flux equations (Goldman, 1943) to express the various ionic currents, in their case K^+, Na^+ and Cl^-. By combining these currents and making the assumption that the net current was zero, they obtained the expression,

$$\psi_{co} = \frac{RT}{F} \ell n \frac{P_{K^+}[K^+]^o + P_{Na}[Na^+]^o + P_{Cl^-}[Cl^-]^i}{P_{K^+}[K^+]^i + P_{Na}[Na^+]^i + P_{Cl^-}[Cl^-]^o} \quad \ldots(1.3)$$

The superscripts i and o indicate the two sides of the membrane, inside (cytoplasm) and outside (bathing solution) respectively. P_j, the permeability coefficient of the j^{th} ion, is a complex parameter and can be defined as $P_j = \mu'_j \frac{RT}{a} k_j$ (after Hodgkin and Katz, 1949; and Dainty, 1962), where μ'_j is the ionic mobility within the membrane, a is the membrane thickness and k_j is the ion partition coefficient between the membrane and the solution.

Equation (1.3) was found to fit the potential of the Characeae under certain conditions. This generally involved the absence or very low concentration of Ca^{++} in the bathing solution (Osterhout, 1949; Kishimoto, 1959; Hope and Walker, 1961; Spanswick, Stolarek and Williams, 1967; Kitasato, 1968; Spanswick, 1972; and Gillet and Lefebvre, 1973). However, the non-independent movement of many of the ions associated with these cells and their potential, must cast doubt on the validity of the application of this expression (MacRobbie, 1968). Spanswick et al. (1967) proposed that, "when Ca^{++} is present in the bathing medium, there is no form of the Goldman equation which can be used to describe Ψ_{co}".

There are also numerous reports in the literature of potentials which are more negative than can be predicted by either equation (1.2) or (1.3) (see for an excellent example, Spanswick, 1972), i.e. there would appear to be some other factor contributing to the membrane potential. Perhaps the most significant short-coming of these equations and the theory upon which they have been based, is their inability to predict the correct experimentally observed membrane conductance. The calculated value is usually about an order of magnitude smaller than the experimentally determined value (Dainty, 1962; Williams Johnston and Dainty, 1964; and Walker and Hope, 1969). However, Spanswick (1970b) showed that the membrane resistance may take several hours to recover from the effect of insertion of the microelectrodes used to measure potential and resistance. He considered that if "all" the ionic fluxes were included, the disagreement between theory and experimentally obtained values would be small. This proposal does not seem to have received support in the ensuing literature, Spanswick himself seems to discard it in favour of an electrogenic transport system which contributes to the total conductance (Spanswick, 1972, 1973, 1974).

Although equation (1.3) and the Goldman equations do not satisfactorily represent the membrane potential of the Characeae, they are still being exployed since, as pointed out by Richards and Hope (1974), there is not a more suitable alternative. This point should be stressed, for the results obtained using these equations should always be viewed with this in mind.

Electrogenic Component of the Membrane Potential

The inability of the Goldman and Hodgkin and Katz equations to fit the experimentally observed potentials, prompted numerous proposals of electrogenic pumps which were considered to contribute towards determining the membrane potential (Slayman, 1965; Hope, 1965; Spanswick et al., 1967, and Kitasato, 1968). An electrogenic transport system can be defined as a carrier system which by its action transfers net charge across the membrane and hence generates electrical potential at the expense of metabolic energy (Slayman, 1965; and Higinbotham, 1973). The general criterion for the existence of an electrogenic pump is the presence of a potential more negative than can be accounted for using either equation (1.2) or (1.3) (Kitasato, 1968; and Spanswick, 1972). Dainty (1962) described the experimental procedure which could be employed to determine whether an electrogenic pump was contributing to the membrane potential. This involved the use of metabolic inhibitors which would stop the electrogenic pump. He suggested that a rapid change (i.e. towards a less negative value in the Characeae) in potential would probably indicate the presence of an electrogenic pump. He proposed that a slow change would indicate the inhibition of a neutral pump, which contributes to the passive diffusion potential by maintaining an asymmetric concentration.

Perhaps the most elegant work demonstrating the existence of an electrogenic pump was that of Slayman (1970) and Slayman, Long and Lu (1973). In this work Slayman and his collaborators showed that the membrane potential of the fungus *Neurospora crassa* dropped rapidly to a new resting level when respiratory inhibitors were added. It was suggested that protons were transported across the plasmalemma in an electrogenic manner (Slayman, 1970) and Slayman et al. provided very convincing evidence that the energy was supplied by ATP. Numerous reports have been made of possible electrogenic contributions to the membrane potential of the Characeae. The main body of this work involves the response of the membrane to changes in the bathing solution pH.

Influence of pH on Characean Ψ_{co}

Kishimoto (1959) was the first worker to report that Ψ_{co} of *C. corallina* was extremely sensitive to the pH value of the bathing solution. He found that increasing the pH caused Ψ_{co} to become more negative, attaining a maximum negative value ($\simeq$ - 205mV) at approximately pH 6.7. The value of Ψ_{co}, at pH values >7.0, decreased in a manner which was almost symmetrical to its increase at pH values < 7.0. Kishimoto did not offer an explanation for this variation of Ψ_{co} with pH.

Hope (1965) inadvertently changed the pH value of the bathing solution by adding $NaHCO_3$. He attributed the observed hyperpolarization to an electrogenic HCO_3^- transport system. (In this present study the membrane is considered to become hyperpolarized when the value of Ψ_{co} becomes more negative than the control value of Ψ_{co}, which existed prior to the particular experimental treatment). It is proposed to discuss this work in detail in the section relating to the influence of light on the value of Ψ_{co} and so no further comment will be made at this point.

The work of Kitasato (1968) was probably the most important report on the influence of pH on Characean Ψ_{co}. His hypothesis was that in *Nitella clavata*, in the pH range 5 to 6, the proton conductance was substantially equal to the membrane conductance, and that there existed a H^+ extrusion mechanism, located in the plasmalemma, which contributed electrogenically to Ψ_{co}, i.e. passive H^+ influx was balanced by an active proton efflux mechanism such that the cytoplasmic pH value was kept constant. He proposed that under these conditions the membrane potential could be expressed by

$$\Psi_{co} \cong \Psi_{H^+} - \frac{F \phi_{H^+}}{g_m} \qquad \ldots\ldots(1.4)$$

where ϕ_{H^+} is the active efflux of protons, Ψ_{H^+} is the diffusion potential with respect to protons and g_m is the passive membrane conductance.

Kitasato observed a depolarization of the membrane when 0.2mM 2,4-dinitrophenol (an uncoupler of respiration) was included in the bathing solution. The decay of Ψ_{co} to a new resting potential was not anywhere near as rapid as that observed by Slayman et al. (1973). A similar effect to that reported by Kitasato, was observed by Richards and Hope (1974); in both reports this depolarization was assumed to indicate the presence of an electrogenic pump.

Kitasato's work stimulated interest in this field and numerous biophysical studies were conducted to test this hypothesis. The main weakness of the hypothesis appeared to lie in the proposal of a high passive permeability to protons (Walker and Hope, 1969; Coster, 1969; Lannoye, Tarr and Dainty, 1970; Spanswick, 1972, 1973, Raven and Smith, 1974; and Richards and Hope, 1974). The high passive proton permeability concept did not appear to be supported by Kitasato's own data nor by the later work of Saito and Senda (1973b)

or Richards and Hope (1974). Inhibition of the electrogenic component caused the membrane potential to fall to a level close to the K^+ diffusion potential, and not the H^+ diffusion potential as postulated by Kitasato. Hence Ψ_{H^+} in equation (1.4) should not be substituted for Ψ diffusion, which can be calculated using equation (1.3).

The main support for Kitasato's hypothesis was the observation by Spear et al. (1969) and Smith (1970) that cells of *Nitella clavata* and *Chara corallina* develop light stimulated acid bands on their surfaces. Lucas and Smith (1973) demonstrated the time-course of this acid efflux, but no identification of its relationship to metabolism has been forthcoming. Rent, Johnson and Barr (1972) measured the passive H^+ influx into *Nitella clavata* at pH 4.7 and from their results they calculated that this flux was of the same order of magnitude as that proposed by Kitasato. However, it is difficult to ascertain whether their experiments, conducted at this pH value, are at all meaningful since later work from this laboratory described the experimental conditions as "rather severe" (Brown, Ryan and Barr, 1973). Brown et al. calculated passive H^+ influx values as high as 220 pmol $cm^{-2}s^{-1}$, a value which appears to be absurdly high. This doubt was given further weight by the work of Richards and Hope (1974) who calculated that the H^+ efflux at pH 5.0 was only 1.2 pmol $cm^{-2}s^{-1}$, i.e. a value which is an order of magnitude smaller than the value obtained by both Kitasato (1968) and Rent et al. (1972). The work was done on different species and it is possible that the proton fluxes are in fact significantly different; however, the similarity in the response of Ψ_{co} with pH suggests that the mechanism, at least, must be common to both species.

It would appear that the situation is far more complex than was first envisaged by Kitasato. For example, his suggestion that high external pH values decreased the H^+ pump activity due to an increase in the cytoplasmic pH value is unsubstantiated by experimental evidence. Added to this was the fact that, rather than the decrease in conductance which would be consistent with this reduced H^+ efflux activity, the experimental conductance often increased as the pH value was raised (Walker, 1962, 1963; Coster, 1969; and Spanswick, 1972). Hence g_{H^+} may not be substantially equal to g_m over a very wide pH range.

Spanswick (1972) proposed a modification of the Kitasato (1968) hypothesis. He assumed that the passive "permeability of the membrane to all ions, including H^+, was low, and the electrical properties of the membrane reflect those of the postulated electrogenic pump". He supported Kitasato in assuming that the electrogenic pump was an active proton efflux system. His main extension to the membrane potential theory was that the pump conductance g_p, in the light, was assumed to be much larger than the passive membrane conductance g_m, i.e. equation (1.3) would contribute very little to Ψ_{co} except when the electrogenic pump was inoperative.

Spanswick based his model on the system proposed by Rapoport (1970) for the Na^+-K^+ pump located in numerous animal membranes. It is not intended to describe in detail Rapoport's entire model, but since both his and Spanswick's models are of importance in this field, the basic postulates will be described before dealing with Spanswick's hypothesis. Rapoport proposed that:

(i) The membrane concerned was anisotropic in that it was partitioned into two regions which acted as if they were electrically connected in parallel; one region was assumed to

function as the site for active transport and through the other, passive ionic fluxes were assumed to occur.

(ii) Hydrolysis of ATP within the active region was assumed to be coupled to the movement of Na^+ out and K^+ into the cell. The rate of this hydrolysis (Jr) was related to the current passing through the active region by the term $JrF(\upsilon_{Na^+} - \upsilon_{K^+})$, where υ_j was the stoichiometric coefficient of the j^{th} ion (i.e. the number of moles of j transported per mole of ATP hydrolysed).

(iii) The pump is only electrogenic when $\upsilon_{Na^+} \neq \upsilon_{K^+}$

(iv) The free energy change of the driving reaction (ΔFr) is dependent upon the membrane potential when the pump is electrogenic, i.e.

$$\Delta Fr = \Delta\bar{\mu}_p - \upsilon_{Na^+}.\Delta\bar{\mu}_{Na^+} + \upsilon_{K^+}.\Delta\bar{\mu}_{K^+} \quad \ldots(1.5)$$

where $\Delta\bar{\mu}_p$ is the change in free energy of the non-transported component of the driving reaction, and $\Delta\bar{\mu}_j$ is the electrochemical potential difference of the j^{th} ion across the membrane.

(v) The rate of the driving reaction is given by

$$Jr = Lrr\ (-\Delta Fr) \quad \ldots\ldots\ldots(1.6)$$

where Lrr is a thermodynamic conductance coefficient.

(vi) When the membrane is in a steady state, the current through the active and passive components of the membrane are equal and opposite.

Turning now to the application of these postulates to the Characean plasma membrane. Spanswick (1972, 1973) proposed that an unidentified metabolic reaction, associated with the plasmalemma, caused the transport of υ moles of H^+ per mole turnover of the

driving reaction. No counter-ion was considered to be transported in the opposite direction, hence the system would always be electrogenic and would generate a current equal to $JrF\nu_{H^+}$. For a Characean cell the expression for ΔFr, from equation (1.5) is simply

$$\Delta Fr = \Delta\bar{\mu}_P - \nu_{H^+} \cdot \Delta\bar{\mu}_{H^+} \qquad \ldots\ldots(1.7)$$

Remembering that $\Delta\bar{\mu}_{H^+} = RT \ln \frac{a^i_{H^+}}{a^o_{H^+}} + ZF\,\Psi_m$, substitution into (1.7) gives

$$\Delta Fr = \Delta\bar{\mu}_P - \nu_{H^+} \cdot \left(RT \ln \frac{a^i_{H^+}}{a^o_{H^+}} + ZF\,\Psi_m\right) \qquad \ldots\ldots(1.8)$$

From equations (1.6) and (1.8) it can be seen that the rate of the driving reaction for the electrogenic system is influenced by the membrane potential.

Spanswick suggested that by equating all passive permeabilities to zero, an expression could be obtained for the maximum emf which the pump could generate, i.e. Ψ_m would increase until ΔFr became equal to zero. Applying this to equation (1.8) gives

$$\Delta\bar{\mu}_P = \nu_{H^+} \cdot \left(RT \ln \frac{a^i_{H^+}}{a^o_{H^+}} + ZF\,\Psi m\right) \qquad \ldots\ldots(1.9)$$

Rearrangement gives

$$\Psi_m = \frac{\Delta\bar{\mu}_P}{ZF\nu_{H^+}} - \frac{RT}{ZF} \ln \frac{a^i_{H^+}}{a^o_{H^+}} \qquad \ldots\ldots(1.10)$$

where, according to Spanswick, Ψ_m = (the pump emf) = Ψ_P

To stop at this point is unrealistic since the passive permeabilities are not zero and it is unfortunate that Spanswick did not develop the steady state expression for Ψ_{co} in terms of its electrogenic and passive diffusion components.

He has suggested, however, that on his model, "most of the current injected during resistance measurements will pass through the active channel", which should result in H^+ being effluxed into the external medium at an increased rate. This statement has not, as yet, acquired experimental support (see for example the attempts by Walker and Hope, 1969). The observed hyperpolarization in the light was proposed to result from a more negative value of $\Delta\bar{\mu}_p$, but just how this could possibly occur was not detailed by Spanswick and it does seem to have been left as a rather vague statement. The other weakness in Spanswick's hypothesis is related to the response of Ψ_m and membrane conductance to changes in external solution pH values. Spanswick (1972, p. 88) suggested that the initial hyperpolarization observed when the external pH value was changed to 7.0, could be explained by a change in $a^o_{H^+}$. One assumes that he considered the expression of a change in $a^o_{H^+}$ to be interpreted by its substitution into equation (1.10). But it must be pointed out that at this pH value he considered the electrogenic pump to be operating, for he suggested that it caused a decrease in $a^i_{H^+}$. (This, he suggested, caused the depolarization of the membrane following the initial hyperpolarization). If the pump was operating $Jr \neq 0$ and hence the results cannot be explained by applying Spanswick's arguments to equation (1.10). This equation only holds for the particular case of $Jr = 0$ and zero passive fluxes.

It also seems that Spanswick's hypothesis cannot explain the observed increase in conductance as the external pH value is raised. If the electrogenic pump does raise the cytoplasmic pH value, in response to an external pH increase, the situation must surely develop where the cytoplasmic pH value actually causes the electrogenic pump to stop. If this was not so, the cytoplasmic pH would soon be raised above physiological limits. Stopping the pump would reduce the membrane conductance. However, Spanswick's own data (Spanswick,

1972, Fig. 3) demonstrated that at pH values greater than 7.0, the conductance actually rises to a maximum value.

Thus, although it is realized that equation (1.3) does not explain the membrane potential under all physiological conditions, there is not at present a comprehensive hypothesis in the literature which can explain all the electrical properties of the Characean plasma membranes. This appears to be especially true for the depolarization of the membrane potential when the cell is placed in contact with solutions of pH > 8.0.

The Response of Ψ_{co} to Illumination

The membrane potential of many green plants cells appears to be sensitive to illumination (Higinbotham, 1973). The phenomenon of the electrical response of the Characean plasmalemma, to illumination, was first reported by Brown (1938). However the response appears to be extremely variable and inter species and seasonal differences may add to the complexity of this phenomenon. Nagai and Tazawa (1962), using cells of *Nitella flexilis*, found that Ψ_{co} became hyperpolarized when their cells were illuminated. Andrianov, Kurella and Litvin (1968), working with the same species, reported a depolarization of approximately the same order of magnitude, following illumination. The work of Nishizaki (1963, 1968) on *Chara braunii* may enable an explanation to be offered for this rather perplexing contradiction in membrane response, observed using the same species. Nishizaki showed that the membrane response to illumination depended upon the ionic composition of the bathing solution and also the duration of the dark period prior to illumination. A long dark period was reported to result in an hyperpolarization, a short dark period of between 8-30 minutes, resulted in the membrane depolarizing upon illumination. Since Andrianov et al. employed alternating light and dark periods of 4-7

minutes, it would appear that their results are consistent with the response reported by Nishizaki.

The electrical changes produced by light have an action spectrum similar to that of photosynthesis (Walker, 1962). It is not surprising, therefore, that the membrane is not responsive to light of wavelengths greater than 700nm (Walker, 1962; and Volkov, 1973). Andrianov et al. also noted that there was an analogous effect between the shape of the response of the membrane potential and the induction of photosynthesis upon illumination. This involvement of photosynthesis has also been shown by the sensitivity of the plasmalemma-response to photosynthetic inhibitors. Walker (1962), using *C. corallina*, and Volkov and Petrushenko (1969), Volkov (1973), Saito and Senda (1973a,b) using *N. flexilis*, all reported that DCMU (or CMU) completely abolished the light sensitivity of the membrane potential to illumination. Excellent conformation of the coupling between changes in Ψ_{co} and photosynthesis was obtained from the work of Andrianov, Bulychev and Kurella (1970). They demonstrated that when the rhizoids of *N. flexilis* were free of chlorophyll, no light induced changes occurred in the resting potential. However, as the rhizoids developed chloroplasts, the resting potential became sensitive to illumination.

In the above studies it appeared that both photosystem I and II were required to enable the cellular expression of a membrane electrical response. However, Vredenberg and Tonk (1973) and Spanswick (1974) have suggested that only photosystem I is required, in *N. translucens*, for this stimulation to occur. This result again serves as a warning that the various Characean cells may differ significantly in their physiological detail.

There has also been the suggestion that the resistance change, produced by light (see Hope, 1965), may be due to an increase in the permeability of the membrane to one or more ions. Walker (1962) suggested that this ion might, in fact, be HCO_3^-. However he did not stipulate the manner in which HCO_3^- was supposed to interact with the light reactions. He reported later (Walker, 1963) that no correlation could be found between increasing the HCO_3^- concentration at a fixed pH, and the hyperpolarization of the membrane which was observed in the light (cf. Volkov, 1973). Nishizaki (1968) demonstrated that the change in electrical resistance associated with the transition from dark to light, had a slower time-course than the light-induced change in Ψ_{co}. This would suggest that the changes in resistance and Ψ_{co} cannot be explained solely by changes in ionic permeabilities.

An electrogenic role for HCO_3^- was first proposed by Hope (1965), Spanswick (1970a) refuted this, claiming that the electrical potential change was independent of the chemical nature of the buffer employed, and that HCO_3^- produced the hyperpolarization via its buffering action. However, it should be pointed out that the conditions used by Spanswick were not free of HCO_3^- and therefore his results do not eliminate a specific role for HCO_3^-. It also is important to note that Spanswick used *Nitella translucens* whilst Hope conducted his experiments on *Chara corallina*.

Hope showed that the hyperpolarization, due to HCO_3^-, was light sensitive, as was the decrease in membrane resistance. This is interesting in two respects; firstly the later work of Hope and Richards (1971) and Richards and Hope (1974) demonstrated a membrane potential which appears to be almost completely light-independent, an inconsistency which has not been accounted for by these workers. Secondly, Spanswick (1970a) reported that the hyperpolarization in

the presence of HCO_3^- was independent of illumination, yet in his later publications he demonstrated that there was a difference between Ψ_{co}, at pH 7.0, in the dark compared with the light (see for example, Spanswick, 1972, Fig. 2). This inconsistency within the literature is confusing. The explanation may lie either in the seasonal variation of the various cells or perhaps by the cells existing in various "states" as demonstrated by Findlay et al. (1969).

Other reports of the influence of HCO_3^- on Ψ_{co} are those of Nishizaki (1968) and Saito and Senda (1973a). Nishizaki found, in contrast to Hope (1965), that changing from unbuffered bathing solutions to solutions containing 0.2mM $NaHCO_3$, in the dark, gave an hyperpolarization of approximately 80mV. Illumination caused a slight further hyperpolarization, followed by a rapid depolarization, a result which is at variance with the response which Hope (1965) obtained using *C. corallina*. However, if the HCO_3^- effect is simply to change the pH from approximately 5.7 to a value of 7.2 - 7.4 (i.e. pH of 0.2mM $NaHCO_3$) then the results obtained by Nishizaki (1968) would fit the response obtained by Spanswick (1972, Fig. 2 or Fig. 6). It would seem that for *Chara braunii* a stable pH-induced hyperpolarization only exists up to a pH value of 7.0 (cf. Kishimoto, 1959, to Spanswick, 1972).

Saito and Senda (1973a), using *Nitella flexilis* and *Nitella axilliformis*, found that 1.0mM $NaHCO_3$ (pH 7.8) added in the dark, gave a small hyperpolarization of approximately 20mV, and illumination caused a further stable hyperpolarization of about 40mV. This response was closer to that observed by Hope (1965). Contrary to Richards and Hope (1974) Saito and Senda always obtained a much more negative Ψ_{co}, in the light, compared with the dark situation. However, in a later paper (Saito and Senda, 1973b) they reported that under some circumstances the high pH-sensitivity of Ψ_{co} was also observed in the dark. This stability of the light induced

membrane response, in the presence of 1.0mM $NaHCO_3$ (pH 7.8), compared with the depolarization observed by Nishizaki (1968) was probably due to the fact that the pH-induced changes in Ψ_{co} were stable to pH values up to 8.5 (see Saito and Senda, 1973a, Fig. 3b). As an indication of the type of variation which can be found in the literature relating to these cells, Andrianov, Vorobeva and Kurella (1968), who also used *N. flexilis*, found that the hyperpolarized state was not stable above pH values of approximately 7.8.

The possible role of HCO_3^- in influencing the membrane potential of *N. flexilis* has also been proposed by Volkov and Misyuk (1969), Volkov and Petrushenko (1969) and Volkov (1973). These workers reported that Ψ_{co} was sensitive to pH and illumination and Volkov and Misyuk proposed that this hyperpolarization of the membrane was a direct result of an increase in the plasmalemma permeability to HCO_3^-, the HCO_3^- entry being passive. What is not clear is whether, during their HCO_3^- concentration experiments, these workers held the pH of the bathing solution constant. If it was not held constant, the observed hyperpolarization would fall into the general category of pH-mediated change in membrane potential. Passive permeation of HCO_3^- was also proposed by Volkov and Petrushenko; however Volkov (1973) suggested that the hyperpolarization may be caused by either the existence of an electrogenic pump or an increase in plasmalemma permeability to some ion. He qualified this statement by suggesting that the connection between the hyperpolarization of the plasmalemma and the commencement of the electron transport chain and hence the Calvin cycle could be through a cytoplasmic change in the concentration of HCO_3^- or H^+. The mechanism that he invoked was a change in membrane permeability to either H^+ or HCO_3^- rather than the operating of an electrogenic pump. The passive proton case has already been discussed and must be discarded, for it cannot

account for the large negative membrane potentials (Kitasato, 1968; and Spanswick, 1972).

The HCO_3^- proposal is difficult to evaluate because of the limited data available. It is possible, however, that if $P_{HCO_3^-}$ is very large and $[HCO_3^-]^i$ fell to a very low level, that equation (1.3) would simplify to equation (1.2) with HCO_3^- acting as the dominant ion. The strongest evidence against this proposal is that it cannot explain the depolarization which occurs at pH values greater than 7.5 to 8.0. This is especially so since HCO_3^- is the dominant species of carbon present in this pH range, remaining so up until pH 10.3. Similarly it does not offer an explanation for the transitory nature of the hyperpolarizing response observed by many workers, including Volkov (1973). Hence the role which HCO_3^- plays in determining Ψ_{co} requires further experimentation, especially in the area of the HCO_3^- - OH^- couple proposed by Lucas and Smith (1973). Unless this proposal is shown to be incorrect, the above hypotheses relating to HCO_3^-, are almost certain to be invalid.

Summary

In conclusion, it has been shown that Characean cells can utilize exogenous HCO_3^- during photosynthesis and that the entry of this ion probably requires an active transport mechanism. However, this membrane transport process and its relationship to OH^- efflux has not been studied in detail. The membrane potential of these cells cannot be successfully fitted to the Hodgkin and Katz (1949) relationship (equation (1.3)), and acceptable agreement between Ψ_{co} (experimental) and Ψ_{co} (equation (1.3)) is only obtained when non-physiological conditions are employed. It can also be accepted that Ψ_{co} is very sensitive to the pH value of the bathing solution

but the nature of this sensitivity has not as yet been completely unravelled. Ψ_{co} is probably composed of a diffusive and an electrogenic component, part of this electrogenicity probably being associated with an active H^+ pump.

Although the perturbation of the membrane potential elicited by light, via the photosynthetic light reactions, has been recorded, the nature of the coupling mechanism between these reactions and the plasmalemma is not well formulated. Whether H^+ is the only ion involved, or whether HCO_3^- and OH^- are also important in determining the value of Ψ_{co} remains to be shown, but there are certainly strong indications that HCO_3^- may be an important ion.

The original aim of the present study was to investigate the acid and alkaline banding phenomena in *Chara corallina* with the view to characterizing these processes. It was hoped that this would provide the basis necessary for a biophysical study on the involvement of H^+, OH^- and especially HCO_3^-, in relation to the electrical properties of the Characean plasma membrane.

CHAPTER TWO

MATERIALS AND METHODS.

I. *Chara corallina* Culture Material

Cells of *Chara corallina** were used throughout the work presented in this dissertation. The cells were cultured in the laboratory in 80 litre plastic containers; illumination was provided by fluorescent lamps (Osram MCFE Daylight tubes) and the intensity at the solution surface was 15-17 Wm^{-2}. A 12h light : 12h dark regime was employed, the light period commencing at 6.30a.m. At least one culture tank was illuminated by direct window light. This provided cells with a lower chlorophyll concentration compared with those grown under the artificial lighting system. The temperature of the cultures was allowed to follow the seasonal variation of this area.

New culture tanks were propagated vegetatively by transplanting branches from an existing culture into a new tank. This was done by covering the bottom of the new tank, to a depth of 12cm, with a later of garden loam. The soil was covered by blotting paper and then 60 litres of deionized water was slowly added; the blotting paper minimized the mixing between the soil and the water and was removed when all the water had been added. The only nutrients added to the deionized water were NaCl, KCl and $CaSO_4$, to give final concentrations of 1.0, 0.1 and 0.2mM respectively. The garden soil appeared to supply all the micronutrients necessary for growth; hence the culture medium detailed by Forsberg (1965) was not used.

---

* The previous name of this species, *Chara australis*, has now been replaced, in accordance with the revised classification of the Characeae (Wood and Imahori, 1965), by the name *Chara corallina*.

In general, it took 6 to 8 weeks before cells could be harvested from a new culture and used for experimental purposes. Once established, a culture tank could be used for several years, and regeneration of young cells was obtained by cutting the culture back to half its mature height. To maintain a constant nutrient level, the unwanted harvested cells were crushed so that the soluble nutrients were extracted and added back to the culture solution.

The ionic composition of the culture tanks was monitored during this work; the indicator ions measured were Na^+, K^+, Ca^{++}, H^+, Cl^- and HCO_3^-. An EEL flame photometer was used to determine the concentrations of Na^+, K^+ and Ca^{++}, Cl^- concentration was measured using an Orion solid state halide electrode and a Radiometer pH meter, in conjunction with a Beckman pH electrode, was used to measure the activity of H^+. The concentration of HCO_3^- was determined by potentiometric (pH) titration (see Appendix A). The data for the culture tanks, from which the majority of cells were harvested during this study, are presented in Table 2.1.

Chara corallina cells were also collected from a site on the River Murray (Mannum, South Australia) and the concentrations of the indicator ions at this location are also presented in Table 2. The Mannum cells were used in ^{14}Carbon fixation experiments to ascertain whether fixation rates of the laboratory cultured cells were comparable with field cells.

The details relating to the cutting of culture cells for experiments will be given in a later section.

II. Experimental Solutions

The standard experimental bathing solution, which was prepared using glass-distilled water, contained 1.0mM NaCl, 0.2mM KCl, and 0.5mM $CaSO_4$. This working solution was prepared from stock solutions, and during all preparations solutions were thermostatted at $20^{o}C \pm 2$. All chemicals used in this work were of Analar Reagent grade. The glass distilled water was prepared from rainwater, which was used in preference to deionized water, since the latter was found periodically to contain ion-exchange residue. The specific conductivity (K_s) of the glass-distilled water was monitored using a Philips conductivity cell (Type P.W. 9510) and a Philips Resistance Meter. After atmospheric equilibration (CO_2), the K_s value was usually 1.09×10^{-6} to 1.18×10^{-6} $ohms^{-1}cm^{-1}$. This value is well within the specification stipulated by Bates (1964) for the preparation of standard buffers to enable pH meter calibration to within 0.01 pH units.

The ionic composition of solutions, which were modified from the basic form, will be specified at the relevant points in the text.

For some experiments a CO_2-free form of the standard bathing solution was required. This was obtained by scrubbing the solution with air from which CO_2 had been removed. Either a commercial source of CO_2-free air was used, or CO_2-free air was prepared in the laboratory by pumping it through two Drechsel bottles (sintered dome pore size 40-60μm) which contained concentrated NaOH and finally through a Drechsel bottle which contained boiled distilled water. This third bottle was used as a "trap" to prevent the transfer of NaOH into the experimental solution. The glass scrubbing vessel was gas-tight except for

the entrance and exit sites for the gas. A 250ml volume of bathing solution was scrubbed by CO_2-free air, which flowed at a rate of 0.6 litres m^{-1}, through a sintered glass bubbler (pore size 40-60μm); the solution was stirred continuously using a magnetic "flea" system. The pH value of the solution was monitored and it was found that a period of at least 1h was required to raise the pH value of the solution from 5.7 up to 7.0 ($\pm$0.05). As an added precaution all CO_2-free solutions were scrubbed for 2h before being employed in an experimental sequence. The apparatus in which these CO_2-free solutions were used is described in Section VII of this Chapter.

III. Techniques and Procedures Employed for ^{14}Carbon Experiments

The CO_2 fixation rate, in the presence of exogenous CO_2 or HCO_3^-, was determined using the radioisotope $H^{14}CO_3^-$ (obtained from the Radiochemical Centre, Amersham, U.K., or New England Nuclear, Massachusetts, U.S.A., as $NaH^{14}CO_3$). A stock solution of $NaHCO_3$ (100mM) was prepared just before it was required in the experimental sequence, and from this the various pretreatment and radioactive solutions were prepared. $NaHCO_3$ was used to prepare stock solutions for some of the initial experiments; however, experimental solutions having pH values higher than 8.3 had to be prepared by titrating the solution with NaOH. This involved the use of freshly prepared, carbonate-free, NaOH, in order that the experimental total carbon concentration remain unaltered. It became obvious that an easier method of obtaining these high pH values was to prepare a stock solution of Na_2CO_3 (pH approximately 10.4). Using this solution, the required pH value was obtained

by titration with 100mM H_2SO_4; the acid did not contaminate the experimental solution with an unknown amount of carbon.

Most experimental HCO_3^- and CO_2 solutions contained concentrations of HCO_3^- or CO_2 that were not in equilibrium with the level of CO_2 in the air. Hence exposure to the atmosphere was minimized and all treatments were conducted in sealed test tubes (25ml). The radioactive $NaH^{14}CO_3$ aliquot was added to the experimental solution not more than 10 minutes prior to the use of this solution in the experimental sequence. The specific activity of the various solutions was determined at the commencement of each experimental sequence. Samples (0.1ml) were pipetted onto planchettes to which 0.2ml of fresh 100mM NaOH had been added. The NaOH was required to convert the $^{14}CO_2$ or $H^{14}CO_3^-$ to $^{14}CO_3^{2-}$ so that during the drying process the loss of $^{14}CO_2$, to the atmosphere, was reduced to a negligible amount. Discs of lens cleaning tissue were used on all planchettes to facilitate the uniform distribution of solution; a condition necessary to minimize 'self-absorption' by the dried sample of $Na_2{}^{14}CO_3$. It was found that this even distribution (for planchettes containing specific activity samples or an experimental cell) could be enhanced by the addition of 0.1ml of ethanol, which probably acted not only on the surface tension of the solution, but also on the cell membranes, rendering them freely permeable to solutes.

It should also be mentioned that a 0.1ml sample of a 2% sucrose solution was added to planchettes containing experimental cells, the sucrose acting as an adhesive between the cell wall and the planchette. This same quantity was added to specific activity planchettes to allow for the 'self-absorption' of this component. The aluminium planchettes used for specific activity

determinations were treated with heat resistant polyurethane to prevent the 100mM NaOH from reacting with the metal. Three planchettes were used, per treatment, to obtain an average specific activity value. These were always dried and counted immediately. Specific activities of the various solutions employed ranged from 250μCi/m Mole to 2mCi/m Mole.

The experimental apparatus, used for these ^{14}carbon experiments, is shown in a diagrammatic form in Figure 2.1. The light source was a Rank-Aldis 24V, 150W Quartz-Iodide projector. Light intensities were attenuated using a range of nickel-nicron neutral density filters. These filters were prepared by the Physics Department, University of Adelaide, and each filter was checked on a Perkin-Elmer spectrophotometer to ensure that its absorption was in fact neutral over the wavelength range 450 to 750nm. Only filters having a Δ optical density of $\leqslant$ 0.03 units, over this wavelength range, were selected for use.

Light intensities were measured using a silicon solar cell (IRC, Type no SO510E 7PL) which was calibrated using a miniature Middleton pyranometer, Model CN6. (The Middleton pyranometer was calibrated by the C.S.I.R.O. Division of Meteorological Physics, Mordialloc, Victoria, Australia, and the calibration was quoted to be accurate to $\pm$ 5%). This silicon solar cell was mounted in a small perspex block so that it could be immersed in the water bath and positioned between two experimental test tubes (for its location see Figure 2.1). This enabled light intensities to be monitored during each experimental run. The output of the silicon solar cell was measured on a current to voltage transducer, which was constructed in this laboratory, and was capable of measuring

the signal reproducibly to ± 0.25mV. The calibration graph used to determine light intensities, when the Quartz-Iodide lamp was employed, is shown in Figure 2.2. Periodic checks on this calibration graph revealed that the silicon solar cell remained stable during the period of this study.

A map of the light intensities within the experimental plane (i.e. the plane in which the test tubes were to be held) was constructed and it was found that a uniform light intensity band, 7cm high by 10cm wide, could be obtained. It was within this band that all experiments were performed and its location is indicated on Figure 2.1. The band width of 10cm restricted the number of test tubes which could be used at any one time to four and the band height of 7cm determined the maximum length of the experimental cells. A mirrored surface was mounted flush against the glass wall of the water bath (see Figure 2.1) and this surface was 1.5cm from the rear of the test tubes. This mirror was incorporated into the apparatus to improve the illumination of the surface of the cells which faced away from the light beam of the lamp. As a further attempt to obtain a sample of uniformly illuminated cells, the test tubes were rotated through 180^{o} every 15 minutes.

The general experimental sequence followed to determine the photosynthetic rate under a given set of conditions was as follows:

(i) Internodal cells were cut from the culture tank and the whorl cells trimmed off close to the node. The experimental cells were cut from the third to fifth internodal region (i.e. back from the apex) and in many cases the fourth and fifth internodal cells were used as pairs. The cells were handled using the remaining small segment of the cell wall of the adjacent internodal cells. Cells were cut into glass

containers, and during the cutting procedure they were bathed in pond water taken from their respective culture tank.

(ii) A 90 minute recovery period was employed immediately after the required number of cells had been cut. During this period the cells were bathed in normal bathing solution (at $20^{o}C$) and were illuminated by fluorescent lighting (8.3 Wm^{-2}).

(iii) At the conclusion of the recovery phase the cells were batched for the various experimental treatments, with 14-16 cells used per treatment. Cell diameters were measured under X100 magnification, using a binocular microscope (Leitz, Wetzlar); the actual diameters could be determined to the nearest 12µm. At the same time the cytoplasmic streaming rate was checked. (It was found that, in general, cells recovered their normal streaming rate of 50 - 70µm s^{-1} within 15 minutes of being cut from the culture.) The length of each individual cell was traced accurately onto graph paper and this trace was used both for determining the cell length and also identifying the cell at the conclusion of the experiment. With these two experimental measurements the cell surface area was computed.

(iv) After batching, the cells were transferred to test tubes containing normal bathing solution and these test tubes were then sealed using Parafilm "M". The test tubes were then placed in the holder housed in the water bath. (It is important to note that stirring of the experimental solution was considered undesirable, because it was found that unless cells were held by some form of rigid support, spontaneous action potentials were induced by the flowing solution. Hence all radioisotope experiments were conducted

in unstirred solutions). The cells were then given a 1h dark pre-treatment.

(v) Cells were then pretreated for 30 minutes in the light (at the intensity specified by the experiment), in non-radioactive experimental solutions. These solutions contained, in addition to the normal bathing solution constituents, x mM Na_2CO_3 titrated to the required pH value. Some solutions were also buffered using "artificial" buffers, the details of which will be given in Chapter 3.

(vi) At the conclusion of (v), radioactive solutions were substituted for the required period, which was usually one hour.

(vii) At the conclusion of the experiment, cells were washed with non-radioactive solutions (5 min) before being cut and dried onto planchettes. (The nodes were discarded before the addition of 0.1ml of a 2% sucrose solution which was followed by 0.1ml of ethanol). The pH value of the radioactive solution was measured before and after the experimental period. In some experiments the streaming rate was also measured before the cells were cut onto the planchettes.

(viii) After drying, the ^{14}Carbon activity in the cells was counted* under a thin end-window Geiger tube (GEC Type E.H. M 2S) using an EKCO Automatic Scaler (Type N 530F), coupled to a Berthold Automatic Sample Changer (Type LB 271).

(ix) Planchettes were then treated with 0.5ml of 100mM Propionic acid to remove the precipitated $Ca^{14}CO_3$ and unfixed $^{14}CO_2$. Propionic

---

* The counting time was generally that required to give 3,000 or 10,000 counts, i.e. the error attributable to the counting procedure was less than ±2%.

acid was selected for this acidification because, owing to its volatile nature, it did not add to the 'self-absorption' layer on the planchettes. A minimum acidification time of 3h was employed, but the most frequent period used was 12 hours. At the end of this acidification period the planchettes were re-dried and the activity counted as in (viii).

(x) The photosynthetic fixation results were computed on a cell surface area basis and are expressed as the mean value of each treatment in pmol $cm^{-2}s^{-1}$ and all errors quoted are expressed as the standard error of the mean.

IV. Chlorophyll Determination

During the months over which these experiments were performed, the chlorophyll concentrations of the various culture tanks were monitored. The cells used for these determinations were given the same treatment as III(i) to (iii), each cell of a particular batch was then cut into 1mm segments and transferred from the end of the cutting scissors to a small (3ml) test tube. A 2ml aliquot of an 80% acetone/H_2O solution was used to extract the chlorophyll from these cells. The test tubes were spun in a Martin-Christ Centrifuge, at 400 x g for 5 minutes, to sediment the cell walls and particulate matter.

The absorption spectrum, in the wavelength range 640 - 700nm, was measured on a Beckman DB Spectrophotometer and from this the optical density values at 645, 652 and 663nm were determined. Chlorophyll concentrations were calculated using the corrected expressions derived by Arnon (1949) (see Appendix B). The mean chlorophyll concentration for each sample was obtained using the equation,

Mean chlorophyll concentration

$$= \left\{ \left([Chl_a] + [Chl_b] \right) + [Chl_{652}] \right\} \div (\Sigma \text{ surface area}) \times 2$$

where [ ] represents concentration, Chl_a, Chl_b and Chl_{652} are the concentrations of chlorophyll a, b and total chlorophyll estimated from the opitcal density at 652nm, respectively (the relationship between these values and the measured optical density is given in Appendix B) and Σ surface area is the cumulative surface area of all the *Chara* cells used in a particular determination. The average value for each culture tank is given in Table 2.1.

V. $^{36}Cl^-$ Time-Course Experiments

A series of time-course experiments were performed using $^{36}Cl^-$ (obtained as Hydrochloric acid, from the Radiochemical Centre, Amersham, U.K.). The stock solution (ampoule) was neutralized, using 100mM NaOH, and diluted with glass-distilled water to give a final volume of 100ml. The NaCl concentration of the bathing solution used for these time-course experiments was obtained by using 0.6mM non-radioactive NaCl and then an aliquot of the radioactive stock solution was added to give a final NaCl concentration of 1.0mM. The specific activity of these solutions was 50 µCi / m Mole.

The experimental procedure was similar to III (i) - (iv); however, following (iv) the cells were given a 30 min dark pretreatment in the radioactive experimental solution. This solution was unbuffered and its pH value was 5.8 ± 0.1. In later experiments the solution was buffered at the same pH value by 5mM HEPES. Following the 30min dark pretreatment, the cells were illuminated, for the required period, and then the sequence was again identical to III, (vii) and (viii).

VI. Measurement of the pH Value at the Surface of *Chara* Cells

(a) The pH Electrodes

Small pH electrodes were prepared in the laboratory (see Bates, 1964) using a fine, solid, pH-sensitive glass rod, which was obtained from Titron (Melbourne). The full details of this procedure were reported by Lucas (1971) and electrodes prepared during this earlier work were employed throughout the period of this study. The characteristics of these electrodes were as follows:

(i) The supporting stem for the pH-sensitive glass tip was approximately 5cm in length and tapered rapidly to a uniform outside diameter of 1mm.

(ii) The pH tips were 1.5mm (approximately) in diameter and the actual pH-sensitive tip area was hemispherical (see Lucas and Smith, Figure 2E).

(iii) The electrodes had Nernstian responses of 55mV to 58mV per pH unit and resistances of approximately $3.6 \times 10^9 \Omega$.

(iv) The electrodes were found to be practically insensitive to illumination, as they gave maximum responses of only 0.015 to 0.02 pH units upon illumination.

(v) The response of the electrodes, with time, was stable in either stagnant or stirred solutions.

(b) *The Electrical System*

A block diagram of the electrical circuit employed for measuring pH with these electrodes is shown in Figure 2.3. The Vibron Electrometer (EIL, Model 33B) was required because of the high resistance of the electrodes. The electrometer input resistance was $10^{13} \Omega$. The signal from the pH electrode

was connected to the high input terminal of the electrometer using thermally insensitive, polythene-insulated, coaxial cable. The low input terminal was connected to the Cambridge Vernier Potentiometer (Type No. 44246) and the circuit was closed by connecting the potentiometer to a calomel reference electrode (Radiometer, Type K401) which made electrical contact with the test solution. The Cambridge Vernier Potentiometer (with an accuracy of ±5μ Volts) was incorporated so that the electrometer signal could be backed off, thereby allowing the use of the more sensitive ranges (10, 30 and 100mV) of this instrument. The pH electrode signal was recorded by connecting the recorder terminals of the electrometer to a Rikadenki (Model TO2N1-H) recorder. As shown in Figure 2.3, the pH and calomel electrodes were housed in a Faraday cage in order that the spurious electrical noise factor be reduced to a minimum. All instruments, except the recorder, were connected to a common earthing terminal.

Calibration of this electrical system was performed in the following manner.

1. Electrometer

The input switch was set to 'positive', then

(i) the hum control was adjusted to give a minimum value on the appropriate test socket;

(ii) the gain control was then adjusted by connecting a low resistance source of 10mV (accurately known) across the high and low terminals and with the range switch on the 10mV scale, the gain was adjusted until the meter gave a full scale deflection;

(iii) the electrometer was then connected back into the circuit with the input switch set to 'negative'.

This procedure was performed at monthly intervals or whenever valves had to be replaced. The daily operation of this instrument simply required the adjustment of the set zero control to give zero on the meter and using the emf supplied by the potentiometer, the accuracy of the various mV ranges was verified.

2. Potentiometer

The voltage to the potentiometer was supplied by two, 2.0 Volt Exide (Type no 042) wet cell batteries connected in parallel (combined capacity of 54 ampere-hours), the current load of the potentiometer was 20 milliamperes. When the circuit was initially assembled, the accuracy of the potentiometer was checked by standardizing the instrument using a Standard Weston Cell and then the emf of a second Standard Weston Cell was determined using the potentiometer. This value agreed exactly with the value quoted on the calibration certificate of the second Standard Weston Cell (given to the nearest 10μV). It was therefore assumed that the potentiometer could be used as an accurate voltage source to apply a backing potential to the electrometer. On a daily basis the potentiometer was standardized using the following procedure:

(i) The potentiometer was disconnected from the measuring circuit.

(ii) The control switch was changed from the test to the standardize position.

(iii) The galvanometer was switched into the potentiometer circuit and the potentiometer was standardized against the standard Weston Cell by rotating the battery rheostats until a null point was achieved.

(iv) The galvanometer was then shorted out of the potentiometer circuit and steps (i) and (ii) reversed.

When the batteries were in good condition, this standardization was adequate for a 6h experimental period.

3. Pen Recorder

The recorder was calibrated at the commencement of each experiment. The zero on the recorder was adjusted to agree with the zero reading on the electrometer. The electrometer was then switched to the range required for the particular experiment and the recorder and electrometer zeros checked, the recorder full scale potential that would be required by the experiment was then applied, via the potentiometer, and the recorder calibrated to give this value.

(c) pH Electrode Calibration

The electrodes were calibrated against the response of a commercial pH electrode used in conjunction with a Radiometer pH Meter. This commercial pH measuring system was standardized using Beckman Buffers and then the Beckman pH electrode and the experimental pH electrode were supported, inside the Faraday cage, such that they were both immersed in the experimental solution.

A series of experimental solutions were employed to calibrate the experimental pH electrode over the pH range 5 to 10.5. The region pH 5.0 to pH 6.5 was measured using 1mM MES buffer, the pH value adjusted using 100mM NaOH; 1mM HEPES was used to buffer the region pH 6.5 to pH 8.0. The region pH 8.5 to pH 10.5 was buffered by 1mM Na_2CO_3, the pH value in this case was adjusted using 100mM H_2SO_4.

All measurements were made in stagnant (i.e. non-stirring) solutions and the simultaneous measurement of the experimental pH electrode response on the electrometer (recorder) and the value on the Radiometer pH Meter enabled the construction of a calibration

graph. A typical calibration graph is shown in Figure 2.4; it was from such a graph that experimental pH values were determined.

On a daily basis the stability of these electrodes, and hence the calibration, was checked using two experimental solutions whose pH values had been predetermined using the standardized Beckman pH electrode-Radiometer pH meter system. It was found that the maximum daily variation was small and random in sign, being of the order of 1mV. The maximum error in pH determinations was therefore approximately ± 0.015 pH units.

(d) Experimental System

The experimental measuring system is shown diagrammatically in Figure 2.5A and B. The thermostatting jacket and central experimental chamber were constructed of clear perspex so that the entire central chamber could be illuminated. The volume of the central chamber was approximately 300ml. Water, from a large thermostatted bath, was pumped through the outer water jacket using the pump as a Braun temperature control unit. In this way the temperature of the central experimental chamber was maintained at 25 ± 0.1^{o}C.

The *Chara corallina* cell under investigation was held in an agar block (see Figure 2.5). The procedure for preparing this agar block, inserting and orientating the *Chara* cell in the block, and positioning the block within the experimental chamber, was as follows:

(i) Bathing solution, containing 0.7% agar powder, was boiled until the agar dissolved and then the agar was poured into petri dishes containing special perspex cell-holders. (The internal measurements of these holders

were 1.4cm wide by 1.0cm high by 9.0cm long. The three supporting walls of these holders were perforated with holes (diameter 1.5mm), to reduce the resistance to diffusion of ions into and out of the agar block).

(ii) Once the agar gel had set, the blocks were cut from the setting-dish and transferred to glass vessels (250ml) which contained specific experimental bathing solutions. In these covered glass vessels, the agar blocks could be stored for 7-10 days without becoming contaminated by bacteria.

(iii) A stainless steel tube, of 1mm outer diameter, was used to make a centrally located hole in the agar block (see Figure 2.5B) into which the *Chara* cell could be inserted. (This technique has been described previously by Lucas (1971) and Lucas and Smith (1973)). While the stainless steel tube was located in the agar block, a suction pipette with a tip diameter of 1mm was used to cut a channel in the agar. This channel, which was cut vertically onto the stainless steel tube, commenced 3-5mm from one end of the agar block and the total length of the channel was determined by the length of the experimental cell, i.e. a 3-5mm lip was left at each end of the cell to hold it firmly along the bottom of the channel.

(iv) The cell to be investigated was then inserted into this chamber via the centrally located hole in the end of the agar block.

(v) The cell was checked to ensure that its streaming rate was normal and then the agar block , which contained the cell, was lowered into the central experimental

chamber which contained the thermostatted experimental solution. The agar block was wedged firmly into place by two pieces of clear perspex (see Figure 2.5B).

(vi) A micromanipulator (Leitz Wetzlar) was used to position the pH electrode directly above the nodal orientation cell (i.e. a whorl cell left attached to the internodal cell, see Figure 2.5A). Using the vertical adjustment control on the micromanipulator (vertical movement could be controlled ± 0.01mm), the electrode was lowered until the crown of the hemispherical pH-sensitive tip just made contact with the cell wall. The electrode was then traversed the small distance to the centre of the node, and the position of the node was then read on the micromanipulator scale. This value of the nodal location was used throughout the experiment to ensure that the cell had not been moved, or it was used for realigning the cell into a fixed position if the experiment required the transfer of the cell to another agar block.

(vii) The electrode was then raised and traversed so that the pH-sensitive tip entered the channel region, the electrode was again lowered until its tip just touched the cell wall. Within this channel, the pH electrode could be traversed along the complete cell wall, except for the 3mm sections at each node.

(viii) An equilibration period of 30 minutes was employed before commencing an experimental sequence. This was to allow full recovery of the cell from the transfer process and to permit the re-establishment of thermal equilibrium.

(ix) When the experimental solution required the presence of a specific concentration of HCO_3^-, procedure (i) above was replaced by the following procedure. The bathing solution, containing the 0.7% agar, was boiled until the agar powder dissolved. The solution was then transferred to a measuring cylinder and hot distilled water added to replace that lost during the boiling process. A water bath was then used to cool the solution to 40°C.

While the hot agar was cooling, a stock solution of Na_2CO_3 (20mM) was prepared and when the agar solution had cooled to 40°C, the Na_2CO_3 stock solution was used to prepare an agar solution with the required HCO_3^- concentration. The pH value, specified by the experiment, was obtained by titrating the warm agar (Na_2CO_3) solution with 100mM H_2SO_4. The setting of the agar blocks was identical to (i), except that sealed petri dishes were used. The bathing solution required for the experimental chamber was also prepared from this Na_2CO_3 stock solution and its pH value was adjusted to the same value as the agar block. Using this procedure the bathing solution and the agar block pH values agreed to within 0.01 pH units.

In all experiments in which HCO_3^- was involved, a liquid paraffin seal (10mm thick) was poured over the surface of the bathing solution to isolate the experimental chamber from atmospheric CO_2. In this way the pH value of the bathing solution and the background value of the agar block remained constant for the duration of the experiment.

(e) Light Systems Employed for Experiments Conducted in the Faraday Cage

(1) Two twin-batten fluorescent fittings (L4530 H) were mounted on opposite walls of the Faraday cage and these held a total of four, twenty watt Osram MCFE Daylight, D65, tubes. This light system gave a light intensity of 13-15 Wm^{-2}, at the centre of the experimental chamber, when measured through a 0.7mm thickness of agar.

(2) The fluorescent light source, detailed above, was used for many preliminary experiments in which an invariable light source was suitable, but when experiments required a range of light intensities, the Rank-Aldis light system detailed in Section III, was employed. Because of the higher infra-red component of the Quartz-Iodide lamp, an additional water jacket was placed between the projected and the permanent water jacket to increase the total water path to 10cm. To prevent the entry of stray light during these experiments, the Faraday cage was covered by heavy duty velvet.

VII *Chara* Cell-Segment Isolating Apparatus

In some experiments a cell segment, containing an operational hydroxyl band, was isolated from the rest of the cell which was in contact with the bulk bathing solution. This isolation was achieved using the apparatus shown in Figure 2.6. It consisted of two clear perspex blocks, of which one was a large basal block and the other a smaller movable block which contained the isolating chamber. The basal block had a channel 1.1cm wide and 1.0cm deep cut into its upper surface (see Figure 2.6A and C) and centrally located in the base of this channel there was a second, much smaller channel. This small channel, which was 1.5mm wide and 1.0mm deep was just large enough to hold a *Chara* cell (see Figure 2.6 B and C). Two removable perspex

plates were used to seal the open ends of the channel in the basal block.

The bottom section of the smaller, movable block, was machined so that it seated, with precision, into the channel of the basal block (see Figure 2.6C). A cylindrical chamber, with an end diameter of 6.0mm, was cut through this block such that it was located over the smaller channel of the basal block. Two stainless steel tubes were set into this smaller block, one was used as an inlet for experimental solutions and this tube entered the isolating chamber close to its base. The second tube was used as an outlet and was located 4mm below the top of the isolating chamber.

Experimental solutions were injected into the isolating chamber using an adjustable volume Manostat Mini-Pet Syringe system. The expelled solutions were drawn off using a vacuum pump connected to the outlet tube. Screw clips were located on the inlet and outlet tubes to seal the system, thereby preventing the movement of solution during an experimental sequence.

The experimental procedure, exployed during the use of this isolating chamber, was as follows:

(i) A *Chara* cell was investigated using the agar block technique described in Section VI(d), and from this the exact location of each OH^- band was determined. A map of the cell length, showing the location of these bands, was drawn on a narrow piece of graph paper.

(ii) The *Chara* cell was removed from the agar block and the cell wall, in the region surrounding the hydroxyl band that was to be isolated, was dried using "Kleenex" tissues. A small quantity of silicon grease (Dow Corning, high vacuum grease) was injected into the small channel, at a distance of 5mm on

either side of the OH^- band centre. The cell was then placed into this small channel such that the selected hydroxyl band was located centrally between the two greased regions.

(iii) The entire lower surface of the small movable block was covered with a uniform layer of silicon grease prior to the performance of (ii). This enabled the small block to be quickly sealed into place over the top of the hydroxyl band. (The silicon grease completely sealed the sections of the cell wall that were beneath the lower surface of the block, but the section of cell wall which was directly beneath the isolating chamber remained free of grease). The unit was then transferred to the central experimental chamber (see Section VI(d) and Figure 2.5A and B) where it was wedged into place using small perspex blocks.

(iv) The level of the bathing solution, in the central experimental chamber, was adjusted so that it was just below the outlet tube. The same experimental solution was quickly injected into the isolating chamber, filling it completely. This gave a head of solution (approximately 6mm) which was used to ensure that the silicon grease gave a water-tight seal.

(v) Using a micromanipulator (see Section VI(d),(vi), the experimental pH electrode was lowered into the isolating chamber until the hemispherical pH sensitive tip was located approximately 3-4mm directly above the cell wall. At this point an agar bridge, was lowered into the isolating chamber (see Figure 2.6B). (This agar bridge was necessary to complete the electrical circuit between the solution in the isolating chamber and the calomel electrode in the outer solution).

The system was allowed 30 minutes, in the light, to equilibrate and for the cell to recover from the isolating process.

(vi) At the end of this recovery period, the pH electrode was very carefully lowered until it just touched the cell wall; the hydroxyl band-centre was then located. The system was then ready for experimentation. The results obtained using this apparatus will be detailed in Chapter 7.

It should be mentioned that all surfaces of these perspex blocks were highly polished so that, when the apparatus was immersed in the central experimental chamber, very little light was prevented from reaching the cell surface.

TABLE 2.1. *Chara corallina* culture tank conditions

Tank	Illumination	Average Chlorophyll conc. ($\mu g\ Chl.cm^{-2}$)	Ionic Composition (mM)					pH*
			Na^+	K^+	Ca^{++}	Cl^-	HCO_3^-	
Delta	Full sunlight	5.2 ± 0.3	--	--	--	--	2.05	9.3-9.5
Delta	Diffuse sunlight	8.9 ± 0.5	2.2	0.17	0.26	1.2	2.13	9.3-9.5
E'	Artificial+	9.1 ± 0.6	1.0	0.22	0.64	0.7	1.56	9.4
A	Artificial	11.2 ± 0.6	1.7	0.25	0.92	1.9	3.63	8.5
XG-1	Artificial	10.93± 0.8	2.5	0.25	0.7	1.0	3.02	9.4
XG-2	Artificial	14.0 ± 1.0	2.2	0.2	0.56	1.0	3.54	8.6
Mannum Cells	Full sunlight	5.0 ± 0.5	2.5	0.22	0.50	--	2.16	7.4

\+ Artificial light was provided by Osram MCFE Daylight Fluorescent tubes, giving an intensity, at the solution surface, of 15-17Wm^{-2}.

* pH values were measured after 6h illumination.

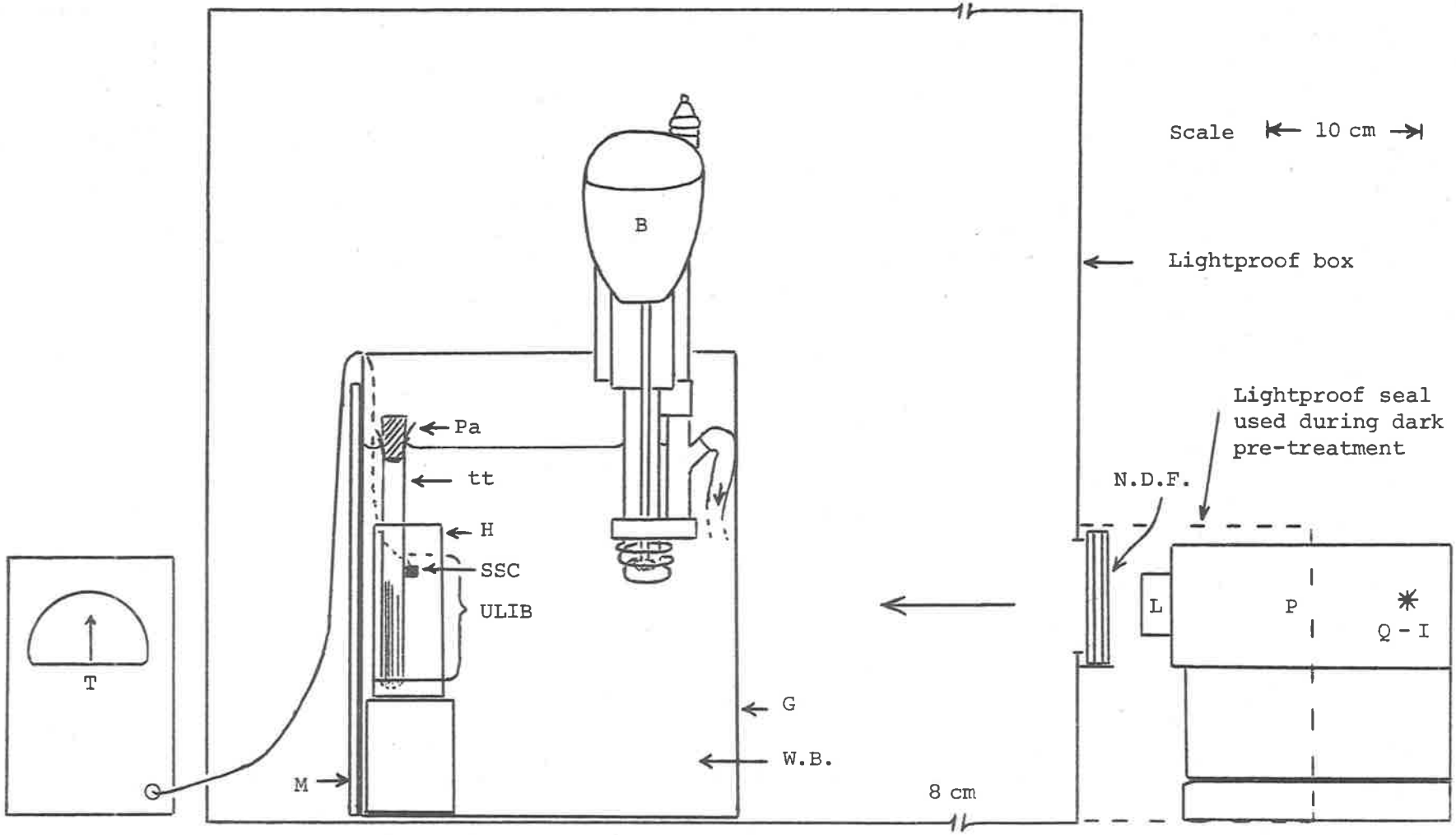

Figure 2.1. Apparatus used for ^{14}Carbon Experiments. Abbreviations are as follows: Braun temperature control Unit, B; Glass walls, G; Holder, H; Lens system, L; Mirrored surface, M; Neutral Density filters, N.D.F; Projector, P; Parafilm "M" seal, Pa; Quartz-Iodide lamp, Q-I; Silicon solar cell, SSC; Transducer, T; Experimental test tube, tt; Uniform light intensity band, ULIB; water bath, W.B.

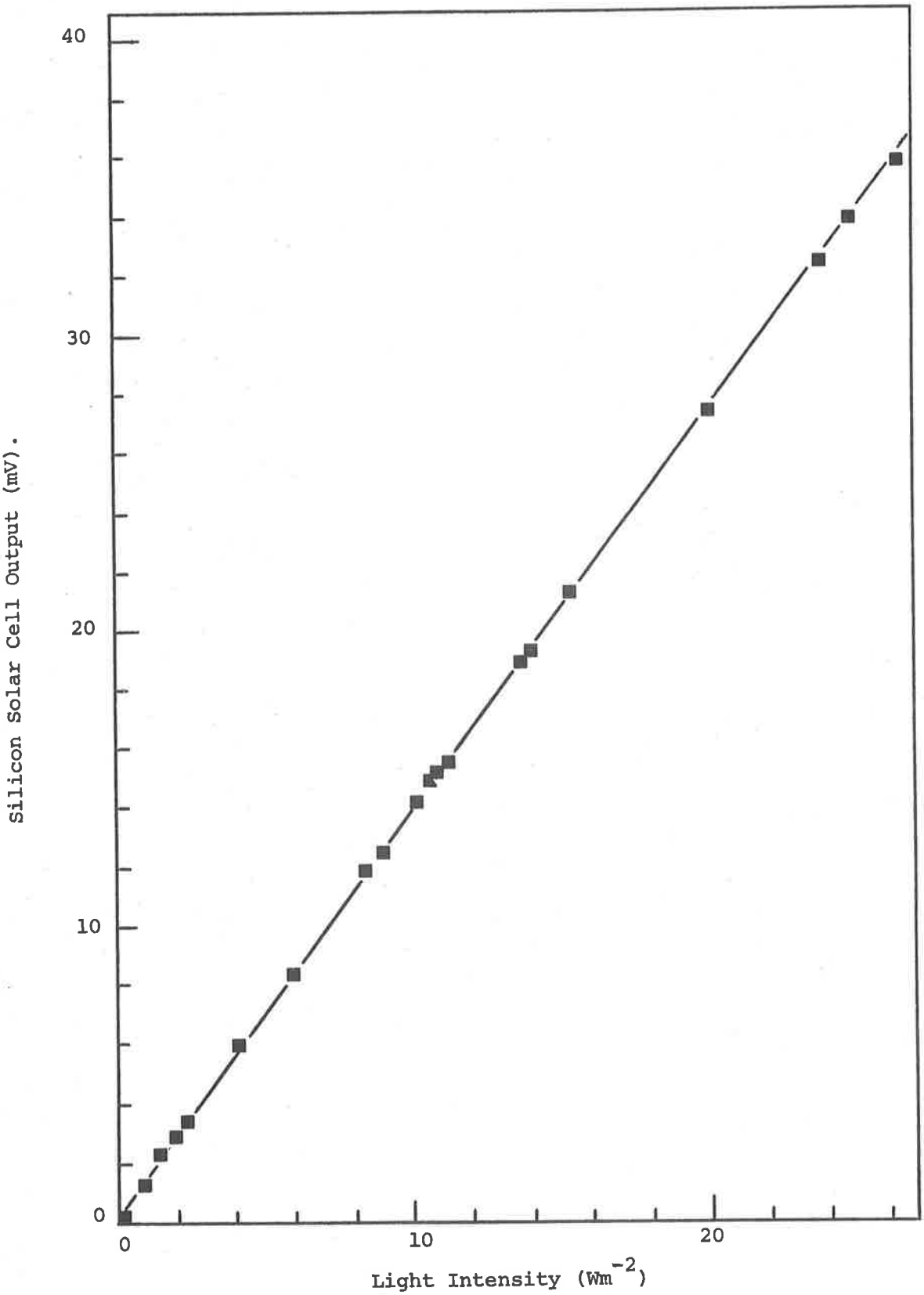

Figure 2.2. Calibration graph of a silicon Solar Cell against the energy output of a Quartz-Iodide lamp.

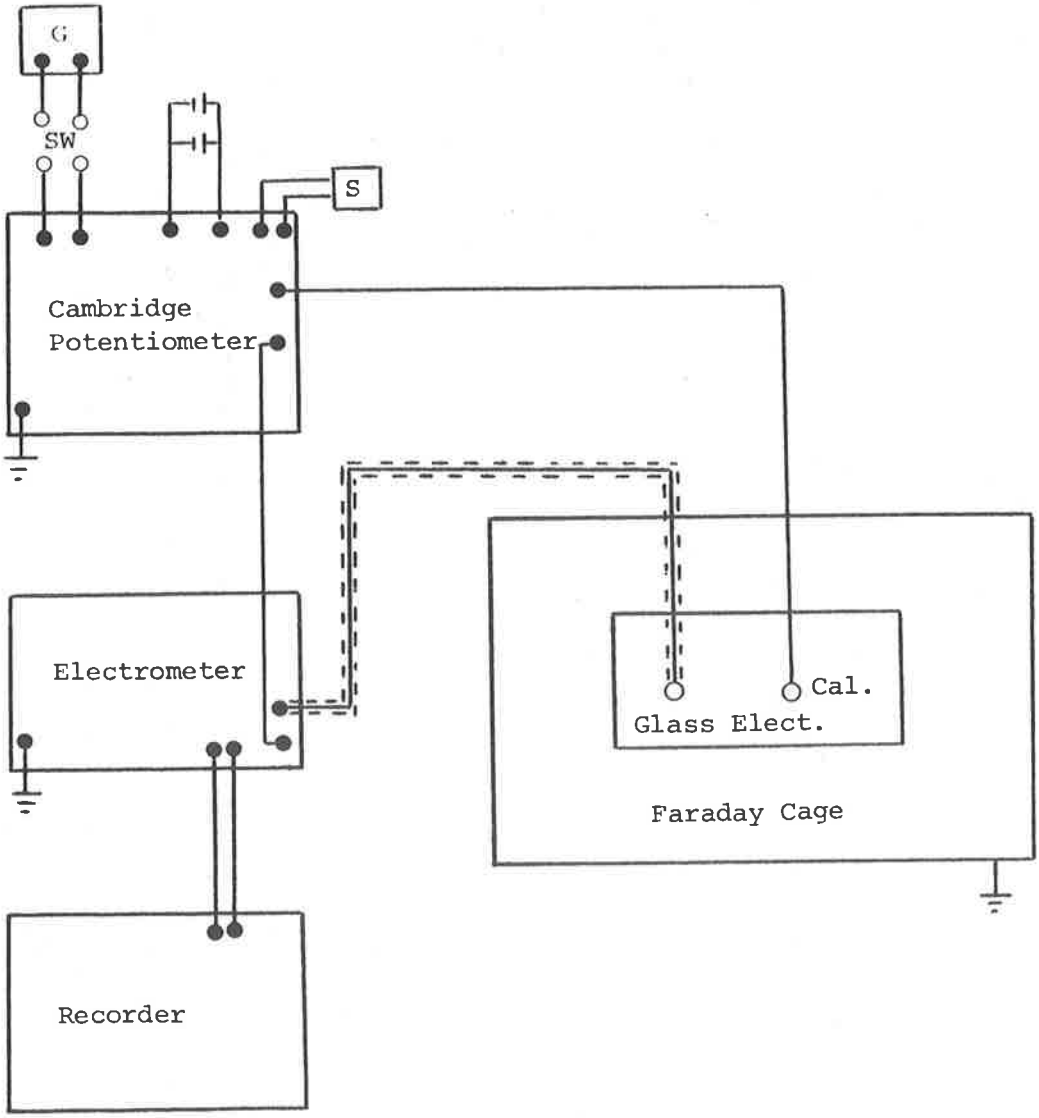

Figure 2.3. Block diagram of the electrical circuit employed to measure pH with the small pH electrodes. The abbreviations used are as follows: Cal., Radiometer calomel reference electrode; G, Cambridge spot galvanometer; S, Standard Weston Cell; S.W., Shorting switch. The electrometer was an E.I.L. Electrometer, Vibron Model 33B, the potentiometer was a Cambridge Vernier Potentiometer and the recorder was a Rikadenki potentiometric recorder, Model TO2N1-H.

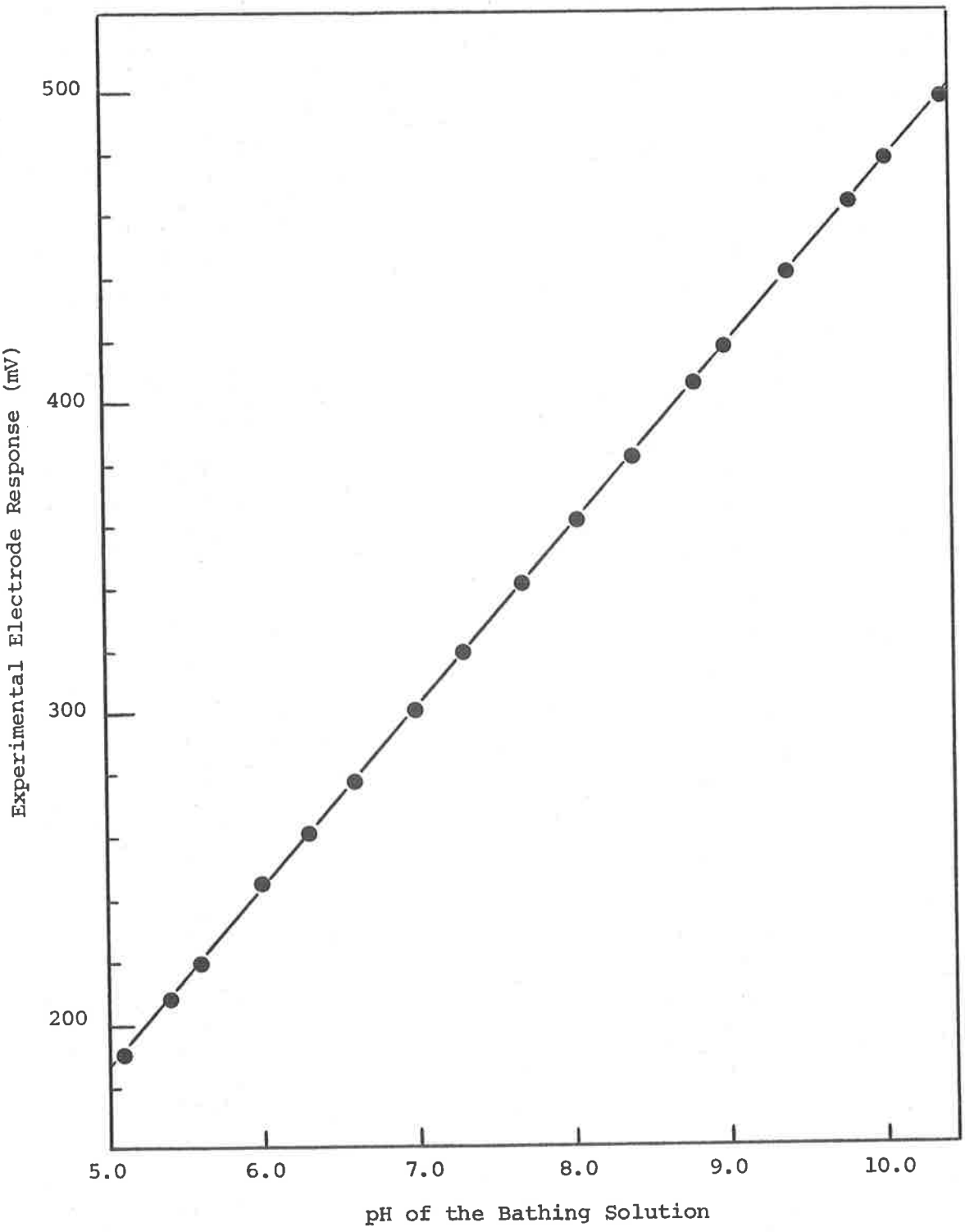

Figure 2.4. pH Calibration Graph of one of the small experimental pH electrodes prepared in this laboratory. The Nernst response of this particular electrode was 57.5mV per pH unit (25°C).

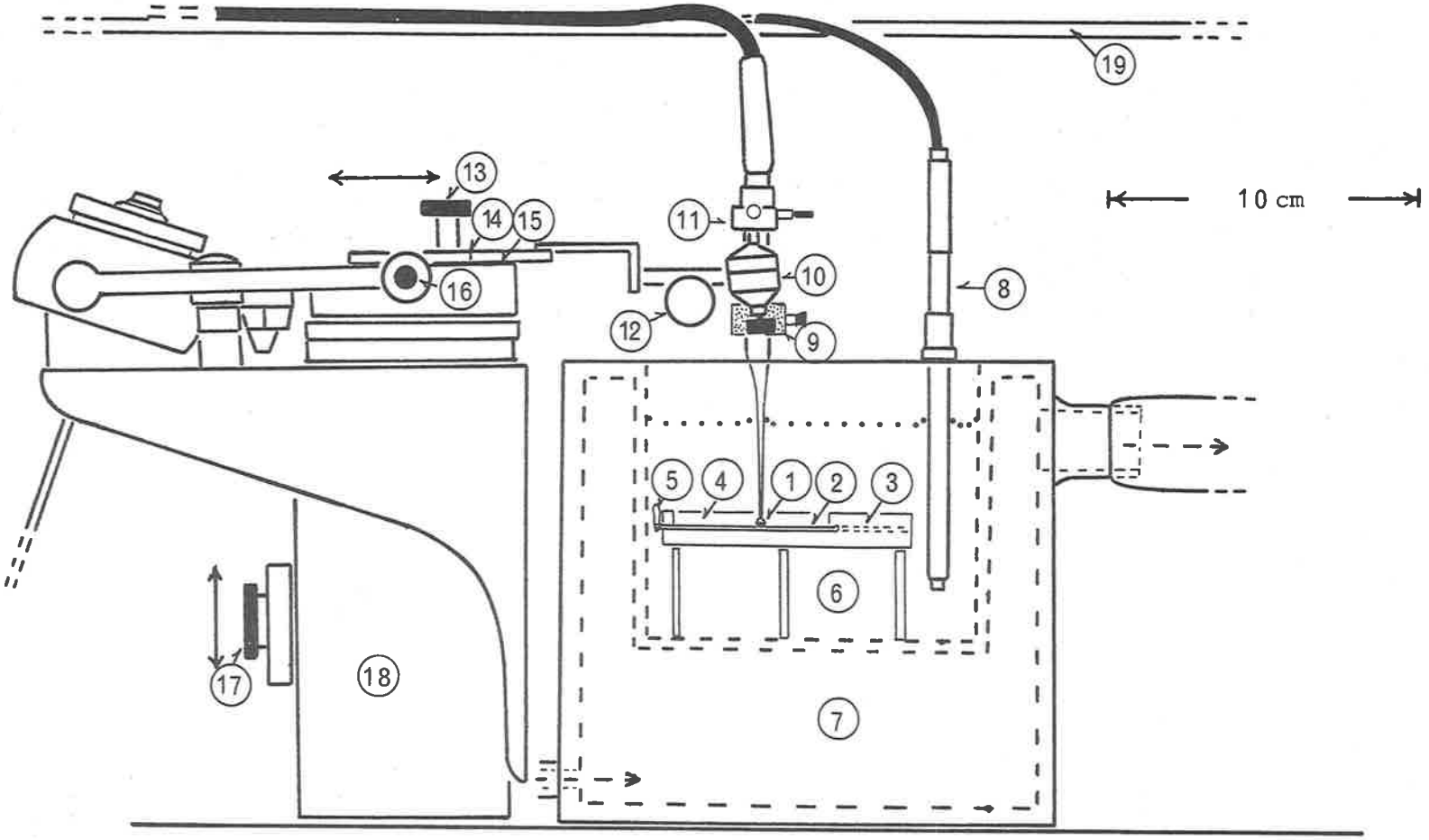

Figure 2.5A. Scale drawing of the pH electrode system used to measure pH changes of the cell surface of *Chara* cells: side view.

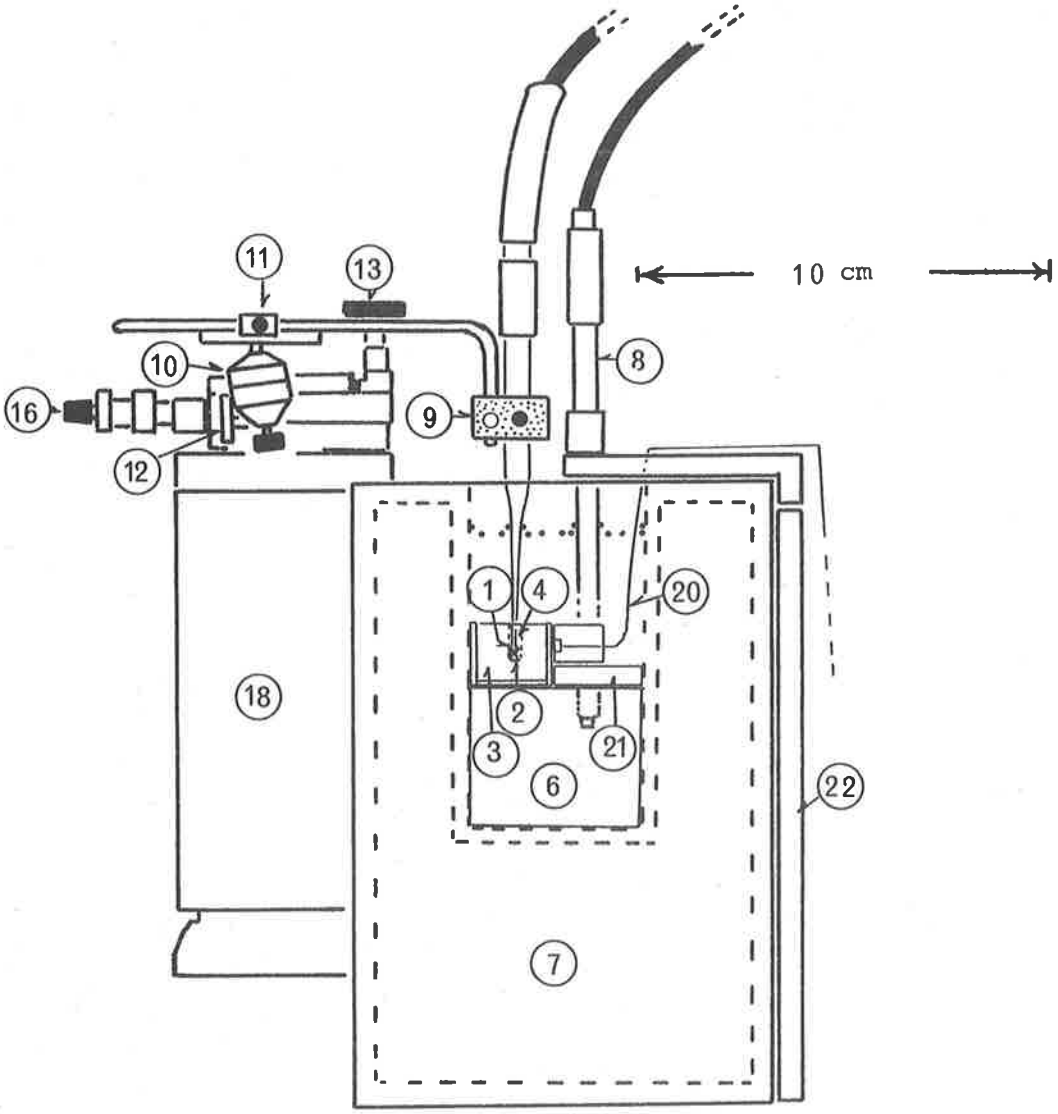

Figure 2.5B. Scale drawing of the pH electrode system used to measure pH changes at the cell surface of *Chara* cells: End view.
Key to Figure 2.5A and B: 1, Hemispherically tipped pH electrode; 2, Experimental *Chara* cell; 3, Agar block; 4, Channel within the agar block; 5, Whorl cell which acts as a nodal orientation cell; 6, Central experimental chamber; 7, thermostatting jacket; 8, Calomel reference electrode; 9, pH electrode mounting; 10, balljoint adjustment; 11, micromanipulator attachment; 12, clamping screw for electrode alignment; 13, Drive for the horizontal movement of the pH electrode; 14, Reference marker used in conjunction with 15; 15, micromanipulator scale; 16, Drive for the lateral (horizontal) movement of the electrode; 17, Drive for the vertical movement; 18, Micromanipulator base; 19, Supporting rod for pH and calomel cables; 20, Electrical leads from the silicon solar cell; 21, One of the clear perspex blocks used to wedge the agar block firmly into place; 22, mirrored surface.

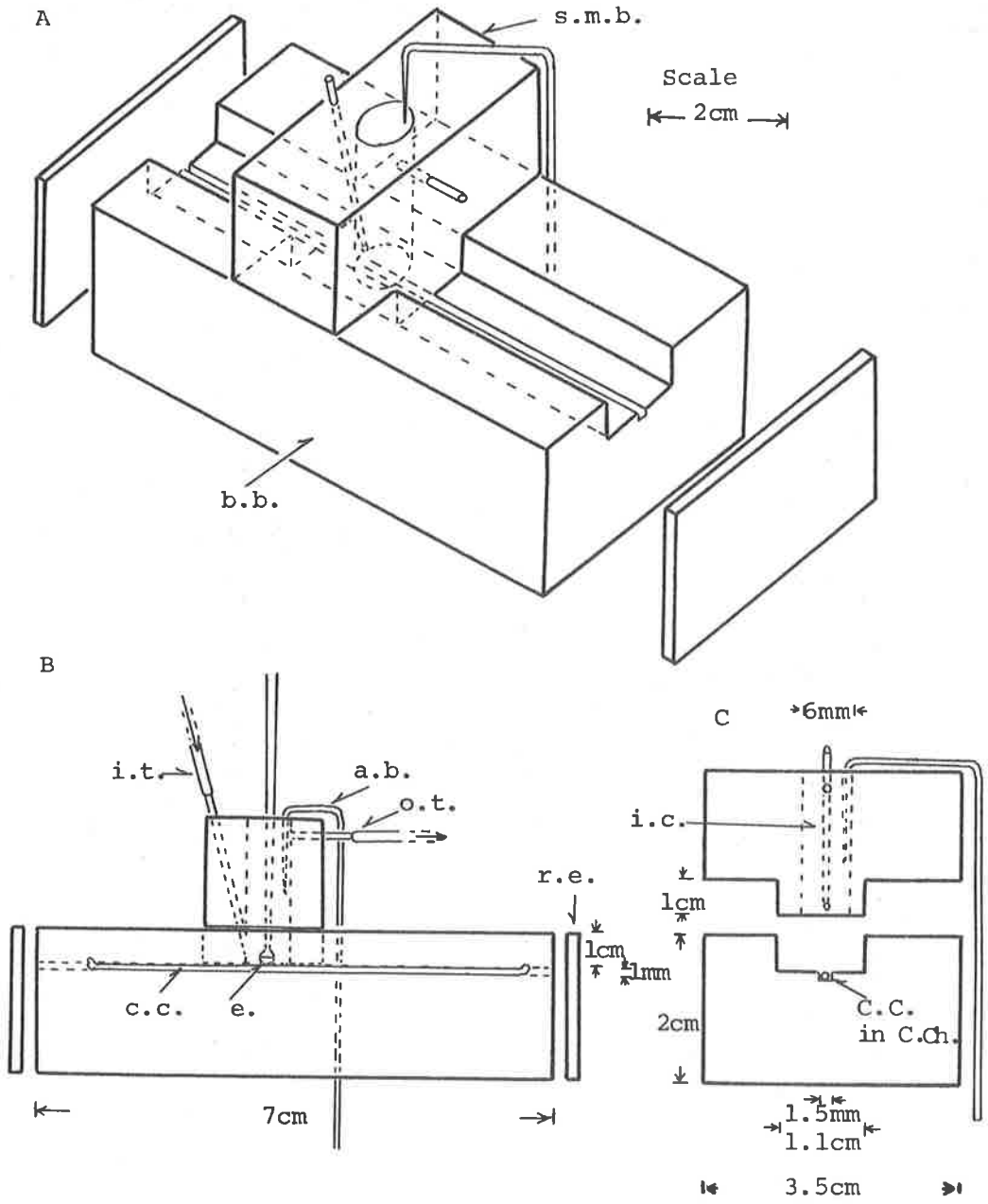

Figure 2.6. Apparatus for isolating *Chara* cell-segments. This apparatus was used to isolate, from the rest of the bathing solution, an external segment of cell which contained an operational hydroxyl band. Abbreviations are as follows: agar bridge, a.b.; basal block, b.b.; *Chara* cell, C.C.; *Chara* cell located in the central channel, C.C. in C.Ch.; pH electrode, e.; isolating chamber, i.c.; inlet tube, i.t.; outlet tube, o.t.; removable end, r.e.; small movable block, s.m.b.

CHAPTER THREE

PHOTOSYNTHETIC PROPERTIES OF *CHARA CORALLINA*: MEASUREMENTS OF ^{14}CARBON ASSIMILATION.

Introduction

Physiological studies have shown that many of the active ionic fluxes of *C. corallina* are light stimulated and that the energy supply for these fluxes is provided, at least in part, by the photosynthetic light reactions. It is possible, therefore, that specific experimental conditions exist, under which competition for ATP and / or reducing power occurs between these fluxes and the fixation reactions of photosynthesis (see for example the proposals of Spanswick, 1974). A situation of this nature may occur when an experiment is conducted under low light intensity and high total carbon concentration.

Experimental data on the photosynthetic capacity of *C. corallina* is limited. Smith (1968a) demonstrated that several Characeae (including *C. corallina*) could fix $^{14}CO_2$ at rates of approximately 30-40 pmol $cm^{-2}s^{-1}$ and $H^{14}CO_3$ at rates of 1-9 pmol $cm^{-2}s^{-1}$. However, he assumed that the saturating conditions of 1.0mM total carbon (pH 6.5) and 13Wm^{-2} light intensity, found for *Nitella translucens* (Smith, 1967a), could be applied to this species. Smith (1968a) also showed that *C. corallina* could assimilate HCO_3^- but his data, relating to the actual rates under conditions of exogenous HCO_3^-, were limited.

Robinson (1969), using the same conditions detailed by Smith, obtained a fixation rate of 50 pmol $cm^{-2}s^{-1}$. Smith and West (1969) reported that using a bathing solution buffered at pH 7.1-7.2 and containing 0.5mM total carbon, they obtained fixation rates of 25-35 pmol $cm^{-2}s^{-1}$. The highest rate for this species appeared to be the value of 55 pmol $cm^{-2}s^{-1}$ reported by Smith (1970) (1.0mM

$NaHCO_3$, pH 7.1, light intensity unspecified). Assimilation when exogenous $H^{14}CO_3^-$ was the dominant species was not investigated in any of this work, except for the original work of Smith (1968a). It is surprising that HCO_3^- has received so little attention since, as pointed out by MacRobbie (1970), the HCO_3^- transport system seems to be particularly active. It appears capable of influx rates which are much greater than the other anionic transport systems present in this species.

Results

Time-course Experiments

The initial experiments in this series were performed to determine whether uptake of ^{14}C, supplied as exogenous $^{14}CO_2$ or $H^{14}CO_3^-$, was linear with time. The procedure employed during these experiments deviated from the general sequence given in Chapter Two Section III, in that step (v) was omitted, i.e. at the conclusion of the 1h dark pretreatment, the cells were transferred immediately into radioactive solutions.

The results obtained indicated that uptake of ^{14}C was linear with time when either $^{14}CO_2$ or $H^{14}CO_3^-$ was present as the exogenous source of carbon. Typical results are presented in Figure 3.1. From this figure it can be seen that, under experimental conditions of 2mM total carbon and light intensities of $12Wm^{-2}$ ($^{14}CO_2$) or 2 and $3Wm^{-2}$ ($H^{14}CO_3^-$), there was not a long lag period associated with photosynthetic induction (Osterhout and Haas, 1918; and Walker, 1973). On the basis of these results, it was assumed that a 30 minute light pre-treatment period followed by a 1h exposure to radioactive solutions would be suitable for all photosynthetic fixation experiments.

Concentration and Light Intensity Results Obtained Using Exogenous $^{14}CO_2$

During exogenous $^{14}CO_2$ experiments the normal bathing solution was buffered at pH 5.3 with 5mM MES buffer. At this pH value 92% of the total carbon existed as $^{14}CO_2$ and it was assumed that no $H^{14}CO_3^-$ influx occurred at this low pH value. Measured $^{14}CO_2$ fixation rates, in response to various levels of exogenous $^{14}CO_2$, are presented in Figure 3.2. These results were obtained using cells cultured in tank XG-2 and a light intensity of $25Wm^{-2}$ was employed throughout. The substrate ($^{14}CO_2$) values were calculated according to Buch (1960, equation 10 and tabulated constants). The fixation rates of tank delta (full sunlight cells) and the River Murray (Mannum) cells, obtained in the presence of 1.8mM exogenous $^{14}CO_2$, are included for comparison.

The influence of light intensity on $^{14}CO_2$ fixation, in the presence of saturating CO_2, was observed for three different cell cultures. The results from these studies are presented in Figure 3.3. Dark fixation rates were also measured during these experiments, and rates of approximately 0.50 ± 0.1 pmol $cm^{-2}s^{-1}$ for both tanks delta and XG-2 were found to be low and insignificant when compared with fixation values obtained under low light intensities of $1\text{-}2Wm^{-2}$. For this reason the values presented in Figure 3.3 were not corrected for dark fixation.

$H^{14}CO_3^-$ Influx: The Effect of "Artificial" Buffers*

Preliminary experiments were conducted to ensure that the use of "artificial" buffers did not interfere with the transport of HCO_3^- across the plasmalemma. It was found that at a solution pH value of 9.0 - 9.2, the buffers Tris, Tricine and borate all significantly reduce the influx of $H^{14}CO_3^-$. Only TES appeared to act as an inert buffer, however its buffer range did not extend to pH 9.0 and so it was used at pH 8.3. The results of these experiments are shown in Table 3.1. The control results indicated that in the pH range 9.0 - 9.2, sufficient HCO_3/CO_3^{2-} buffering capacity was present to reduce changes in the pH value of the bathing solution to an acceptable level. Because of the influence of the "artificial" buffers tested, it was decided to conduct $H^{14}CO_3^-$ experiments at an initial pH value of 9.0 and to omit "artificial" buffers from the solutions. (For a sealed experimental system, the amount of CO_2 which existed at this initial pH of 9.0 was so low that it was considered to be insignificant, but see Appendix C).

$H^{14}CO_3^-$ Influx: The Influence of Exogenous $H^{14}CO_3^-$ Concentration and Light Intensity

The relationship between $H^{14}CO_3^-$ influx and exogenous $H^{14}CO_3^-$ concentration is indicated in Figure 3.4. As in Figure 3.2, a light intensity of $25 Wm^{-2}$ was used throughout, and the $H^{14}CO_3^-$ substrate concentrations were calculated according to Buch (1960,

---

* In Chapter Four it will be shown that excellent correlation was obtained between $H^{14}CO_3^-$ uptake and OH^- efflux, hence the loss of ^{14}C from the $H^{14}CO_3^-$ influx via gaseous $^{14}CO_2$ escape was minimal. On this basis, ^{14}C fixation values obtained at pH values ≥ 9.2 will be assumed equivalent to $H^{14}CO_3^-$ influx.

equation 9, and Tabulated constants). In this figure, the curve marked A was obtained using cells from tank delta which were cultured under full sunlight, while curves B and C were obtained with cells from the same tank cultured under diffuse sunlight. (See Table 2.1 for the variation in chlorophyll concentration which results under these two light regimes).

The removal of precipitated $Ca^{14}CO_3$ and unfixed $^{14}CO_2$, using the propionic acid treatment, is represented by the difference between curve B and C, i.e. curve C represents the true $H^{14}CO_3^-$ influx value. The results expressed in curve A represent values corrected for $Ca^{14}CO_3$ and unfixed $^{14}CO_2$.

The influence of light intensity on $H^{14}CO_3^-$ influx is expressed, for cells cultured in tank delta under diffuse sunlight, in Figure 3.5. The bathing solution contained 3mM total carbon throughout these experiments and the pH value was maintained within the limits of pH 9.0 - 9.2. The dark fixation rate was also determined under these conditions and the observed value of 0.81 ± 0.03 pmol $cm^{-2}s^{-1}$ has been subtracted from the values plotted on Figure 3.5.

The Relationship Between $^{14}CO_2$ Supplied by Diffusion and Transported $H^{14}CO_3^-$

There is very little known about the relationship between the supply of $^{14}CO_2$ by diffusion and the activity of the HCO_3^- transport system of *Chara corallina*. Raven reported that the ^{14}C assimilation of *H. africanum* appeared to show "differential effects" at pH values of 6.0 and 10.0. He suggested that these "differential effects" could still be distinguished between solutions with pH values of 7.3 and 10.2 (Raven, 1968, p. 195 and Figure 2). On the basis of these results, Raven suggested that in this species

"photosynthesis has the characteristics of CO_2 use at the two lower pH's (i.e. pH 6.0 and 7.3) and that of HCO_3^- use at pH 10.2." He went on to conclude that, "it would appear that the characteristics of the system are determined by CO_2 at any pH below 7.3, where CO_2 comprises more than 10% of the total carbon supply".

It is not clear just exactly what Raven is proposing. For example, is he saying that below pH 7.3 only CO_2 is involved in photosynthetic carbon assimilation, or is he proposing that below this pH value of 7.3, CO_2 predominates as the source of inorganic carbon for photosynthesis?

His results do not help to clarify this situation. Admittedly Figure 2 (Raven, 1968) shows that fixation in the presence of predominantly exogenous $^{14}CO_2$ was higher when compared with the exogenous $H^{14}CO_3^-/CO_3^{2-}$ condition. However, lowering the temperature from 15° to 5°C reduced the ^{14}C assimilation under the exogenous $^{14}CO_2$ and $H^{14}CO_3^-$ conditions by 56 and 59 per cent respectively. This result could not be termed a "differential effect". The same is true for the high and low light intensity results, in the same order given above, the percent reduction was 81 and 87 respectively. The results of Figure 2B, in which the influence of temperature and HCO_3^- concentration on $H^{14}CO_3$ assimilation was investigated under low light intensity, are of limited use in determining the properties of the HCO_3^- system. This is because under these conditions ^{14}C assimilation was light limited, hence an increase in HCO_3^- concentration from 1 to 4mM would be expected to yield a negative response. Raven should have conducted these experiments in the 0 to 0.25mM HCO_3^- concentration range, if he wanted to distinguish between a diffusion or photochemical limiting process.

Unfortunately Raven did not include the "differential effects" that he obtained between pH values of 7.3 and 10.2. No comment can therefore be made regarding these results, but it is obvious from Raven's Figure 1A that at pH 7.3 the ^{14}C fixation rate was higher when compared with the same level of CO_2 at pH 5.7. This indicates that at pH 7.3 $H^{14}CO_3^-$ was in fact contributing ^{14}C for photosynthetic assimilation.

If it is assumed that Raven was suggesting that the HCO_3^- contribution to ^{14}C assimilation was insignificant below pH 7.3, the proposal acquires a degree of importance. This is because the transport of HCO_3^- has been implicated as a contributing factor in the determination of the electrical properties of the plasmalemma (Walker, 1962; Hope, 1965; Volkov and Misyuk, 1969; Volkov and Petrushenko, 1969; Saito and Senda, 1973a; Volkov, 1973). On the basis of Raven's proposal, the electrical contribution of HCO_3^- would be minimal or entirely absent when cells were bathed in solutions having pH values below 7.3.

To investigate this relationship, it was decided to conduct experiments over the pH range 4.8 to 10.8, using a concentration of total carbon which would saturate fixation over this range. The results of Figures 3.2 and 3.4 indicated that 3mM total carbon would be suitable and hence this concentration, in conjunction with a saturating light intensity of $25 Wm^{-2}$, was used throughout this series of experiments. The results obtained, using cells from three different cultures, are presented in Figure 3.6. In these experiments the pH region 4.8 to 6.2 was buffered using 5mM MES, the region pH 7.0 to 8.6 by 5mM TES and the region pH 9.0 to 10.8 by the 3mM HCO_3^- / CO_3^{2-} buffer which also acted as the substrate for fixation.

Discussion

Apparent K_m and Theoretical V_{max} Values for $^{14}CO_2$ Fixation

In this study the apparent K_m is used in the operational sense of the substrate concentration (either $^{14}CO_2$ or $H^{14}CO_3^-$) required to give half maximal velocity. $^{14}CO_2$ fixation at pH 5.3 gave an apparent K_m of 0.71mM ± 0.20 and a V_{max} of 159.5 ± 17.6 (pmol $cm^{-2}s^{-1}$). The values when $H^{14}CO_3^-$ was the exogenous carbon species (pH 9.0 - 9.2) were K_m, 0.59mM ± 0.16 and V_{max}, 71.2 ± 6.2 (pmol $cm^{-2}s^{-1}$) for the 8.9µg chl.cm^{-2} cells from tank delta, and a K_m, 0.58mM ± 0.19 and V_{max}, 46.9 ± 4.6 (pmol $cm^{-2}s^{-1}$) for the 5.2µg chl.cm^{-2} cells from tank delta. These kinetic values were obtained using the computer programme developed by Cleland (1963). The computed V_{max} values are larger than the experimentally determined maximum values of 114.0 ± 5.1 - 130 ± 6.3 pmol $cm^{-2}s^{-1}$ ($^{14}CO_2$, pH 5.3) or 59.6 ± 2.9 and 40.5 ± 1.7 pmol $cm^{-2}s^{-1}$ ($H^{14}CO_3^-$, pH 9.0) for the 8.9 and 5.2µg Chl. cm^{-2} cells respectively. However, the rates are higher than those previously reported for $^{14}CO_2$ or $H^{14}CO_3^-$, the latter demonstrating that *C. corallina* cells are capable of large anionic fluxes when alkaline solutions containing HCO_3^- are employed.

A theoretical consideration of the maximum rate at which HCO_3^- can be converted to CO_2 is presented in Appendix C. The values obtained indicate that at pH 9.0 and in the presence of 1mM total carbon, the maximized rate of supply of CO_2 cannot account for the observed rate of ^{14}C fixation. Under the experimental conditions employed, the free CO_2 contribution would be small; the discrepancy between the calculated CO_2 and experimentally observed rates demonstrates beyond doubt that cells of this species can assimilate HCO_3^-.

Seasonal Variation in Cell Capacity

The discrepancy between the high ^{14}C fixation values reported in this work and those of Smith (1968a), cannot be due to differences in chlorophyll concentrations. This is because the value of 11µg Chl.cm^{-2} quoted by Smith (1968a, Table 1) is in very close accord with the actual chlorophyll concentrations present in the cells used during this work (see Table 2.1). No conclusions can be drawn regarding the influence of chlorophyll concentrations on the values reported by Robinson (1969), Smith and West (1969) or Smith (1970), since chlorophyll concentrations were not specified in any of these reports.

All the ^{14}C experiments reported thus far were conducted during the summer growing season, during which time optimal growth rates ensured that uniform mature cells were obtained. However, Smith (1968a) conducted his ^{14}C experiments during the northern hemisphere winter months (F.A. Smith, personal communication). If there was a seasonal difference in the cellular capacity to fix ^{14}C, it would account for part of the discrepancy in results. To test this possibility, a series of experiments was performed during the mid-winter period.

Experimental cells were cut from a culture which had been allowed to mature from autumn to mid-winter. The culture conditions of this tank, on the day the cells were harvested, are detailed in Table 3.2. A bulk harvest of the cells was necessary because the branches had become intertwined, forming a dense mass of cells from which it was extremely difficult to separate and cut cells suitable for experimentation. The bulk harvest involved cutting the dense mass of cells at a depth of approximately half the height

of the mature culture. The top section was then transferred to a large container of tap water, and in this container the individual branches were sorted and cells suitable for experimentation were harvested. These cells were stored in glass dishes which contained normal bathing solution to which 3.0mM $NaHCO_3$ had been added and the pH value adjusted to 8.6. Cells were stored in these containers for up to 9 days*, with the solution being prepared and changed twice daily. Illumination was provided by fluorescent lighting at an intensity of $8.3 Wm^{-2}$ at the solution surface and a 12h light : 12h dark regime was employed.

The results of this series of winter experiments is presented in Table 3.3. The exogenous $^{14}CO_2$ results indicated that the photosynthetic fixation and cytoplasmic streaming rates were lower on the day that the cells were cut. By the following day the cytoplasmic streaming rate had returned to the normal value observed in these cells (50-70µm s^{-1}), and the measured $^{14}CO_2$ fixation rate had also recovered to a value equivalent to the rates observed during the summer months. Hence seasonal differences in tissue cannot explain the discrepancy in $^{14}CO_2$ fixation rates.

Cells treated in exogenous $H^{14}CO_3^-$ did not follow this simple pattern of recovery. Of the three experiments conducted on the day that the cells were cut, the average cytoplasmic streaming rate of the cells cut using the bulk harvest technique (rough handling) was much lower than the normal value obtained for the cells which were cut directly from the culture tank. (It was assumed that this reflected slight cellular injury inflicted during the bulk harvesting procedure). The interesting point to note is

---

* During this period the cells were thermostatted at 20°C.

that the lower cytoplasmic streaming rate did not correlate with a lower value of $H^{14}CO_3^-$ influx; all three treatments gave approximately the same rate. The change in $H^{14}CO_3^-$ influx with post-harvest age is noteworthy. On the first and second days after the harvest, the rate dropped to almost half the value observed on the day that the cells were harvested. From the fourth post-harvest day the influx increased, until by the ninth day it had recovered to a value which was equivalent to the results obtained during the summer months.

The exogenous $^{14}CO_2$ fixation results indicate that the cause of this slow $H^{14}CO_3^-$ influx response is not directly related to a limit on fixation, imposed by the chloroplasts. It is more likely that the limit on $H^{14}CO_3^-$ influx is imposed at the plasmalemma, in that the mature winter cells may have fewer operational HCO_3^- carriers. Hence, part of the discrepancy in $H^{14}CO_3^-$ influx results may be due to seasonal variation in tissue. The difference in $^{14}CO_2$ results is probably due to the employment of a light system which did not illuminate the entire surface of the cell with a saturating light intensity.

These results are important in two respects. Firstly, they demonstrate that there may exist seasonal variation within the influx capacity of the $H^{14}CO_3^-$ transport system. Secondly, they show that the post-harvest age of the cell may be extremely important in terms of the capacity of the $H^{14}CO_3^-$ transport system. Consequently future biophysical studies, on the influence of HCO_3^- in relation to the electrical properties of the plasmalemma, must ensure that the status of the HCO_3^- transport system is determined simultaneously with the electrical measurements.

Interpretation of the Kinetic Data

It is not possible to assign categorically the observed apparent K_m values to specific binding sites. This is because the measured ^{14}C fixation rate depends upon the combined processes of CO_2 diffusion, from the bulk solution to the chloroplasts, and carboxylation. The relationship between the carbon concentration (e.g. CO_2) in the bathing solution and the concentration actually present at the carboxylating site in the chloroplasts, is very difficult to obtain for cells of macroscopic size. This is particularly so for the results obtained in this study because the experimental medium was not stirred. Hence the unstirred diffusion layer (see Dainty, 1963) would have been greater than the estimated value of 100μm obtained by Dainty and Hope (1959) for isolated *Chara* cell walls in a stirred medium. According to Raven (1970), the total diffusion path in a situation of this nature would probably be at least 400-500μm.

Consequently the apparent K_m, obtained with the unstirred experimental solution buffered at pH 5.3, would have been influenced significantly by the diffusive resistance of the system to CO_2 (see Raven, 1970). Under these conditions (i.e. the presence of a large diffusive resistance component) it has been found that the apparent K_m for photosynthetic CO_2 fixation is similar to the K_m for the isolated carboxylating enzyme, ribulose-diphosphate carboxylase (Steemann Nielsen, 1960; and Raven, 1970). In this respect the obtained apparent K_m value of 0.7mM is in reasonable agreement with the adjusted value of 0.45-0.54mM, calculated for the isolated enzyme (Cooper, Filmer, Wishnick and Lane, 1969; and Walker, 1973). However, it should be pointed out that firstly, the *in vitro* K_m for the isolated enzyme is sensitive to the level

of magnesium ions present (Pon, 1959), and under these conditions a reduction in the value of the K_m to 0.12mM was reported by Paulsen and Lane (1966). Secondly, the reported *in vivo* apparent K_m values for CO_2 fixation range from 1μm for *Chlorella* (see for example Whittingham, 1952; and Steemann Nielsen, 1955) to 10-12μM for most land plants (see Goldsworthy, 1968) and up to 0.3mM for some aquatic species (see, for example, Steemann Nielsen, 1946; 1947; Smith, 1967; and Raven, 1968a). There is an obvious discrepancy between the *in vivo* and *in vitro* values for the K_m of this enzyme system (Raven, 1970; and Walker, 1973).

The exogenous $H^{14}CO_3^-$ situation is as complicated, since the photosynthetic fixation rate is dependent upon the properties of the carrier associated with the transport of HCO_3^- across the plasmalemma, the rate of HCO_3^- diffusion to the carrier and from the carrier to the chloroplasts, and finally the carboxylating process. The apparent K_m value, determined in the presence of exogenous $H^{14}CO_3^-$ is very similar to the values reported by Steemann NIelsen (1946; $K_{m\ HCO_3^-}$ - 0.5mM for *Myriophyllum spicatum*) and Raven (1968a $K_{m\ HCO_3^-}$ - 0.7mM for *H. africanum*). The complexity of the experimental situation does not permit the K_m to be assigned either to the actual carboxylating process or to the binding site associated with the HCO_3^- transport system of the plasmalemma.

The requirement of a low K_m value (<1μM) for photosynthetic fixation, which Raven (1970) suggested would be imposed by a facilitated diffusion system for HCO_3^-, does not appear to be supported by the $H^{14}CO_3^-$ results. However, this conclusion is valid only if the diffusive resistance of the system does not

prevent the establishment, by the HCO_3^- transport system, of a stromal $^{14}CO_2$ level greater than 1μM when 0.6mM exogenous $H^{14}CO_3^-$ is present in the bathing solution. It is therefore assumed that the data tentatively supports the hypothesis that the entry of HCO_3^- occurs by an active process. It should be remembered though that Lucas and Smith (1973) considered the HCO_3^- movement to be obligately coupled to OH^- efflux. The independent or coupled nature of these two fluxes must be resolved before a final statement can be made as to the active nature of the HCO_3^- transport system.

A comparison of the fixation rates obtained in the presence of exogenous $^{14}CO_2$ and $H^{14}CO_3^-$ (cf. Figures 3.2 and 3.4) indicates that for the same carbon concentration, the rate is always lower when exogenous $H^{14}CO_3^-$ is present. A similar situation was observed for *H. africanum* (Raven, 1968a). Unfortunately the results presented in Figures 3.2 and 3.4 were obtained using cells from culture tanks XG-2 and delta respectively, in which the respective chlorophyll concentrations were 140 and 8.9μg Chl.cm^{-2}. However, the difference in V_{max} between exogenous $^{14}CO_2$ and $H^{14}CO_3^-$ cannot be due simply to differences in chlorophyll concentrations. This is demonstrated by the results presented in Figure 3.6, which show that uniform cells, cultured in tanks delta and E', fixed exogenous $^{14}CO_2$ at maximum rates of approximately 130 pmol $cm^{-2}s^{-1}$, but under exogenous $H^{14}CO_3^-$ conditions the maximum fixation rate was only 60 pmol $cm^{-2}s^{-1}$. This implies that the fixation rate, in the presence of exogenous $H^{14}CO_3^-$, is limited by a process other than the carboxylating reaction. The limiting process may be the transport of HCO_3^- across the plasmalemma. If this was in fact the case, the value of V_{max} may be determined by the total number of operational carriers in the plasmalemma.

Influence of Light Intensity in the Presence of Saturating Substrate

Over a significant range of light intensities the $^{14}CO_2$ fixation rate was found to be directly proportional to the light intensity (Figure 3.3). A similar response was observed by Raven (1969a) and in fact this appears to be the most commonly observed photosynthetic response (Smith, 1936; Rabinowitch, 1951). Under saturating CO_2 concentrations, the rate limiting step at low light intensities may be either the production of ribulose-diphosphate or the conversion of 3-phosphoglyceric acid to glyceraldehyde-3-phosphate. Independently of which site is limiting, the level of ribulose-diphosphate should be small compared with the level of CO_2. If this was so, it would explain the observed pseudo-first order reaction.

Recent studies have shown that several of the reductive pentose phosphate enzymes may require photoactivation (Pedersen, Kirk and Bassham, 1966; Buchanan, Kalberer and Arnon, 1967; Wildner and Criddle, 1969; and Bassham, 1971). It is possible that this form of activation and regulation could result in a linear response between fixation and light intensity. The different saturating rates of fixation observed in Figure 3.3 could be due to any number of rate limiting factors (Bassham, 1971), but since the lower two curves also had very much lower chlorophyll levels, the most simple explanation is that the rates were depressed by lower supplies of $NADPH_2$ and ATP.

The $H^{14}CO_3^-$ light intensity response was slightly sigmoidal (Figure 3.5); the significance of this response is not known. A comparison of fixation rates, at a particular light intensity, for exogenous $^{14}CO_2$ and $H^{14}CO_3^-$ reveals that the value is always

lower when $H^{14}CO_3^-$ is being assimilated rather than $^{14}CO_2$. (Compare, for example, the rates of tank delta cells presented in Figures 3.3 and 3.5). This indicates that more light (quanta) is required to fix a mole of carbon, supplied as $H^{14}CO_3^-$, than is required for a mole supplied as $^{14}CO_2$. It is possible that this extra energy is required for the transport of HCO_3^- across the plasmalemma and the possibility of an energy requirement for the efflux of OH^- should not be discounted. Other transport processes (ionic or non-ionic) which require photosynthetic energy may also contribute to this "apparent" higher energy requirement for photosynthetic ^{14}C fixation. However, for this additional transport energy "load" to be significant, the actual fluxes would have to be stimulated by raising the pH of the bathing solution, or alternatively the energy requirement per mole transport would have to increase as the pH was raised. (Irrespective of what cellular processes are utilizing this additional photosynthetic energy, it is apparent that light-limiting conditions should be avoided unless they are specifically required by the experiment (cf. Spear et al., 1969; and Richards and Hope, 1974).

Simultaneous Supply of ^{14}C by Diffusion of $^{14}CO_2$ and Transport of $H^{14}CO_3^-$

To determine whether diffusion of $^{14}CO_2$ and $H^{14}CO_3$ transport are operating simultaneously to give maximum possible fixation values, it was necessary to calculate the concentrations of CO_2, HCO_3^- and CO_2^{2-} present over the experimentally employed pH range (see Figure 3.6). The results of these calculations are shown in Figure 3.7. Using Figure 3.2 it was estimated that the

$^{14}CO_2$ fixation rate saturated over the concentration region 1.0 to 1.5mM (exogenous $^{14}CO_2$). Similarly the saturating concentration region for $H^{14}CO_3^-$ influx was estimated to be from 1.5 to 2.0mM (Figure 3.4). These regions have been marked on Figure 3.7 and using the data in this figure it is evident that saturating CO_2 concentrations are present until the employment of pH values higher than 6.7. Applying Raven's (1968a) proposal, the exogenous CO_2 concentration should fall to 0.3mM (i.e. 10% of the total carbon present) before the HCO_3^- transport system becomes operational. The pH value at which this 1 : 10 (CO_2 : HCO_3^-) ratio occurs is 7.28 and is marked on Figure 3.7. Now, if Raven's proposal is correct, the fixation rate in the pH region 6.7 to 7.28 would be expected to fall and then recover once the HCO_3^- transport system could contribute carbon for fixation. An examination of Figure 3.6 reveals that the experimentally obtained fixation rate does not decline until the bathing solution pH value is raised to pH 7.4. The observed fixation value of 120 pmol $cm^{-2}s^{-1}$ at pH 7.0 cannot be due simply to $^{14}CO_2$ supplied by diffusion, for at this pH value 0.54mM CO_2 is present and this CO_2 level would support a fixation rate of only 60 pmol $cm^{-2}s^{-1}$. (This fixation rate was estimated from Figure 3.2). However, at this pH value exogenous $H^{14}CO_3^-$ is present at a concentration greater than that required for saturation of the HCO_3^- transport system. Consequently the ^{14}C which would be supplied were the $H^{14}CO_3^-$ transport system operating, would be 60 pmol $cm^{-2}s^{-1}$ (derived from Figure 3.4).

Thus combining the two rates gives a maximum value of 120 pmol $cm^{-2}s^{-1}$ and the agreement between this value and the experimentally observed rate must be taken as conclusive evidence for the simultaneous supply of ^{14}C by diffusion of $^{14}CO_2$ and

transport of $H^{14}CO_3^-$. It is assumed that these two processes combine to give the maximum possible rate which is governed by the prevailing experimental conditions. This assumption is supported by the observed fall in the ^{14}C fixation rate over the pH range 7.4 to 8.4. (Over this pH range the CO_2 concentration falls from 0.25 to 0.03mM). The combined rates in this region still agree with the experimentally observed value, for example, at pH 8.0 the exogenous CO_2 concentration is 0.06mM and this would facilitate a fixation rate of 7 pmol $cm^{-2}s^{-1}$, which when added to the maximal $H^{14}CO_3^-$ influx value of 60 pmol $cm^{-2}s^{-1}$, gives a combined rate of 67 pmol $cm^{-2}s^{-1}$. The experimentally observed rate at this pH value was in fact 64 ± 5 pmol $cm^{-2}s^{-1}$. Since, over this pH range, the HCO_3^- concentration actually increases to a maximum value, it can be seen that the $H^{14}CO_3^-$ does not act simply as a reservoir for $^{14}CO_2$. This is also supported by the plateau in the fixation rate over the pH range 8.4 to 9.4, i.e. the exogenous $H^{14}CO_3^-$ concentration remains super-saturating whilst the exogenous $^{14}CO_2$ concentration decreases to 2.5μM and the concentration of CO_3^{2-} remains reasonably low. The reference to the CO_3^{2-} concentration will be explained in the following section.

It would appear that the control of $H^{14}CO_3^-$ transport into *C. corallina* is different from that proposed for *H. africanum*, or that Raven's proposal is invalid. The ^{14}C results presented in this work support the earlier work of Lucas and Smith (1973) and taken together they demonstrate conclusively that this species can transport HCO_3^- when the bathing solution has a pH value as low as 6.7 and this value can probably be extended down to pH 5.7 (but this will depend upon the external conditions).

Decrease in $H^{14}CO_3^-$ Influx in the pH Range 9.5 to 10.8.

It was assumed that $H^{14}CO_3^-$ influx would remain constant from pH 8.4 ($H^{14}CO_3^-$ concentration 2.93mM) to 10.33 ($H^{14}CO_3^-$ concentration 1.50mM). Above pH 10.33 exogenous $H^{14}CO_3^-$ would fall below the level required to saturate the $H^{14}CO_3^-$ influx system and hence a decline at values > pH 10.33 was expected. Experimental results did not confirm the first assumption; at pH values $\geqslant$ 9.5 considerable inhibition of $H^{14}CO_3^-$ influx occurred (see Figure 3.6). In fact at pH 9.9, an apparent inhibition of 80% in the $H^{14}CO_3^-$ influx occurred in the presence of a saturating HCO_3^- concentration (see Figure 3.7). (It is interesting to note that a decrease of this nature, at a slightly lower pH value, was observed by Smith (1968) for *N. translucens* and *Tolypella intricata*). Raven (1968) conducted his experiments at pH 9.6 or 10.2 to 10.4, consequently his low fixation rates may have been due to the experimental conditions rather than an inability of *H. africanum* to utilize $H^{14}CO_3^-$ at higher rates.

The inhibition observed at these pH values may have been due to either the influence of high pH *per se* on the membrane properties (or cytoplasmic pH) or to the presence of CO_3^{2-} which could interfere with the HCO_3^- transport system. Since cells actually grow in culture tanks in which the pH value can equal 9.5 (see Table 2.1) or exceed this value (Smith, 1968), it would appear that inhibition by CO_3^{2-} is the more likely explanation of this decline in $H^{14}CO_3^-$ influx. This conclusion is also supported by the results of earlier workers in the field of HCO_3^- assimilation. Österlind (1949), in his review of this work, discussed the inhibiting effect of CO_3^{2-} on culture growth and photosynthetic assimilation of HCO_3^-. However, he assumed that the CO_3^{2-} ions could cross the plasmalemma and that their inhibiting influence

was expressed through their displacement of the cytoplasmic pH towards more alkaline values. Österlind's assumption that CO_3^{2-} can penetrate to the cytoplasm is unsubstantiated by experimental evidence and it is considered that, in *Chara corallina* at least, the inhibition is expressed via a competitive blocking of the HCO_3^- carrier system by the CO_3^{2-} ion.

If this is in fact the case, it indicates that for normal transport the carrier requires at least a C - OH group and very possibly a C $\overset{\delta\ominus}{\text{---}}$ group on its substrate. When this C - OH group is ionized the substrate can still bind to the carrier through the C $\overset{\delta\ominus}{\text{---}}$ O group, but the successful orientation of the ion onto the carrier cannot be accomplished, because of the absence of the hydrogen binding group. It is just possible that the "artificial" buffer inhibition of $H^{14}CO_3^-$, demonstrated in Table 3.3, is also due to competitive blocking of the carrier site. It should be pointed out that if CO_3^{2-} does act as an inhibitor of the HCO_3^- transport system, then the maximum influx rates obtained at pH 9.0 to 9.2 would be lower than the true maximum rates. This may also explain the discrepancy between the observed V_{max} values of HCO_3^- influx and the computed V_{max}.

Buffer Effects at Alkaline pH.

The experiments with the various "artificial" buffers (see Table 3.3) showed that their presence interfered with the cellular utilization of exogenous $H^{14}CO_3^-$. The pronounced inhibition of $H^{14}CO_3^-$ influx by Tris and Tricine buffers is particularly noteworthy, because these buffers are still being used in membrane potential studies (see Kitasato, 1968; and Saito and Senda, 1973 a and b), and in artificial culture media (see Rent, Johnson

and Barr, 1972). Lannoye, Tarr and Dainty (1970) reported that "Tris-buffer, in particular, had a secondary effect on the membrane potential not due to pH". The "secondary effect" was not detailed but it is possible that it may have been associated with an effect on HCO_3^- influx. Of the four buffers used, excluding HCO_3^-/ CO_3^{2-}, only TES was found not to interfere with the HCO_3^- influx system.

In this respect it is interesting to note that Spanswick (1970a, Fig. 4) used TES-buffer, at pH 7.1, to investigate the electrogenic HCO_3^- hypothesis proposed by Hope (1965). The parallel in response when TES or 0.1mM HCO_3^- was used, would be expected because TES does not inhibit the HCO_3^- influx, and the buffer at pH 7.1 would contain 0.072mM HCO_3^- if the solution was equilibrated with atmospheric CO_2.

The mode of action, by which the Tricine, Tris and borate buffers inhibit HCO_3^- influx is not known with any certainty. However, it is possible that the Tricine-buffer acts as a competitive inhibitor on the HCO_3^- carrier site. The formula of Tricine is $(CH_2OH)_3\text{-}CNH\text{-}CH_2\text{-}COOH$ and its pK_a is 8.15. Hence, at pH 9.0 a large proportion of the buffer will exist in the ionized form $(CH_2OH)_3\ CN^+H_2\text{-}CH_2\text{-}C{=}O$ with $O^\ominus$. The carboxyl group may act as an analogue for HCO_3^- and bind to the carrier.

Once bound, the rest of the ion may act to sterically hinder its release. TES, in this respect, would be inert because the sulphonate group of this buffer $\left((CH_2OH)_3\ \overset{+}{N}H - CH_2 - CH_2 - SO_3^\ominus\right)$ could not act as an analogue of HCO_3^-.

Tris-buffer could inhibit the influx of HCO_3^- in at least two ways. Firstly, the buffer could react with CO_2 to produce Tris carbamate by the reaction,

$$R - NH_2 + CO_2 \rightleftharpoons R - NH\,COOH \rightleftharpoons R - NH\,COO^- + H^+$$

where R represents $(CH_2OH)_3C$ (Edsall and Wyman, 1958; and Jensen and Faurholt, 1952). Since this reaction is very rapid and the carbamate is stable only at alkaline pH values, it is possible that an amount of Tris carbamate was present and that it acted in the same way as Tricine, namely as an analogue for HCO_3^-.

Secondly, in Chapter 8 it will be shown that NH_4^+ (or NH_3) specifically inhibits the OH^- efflux system of *C. corallina*. Tris may be capable of acting in the same way, and the resultant inactivation of the OH^- efflux system would prevent the HCO_3^- transport system from operating normally.

The mode of action of the borate buffer remains completely obscure. The solution chemistry of boric acid and $Na_2B_4O_7.10H_2O$ is not known in detail, but it appears that boron may exist as polymeric species. In this form borate buffer may have a deleterious effect on the plasmalemma.

Comparison between Field and Laboratory Cultured Cells

Finally, there does not appear to be any significant difference in $^{14}CO_2$ fixation rates between field cells and cells cultured in the laboratory under full sunlight (see Figure 3.3). Unfortunately comparative experiments under exogenous $H^{14}CO_3^-$ conditions were not conducted, so no comment can be made regarding $H^{14}CO_3^-$ influx rates. (However, the field cells were banded with $CaCO_3$ and they formed alkaline bands when treated in a bathing solution which contained HCO_3^- and the pH-indicator, phenol red). The total exogenous carbon required to saturate the photosynthetic system appears to be between 1.0 and 1.5mM and both field and

culture tank systems had HCO_3^- in excess of this amount (see Table 2.1). The summer light intensity in the field situation may be in excess of the saturation level, but would depend to some extent upon the density of surface-floating vegetation. It would seem, therefore, that the rates obtained in this study are realistic in terms of the natural growth of this particular species (cf. Smith, 1965).

TABLE 3.1

Effects of various buffers on $H^{14}CO_3^-$ Influx.

Solution	$H^{14}CO_3^-$ Influx (pmol $cm^{-2}s^{-1}$)				pH of the Expt. Soln.
	Culture Tank				
	E'	Delta	XG-2	A	
Control*	59.3 ± 3.6	58.9 ± 2.6	55.5 ± 3.0	51.6 ± 2.4	9.0†, 9.2
+ 5mM Tricine	5.85 ± 0.37	18.3 ± 1.0	5.28 ± 0.56	3.99 ± 0.35	9.0, 9.0
+ 5mM Tris	—	4.03 ± 0.21	4.6 ± 0.33	—	9.2, 9.2
+ 5mM Borate	4.18 ± 0.40	6.81 ± 0.45	—	—	9.0, 9.0
+ 5mM TES	—	—	—	52.6 ± 2.6	8.34, 8.35
Control*	91.7 ± 7.1				7.35, 7.7
+ 5mM TES	98.5 ± 5.9				7.4, 7.4

* Normal bathing solution plus 2mM total carbon, the solution pH value was adjusted using either 100mM NaOH or 100mM H_2SO_4. (A saturating light intensity of 25Wm^{-2} was employed.)

† Initial and final pH values respectively

TABLE 3.2

Winter Culture Tank (XG-1) Conditions.

Date	Average Chlorophyll concentration ($\mu g\ Chl.\ cm^{-2}$)	Ionic Composition (mM)					pH*
		Na^+	K^+	Ca^{++}	Cl^-	HCO_3^-	
29th July 1974	10.8 ± 0.5	3.5	0.15	0.7	0.8	3.24	9.5

* pH value of the culture tank measured after 6h artificial illumination (as in Table 2.1).

TABLE 3.3

^{14}Carbon Fixation Rates Obtained Using Mature Winter Cultured Cells

Day No*	Exogenous $^{14}CO_2$ +		Exogenous $H^{14}CO_3^-$ ‡	
	$^{14}CO_2$ Fixation (pmol $cm^{-2}s^{-1}$)	Cyclosis (Av.) ($\mu m\ s^{-1}$)	$H^{14}CO_3^-$ Influx (p mol $cm^{-2}s^{-1}$)	Cyclosis (Av.) ($\mu m\ s^{-1}$)
0	67.57 ± 7.75	20	13.21 ± 2.1	20
	58.84 ± 8.10	20	17.81 ± 2.1	21
0**			17.77 ± 2.7	50
1	107.29 ±13.95	62	10.71 ± 0.98	60
2			9.02 ± 1.43	60
4			21.95 ± 3.82	62.9
5			19.21 ± 2.74	61.5
7			32.79 ± 4.58	70.4
			38.40 ± 6.15	
9			47.93 ± 2.37	65

* This indicates the number of days which elapsed between harvesting and employing the cells in an experiment.

\+ Experimental conditions were, 3mM total carbon buffered at pH 5.3 with 5mM MES buffer and a saturating light intensity of $25 Wm^{-2}$.

‡ Experimental conditions were, 3mM total carbon buffered at pH 9.0 by the exogenous HCO_3^-/CO_3^{2-} buffer.

** The cells employed in this experiment were cut directly from the culture tank before the bulk harvest of the remaining cells.

The brackets indicate duplicate experiments.

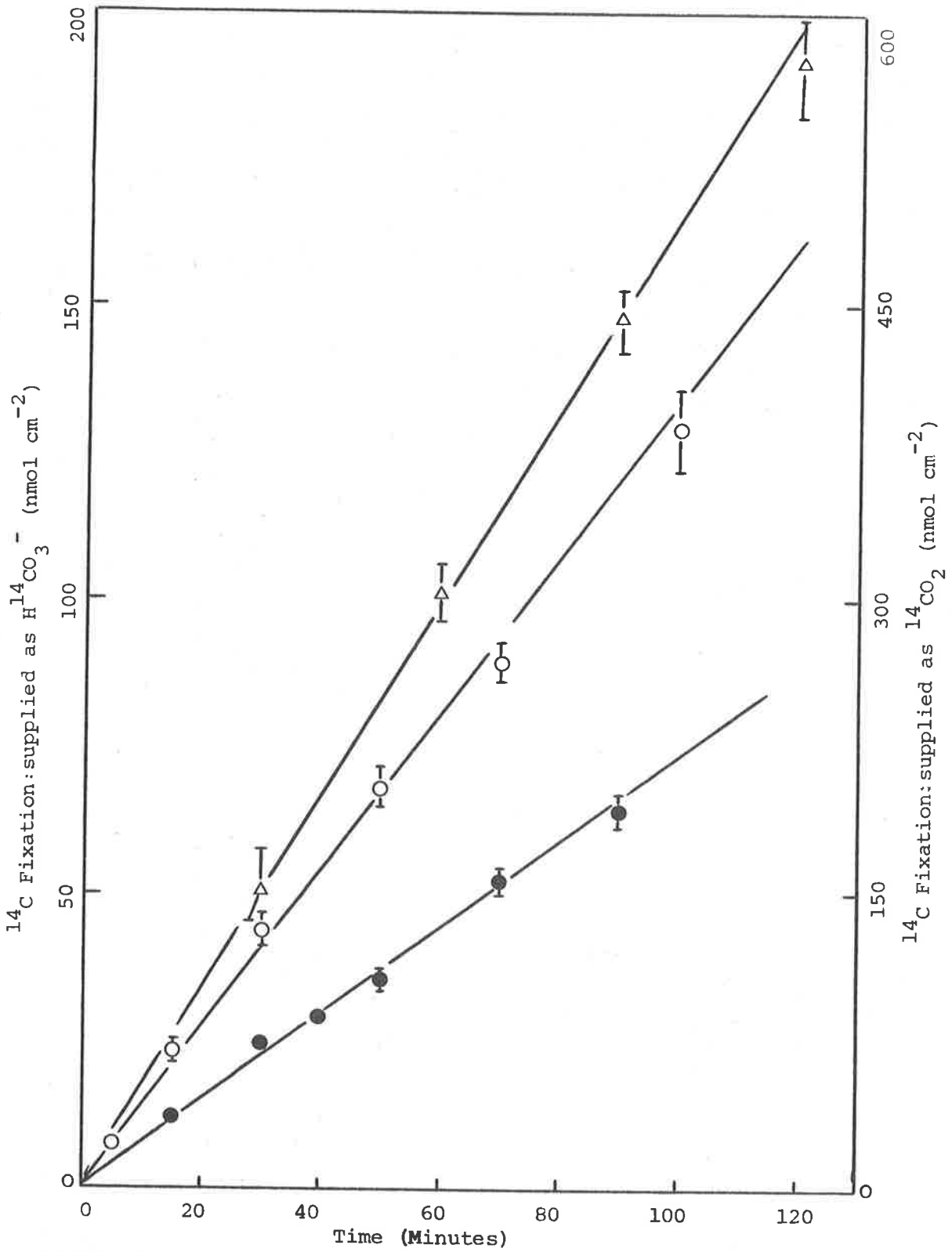

Figure 3.1.

Time-course of ^{14}C.fixation. $^{14}CO_2$ fixation (Δ) was determined in the presence of 2mM total carbon, pH 5.3 and 5mM MES-buffer; light intensity was 12Wm^{-2}. $H^{14}CO_3^-$ uptake was determined in the presence of 2mM total carbon, pH 8.6 and 5mM TES Buffer. The $H^{14}CO_3^-$ time-courses (●) and (○) were obtained using light intensities of 2 and 3Wm^{-2} respectively.

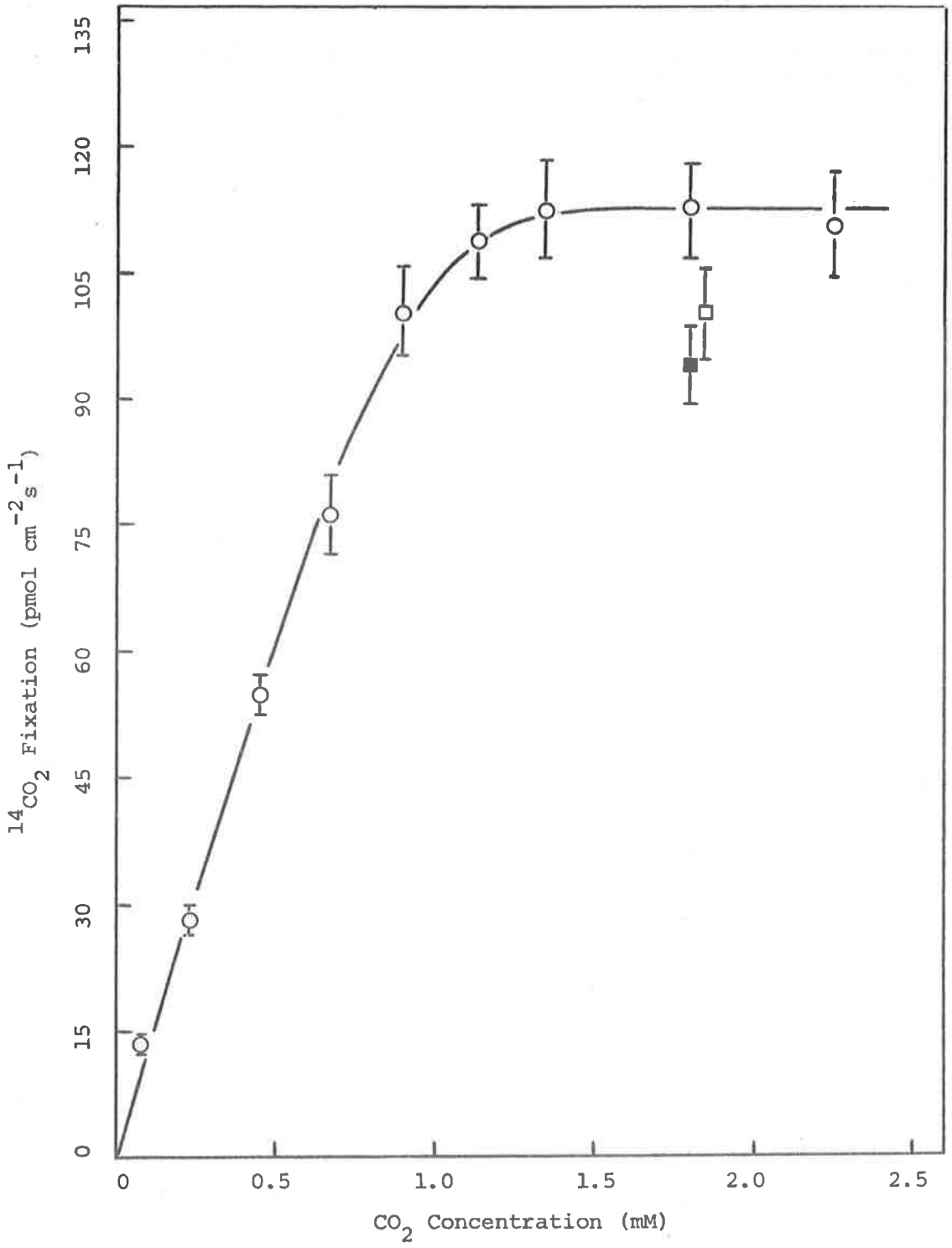

Figure 3.2. $^{14}CO_2$ Fixation in response to increasing substrate concentration. The bathing solution was buffered at pH 5.3 with 5mM MES buffer and a light intensity of 25Wm^{-2} was used throughout. (O), rates using cells cultured in tank XG-2; (□), Mannum cells; (■), delta tank cells.

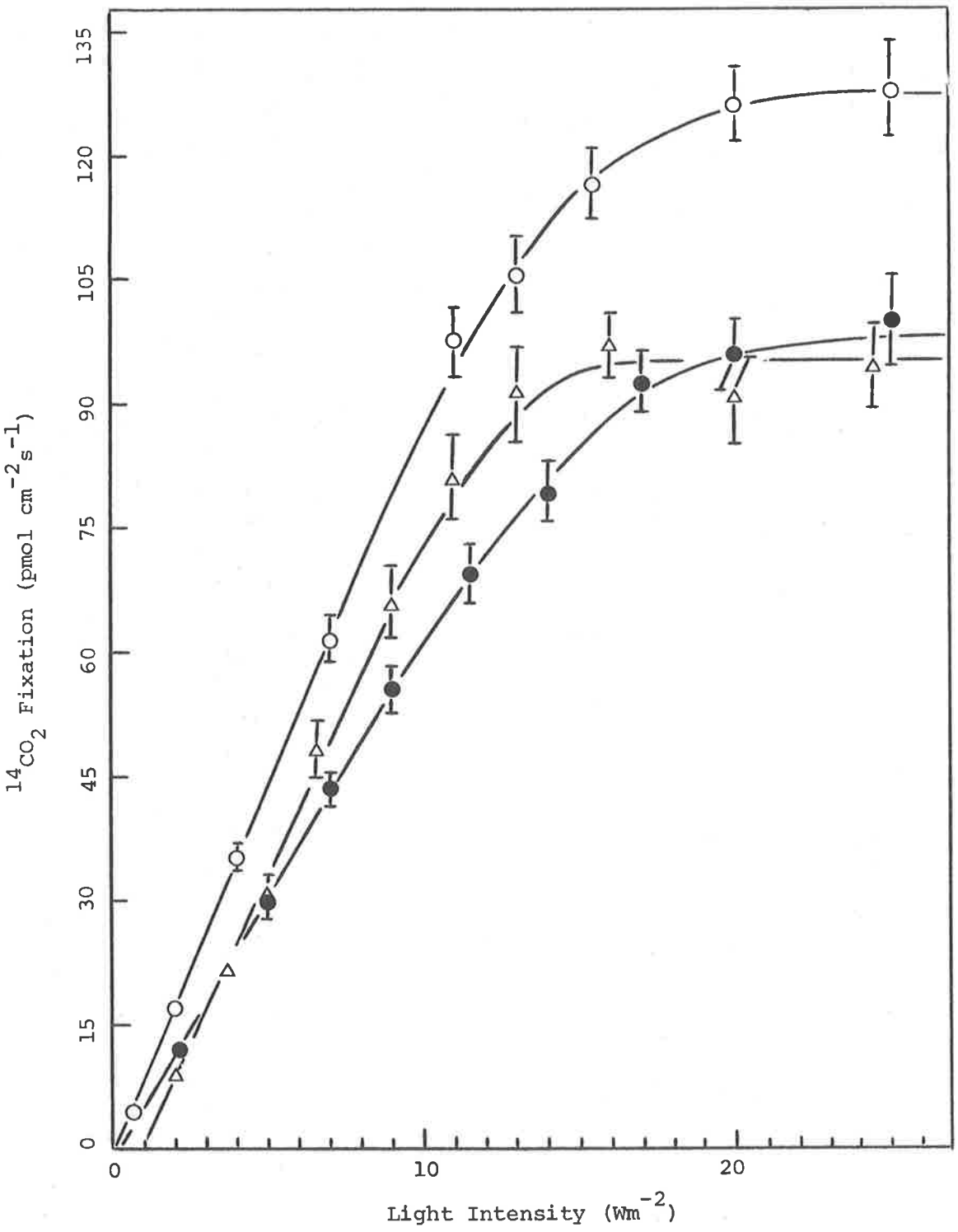

Figure 3.3. The effect of light intensity on $^{14}CO_2$ fixation. The bathing solution contained 2.0mM total carbon and was buffered at pH 5.3 with 5mM MES buffer. The symbols (O), (Δ) and (●), represent the responses obtained using XG-2, delta (full sunlight) and Mannum cells respectively.

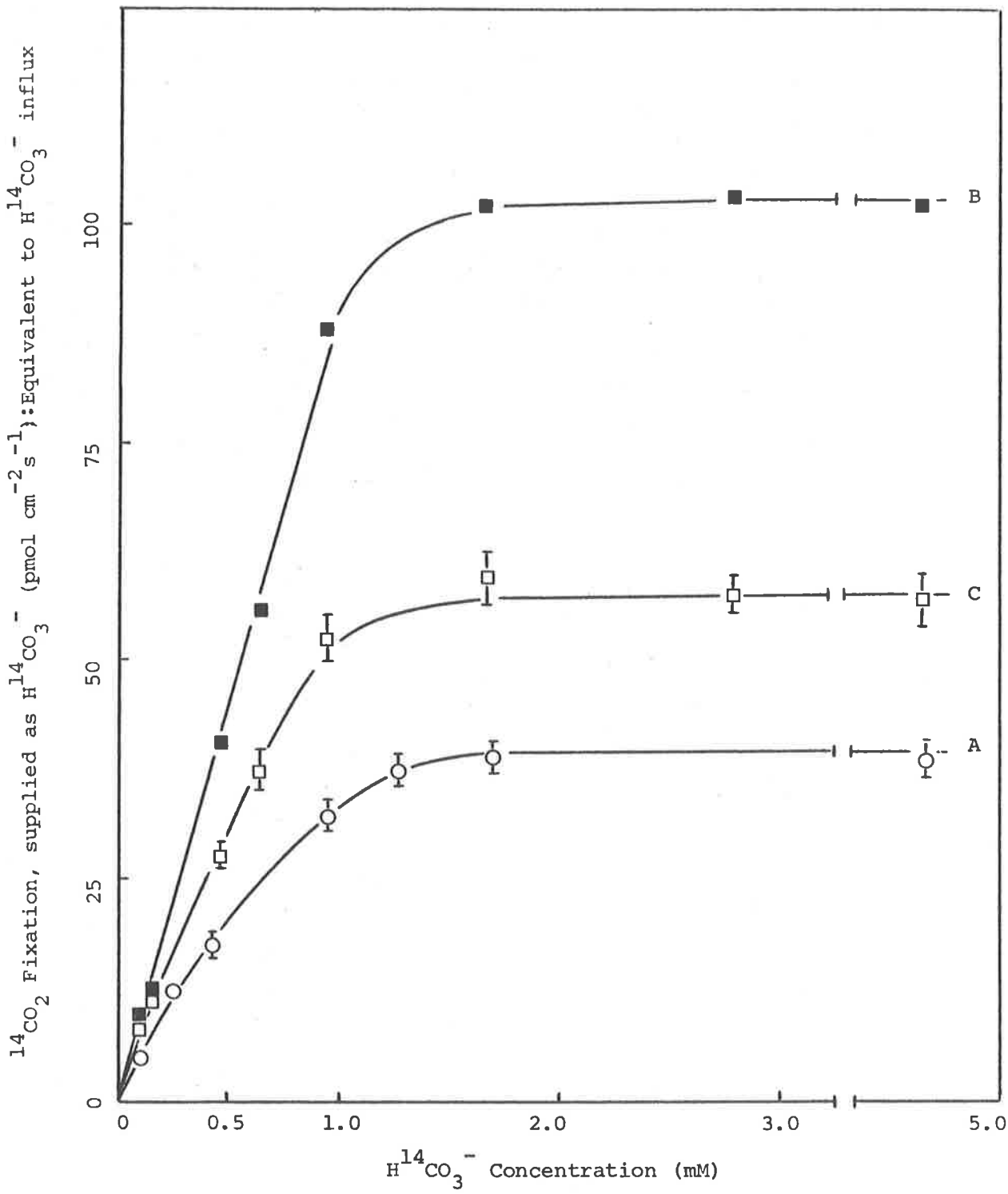

Figure 3.4. $H^{14}CO_3^-$ influx in response to increasing substrate concentration. The bathing solution pH was controlled by the buffering effect of the added $NaHCO_3$ and experimental pH values were held between 9.0 and 9.2. See the text for full details in relation to Curves A, B and C.

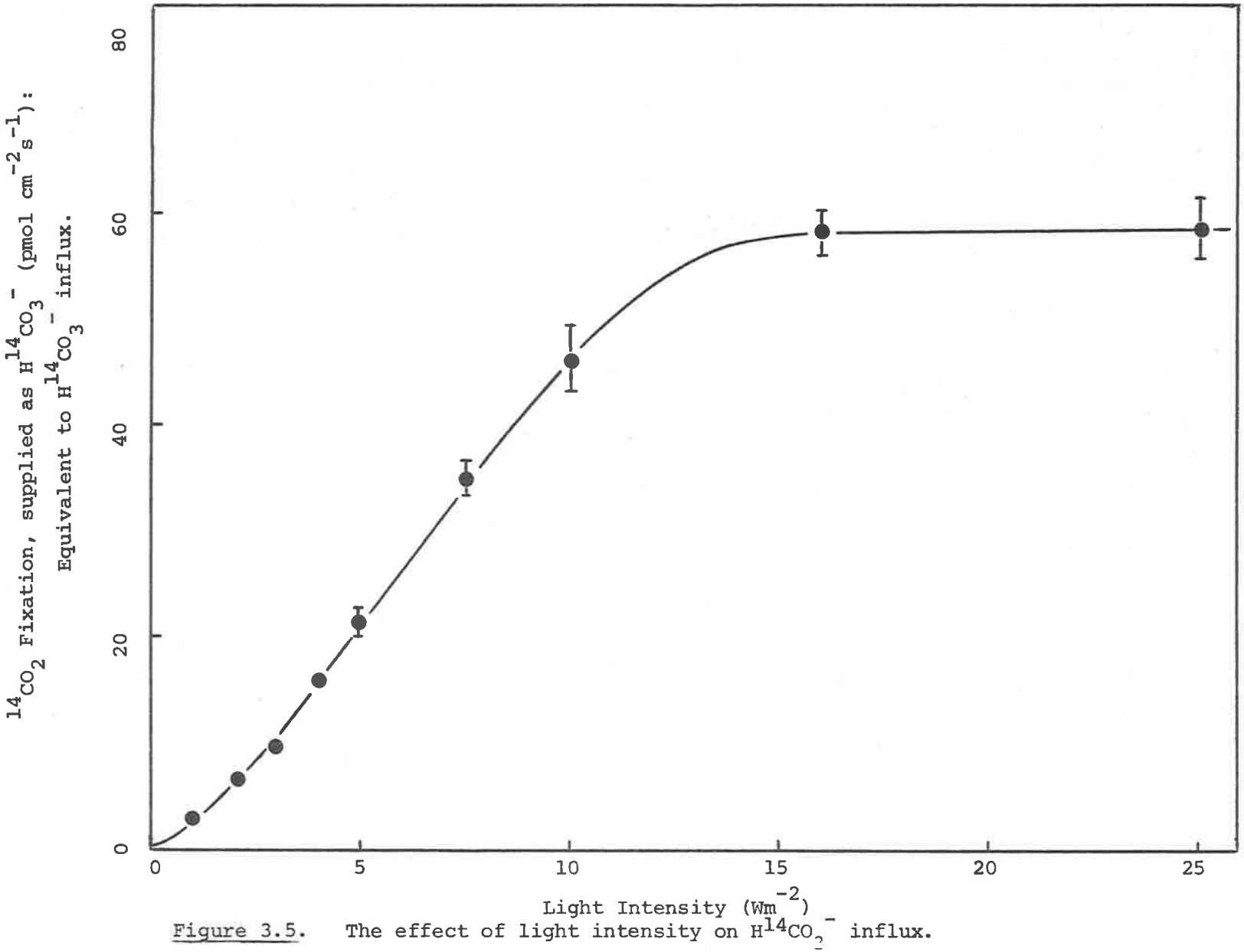

Figure 3.5. The effect of light intensity on $H^{14}CO_3^-$ influx.

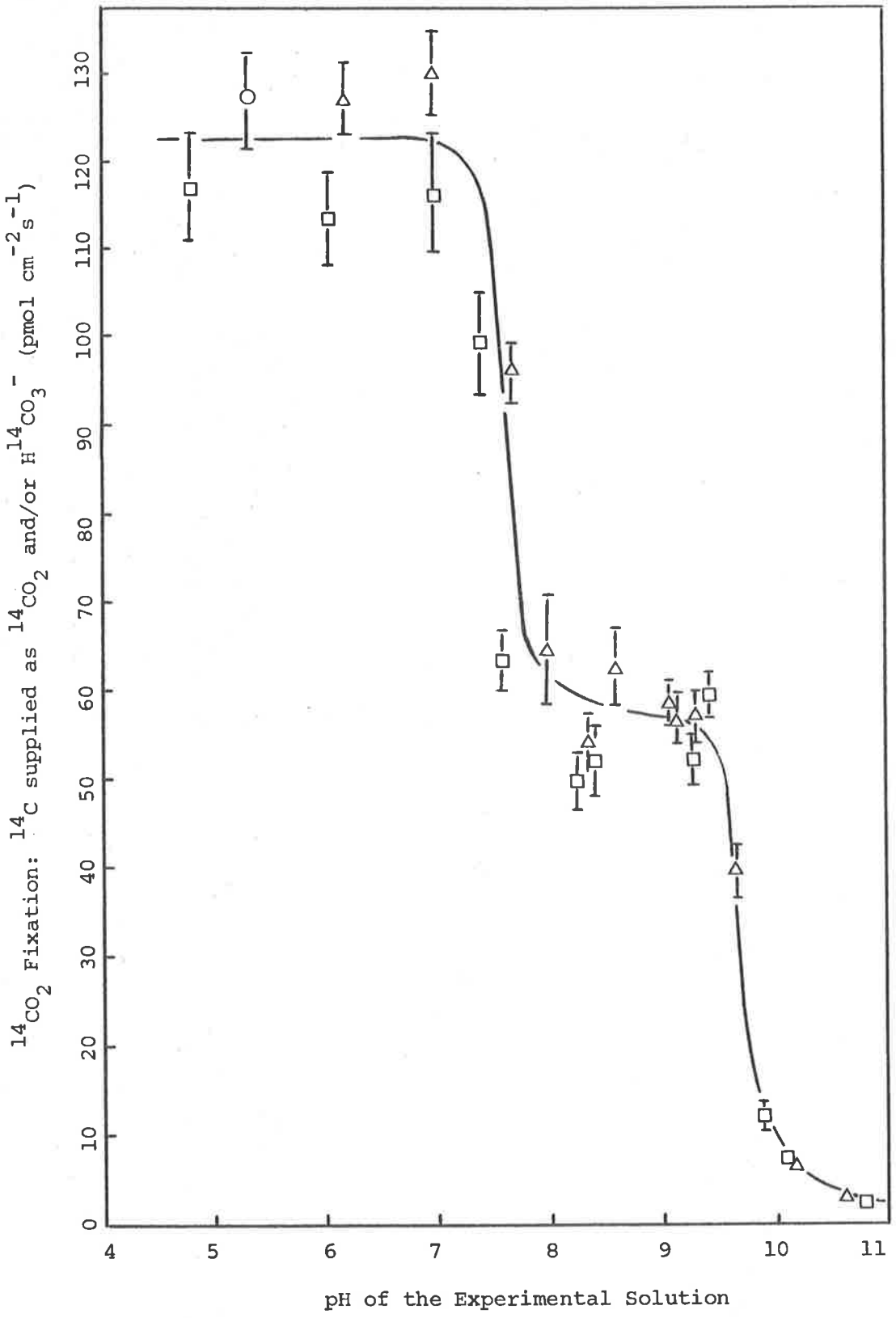

Figure 3.6. The influence of pH on ^{14}C. fixation. A total ^{14}C. concentration of 3mM and a light intensity of $25Wm^{-2}$ were employed for each experiment. The pH region 4.8 - 6.2 was buffered by 5mM MES, the region 7.0 - 8.6 by 5mM TES and the region 9.0 - 10.8 by the 3mM HCO_3^- / CO_3^{2-} buffer. The symbols (O), (Δ) and (□) represent cells cultured in tanks XG-2, delta and E' respectively.

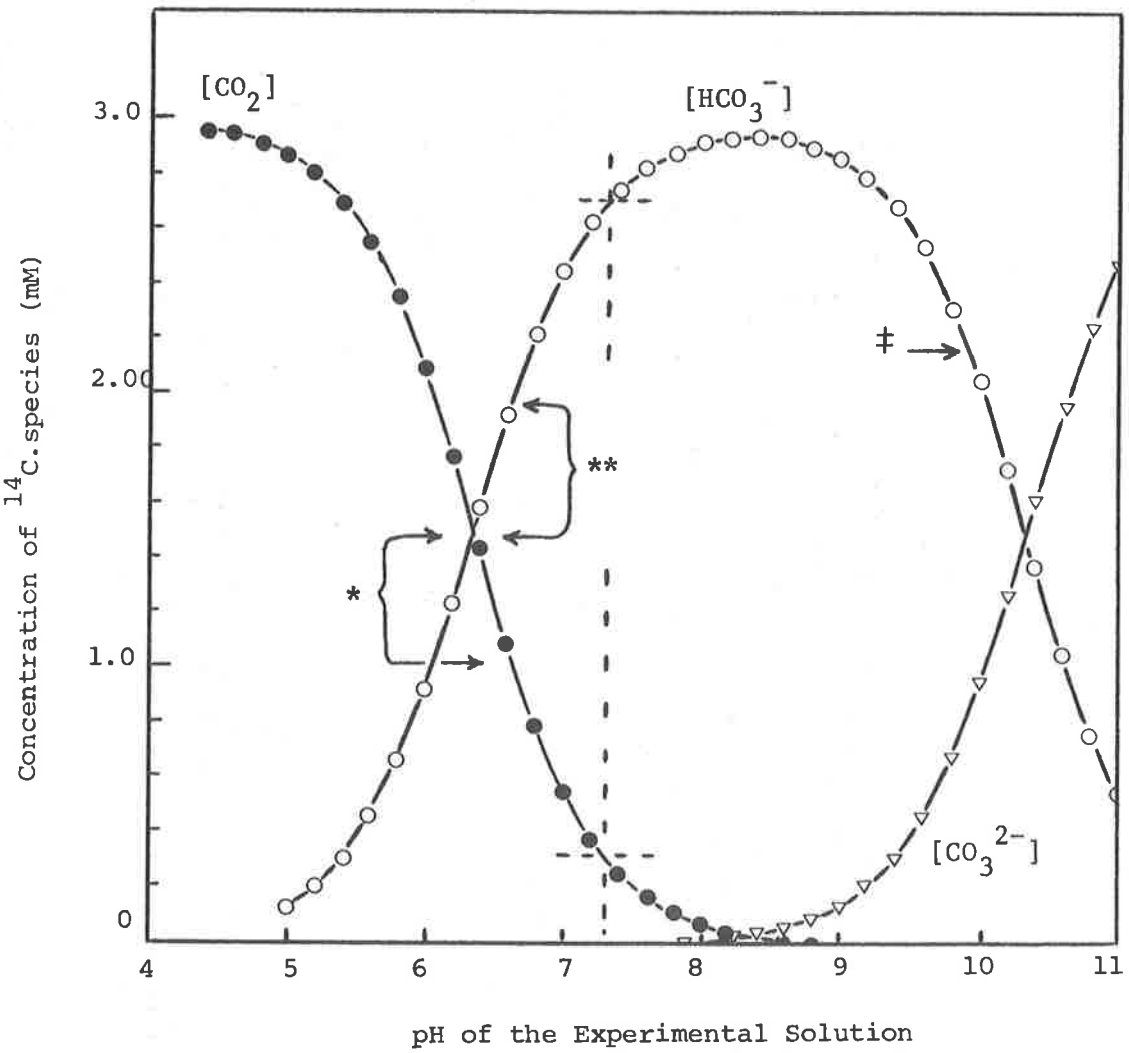

Figure 3.7. Calculated concentrations of CO_2, HCO_3^- and CO_3^{2-} present over the experimentally employed pH range. The concentrations were calculated using the equations and Tabulated constants of Buch (1960).

* The saturating exogenous $^{14}CO_2$ concentration region for ^{14}C. fixation.

** The saturating exogenous $H^{14}CO_3^-$ concentration region for ^{14}C. fixation.

‡ pH value at which $H^{14}CO_3^-$ influx was inhibited by 80% in the presence of saturating exogenous $H^{14}CO_3^-$. The concentration of CO_3^{2-} was 0.8mM.

The broken lines represent the 1:10 concentration ratio (CO_2:HCO_3^-) proposed by Raven (1968, 1970).

CHAPTER FOUR

THE pH BANDING PHENOMENA : A MATHEMATICAL ANALYSIS

Introduction

Several Characean species develop alkaline and acid regions on their cell surface. Spear et al. (1969) reported that these phenomena occurred on the cell surface of *Nitella clavata* and Smith (1970) similarly demonstrated that *Chara corallina* developed these pH regions. *Nitella flexilis* can also be added to this list (J. Lefebvre, personal communication).

Spear et al. considered that their results gave support to the hypothesis proposed by Kitasato (1968). They observed the acid and alkaline banding pattern by using a bathing solution which contained 0.1mM $KHCO_3$ (pH 6.9) and a 0.1mM concentration of the acid/base indicator phenol red. By means of partitions, they could also isolate an acid and an alkaline region from the rest of the cell. Using an experimental system of this nature, they suggested that over several hours, measurable pH changes occurred in the isolated solutions. However, no details were given as to the volume of these isolating compartments or the procedure by which the pH changes were measured. This is particularly important, because these workers suggested that under these conditions they could actually estimate a value for the rate of H^+ extrusion. A value of 5-20 pmol $cm^{-2}s^{-1}$ was reported, which was of the same order of magnitude as the passive influx value inferred by Kitasato (1968) (based on his electrical studies). However, it is doubtful whether this extrusion rate, reported by Spear et al., provides any real support for the electrogenic H^+ pump proposed by Kitasato. This is because of the

inherent errors which would have resulted from the experimental system employed by these workers.

For example, the solution in the isolating compartments contained 0.1mM total carbon which was added as $KHCO_3$. Therefore, since the initial pH was 6.9, the initial HCO_3^- and CO_2 concentrations in the solution would have been 78.3μM and 21.7μM respectively. At this point it should be stressed that the experimental system was open to the atmosphere. Hence, the processes which would have influenced the pH value of the bathing solution are:

(i) diffusion of CO_2 into the atmosphere,

(ii) removal of CO_2 by photosynthetic fixation,

(iii) transport of HCO_3^- (influx) across the plasmalemma,

(iv) efflux of H^+ via the "proton pump",

(v) influx of H^+ by passive diffusion down its electrochemical gradient.

This situation can best be represented by the following equilibria:

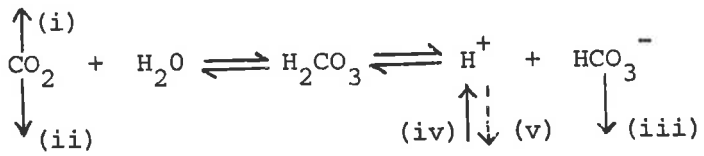

Spear et al. considered the pH change within the acid band resulted solely from process (iv); this would not have been so. Firstly, process (i) would remove CO_2 from the solution to the atmosphere (the concentration of CO_2 which is in equilibrium with the atmosphere is 12μM) and this would tend to force the equilibria to the left. This would result in the removal of H^+ and HCO_3^- from the solution. The experiments were conducted under a light intensity of $4.4Wm^{-2}$, and so photosynthetic CO_2 fixation (process (ii)) would enhance the removal of H^+ and HCO_3^-. However, since the cells developed alkaline regions, it is obvious from the work of

Lucas and Smith (1973) that the cells were assimilating HCO_3^-. If the HCO_3^- influx and OH^- efflux can be spatially separated (see Chapter 7), then HCO_3^- influx (process (iii)) would cause a tendency for the equilibria to move to the right, i.e. H^+ may be generated by the conversion of CO_2, via carbonic acid, to HCO_3^-. Spear et al. proposed that the alkaline regions were formed by passive H^+ influx (i.e. process (v)) and so they would have assumed that this back flux of H^+ was negligible in the acid region. This hypothesis has been refuted by Lucas and Smith (1973). Unfortunately there is no accurate technique available at present by which processes (iv) and (v) can be evaluated separately. Hence if the passive permeability of the plasmalemma is as high as Kitasato proposed, process (v) would result in a large underestimation of the actual H^+ efflux rate. (Actually Kitasato proposed that the passive H^+ influx was balanced by an active H^+ efflux and hence his hypothesis would demand a net H^+ efflux tending to zero). In view of all these complicating factors, it is proposed that the H^+ efflux rate reported by Spear et al. contains so many sources of error that it is completely unreliable.

Other attempts to evaluate the H^+ fluxes have been made by Rent et al. (1972), Brown et al. (1973) and Richards and Hope (1974). Rent et al. attempted to measure the H^+ influx which occurred when cells of *N. clavata* were bathed in solutions of pH 4.5 to 4.7. These workers also seem to have misinterpreted Kitasato, for on his hypothesis the influx that they were attempting to measure should have been cancelled by his proposed active H^+ efflux (providing that it operates at this low pH value). Their results tend to suggest that the plasmalemma had been damaged by this low pH treatment and in fact they may have been titrating some

component of the cytoplasm. Brown et al. and Richards and Hope attempted an evaluation of H^+ fluxes using electrical measurements. Both of these works are of limited value because of the poor predictive nature of the theoretical equations which must be used to calculate these flux values.

Lucas and Smith (1973) measured the pH of the acid and alkaline bands that developed at the surface of *Chara corallina* cells. They attempted to calculate values for the HCO_3^- and OH^- fluxes, but this required an accurate knowledge of the alkaline band dimensions. Since this information was not available, various simplifying assumptions had to be made concerning the geometry of the alkaline bands. Consequently only approximate fluxes could be estimated. These workers were also unable to calculate a meaningful value of the net H^+ efflux associated with the acid bands.

It is important that these fluxes be measured. Firstly, although Kitasato's hypothesis would suggest that the net H^+ efflux is very close to zero, the modification of this hypothesis proposed by Spanswick (1972, 1973, 1974) would suggest that almost all the flux through the H^+ pump should be measurable in the bathing solution. Secondly, there still exists a discrepancy between the electrically measured and calculated value of the conductance of the plasmalemma. The calculated conductance is obtained by applying the measured (known) ionic fluxes to a theoretical conductance equation. It is possible that the acid or alkaline regions are associated with ionic fluxes which contribute to the actual membrane conductance. If this is so, their omission from the theoretical conductance calculations may account for part of the observed discrepancy.

As a result of the large HCO_3^- influx rates observed in Chapter 3, the role of the HCO_3^- and OH^- transport systems must now be viewed in a new light.

Preliminary Results.

By embedding a *Chara* cell in a solid agar block (i.e. an agar block which did not have a channel cut above the cell surface) it was possible to map the diffusion symmetry established by the respective acid and alkaline bands present on the cell surface. However, before the results of this investigation are presented, the nature of the acid and alkaline banding patterns will be briefly reviewed. This will be done so that the reader is familiar with the type of results previously obtained using this technique (Lucas (1971) and Lucas and Smith (1973)).

Using the apparatus and procedures detailed in Chapter 2 Section VI (see particularly Figure 5A and B in conjunction with VI(d)) the pH electrode was located on the wall of a *Chara* cell which was positioned in the channel of an agar block. After an illumination period of 2h, the pH electrode was traversed along the cell wall and the pH value of the bathing solution at the cell surface measured. Steady state measurements were made by recording the pH electrode response on the chart recorder; the pH-sensitive tip was not moved to another position until a steady reading was attained. A typical banding pattern which was established under these conditions is illustrated in Figure 4.1. The bathing solution for this experiment contained 0.1mM $NaHCO_3$ and its pH value of 6.94 is indicated by a broken line on the figure. (Note that Chapter 2 section VI(d)(i) is replaced by VI(d)(x) under these solution conditions). The four band-centres of the alkaline bands are labelled A to D and their locations are indicated on the figure by vertical (solid) arrows. The centres of the inter-alkaline band regions are also marked by (broken) arrows. When

the pH value on the cell surface was depressed below the bulk solution value, this region was termed an acid band, i.e. in Figure 4.1 acid bands existed to the left of alkaline band A, between alkaline bands B and C, and C and D, and to the right of alkaline band D.

By locating the pH-sensitive tip of the electrode on an alkaline band-centre, the response of the cell to illumination could be observed. Figure 4.2 was obtained by placing the electrode on the centre of band A and following a 1h dark treatment, the cellular response to illumination was recorded. From this figure it can be seen that there was a short lag period before the pH value of the bathing solution at the alkaline band-centre began to increase rapidly. Within 30 minutes of the cell being illuminated, this band had established a steady pH value at the cell surface.

An acidification time-course for this same cell is presented in Figure 4.3. For this experiment the electrode was located between alkaline bands C and D. It should also be noted that the cell was transferred to a new agar block and bathing solution prior to the 1h dark period; this new experimental system did not contain added $NaHCO_3$. Following illumination the pH value at the acid band-centre actually increased for the first 8 to 10 minutes and then the value steadily became more acidic. (An explanation of the initial slow rise in pH at the cell surface, for both acid and alkaline bands, will be given in Chapter 5). In general it took between 60 to 100 minutes for the establishment of a steady pH value at cell surface of an acid band-centre.

Diffusion Symmetry of the Alkaline Bands

The first step towards determining the diffusion symmetry developed by alkaline bands involved measuring the pH banding pattern along the cell wall. This was obtained using the procedure described above. Using these results the alkaline band-centres were located (see Figure 4.4A). The cell was then transferred to an agar block which, although it had a centrally located hole for the cell, it did not have a channel cut into the upper surface of the agar. This provided a completely stable medium in which the cell could develop acid and alkaline bands, and no convective forces could act on the concentration gradients thus established at these H^+ and OH^- sites.

The cell was illuminated ($10 Wm^{-2}$) for 4h and then vertical scans were conducted, through the agar medium, onto the cell wall. (The exact location of each alkaline band-centre was determined using the previously obtained data and the scale on the micro-manipulator). The results obtained for a single alkaline band are presented in Figure 4.4. Vertical pH scan locations are indicated on Figure 4.4A, and actual pH values recorded during these scans are presented in Figures 4.4B and C. Using the horizontal (i.e. in the immediate vicinity of the alkaline band) and vertical pH scan values, a two dimensional OH^- diffusion pattern was mapped using iso-concentration lines. Figure 4.5 represents the iso-concentration pattern developed using the results presented in Figure 4.4. (This mis-match between the 1.0 and 10 (moles cm^{-3} x 10^{-10}) iso-concentration lines was due to the elapsed time between scans 1 and 6, i.e. at least 40 minutes was required per scan).

Figure 4.5 typified the results obtained when alkaline bands were investigated and it indicated that these bands established a diffusion pattern which approximated to that of a spherical co-

ordinate system. However, the band or diffusion centre on the cell surface appeared to be wider (0.05cm) than would be expected if the alkaline bands develop from localized point source efflux centres (see Lucas and Smith, 1973). It was also evident that although the pH value at the alkaline band-centre reached a steady state within 30 minutes (see, for example, Figure 4.2), the steady state at vertical distances of 2mm or more required considerably greater periods. Experience showed that this period could be up to, or greater than 6h.

Diffusion Symmetry of the Acid Bands

As in the symmetry studies conducted on the alkaline bands, the acid bands were located and mapped using the open channel agar block procedure. The bathing solutions used in the acid band studies were normal, in that they did not contain added $NaHCO_3$, but the pH value was adjusted to a value of approximately 6.65. This was done using freshly prepared NaOH. The resultant medium was very low in terms of buffering capacity but had a background value upon which could readily be discerned the influence of the acid bands.

Employment of this experimental system lengthened considerably the time required to establish steady pH values along the acid band cell surface. An indication of the time required to establish this situation is given by the results presented in Figure 4.6. (This figure also demonstrated that non-activated alkaline bands can exist in an acid region; this situation will be discussed in Chapter 5). From these studies it was evident that illumination periods of at least 6 to 7h were required before the values on the cell surface began to stabilize. Consequently a pretreatment illumination period of at least 6h was employed prior to performing scans either along or vertically onto the cell wall.

Typical results obtained from a two dimensional analysis of an acid band are presented in Figure 4.7. The two dimensional acid iso-concentration pattern which was constructed from these results is shown in Figure 4.8. This revealed that the diffusion pattern established by acid bands approximated to that of a cylindrical co-ordinate system. However, it was obvious that the alkaline bands, which were present on either side of the acid band, distorted the diffusion pattern by neutralizing H^+ at their boundaries of overlap. This meant that, in order to evaluate the total net H^+ efflux for a single cell, it would be necessary to correct for these neutralization zones.

Alkaline Bands: Point or Band Surface Source?

Lucas and Smith (1973) considered the development of an alkaline band to be due to the localized efflux of OH^- from a point on the cell surface; accumulation of OH^- near the surface eventually forming a band. As previously mentioned, the results presented in Figure 4.5 do not support this hypothesis. By analysing the experimental data in terms of the mathematical equations which describe the concentration distribution established by a continuous point source, it was possible to test this hypothesis.

A cell was located in a normal agar block, with its single orientation cell (see Figure 2.5A) in the vertical (upright) position. This orientation was referred to as the 0^o position. The cell was illuminated for 2h and a cell wall pH scan was then performed. After completing this scan the cell was carefully transferred to an identical agar block, which had been equilibrated in the same bathing solution. The nodal orientation cell was rotated to the horizontal or 90^o position and the procedure repeated. The entire sequence was repeated for the nodal orientation cell in the 180^o position. A

typical pattern of the pH values obtained from such a sequence of scans is shown in Figure 4.9. For clarity only the 0° and 180° values have been plotted on this figure. These results indicated that there was very little change in the concentration of OH^{-} around the surface of the cell, within any particular band. This situation would not be expected if OH^{-} ions were being effluxed through localized point sources. The small band, illustrated on the extreme left of Figure 4.9, was an exception and demonstrated the presence of a very small localized OH^{-} efflux system.

It was also found that the alkaline band-centres attained the steady state situation within the 2h pre-scan illumination period. If it was assumed that for a particular band, the efflux point source was located at the 0° position, the time required to establish the steady state OH^{-} concentration at the 180° position could be obtained from the continuous point source equation derived by Carslaw and Jaeger (1959, p. 261,(2)) i.e.

$$C = \frac{q}{4\Pi DR} \quad \text{erfc} \quad \frac{R}{(4Dt)^{\frac{1}{2}}} \qquad \ldots\ldots(4.1)$$

where C is the concentration of OH^{-} at a radial distance of R_{cm} from the point source, D is the diffusion coefficient for OH^{-}, q is the steady state rate at which OH^{-} is being effluxed through the point source and t is the time the point source has been operating. The diffusion distance for the above situation would be $\Pi.R_{Chara}$ (where R_{Chara} is the radius of the cell in question) and this could be substituted into equation (4.1). This would result in a steady state time actually shorter than the true time required, because equation (4.1) assumes radial flow, whereas the OH^{-} diffusion being considered would be around the cell wall.

For large values of time t, erfc $\frac{R}{(4Dt)^{\frac{1}{2}}}$ tends to 1.0 and the result at position R is the steady state concentration, i.e.

$$C = \frac{q}{4\Pi DR} \qquad .....(4.2)$$

The way in which the steady state is approached will depend upon the distance R from the source. Hence C will have attained 95% of the steady value given by equation (4.2) when erfc $\frac{R}{(4Dt)^{\frac{1}{2}}}$ = 0.95 or $\frac{R}{(4Dt)^{\frac{1}{2}}}$ = 0.044 (value obtained from Appendix II of Carslaw and Jaeger, 1959). So the time to attain 95% of the steady value at R would be

$$t = \frac{R^2}{4(0.044)^2 D} \qquad .....(4.3)$$

Substituting values of 2.129×10^{-5} cm ^{2}s^{-1} for D* and R = $\Pi.4.62 \times 10^{-2} = 1.451 \times 10^{-1}$cm, a value of t = 35.5h was obtained.

The general conclusion was therefore that the alkaline bands could not be formed from point source OH^- effluxes since they can establish the steady state within much shorter periods of time. This conclusion was supported by time-course experiments in which alkaline band activation and steady state establishment were recorded. It was found that the response of a particular alkaline band, to illumination, was the same whether observed from the 0°, 90° or 180° positions (Figure 4.10). In Figure 4.10, traces 1 and 3 were obtained when the cell was held in the 0° position and traces 2 and 4 in the 180° position. (The alkaline band and pH electrode location employed in the experiment associated with Figure 4.10, are indicated on Figure 4.9; the same cell was used for both experiments). The attainment of the steady state OH^- concentration, around the surface of the alkaline band, within a period of 12-14

---

* This value of D is the limiting diffusion coefficient for NaOH, at 25°C, calculated using the Nernst-Hartley relation. This equation and the experimental values are given in Robinson and Stokes (1965) p. 287-8 (11.3) and (11.4) and Appendix 6.2).

minutes (see Figure 4.10) could not possibly occur if a point source OH^- efflux system was operating.

It would therefore appear that most alkaline bands were formed via efflux of OH^- ions over band surfaces whose width was usually equal to or less than 0.05cm. The results presented in this section and the iso-concentration diffusion pattern presented in Figure 4.5 suggest that the diffusion symmetry of an alkaline band might fit the equation for a spherical surface source of radius R_{Chara}, provided radial values too close to the surface of the cell were not used.

Limiting Hydroxyl Ion Capture

Any attempt to analyse the concentration diffusion pattern of OH^- ions, with the ultimate aim of obtaining an absolute value of the flux crossing that band surface, must ensure that OH^- capture is reduced to its minimum possible value. It was proposed that the bathing solutions to be employed in these diffusion analysis experiments would have HCO_3^- concentrations of 0.2 to 0.5mM. Consequently within a normal band centre (pH of approximately 9.9 and with 0.5mM HCO_3^- present) the equilibrium,

$$HCO_3^- + OH^- \rightleftharpoons H_2O + CO_3^{2-}$$

would establish a CO_3^{2-} concentration of 0.136mM. If the Ca^{++} concentration of the normal bathing solution was left at 0.5mM, the ionic product $[Ca^{++}]\,[CO_3^{2-}]$ would be 6.8×10^{-8}(moles$^2\ell^2$) which would exceed the solubility product for these ions at 25°C (0.87×10^{-8}moles$^2\ell^2$). Consequently this concentration of Ca^{++} could not be employed, for it would result in the precipitation of $CaCO_3$ onto the cell wall, and this would result in the continued removal of OH^- from the diffusion system. Using this level of total carbon (0.5mM), the solubility product indicated that Ca^{++}

at 0.06mM would be low enough to prevent $CaCO_3$ precipitation.

A series of $H^{14}CO_3^-$ influx experiments was performed at various Ca^{++} concentrations, to determine whether the influx remained unaffected by such low Ca^{++} concentrations ($\leq$ 0.06mM). *Chara* cells were cut and given the normal pretreatment used for ^{14}C experiments. At the end of the recovery period the cells were washed with Ca^{++}-free bathing solution and then pretreated for 1h in their respective bathing solutions, which contained Ca^{++} levels ranging from 0 to 0.5mM and 0.5mM $NaHCO_3$. The pH value of all solutions was adjusted to 8.6 and no other buffer was used. A saturating light intensity of $15Wm^{-2}$ was employed for both the 1h pretreatment and 1h experimental (^{14}C) periods. The results of this series of experiments, which are presented in Figure 4.11, showed that Ca^{++} levels as low as 0.02mM did not reduce the $H^{14}CO_3^-$ influx.

These results were encouraging for they indicated that suitable Ca^{++} levels could be employed in the diffusion analysis experiments. However, longer exposure times to low Ca^{++} levels would be required during these experiments, since preliminary studies indicated that at least 10-12 were required to establish the steady state situation at radial distances of up to 7mm from the cell surface. To ensure that this prolonged contact with low Ca^{++} levels was not deleterious to the cellular assimilation of $H^{14}CO_3^-$, a further series of $H^{14}CO_3^-$ experiments was performed. After the 2h recovery period, the cells were bathed in a solution which contained 0.02mM $CaSO_4$, 0.5mM $NaHCO_3$, 1.0mM NaCl and 0.2mM KCl (pH 8.6). The cells were treated in this solution for 10h, 6hL, $8.3Wm^{-2}$, 4hD. The 1h pretreatment and 1h $H^{14}CO_4^-$ exposure were as previously described. The results obtained are also presented in Figure 4.11 and they indicated that prolonged contact with 0.02mM Ca^{++} did not reduce $H^{14}CO_3^-$ influx.

The Alkaline Band: Diffusion Analysis Based on the Hollow Sphere Model

A *Chara* cell, whose alkaline banding pattern had been mapped and checked for consistency on the previous two days, was inserted into an agar block which did not have a channel cut into its upper surface. The solution used for this particular experiment contained 0.02mM $CaSO_4$, 0.2mM $NaHCO_3$, 1.0mM NaCl and 0.2mM KCl. After a 10h illumination period ($15Wm^{-2}$), vertical scans were performed onto each of the alkaline band-centres, i.e. the cell nodal position was re-measured, and from this value the positions of the various alkaline band-centres were determined. The vertical scans were through the centre of symmetry of the bands, provided the banding pattern had not moved relative to its previously determined pattern.

Table 4.1 gives a typical set of results obtained using this procedure. The cell studied in this case had four alkaline bands present during the pre-scan experimental investigation. However, band C was not operational at the end of the 10h illumination period. If the OH^- efflux sites on the cell surface are acting to establish spherical diffusion patterns, the steady state OH^- concentration diffusion pattern should fit the diffusion equation of a hollow sphere. The hollow sphere system was selected for the initial analysis because its diffusion pattern was the closest to that obtained in Figure 4.5. If the width of the OH^- efflux band approximates to the radius of the hollow sphere, then the concentration diffusion pattern which these two systems develop (i.e. a band and a spherical effluxing surface), should become equivalent at a short distance from their surfaces.

The steady state hollow sphere equation derived by Carslaw and Jaeger (1959, p. 231 (3)) can be expressed as,

$$C_{(r)} = \frac{aC_1(b-r) + bC_2(r-a)}{r(b-a)} \qquad \ldots(4.4)$$

where $C_{(r)}$ is the concentration at the radial distance rcm, a is the radius of the hollow sphere (equivalent to the radius of the *Chara* cell, R_{Chara}), and C_1 is the concentration at the surface of the hollow sphere, and b is the radial distance at which C_2 is equal to the concentration of the bulk solution. The boundary conditions are that $a < r < b$, $C = C_1$ at $r = a$, and $C = C_2$ at $r = b$. For a particular alkaline band, in the steady state, a, b, C_1 and C_2 are constant and hence equation (4.4) can be reduced to,

$$C_{(r)} = K.\frac{1}{r} - B \qquad \ldots(4.5)$$

where K and B are numerical constants whose values are determined by the boundary conditions. It should be pointed out that the value of r appearing in equations (4.4) and (4.5) is equal to $(R_{Chara} + R)$ where R is the radial distance from the surface of the cell to a particular point in the bathing solution.

If a close approximation to the hollow sphere diffusion system is operating, the graph of $C_{(r)}$ against $\frac{1}{r}$ should be linear. Graphical analysis of $[OH^-]_{(R_{Chara} + R)}$ against $(R_{Chara} + R)^{-1}$ for alkaline band D of Table 4.1 is shown in Figure 4.12. A linear relationship appeared to hold for distances of R greater than 0.04cm. The deviation from linearity in the region of the graph where $[OH^-]$ approached the background value was expected. This was because the effective radial diffusion distance for the OH^- ion would be finite for the time scale employed in this experiment. Hence, at the outer boundary of the alkaline band there would always be a region which was not in the steady state. The non-linear section of the graph in the region where R tended to

zero might have been due to the fact that the band surface source was not an accurate approximation to a spherical surface source, for these small values of R. However, since in this region very small radial distances were involved, it should be pointed out that the pH-sensitive tip was not a "point measuring source". In fact it will be recalled that the hemispherical tips had diameters of approximately 0.15cm and the height of the hemisphere was 0.08 - 0.09cm. This meant that the electrode would measure an average pH value and this value would have been associated with an average height "x", back from the electrode tip, i.e. the pH value observed when the pH-sensitive tip was just touching the cell surface would be,

$$[OH^-]_{(R_{Chara} + R + x)} \neq [OH^-]_{(R_{Chara} + R)}, \quad R = 0 .$$

Consequently each of the radial distances may have been underestimated by a small amount equal to "x". At small values of R, this error would have had a significant effect on the value of $(R_{Chara} + R)^{-1}$. Therefore part of the deviation from linearity observed in Figure 4.12 at large values of $(R_{Chara} + R)^{-1}$, could have been due to an error in R. An attempt was made to evaluate this error (x). Experimentally measured values of R for band D (Table 4.1) are listed in Table 4.2, and corrected values of $(R_{Chara} + R + x)^{-1}$, using x values from 0 to 0.06cm have also been given. These values, in conjunction with the alkaline band D $[OH^-]_{(r)}$ results presented in Table 4.1, were plotted to give Figure 4.13. From this form of "corrective" analysis, it was found that an "x" value of 0.03cm gave an almost perfect linear relationship for all the measured values of $[OH^-]_{(r)}$. This value of 0.03cm for the mean pH-sensing height of the electrode appeared to be a sensible value with respect to the actual hemispherical height of 0.08 - 0.09cm. Over-correction at higher "x" values resulted in the reintroduction of non-linear responses and this

was taken as supporting evidence for the validity of this corrective value of x = 0.03cm. This value was used to graph the diffusion results for the three alkaline bands of Table 4.1; the results are presented in Figure 4.14.

Linear relationships were observed for all three bands, and linearity was also obtained for all other alkaline diffusion experiments. Thus the corrective value of 0.03cm was used throughout the rest of this work. (If a point measuring source for pH had been available, the results which would have been obtained for the distance $R \leqslant 0.03$cm would have deviated from linearity because of the limitation of the basic assumption that the diffusion systems established by the band and the sphere are equivalent).

Characteristics of the Alkaline Diffusion System

The correlation between the corrected experiment results and equations (4.4) and (4.5) indicated that actual OH^- fluxes from each alkaline band could in fact be calculated. The solution for a continuous spherical surface source was given by Carslaw and Jaeger (1959, p. 231,(7)), i.e.

$$Q_t = \frac{4\Pi D\, r_1 r_2\, (C_1 - C_2)}{r_2 - r_1} \qquad \ldots(4.6)$$

where Q_t is the steady state efflux of OH^- (moles s^{-1}), r_1 is equivalent to $(R_{Chara} + R_1)$, r_2 is $(R_{Chara} + R_2)$ and $R_2 > R_1$ (these $R_{1,2}$ are corrected values of R), C_1 and C_2 are the respective OH^- concentrations at r_1 and r_2 and D is the OH^- diffusion coefficient. For the calculation of Q_t, r_1 and r_2 must be selected from the linear section of the $[OH^-]$ vs. $(R_{Chara} + R + x)^{-1}$ graphs and these values were selected from the linear section as far from the band OH^- efflux source as possible. At this distance, and in the

steady state, the flux through the spherical shell could be obtained as an accurate measure of the flux through the band surface, with the least assumptions about the nature of the OH^- efflux site.

Before equation (4.6) is applied to the results presented in Figure 4.14, the OH^- diffusion system will be examined to ascertain whether there are any processes present which will influence the pH of the solution in a spurious manner. The equilibria and other processes which could influence the pH value in the vicinity of an alkaline band are shown below:

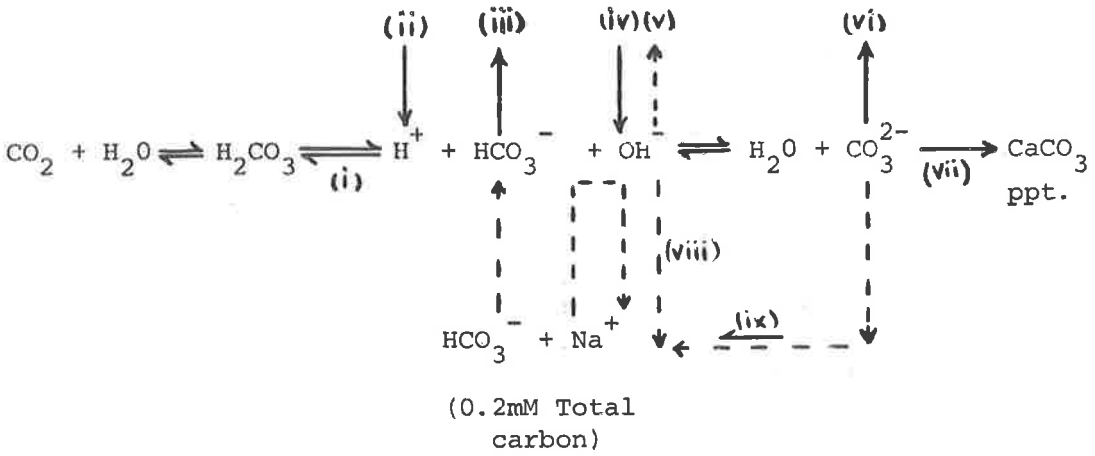

The background pH of the experimental bathing solution was 8.6 and this value increased within the alkaline bands to a value in excess of 10.0. This would mean that the CO_2 concentration would be so low that component (i) would have no influence on the OH^- concentration. The results presented in Figure 4.5 indicated that the iso-concentration lines were not distorted where they met the cell surface. Hence it can be assumed that within the immediate vicinity of the OH^- efflux band, H^+ is not being effluxed and so component (ii) can also be assumed to play no part in influencing the pH value. The influx of HCO_3^- (component (iii)) would lower the concentration of this ion near the cell surface. This would be an advantage because it would maintain the HCO_3^-/CO_3^- equilibrium

in favour of the HCO_3^- species. Under this situation the OH^- ions which are effluxed (component (iv)) will produce their maximum influence on the pH value.

Using the same argument as proposed for H^+ efflux, the rate of OH^- diffusion back into the cell is likely to be extremely small and so component (v) can also be disregarded. No experimental evidence is available which indicates that this species can transport CO_3^{2-}, so (vi) can likewise be assumed to be insignificant. (If CO_3^{2-} could be transported, the process would, in effect, remove one OH^- for every CO_3^{2-} moved). The experimental solution was designed to prevent the precipitation of $CaCO_3$ (component (vii)) and so the loss of OH^- by this reaction will be extremely low. The employment of cells with walls free of visible $CaCO_3$ also aided in the control of this precipitation process.

The remaining components are (viii) and (ix). The removal of OH^- by the conversion of HCO_3^- to CO_3^{2-} is unavoidable since HCO_3^- is a necessary requirement for the photosynthetic production of OH^-. However, this "buffering effect" is not serious because the equilibrium constant for this reaction has a pK of 10.32 (25^oC) and at pH values below this the amount of OH^- removed decreases almost exponentially. A further point to note is that since both the OH^- and CO_3^{2-} ions diffuse away from the OH^- efflux site, down their respective concentration gradients, all the CO_3^{2-} will be converted back to HCO_3^- and OH^- under the influence of the decreasing OH^- values (component (ix)). Consequently it is considered that almost all of the OH^-, efflux from a particular alkaline band, can be measured by an analysis of the concentration gradient established by component (viii), i.e. applying the spherical surface source equations (see equation (4.6)) should enable the calculation

of the rate of OH^- efflux and the error associated with the physical system will be small.

Equation (4.6) was therefore applied to the results presented in Figure 4.14 and the individual alkaline band efflux rates are presented in Table 4.3. The total OH^- efflux for this cell, based on surface area, was 11.69 pmol $cm^{-2}s^{-1}$ in the presence of 0.2mM $NaHCO_3$. This procedure was repeated several times to test the accuracy of the technique. The results of these experiments are tabulated in Table 4.4. The average OH^- efflux, on a cell surface area basis, was 12.45 ± 0.47 pmol $cm^{-2}s^{-1}$. The very close agreement between the respective experimental values was reflected in the small standard error of the mean. This average OH^- efflux value was compared with the $H^{14}CO_3^-$ influx results obtained under the same total carbon concentration (0.2mM $NaHCO_3$). The $H^{14}CO_3^-$ influx value, which was determined using graph (C) presented in Figure 3.4, was 13.0 ± 0.5 pmol $cm^{-2}s^{-1}$. The agreement between these independently obtained values was extremely encouraging.

Figures 4.14 and 4.15 (the results of which are expressed as Exp. No. 1, Table 4.4) are included to illustrate the relationship between the pH scans along the cell surface and the actual OH^- efflux value determined for a particular alkaline band. For example, a band-centre pH value of 9.4 corresponded to an OH^- efflux of 0.57 pmol s^{-1} (band C), a pH value of 9.95 to an efflux of 1.51 pmol s^{-1} (band A) and a pH value of 10.2 was associated with an efflux value of 3.53 pmol s^{-1} (band E) for this particular cell. These values indicated that the OH^- efflux estimations reported by Lucas and Smith (1973) were too large; this overestimation resulted from the invalid assumptions relating to the alkaline band geometry.

Correlation between ΣO_t for OH^- and the Influx of $H^{14}CO_3^-$

An internal test, which was applied to further examine the validity of the diffusion analysis model (spherical surface source), firstly involved the evaluation of the total OH^- efflux for a particular cell. The $H^{14}CO_3^-$ influx, by this cell, was then measured under exactly the same conditions as used for the diffusion analysis. These experiments were performed using 0.5mM $NaHCO_3$ in the low Ca^{++} (0.02mM) bathing solution and the values which were obtained are presented in Table 4.5. An examination of the calculated total OH^- efflux and the measured $H^{14}CO_3^-$ influx values indicated that the correlation between these fluxes was excellent. The agreement between the calculated total OH^- efflux and $H^{14}CO_3^-$ influx values of Table 4.5 and the $H^{14}CO_3^-$ influx values presented in Figure 4.11 and the earlier results of Figure 3.4, was also assumed to add support to the validity of the OH^- efflux analysis.

HCO_3^- Uptake Equivalent to Influx

Under the experimental conditions employed for exogenous HCO_3^-, the concentration of CO_2 in the bathing solution was very low. Hence an outward diffusion gradient would exist across the plasmalemma as well as an inward CO_2 diffusion gradient from the cytoplasm to the stromal matrix of the chloroplasts. If a significant component of the $H^{14}CO_3^-$ influx was lost from the cell via $^{14}CO_2$ diffusion back into the bathing solution, then the ^{14}C fixation value would be smaller than the total OH^- efflux value by this amount. This would be because the diffusion of CO_2, from the cytoplasm to the bathing solution, would leave within the cytoplasm one OH^- ion for every CO_2 molecule which escaped to the bathing sclution. Since there was little difference

between the ^{14}C and total OH^- efflux values it was assumed throughout this dissertation that $H^{14}CO_3^-$ uptake was equivalent to $H^{14}CO_3^-$ influx.

The Acid Band: Diffusion Analysis Based on the Diffusion in a Cylindrical Coordinate System

It was apparent from Figure 4.8 that the diffusion pattern developed by an acid band approximated to that of a continuous cylindrical surface source. The length of the individual bands, present on the cell surface, was always influenced by the number of operational alkaline bands; the more OH^- efflux sites, the shorter the individual acid band lengths. This alkaline band dominance made the analysis of the acid diffusion system very much more difficult than would have resulted if the measurements could have been made in the absence of the alkaline banding system.

The steady state hollow cylinder diffusion equation was derived by Crank (1956, p. 62 (5.4)),

$$C_{(r)} = \frac{C_1 \ln \frac{b}{r} + C_2 \ln \frac{r}{a}}{\left(\ln \frac{b}{a}\right)} \qquad \text{.....(4.7)}$$

where the longitudinal axis of the cylinder is considered to lie along the Z axis, $C_{(r)}$ is the H^+ concentration at the radial distance r(cm) (perpendicular to the Z axis), a is the radius of the cylinder and all other terms follow the terminology of equation (4.4). As before, equation (4.7) can be reduced to,

$$C_{(r)} = A + D \ln r$$

where A and D are numerical constants whose values are determined by the boundary conditions.

A plot of $C_{(r)}$ against $\ell n\ r$, for the results expressed in Figure 4.7B (S1) is presented in Figure 4.17. (Note that the value of r has been corrected for the mean pH electrode sensing height, and hence is expressed as (R_{Chara} + R + x cms)). A linear relationship appeared to hold until values of r were encountered where the steady state situation had not been established. This linearity suggested that the acid bands could be analysed using an expression for a continuous cylindrical surface source. Carslaw and Jaeger (1959, p. 262) dealt with this particular situation, and they stated that it could not be solved in terms of known tabulated functions.

However, these workers derived the steady state equations relating to a circular cylinder of infinite length in which the diffusing substance (in this case H^+) was being supplied at a constant rate F_t per unit cylinder length. In this analysis they showed that the concentrations C_1 and C_2, at r_1 and r_2 respectively, were related to the constant flux F_t by:

$$F_t = \frac{2\pi D\ (C_1 - C_2)}{\ell n\ \frac{r_2}{r_1}} \qquad .....(4.9)$$

The important points concerning this expression are that the relationship is independent of how the H^+ is supplied and also of the boundary conditions at the inner cylindrical surface.

Equation (4.9) was used to obtain an estimate of the net H^+ efflux associated with the results presented in Figures 4.7 and 4.17. In this calculation the value used for D* was 3.3356 x 10^{-5} $cm^2 s^{-1}$ and C_1 and C_2 were selected from the linear portion

---

* Limiting diffusion coefficient for HCl; see footnote concerning calculation of D_{NaOH} for full details.

of the graph (see Figure 4.17). The value for F_t was 0.43 pmol s^{-1} and it should be stressed that this is the quantity being effluxed through a unit length (1cm) of cell surface. This value can only be taken as an approximate value of the net H^+ efflux because the acid bands were of finite length. To allow for this finite length, end corrections would have to be applied because the H^+ flow can no longer be assumed to occur solely in the radial direction.

Other complicating factors also exist which cause an underestimation of the actual net H^+ efflux. The first was the neutralization component associated with each acid / alkaline overlap region. The exact amount of H^+ which would have been removed by this process would be difficult to evaluate. Secondly, there would also have been a slight reduction in H^+ concentration due to the conversion of HCO_3^- to H_2CO_3 and hence to CO_2. However, since the bathing solution only contained carbon supplied by equilibration with the atmosphere, the depression of F_t due to this interaction would be small.

Most cells of 3-4cm in length were observed to have a combined acid band length of approximately 1cm (see for example Figure 4.1, 1cm in 3.9, Figure 4.9, 1.4cm in 4.0). Hence without allowing for any of the above factors, the net H^+ efflux on a cell surface area basis would be between 0.8 and 1.2 pmol $cm^{-2}s^{-1}$. It would seem, therefore, that the net H^+ efflux in these cells is either considerably smaller than that present in *Nitella clavata*, or that other workers have overestimated their values by an order of magnitude (cf. Spear et al., 1969; Rent et al., 1972; and Brown et al., 1973).

Finally it should be emphasised that the measured H^+ flux was a net component of H^+ escaping from the cell. The relationship of this value to total H^+ efflux cannot be determined using this technique.

DISCUSSION

It is clear from this study that the basic mechanisms of the acid and alkaline systems differ. The localized band surface sources of OH^- are quite obviously acting as disposal sites for the internally generated OH^- ions, that is, these ions result when CO_2, supplied as HCO_3^-, is fixed photosynthetically. The plasmalemma mechanism which operates to transport these ions will be considered in detail in Chapters Five and Seven.

The acid bands appear to form as a result of uniform H^+ efflux over the cell surface in regions where the OH^- efflux systems are not operational. The H^+ efflux analysis would be very much simpler if the alkaline bands could be inhibited in such a way that the acid efflux remained unaffected. It may be possible to find an analogue for HCO_3^- which would competitively inhibit this system at pH values of approximately 7.0. However, the analogue would have to be effective at very low concentrations or the combined buffering capacity of the analogue and HCO_3^- would become a serious problem. Studies in search of this analogue have as yet been unsuccessful.

It was also found during these studies that, under conditions of 0.1 - 0.2mM $NaHCO_3$ and bathing solution pH values of 7.5 to 8.6, very little net H^+ efflux could be detected, i.e. very few of the experimental scans conducted along the cell wall revealed pH values lower than the pH of the bathing solution (see Figure 4.15 as a typical example). Admittedly the $NaHCO_3$ would tend to buffer the influence of the H^+ ions that were being effluxed, but if acid fluxes of the magnitude reported by Spear et al. (1969) were present, they certainly would have been observed. The small values of net H^+ efflux inferred from this study do not

give support to Spanswick's extension of Kitasato's hypothesis.

When the pH values along the cell surface between two OH^- efflux sites are raised above that of the background solution, it is proposed that this arises by the combined OH^- diffusion from the two efflux sites, that is the spherical diffusion pattern extends out into the bathing solution and along the cell surface until eventually the alkaline spheres overlap. At the area of overlap the concentration of OH^- ions will increase at a faster rate and this in turn will eventually cause distortion of the spherical diffusion pattern. The extent to which the pH value in this inter-alkaline region is increased will depend upon the distance between the operational OH^- efflux sites and on the actual efflux rates from these sites.

Connection between the Alkaline System and Other Membrane Properties

If the HCO_3^- and OH^- ions are transported across the plasmalemma on an obligate coupled non-electrogenic system they could not contribute to the membrane conductance. If the passive permeability coefficients of these ions are also very low, their contribution to the membrane potential would also be insignificant. The $H^{14}CO_3^-$ results, which indicate the accuracy of the analysis used to evaluate the total OH^- efflux for each cell, do not indicate the manner in which the HCO_3^- enters the cell, i.e. it is not possible to say whether the HCO_3^- enters only in the OH^- efflux regions or in fact uniformly over the entire cell surface. (The latter may in fact be the expected situation). Hence, because the nature of these transporters is not known, their contribution to the electrical properties of the plasmalemma should not be rejected (cf. Richards and Hope, 1974). If the obligate coupling between the very active HCO_3^- influx and OH^- efflux systems can be disproved,

the relationship between these carriers and the electrical properties of the plasmalemma may in fact be very important.

In fact this successful analysis of the alkaline banding system will enable an investigation to be conducted on the response of the OH^- efflux system to illumination, i.e. this response can be fitted to the continuous spherical surface source equation (see Carslaw and Jaeger, 1959, p. 263 (10)) and the manner in which Q_t (OH^- efflux) changes after the onset of illumination, and approaches the steady state, can be obtained. These results can then be compared with the cellular response of the membrane potential and resistance to illumination, to determine whether any correlation exists between the two phenomena.

TABLE 4.1

Alkaline Band Diffusion Analysis: Vertical pH Scan Values

Alkaline Band	Vertical Height* above the cell surface, "R" (mm)	Steady pH electrode value (mV)	pH (converted using calibration graph)	$[OH^-]^{**}$ (moles cm^{-3} x 10^{10})
A	0.0	486	10.18	1524
	0.1	482.5	10.13	1349
	0.2	480	10.08	1208
	0.3	477	10.04	1084
	0.4	474.5	9.99	966
	0.5	472	9.95	881
	0.6	469.5	9.90	794
	0.7	467	9.86	724
	0.9	462	9.77	596
	1.1	456.5	9.68	479
	1.3	452	9.60	398
	1.5	448	9.54	343
	1.7	444	9.46	290
	1.9	440	9.39	247
	2.1	436.5	9.32	208
	2.3	432	9.26	182
	2.6	426	9.16	143
	2.9	420	9.05	112
	3.2	414	8.94	88
	3.5	407.5	8.83	68
	3.8	400.5	8.71	51
	4.1	393.5	8.59	39
	5.1	368	8.15	14.1
	7.1	332	7.52	3.32
B	0.0	476	10.01	1028
	0.2	472	9.95	881
	0.4	465	9.83	668
	0.6	459	9.72	525
	0.8	453	9.62	417
	1.0	448	9.54	343
	1.2	443	9.44	279
	1.5	434.5	9.30	199
	1.8	426	9.16	143
	2.1	419	9.03	108
	2.4	411	8.89	78
	2.7	402	8.74	55
	3.0	392.5	8.57	37
	5.0	336	7.59	3.9
	7.0	320	7.31	2.0

..(contd.)

TABLE 4.1 (contd.)

Alkaline Band	Vertical Height* above the cell surface, "R" (mm)	Steady pH electrode value (mV)	pH (converted using calibration graph)	$[OH^-]^{**}$ (moles cm^{-3} x 10^{10})
C	0.0	310	7.14	1.30
	0.3	320	7.31	2.04
	*1.3	321	7.32	2.1
	3.3	317	7.26	1.8
	7.3	314	7.21	1.6
D	0.0	482.5	10.13	1349
	0.1	479	10.07	1175
	0.2	475.5	10.00	1004
	0.3	472	9.95	881
	0.4	469	9.89	780
	0.5	466.5	9.85	708
	0.6	463.5	9.80	631
	0.7	461	9.75	569
	0.9	455	9.66	457
	1.1	449.5	9.56	361
	1.3	444	9.47	292
	1.5	439	9.38	240
	1.7	434	9.29	196
	1.9	429	9.21	161
	2.2	419.5	9.04	110
	2.5	409.5	8.87	74
	2.8	399	8.68	48
	3.1	388	8.49	31
	4.1	350	7.84	6.9
	5.1	330	7.48	2.7
	7.1	314	7.21	1.6

* This value of the vertical height above the cell surface was the vertical (radial) distance from the cell wall to the lowest part of the hemispherical pH-sensitive electrode tip. Thus when the tip just touched the cell wall, this situation was assigned the value of 0.0(mm)

** [OH] is actually the activity of the OH^- ion.

TABLE 4.2

Mean Electrode Sensing Distance

Vertical Height above the cell surface, R (mm)	Electrode Correction Factor "x" $\frac{1}{R + R_{Chara} + x}$ (cm^{-1})					
	x = 0	x = 0.01cm	x = 0.02	x = 0.03	x = 0.04	x = 0.06
0.0	23.53	19.05	16.00	13.80	12.12	9.76
0.1	19.05	16.00	13.80	12.12	10.81	8.88
0.2	16.00	13.80	12.12	10.81	9.76	8.16
0.3	13.80	12.12	10.81	9.76	8.88	7.55
0.4	12.12	10.81	9.76	8.88	8.16	7.02
0.5	10.81	9.76	8.88	8.16	7.55	6.56
0.6	9.76	8.88	8.16	7.55	7.02	6.15
0.7	8.88	8.16	7.55	7.02	6.56	5.80
0.9	7.55	7.02	6.55	6.15	5.80	5.19
1.1	6.56	6.15	5.80	5.48	5.19	4.71
1.3	5.80	5.48	5.19	4.93	4.71	4.30
1.5	5.19	4.94	4.71	4.49	4.30	3.96
1.7	4.71	4.49	4.30	4.12	3.96	3.67
1.9	4.30	4.12	3.96	3.81	3.67	3.42
2.2	3.81	3.67	3.54	3.42	3.30	3.10
2.5	3.42	3.31	3.20	3.10	3.01	2.84
2.8	3.10	3.01	2.92	2.83	2.76	2.61
3.1	2.83	2.76	2.68	2.61	2.55	2.42
4.1	2.20	2.16	2.12	2.07	2.03	1.95
5.1	1.81	1.77	1.75	1.72	1.69	1.63
7.1	1.33	1.31	1.29	1.28	1.26	1.23

R_{Chara} = 0.0425cm (Radius of the experimental *Chara* cell).

TABLE 4.3

Calculation of the Total OH^- Efflux for a Single *Chara* cell

r_1 (cm)	r_2 (cm)	(r_2-r_1) (cm)	D (cm^{-2} s^{-1})	$4\pi D \frac{r_1-r_2}{r_2-r_1}$ (cm^3 s^{-1})	Band No									ΣQ_t (pmol s^{-1})	$\frac{\Sigma Q_t}{\text{Surface area}^*}$ (pmol cm^{-2} s^{-1})
					A			B			D				
					C_1+	C_2	Q_t	C_1	C_2	Q_t	C_1	C_2	Q_t		
0.1	0.2	0.1	2.129 x 10^{-5}	5.351 x 10^{-5}	1101	422	3.63	786	256	2.83	908	306	3.22	9.68	11.69

* The surface area of this cell was 0.828 cm^{-2}

\+ C_1 and C_2 are in moles cm^{-3} x 10^{-10}

TABLE 4.4

Tabulation of Q_t values for each OH^- band obtained using equation (4.6) and the summation of Q_t to give total OH^- efflux per cell

Exp. No.	Band No.							ΣQ_t (pmol s^{-1})	$\frac{\Sigma Q_t}{\text{Surface area}}$ (pmol $cm^{-2}s^{-1}$)	+ Chlorophyll concentration (µg Chl cm^{-2})
	A	B	C	D	E	F	G			
1	1.51*	3.02	0.57	2.76	3.53			11.39	12.95	
2	1.0	2.10	2.10	1.78	5.98	0.35	0.07	13.38	10.40	10.82
3	1.25	1.43	2.79	0.80	2.54			8.81	11.49	8.71
4	5.64	4.78	1.43					11.85	13.62	8.90
5	1.51	3.02	0.57	2.76	3.53			11.39	12.95	10.62
6	1.73	1.74	1.41	1.61	1.48	1.74	1.70	11.41	13.85	

Experimental conditions were 15 Wm^{-2} illumination for 12h before commencing the vertical scans and the bathing solutions contained 0.2mM $NaHCO_3$, 0.02mM $CaSO_4$, 1.0mM NaCl and 0.2mM KCl.

* Values of Q_t for each band in pmol s^{-1}.

\+ Determined using the equations derived by Arnon (1949) (see Appendix B).

TABLE 4.5

Correlation between total OH^- efflux calculated using the diffusion analysis and $H^{14}CO_3^-$ influx obtained on the same cell

Exp. No.	Band No.					ΣQ_t (pmol s^{-1})	$\frac{\Sigma Q_t}{\text{surface area}}$ (pmol $cm^{-2}s^{-1}$)	$^{14}HCO_3^-$ Influx (pmol $cm^{-2}s^{-1}$)
	A	B	C	D	E			
16	2.15*	4.54	5.35	--	--	12.04	25.40	28.60
18	5.13	1.39	1.49	1.92	2.67	12.60	24.43	25.14
20	2.72	5.95	4.60	3.99	--	17.26	27.61	25.93

Experimental conditions were 15 Wm^{-2} illumination for 6h before commencing the vertical scans and the bathing solutions contained 0.5 mM $NaHCO_3$, 0.02mM $CaSO_4$, 1.0mM NaCl and 0.2mM KCl.

* Values of Q_t for each band (pmol s^{-1}).

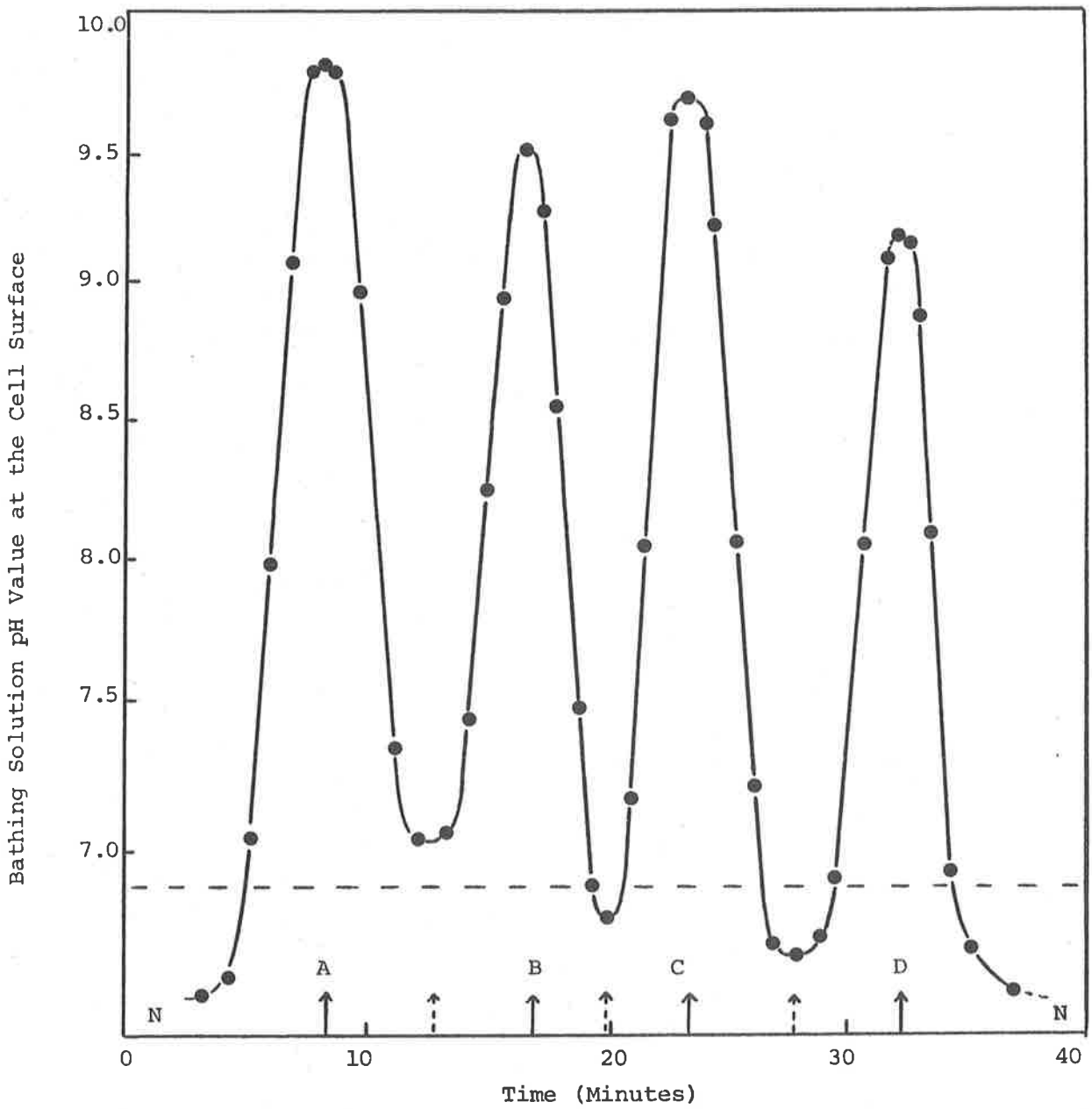

Figure 4.1. Alkaline and acid bands developed at the surface of a *Chara corallina* cell. The cell was given a 2h illumination period ($15 Wm^{-2}$) in bathing solution which contained 0.1mM $NaHCO_3$, pH 6.94. (The surface of the experimental chamber was sealed with liquid paraffin). At the end of this 2h period the pH-sensitive tip of the electrode was used to measure the pH values which had developed on the cell surface. The alkaline band-centres are labelled A to D and their locations are indicated by the solid arrows. The broken arrows indicate the inter-alkaline regions and when their pH value falls below that of the bathing solution, they are termed acid bands.

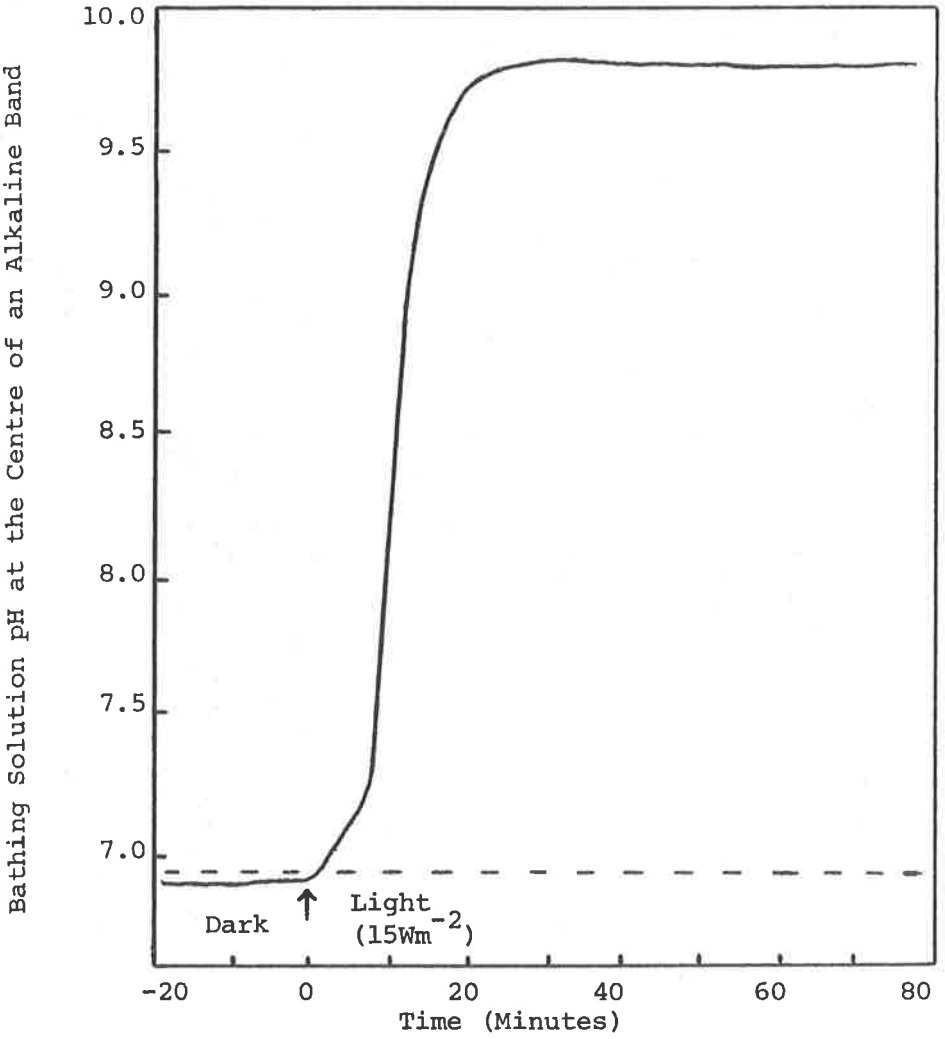

Figure 4.2. Alkalinization Time-Course following illumination.

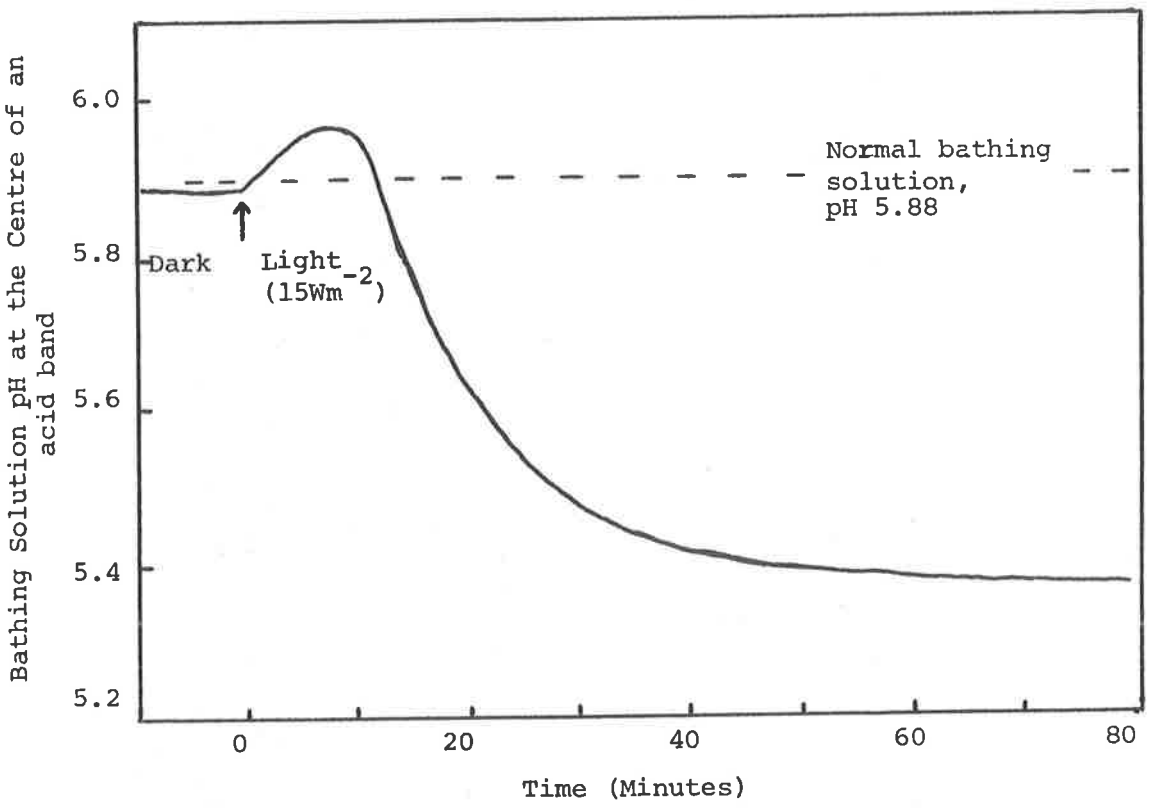

Figure 4.3. Acidification Time-Course following illumination.

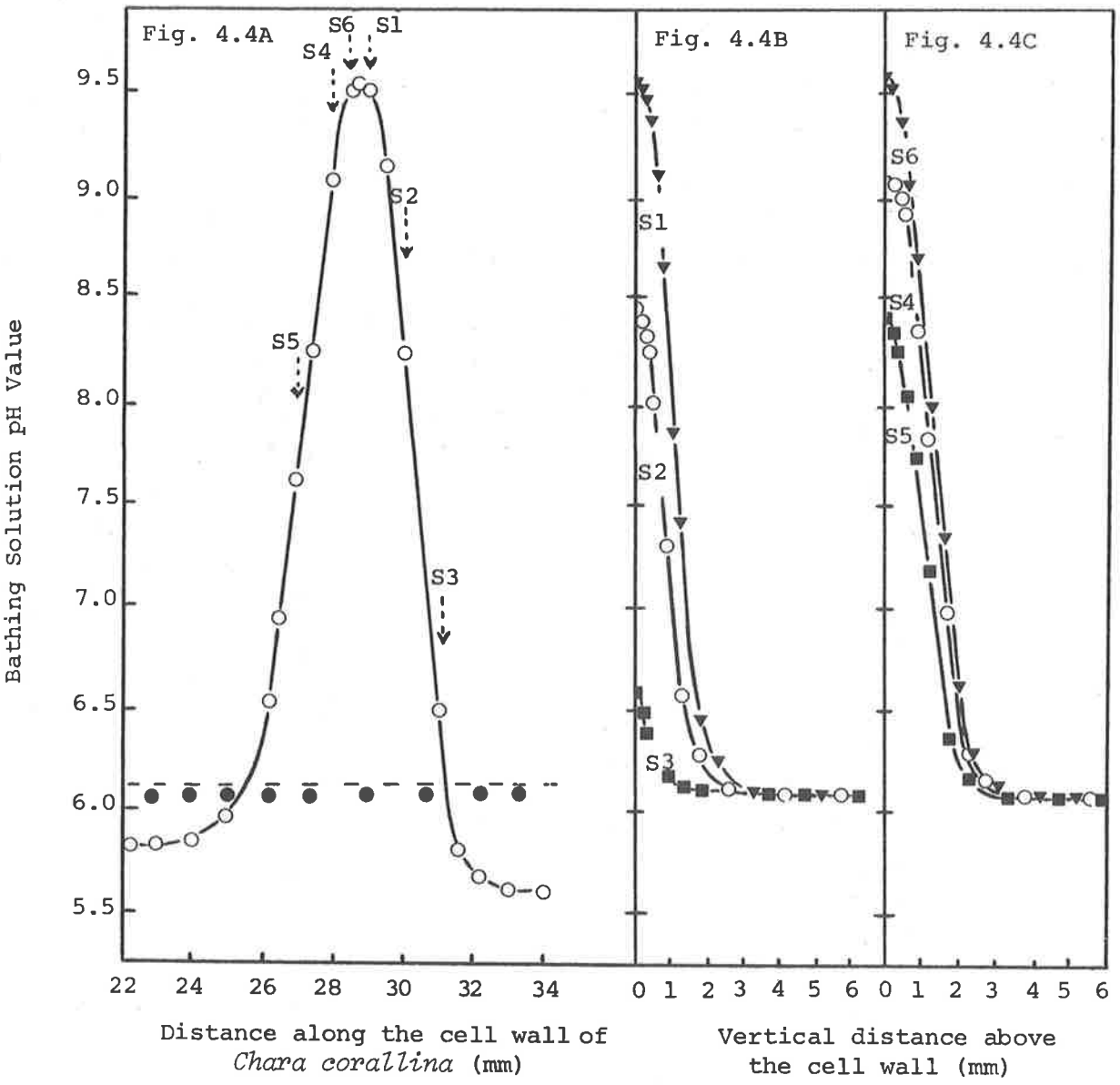

Figure 4.4. Two dimensional analysis of the pH values associated with an alkaline band. A; presents the results of a pH scan along the cell surface after 2h illumination; a normal agar block was employed. The arrows represent the positions of the vertical scans, the results of which are presented in B and C.
B and C; the vertical scans conducted after 4h illumination ($10 Wm^{-2}$). Each scan took approximately 40 minutes to perform and involved the step-wise lowering of the electrode, through the agar, onto the cell wall. The broken line represents the pH of the bathing solution, and (●), the dark cell wall values. The symbol S represents the vertical scan and they were conducted in the order S1 to S6.

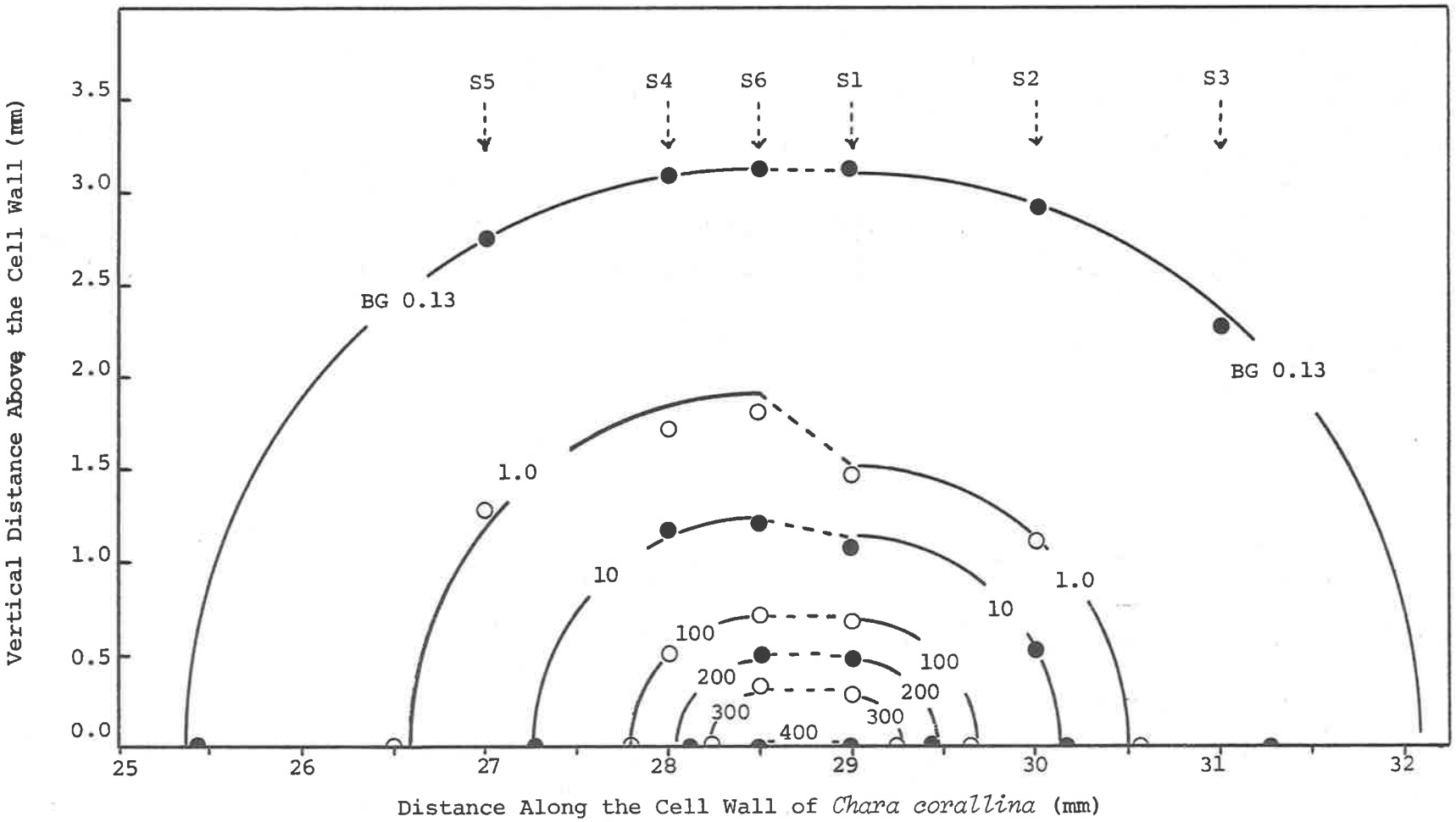

Figure 4.5. Two dimensional iso-concentration pattern of an hydroxyl band, constructed using the results presented in Figure 4.4. The hydroxyl band-centre extends from 28.5 to 29.0mm. The number associated with each iso-concentration line is its actual OH^- concentration in moles cm^{-3} x 10^{-10}. BG 0.13 indicates the background OH^- value of the bathing solution.

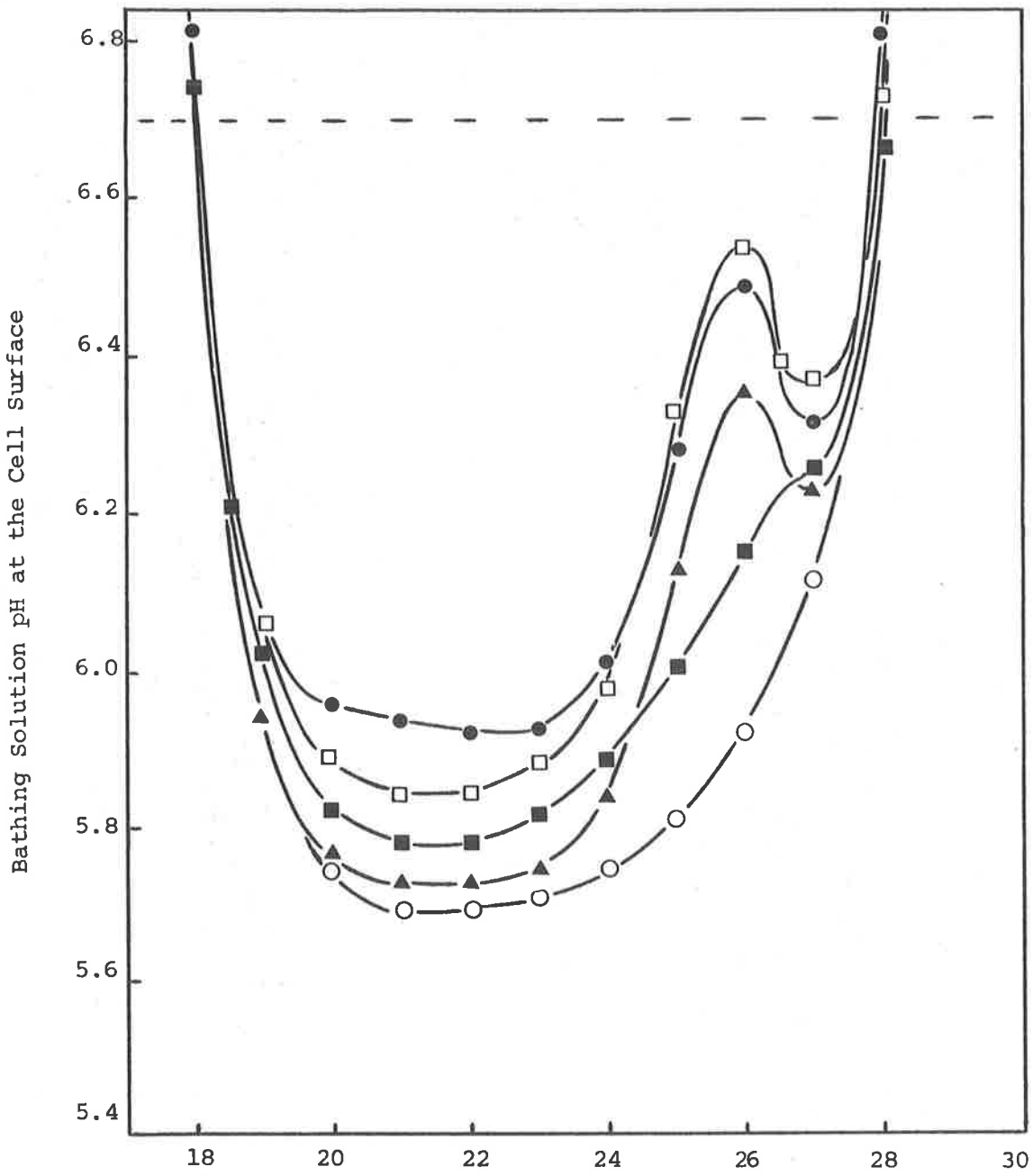

Figure 4.6. Cell surface pH values in an acid band: variation with time. This acid band was first scanned after 70 minutes illumination (●). Scans were repeated at 120 (□), 180 (■), 300 (▲) and 400 (○) minutes after the onset of illumination. After the (▲) scan, the cell was given a 10 minute dark period; this was successful in removing the non-active alkaline band which was located at the 26mm site.

Figure 4.7. Two dimensional analysis of the pH values associated with an acid band.

Figure 4.7A. represents the results of a pH scan conducted along the cell wall after 6h illumination. The arrows on this figure represent the positions of the vertical scans conducted when the cell was held in a channel-free agar block.

Figure 4.7B, C and D represent the results of the vertical pH scans conducted through the agar block, onto the cell surface. The cell was illuminated for 6h prior to the commencement of these scans. Each scan took approximately 30min, and they were conducted in the order S1 to S5.

The broken line represents the pH value of the bathing solution.

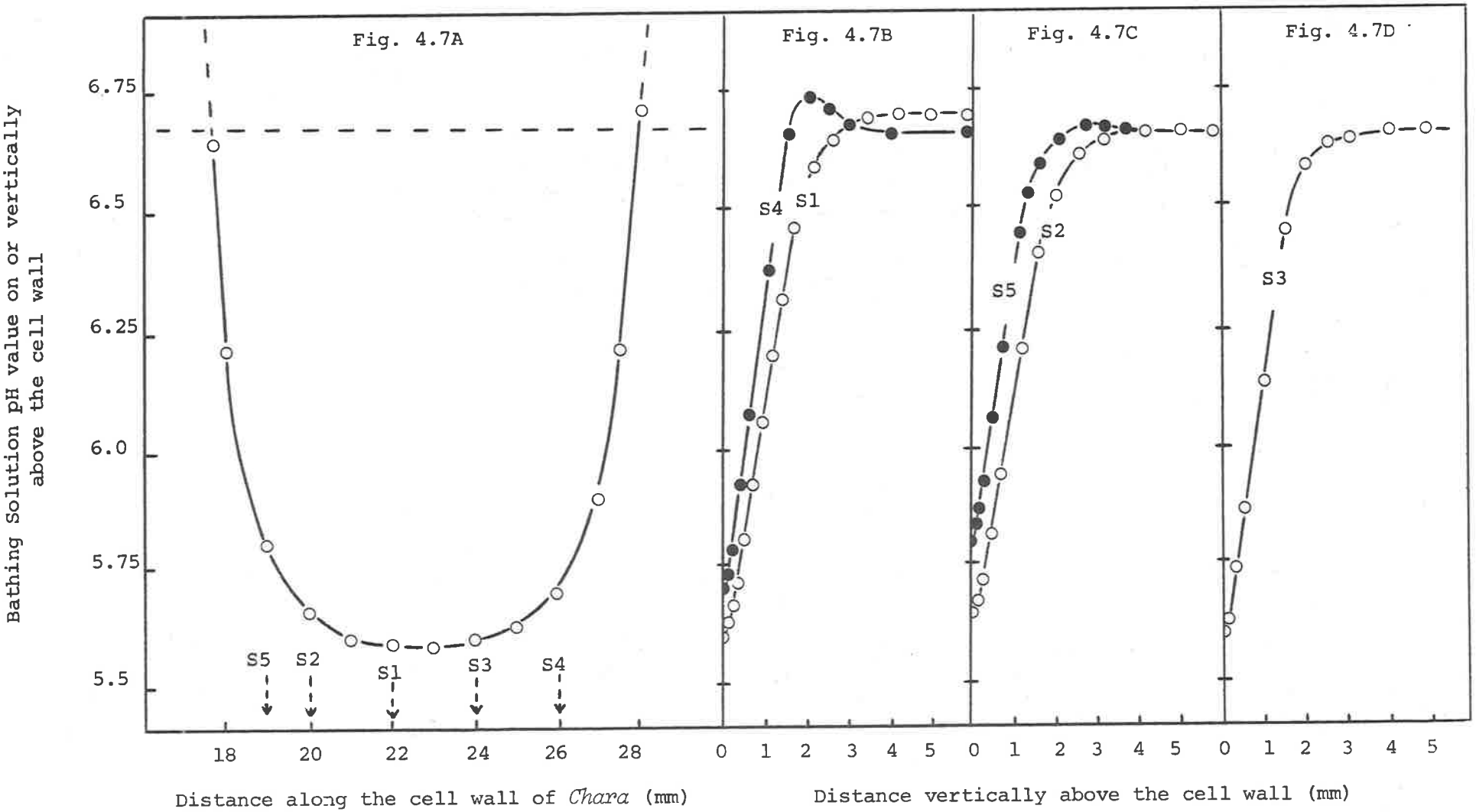
Fig. 4.7A
Fig. 4.7B
Fig. 4.7C
Fig. 4.7D
Bathing Solution pH value on or vertically above the cell wall
6.75
6.5
6.25
6.0
5.75
5.5
S5
S2
S1
S3
S4
18
20
22
24
26
28
0 1 2 3 4 5
Distance along the cell wall of *Chara* (mm)
Distance vertically above the cell wall (mm)

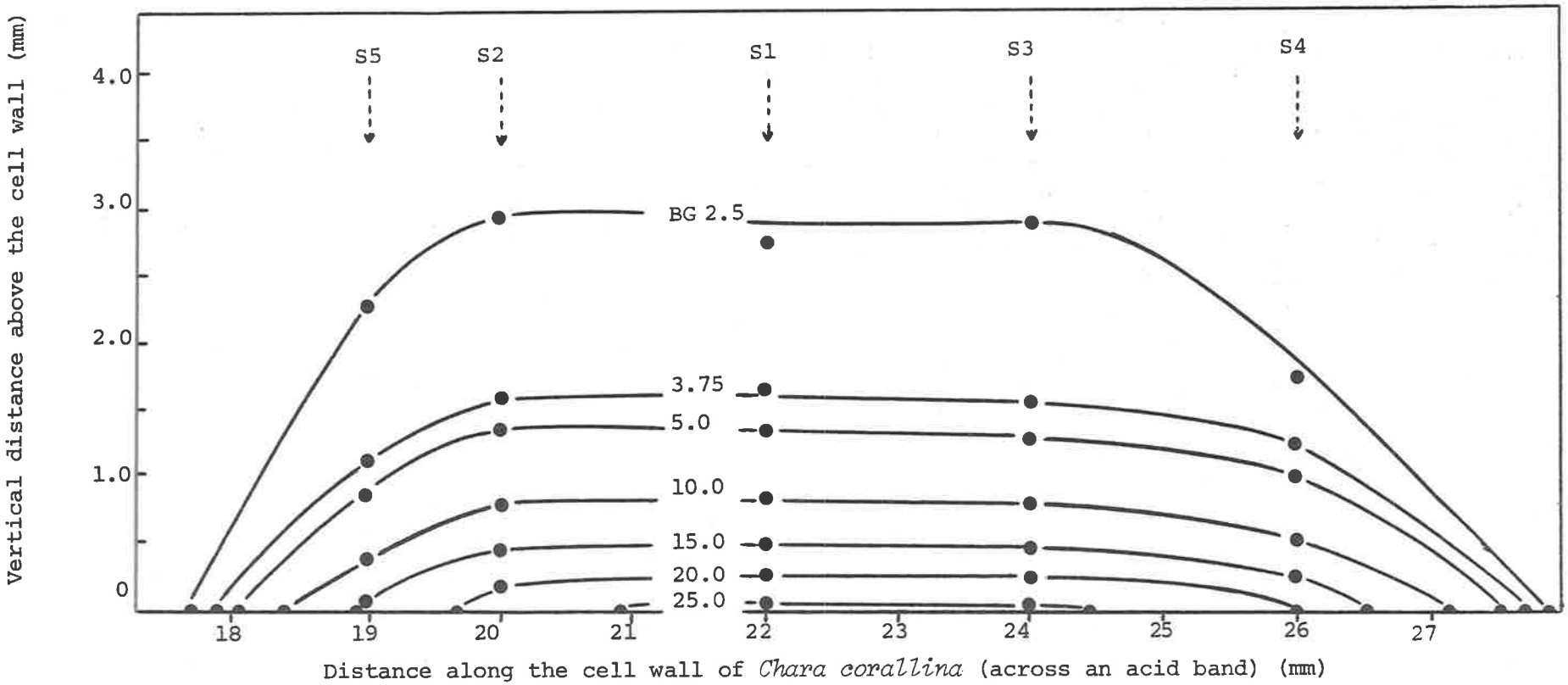

Figure 4.8. Two dimensional iso-concentration pattern, of an acid band, constructed using the results presented in Figure 4.7. The number associated with each iso-concentration line is its actual H^+ activity in mol cm^{-3} x 10^{-10}. BG 2.5 indicates the background value of the bathing solution.

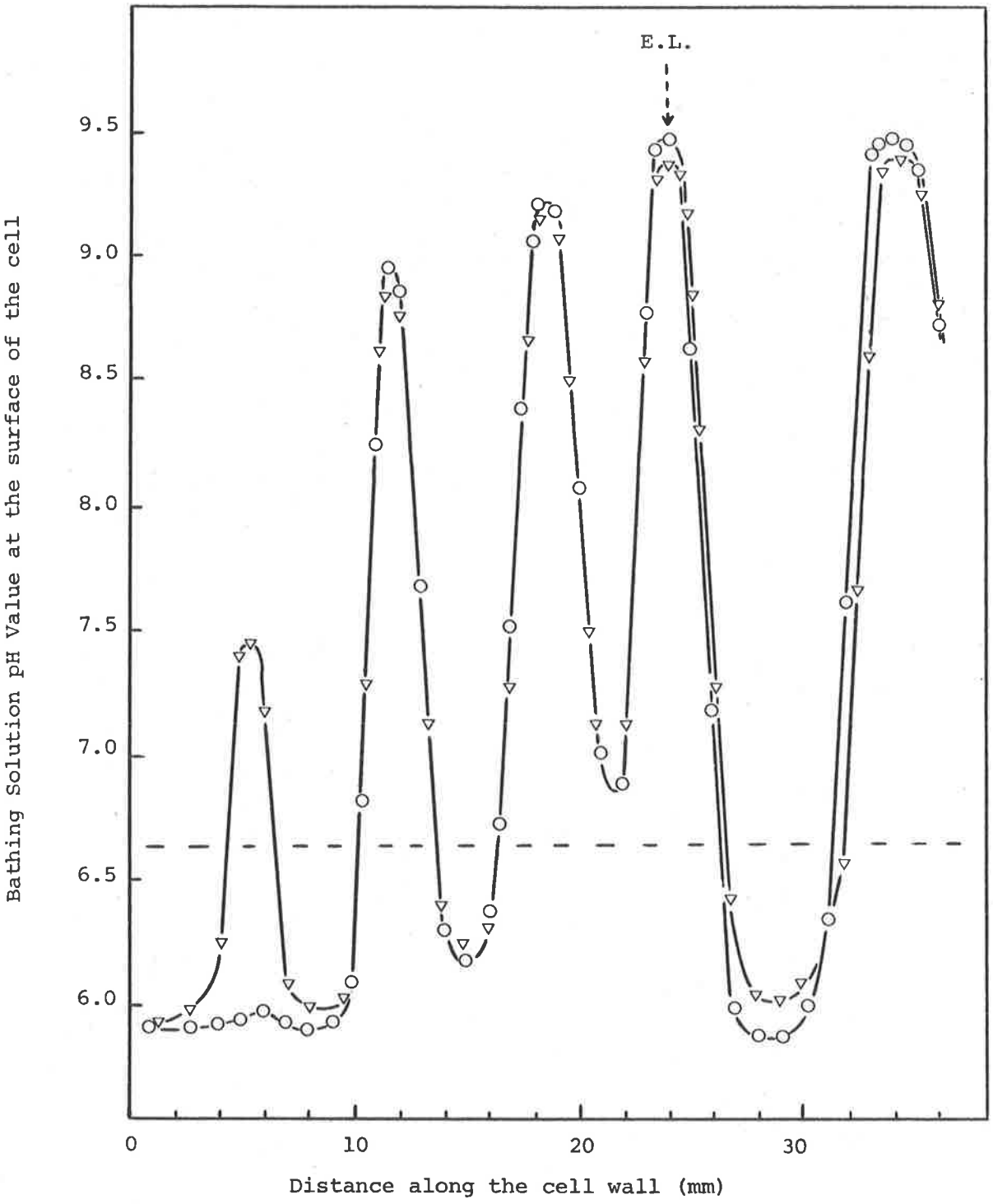

Figure 4.9. pH values around the surface of a cell. Cell wall pH values were obtained after 2h illumination in normal bathing solution, (O) indicates values obtained when the cell was in the 0° position and (▽) the 180° position. E.L. refers to the pH-sensitive electrode position used to obtain the results presented in Figure 4.10.

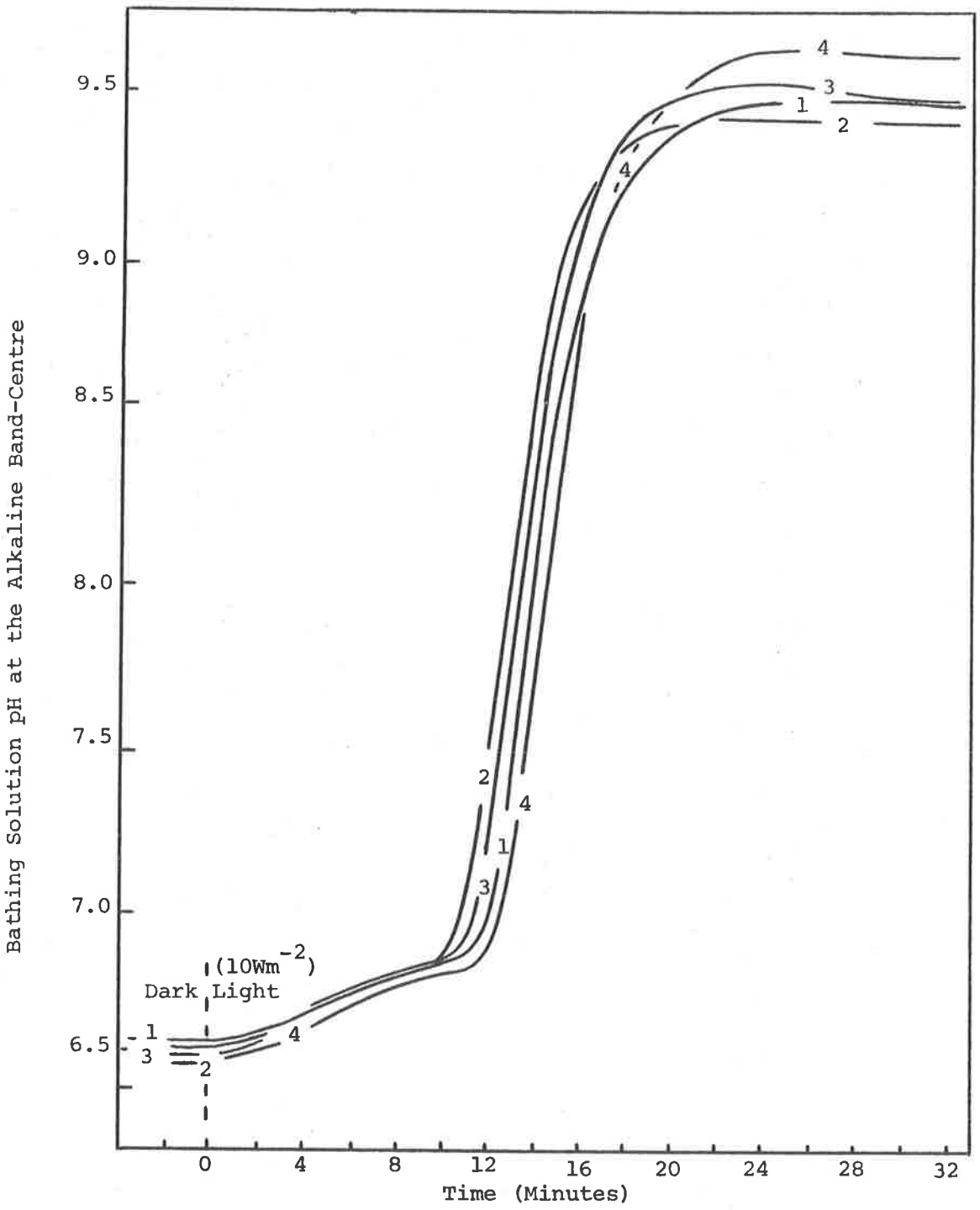

Figure 4.10.

An alkaline band response to illumination (10Wm^{-2}). Each trace is part of the alkaline band response to 1h dark treatment followed by a 1h light treatment. The alkaline band used for this experiment and the electrode location are indicated on Figure 4.9. Traces 1 and 3 represent the alkaline band response when the cell was in the 0° position and traces 2 and 4 the response when the cell was in the 180° position.

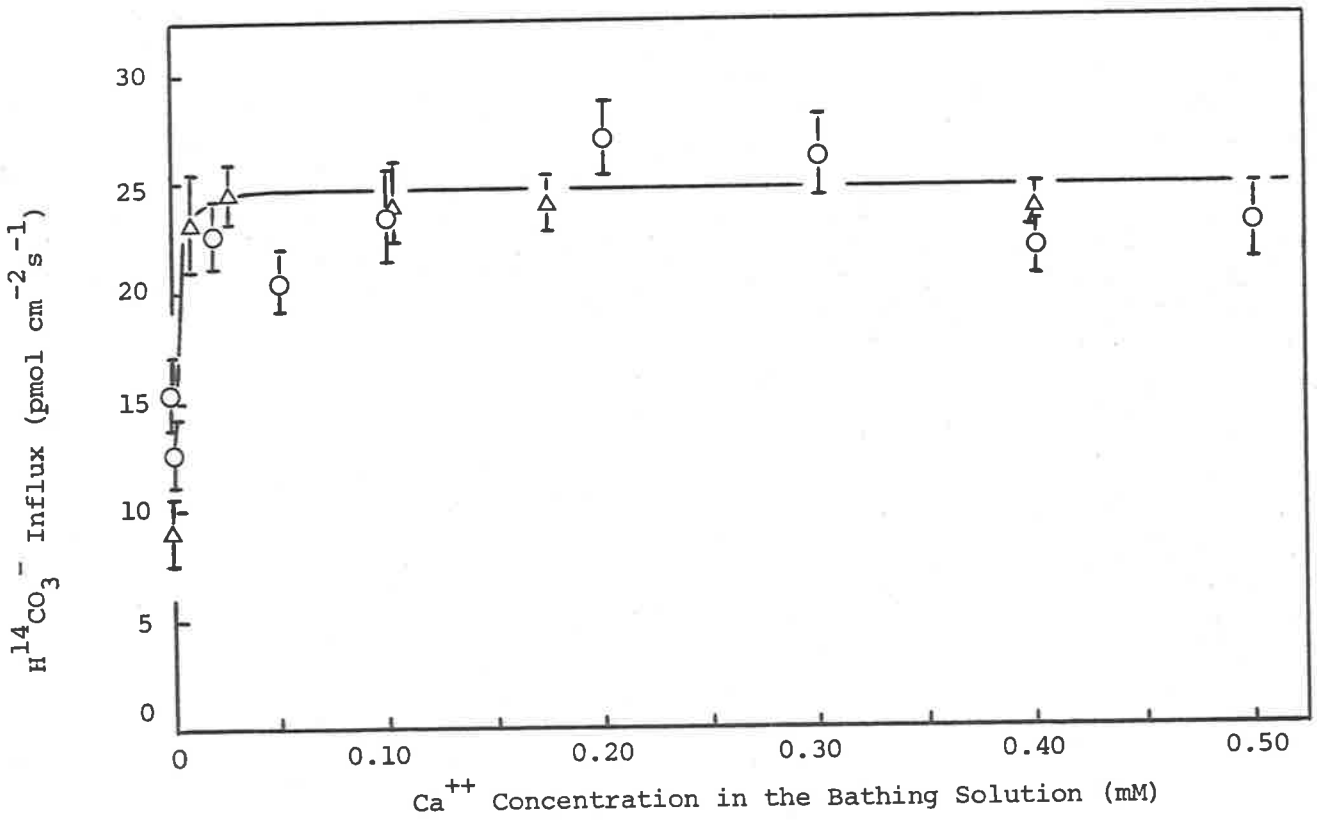

Figure 4.11. Influence of Ca^{++} concentration, in the bathing solution, on $H^{14}CO_3^-$ influx. The light intensity for all experiments was $15Wm^{-2}$. The symbol, (O) represents the experimental sequence: 2h recovery period after cutting followed by 1h pretreatment in experimental solutions and a further 1h in the $H^{14}CO_3^-$ solutions. The symbol, (△) represents the experimental sequence in which a 10h pretreatment in 0.02mM $CaSO_4$ bathing solution was included. This was incorporated between the 2h recovery phase and the 1h experimental pretreatment. The solutions contained 0 - 0.5mM $CaSO_4$, 1.0mM NaCl, 0.2mM KCl and 0.5mM $NaHCO_3$ and were buffered at pH 8.6.

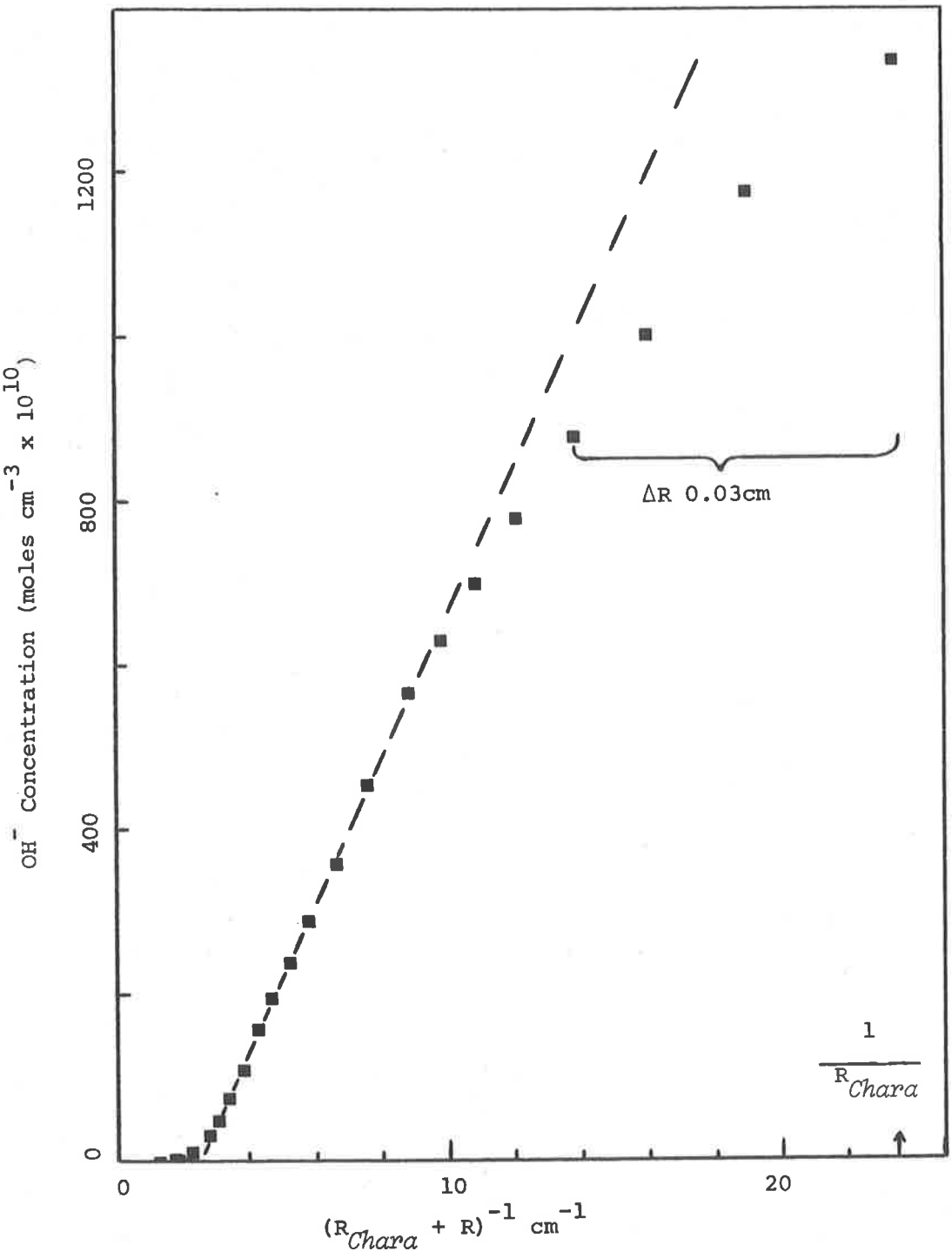

Figure 4.12. Graph of $[OH^-]_r$ against $(R_{Chara} + R)^{-1}$. The results for this graph were obtained from Table 4.1, band D. The value of $1/R_{Chara}$ is marked on the ordinate axis, at this value R is assumed equal to zero. The bracketed points represent the $[OH^-]$ values measured close to the cell surface.

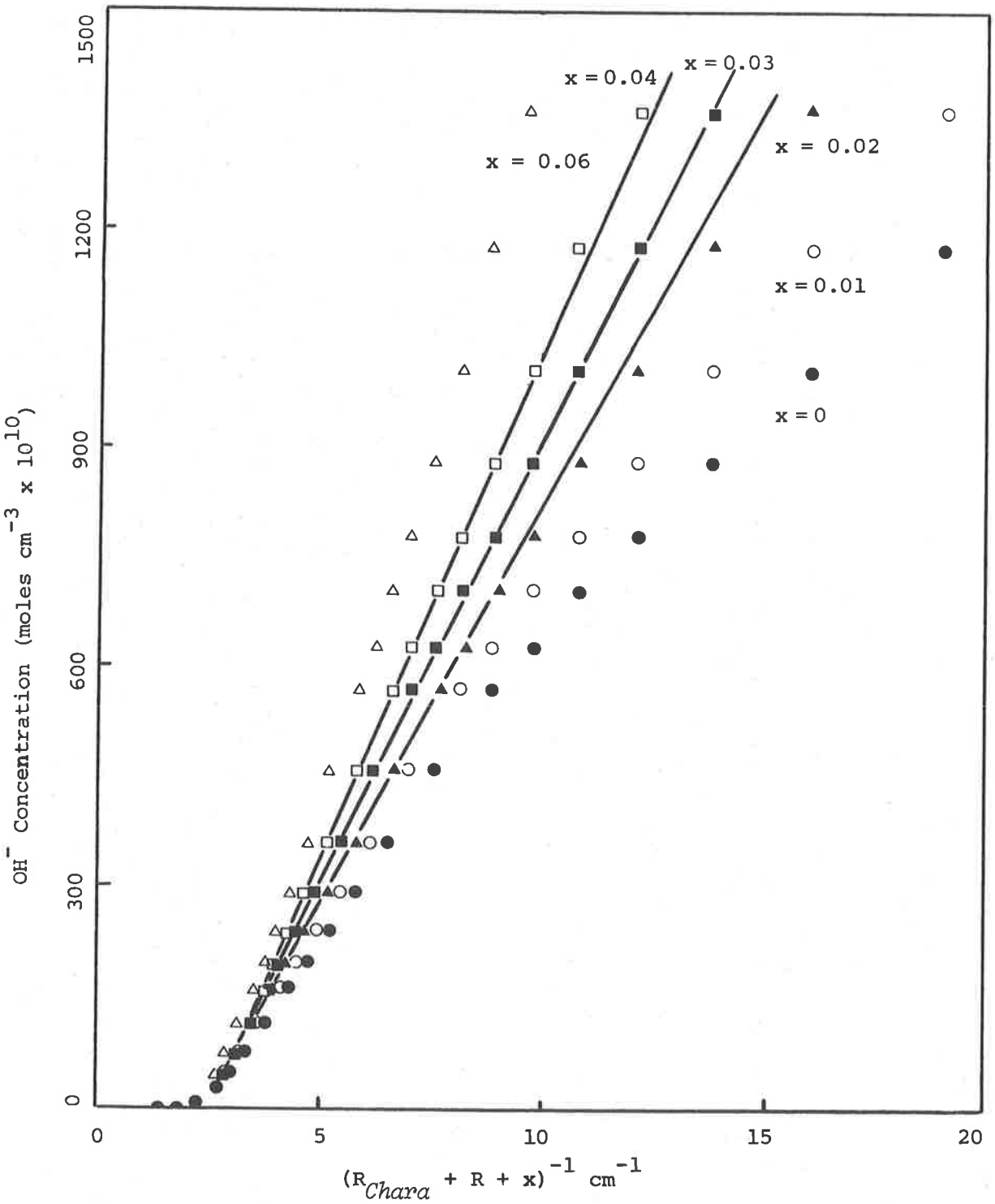

Figure 4.13. The influence of "x" values on the graph of $[OH^-]_r$ against $(R_{Chara} + R + x)^{-1}$. The value of x = 0.03cm was assumed to be the mean sensing height of the pH-sensitive hemispherical tip.

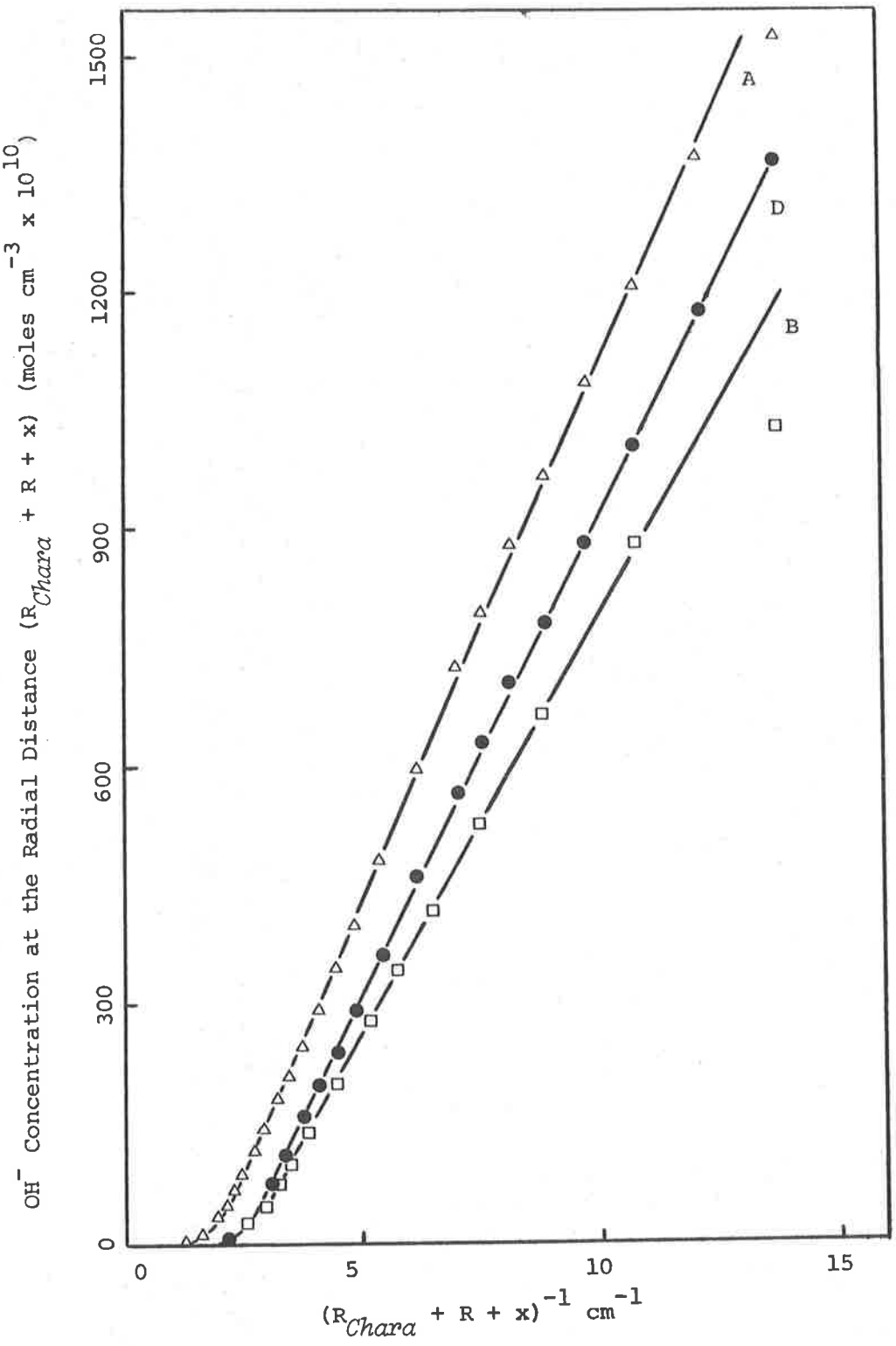

Figure 4.14. Graph of $[OH^-]_r$ against $(R_{Chara} + R + x)^{-1}$. The values of $[OH^-]_r$ for bands A, B and D were obtained from Table 4.1. The value of R_{Chara} for this experimental cell was 0.0425cms and "x" was 0.03cm.

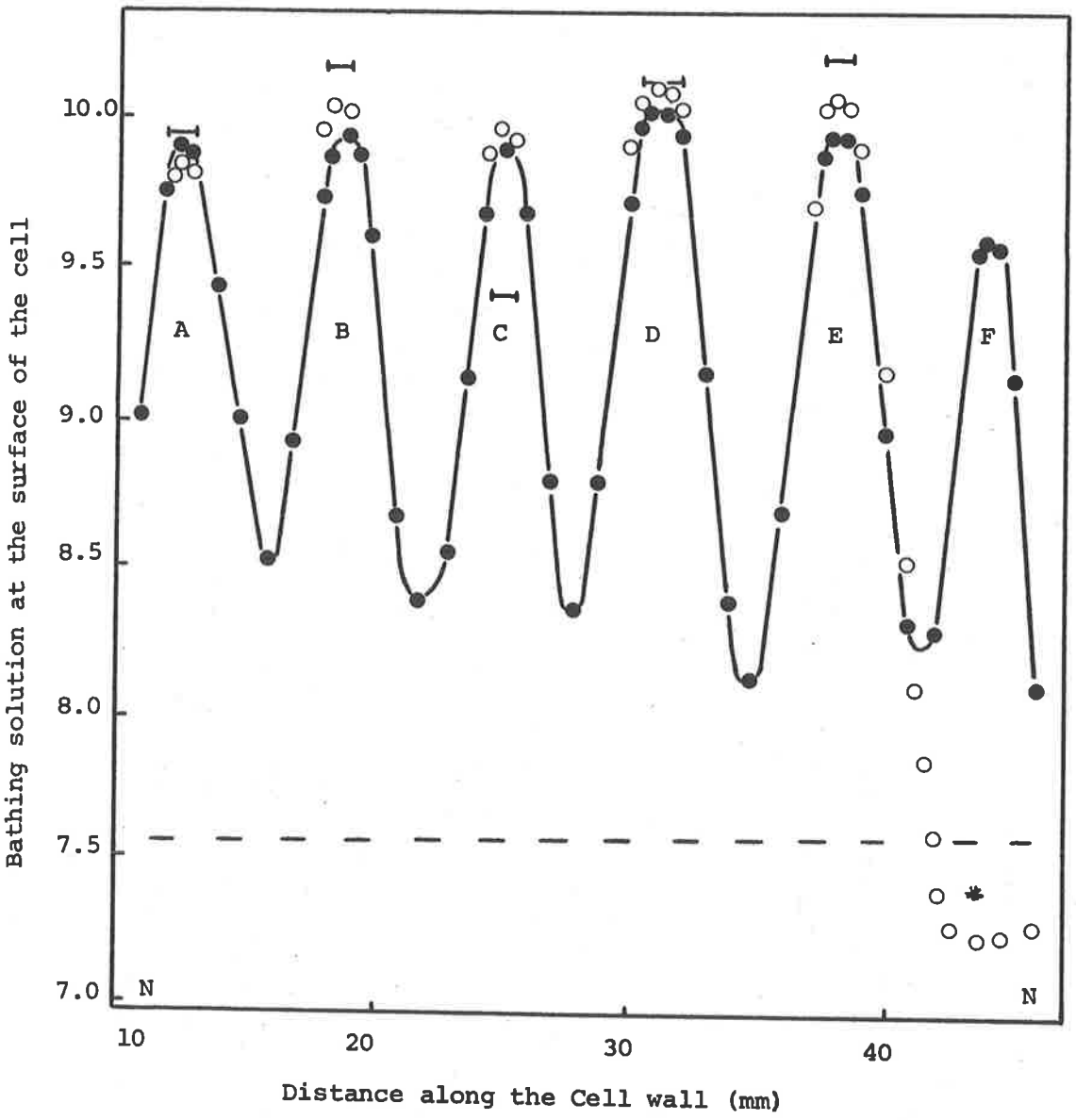

Figure 4.15. Typical cell response to illumination ($15 Wm^{-2}$). The bathing solution contained 1.0mM NaCl, 0.2mM KCl, 0.02 $CaSO_4$ and 0.2mM $NaHCO_3$. The banding pattern developed after 2h, (●) was checked after a 4h dark period followed by re-illumination for 2h, (○). The nodal positions are represented by N, the broken line represents the pH of the bathing solution. The horizontal bars represent the peak heights developed after 12h illumination; the cell was held in this instance in a solid agar block.

* Note the occurrence of only one acid band under these conditions.

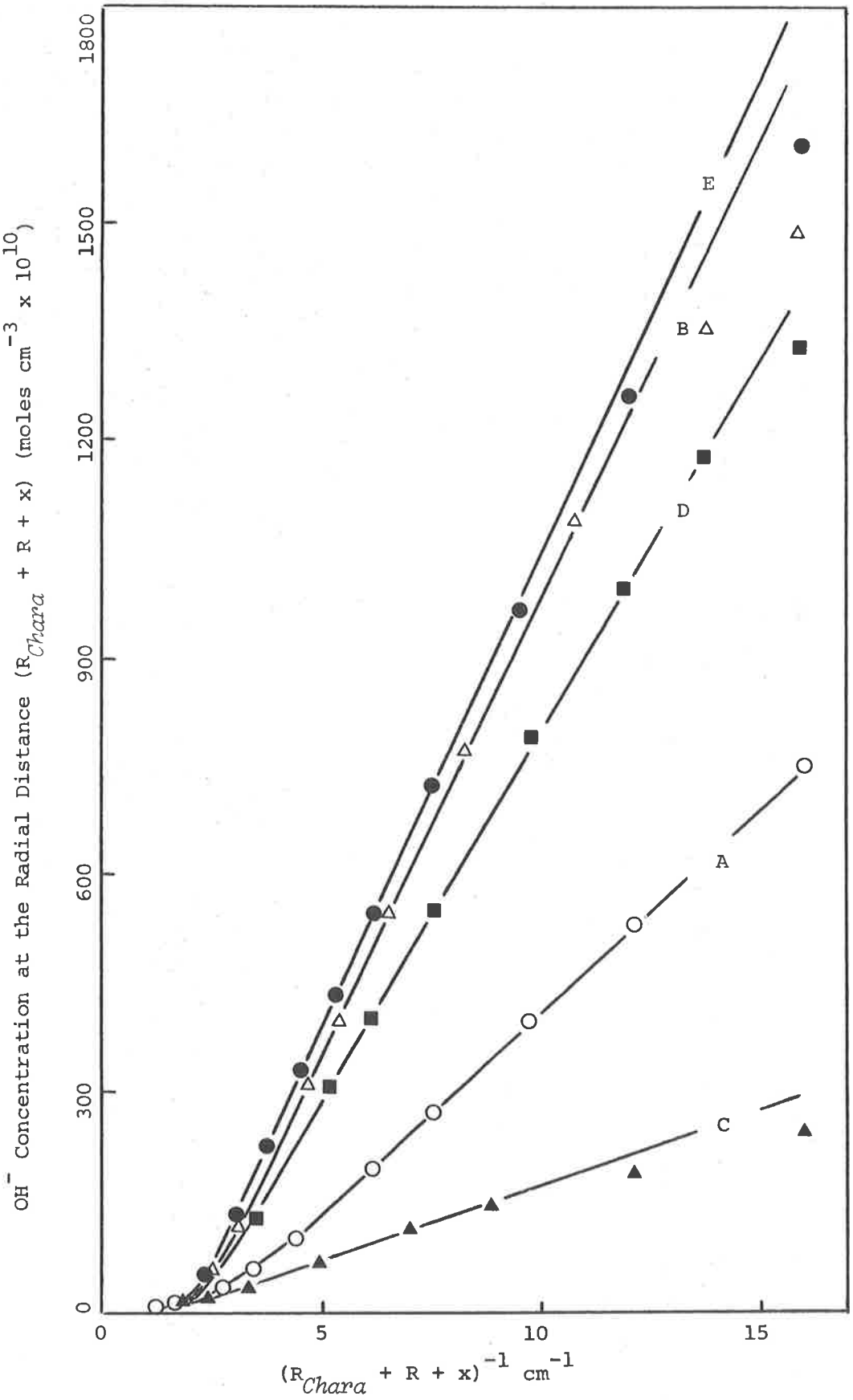

Figure 4.16. A complete hydroxyl ion band analysis. The OH^- concentrations, obtained from the vertical scans onto five alkaline band-centres, are plotted against the reciprocal of (R_{Chara} + R + x).

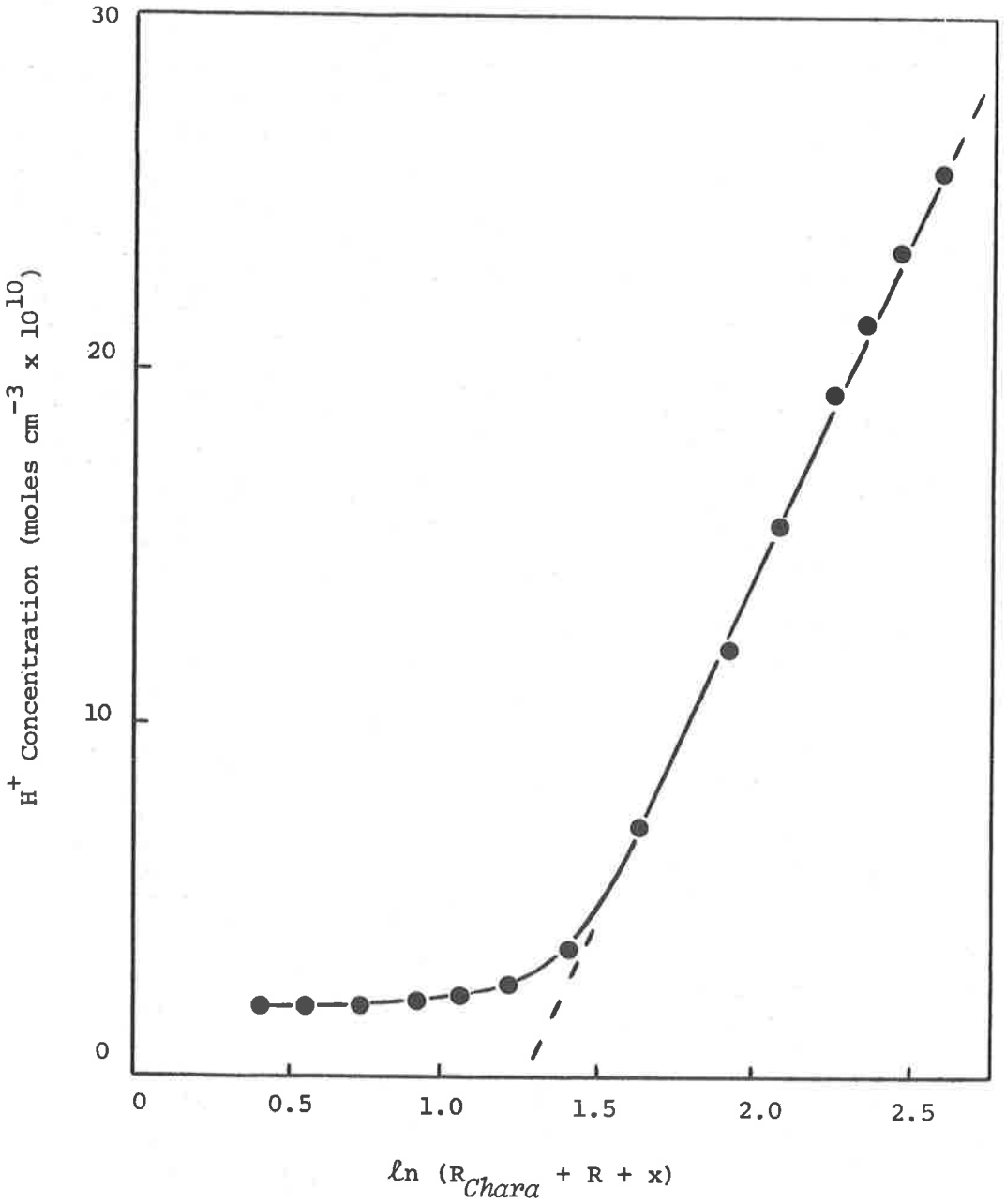

Figure 4.17. Graph of $[H^+]_r$ against $\ell n\ (R_{Chara} + R + x)$. The values of $[H^+]_r$ were obtained from the experimental results employed in the construction of Figure 4.7B (Scan 1). The Scan 1 data were chosen because this vertical pH Scan was conducted at approximately the centre of the acid band that was being studied.

CHAPTER FIVE

THE ACTIVATION AND OPERATION OF THE OH^- EFFLUX SYSTEM: THE INFLUENCE OF LIGHT INTENSITY

Introduction

In Chapter Three it was demonstrated that internodal cells of *Chara corallina* can assimilate HCO_3^- at extremely rapid rates. It has also been shown that when these cells photosynthetically fix CO_2, supplied by the transport of HCO_3^- across the plasmalemma, they develop alkaline bands on their cell surface (Lucas and Smith, 1973). The quantitative correlation between the $H^{14}CO_3^-$ influx and the OH^- extruded at these alkaline bands (see Chapter Four) indicates that these two processes must be under tight cytoplasmic control. If this was not the case, the cytoplasmic pH could be raised to deleterious levels during HCO_3^- assimilation.

Since the rate of $H^{14}CO_3^-$ assimilation is dependent upon the light intensity and substrate level employed, the total OH^- efflux should also correlate with light intensity. The nature of the interrelationships between light energy and the activation and regulation of the OH^- transport system will be examined in this Chapter.

Results

The Lag Period Prior to Activation of the OH^- Efflux System

It was shown previously that, following a 1h dark pretreatment, the pH electrode located on an alkaline band-centre recorded a lag*, prior to the activation of the OH^- efflux system (Chapter 4, see Figure 4.2). The nature of this lag is shown in Figure 5.1 in which the cellular and hence alkaline band response to $10 Wm^{-2}$

---

* This lag will be called the OH^- lag period.

illumination was recorded. The lag period in this experiment was 8.6 minutes. At the end of this lag period the OH^- concentration, in the alkaline band-centre, began to increase at a rapid rate; approximately 15 minutes were required before the activated steady state concentration was established at the band-centre. This type of response suggested that upon illuminating the cell, it was necessary to develop a certain cytoplasmic state before the OH^- efflux system was activated. This cytoplasmic state could have been associated with the commencement of fixation at the chloroplasts or the establishment of a certain requirement at the plasmalemma. Since both processes were considered to be connected indirectly to the light reactions of photosynthesis, it was proposed that a relationship should exist between the light intensity being employed and the observed lag period.

This proposal was not supported by initial experiments, which failed to show a simple relationship between the OH^- lag period and light intensity. This was particularly so for intensities below $4Wm^{-2}$. It was discovered that when a cell was placed under low light intensities ($1\text{-}4Wm^{-2}$), the banding pattern which developed on the cell surface was not uniform. In fact not all bands were activated under these intensities. This is demonstrated by the results presented in Table 5.1. From these results it was obvious that by locating the pH electrode on any particular alkaline band, there existed an element of chance as to whether this band would activate. Hence the erratic nature of the initial OH^- lag period experiments can be partially explained.

Primary and Subsidiary OH^- Band Status

Typical stable alkaline banding patterns, developed by a particular cell under a range of light intensities, are shown in Figure 5.2. A light intensity of $10Wm^{-2}$ caused six OH^- bands to develop, but under $1.6Wm^{-2}$ only three formed (Figure 5.2A), i.e. the six bands did not reactivate and operate at lower OH^- efflux rates. This situation would have been reflected in lower band-centre pH values. What should be noted is that band B and band F actually increased their OH^- efflux rates under the lower intensity of $1.6Wm^{-2}$, i.e. on the basis of the OH^- band analysis presented in Chapter 4, an increase in band-centre pH value must reflect a higher OH^- efflux rate, provided the physical conditions of the experiment remained constant.

A light intensity of $1.1Wm^{-2}$ also caused three OH^- bands to develop, but in this experimental sequence band E replaced band D and bands B and F remained the more active sites of OH^- efflux (Figure 5.2B). At a still lower light intensity of $0.8Wm^{-2}$, only band B activated; no reduction in its efflux activity was observed (Figure 5.2C). Repeated experiments at this low light intensity always resulted in the activation of this OH^- band (B). The very small increase in OH^- concentration at the band-centres D, E and F, indicated that an extremely small amount of OH^- was being transported at these sites. These were called non-activated OH^- bands as opposed to the completely inactive nature of band C. The nature of band A was masked by the OH^- diffusion pattern established by band B.

Light intensities below a certain value would not activate any OH^- bands (Figure 5.2D), unless the OH^- efflux system was previously established using a higher light intensity. For example,

$0.6Wm^{-2}$ (Figure 5.2D) caused the pH value of the entire cell wall to be raised above the background or dark value, but no OH^- bands had formed at the end of a 2h illumination period. This rise in pH value along the cell wall is also observed at the acid band-centre during the early stages of acid band activation (see Figure 4.3). It may be due to the removal of CO_2 from the bathing solution into the cell, which would cause a pH rise (Lucas and Smith, 1973 and see also the CO_2 equilibria detailed on page 24). This proposal has difficulty in explaining the result obtained under low light intensities. For example in Figure 5.2C and D, it can be seen that very little acid efflux can be detected, and yet the cell surface shows an irregular pH pattern in the regions where the OH^- bands have not activated, i.e. the pH seems to have been raised to a higher value in the vicinity of the non-activated OH^- bands. Hence this initial pH rise may be due to the combined effect of two processes, the first being the CO_2 effect, and the second is that non-activated OH^- bands can transport a very small amount of OH^- prior to activation. The CO_2 contribution will depend upon the pH of the bathing solution, for the lower the HCO_3^- level, the smaller will be the pH change. Once activated, using an intensity of $3Wm^{-2}$, a stable OH^- band could be maintained when the intensity was reduced from 3 to $0.6Wm^{-2}$, with no intervening dark period. It should also be noted that band F had also retained slight OH^- efflux activity following this 3 to $0.6Wm^{-2}$ treatment.

These results revealed that all OH^- bands developed by a cell are not equivalent in status. The most permanent band (for example see band B of Figure 5.2, and also Table 5.1) was also found to be the main OH^- efflux site. Apparently this band acts as the sole OH^- efflux site until the physiological conditions

of the cytoplasm are such that other efflux sites are required. This main OH^- efflux band, therefore, was termed the primary OH^- system. Another band (e.g. band F of Figure 5.2) which increased in activity under lower light intensities, but which deactivated before the primary OH^- band, was assigned the status of sub-primary OH^- band. All other alkaline bands were termed subsidiary OH^- bands since their OH^- efflux activity was supplementary to the primary OH^- system.

This concept of OH^- band status was strongly supported by the diffusion analysis results presented in Chapter 4. An examination of the individual alkaline band OH^- efflux values which were presented in Tables 4.3, 4.4 and 4.5, showed that for each cell examined, there was an OH^- efflux rate which was considerably higher than the others. (The only exception was the results of Exp. No. 6, Table 4.4). The diffusion analysis results enabled the assignment of primary, sub-primary and subsidiary status to the OH^- bands of most of the cells studied.

Primary Band Lag Period as a Function of Light Intensity

It was obvious that the relationship between light intensity and the OH^- lag period could only be studied successfully using the primary OH^- band of each cell. This meant that priot to conducting a light intensity experiment, the primary OH^- band of the experimental cell had to be identified. This was achieved by placing the cell in its experimental agar block and illuminating it for 30 minutes under a light intensity of $5Wm^{-2}$. At the conclusion of this 30 minute period the intensity was decreased in a step-wise manner until an intensity was reached at which only the primary OH^- band remained operational. The band-centre was then mapped accurately. A 1h dark treatment was then employed

and the above sequence repeated to ensure that the location of the primary band-centre was stable.

Following this identification of the primary OH^- band, the cell was given another 1h dark treatment, at the conclusion of which the primary OH^- band response to a particular light intensity was recorded. Each response was recorded for 2h, and at the end of this period the band-centre pH values of the sub-primary and subsidiary bands were measured. This dark to light sequence was repeated using a range of suitable light intensities. Typical results are presented in Figures 5.3 and 5.4. It was apparent that as the light intensity decreased, the OH^- lag period increased. The results presented in Figure 5.3 demonstrated that a light intensity of $0.6Wm^{-2}$ did not cause activation, even after an illumination period of 200 minutes. Furthermore, it was found that when the intensity was increased to $0.8Wm^{-2}$, the band was still in the non-activated state even after 100 minutes at this new intensity. This was surprising since the lag period associated with the dark to $0.8Wm^{-2}$ situation was 56.5 minutes. A similar inability to cause activation was also found for $1.0Wm^{-2}$, however, a higher intensity ($3.0Wm^{-2}$) did activate the primary OH^- band. At the end of a 15 minute treatment under this $3.0Wm^{-2}$ intensity, the light intensity was reduced to 1.0, 0.8 and finally $0.6Wm^{-2}$. The alkaline band remained active and stable under this final intensity.

A similar response was observed in the experiment illustrated in Figure 5.4. For this particular cell, $0.8Wm^{-2}$ would not activate the primary OH^- band and the response to this intensity was investigated over a 14h period. The pH values along the entire cell wall were checked at the 2, 10 and 14h stages of the experiment. This was to ensure that the primary OH^- band

had not moved or that some other band had not activated. At the end of the 14h period no activated alkaline band was present on the cell surface. When the light ($0.8Wm^{-2}$) was switched off, the pH value at the primary OH^- band-centre decreased back towards the background value. Hence the band was in the non-activated state as opposed to the inactive state where no OH^- efflux occurs at all.

In the light intensity region where only the primary OH^- band was active, a reduction in intensity resulted in a decrease in the steady state pH value of the band-centre (1.5 to $1.1Wm^{-2}$ and 1.3 to $0.8Wm^{-2}$), i.e. the decrease in the rate of OH^- production by the cell at intensities lower than $1.5Wm^{-2}$, could be observed by measurements on just this band. In the light intensity region where the primary and sub-primary bands are operating a reduction in intensity may not result in a change in the steady state pH value of the primary OH^- band (e.g. 1.7 to $1.5Wm^{-2}$). This is because the reduction in OH^- produced by photosynthesis is reflected in a decrease in the pH value of the sub-primary band.

Another feature which was demonstrated in both Figure 5.3 and Figure 5.4 was the characteristic increase in band-centre pH value of the primary band which resulted when the light intensity was reduced.

Subsidiary OH^- Band Response to Decreasing Light Intensity

It was found that deactivation of any particular subsidiary OH^- band occurred over a relatively short decrease in light intensity. An example is given in Figure 5.5. The initial part of the trace (0-180 minutes) demonstrated the response of this band to the transition from $14Wm^{-2}$ to the dark and the reactivation of the band when this sequence was reversed. It should be noted that

the physical system required approximately 40 minutes for the dissipation of the OH^- diffusion gradient, established at the cell surface by this particular band. The decrease in intensity from 14 to 2.7 Wm^{-2} resulted in a small reduction in the steady state band-centre pH value. This is a characteristic response of a subsidiary OH^- band.

The cell was then subjected to a range of light intensities from $2.3Wm^{-2}$ down to $1.3Wm^{-2}$. The respective pH traces indicated that a reduction in the steady state value always resulted, and the time required to establish the new steady state was considerable. For example, the decrease in light intensity from 14 to $1.5Wm^{-2}$ required a period of greater than 1h for the establishment of the new steady state. This slow response was due to some aspect of cellular activity, because the response of the measuring system was much faster, i.e. compare this response with the $14Wm^{-2}$ to dark response. In transferring the cell from a 14.0 to a $1.3Wm^{-2}$ light regime, the photosynthetic system would be changed from a substrate- to a light-limited condition. The slow response of the subsidiary band suggested that either there was a slow re-adjustment of the rate of CO_2 fixation (and hence OH^- generation) or that a "pool" of OH^- was present in the cytoplasm.

The subsidiary band response, when an intensity of $1.3Wm^{-2}$ was employed, revealed that at this intensity the OH^- efflux rate from this band decreased to that of a non-activated OH^- band. This was demonstrated by the fact that the pH value fell to the value maintained by this band when it was in the non-activated state.

Its existence in the non-activated state was also supported by the response elicited by the dark treatment. Hence this subsidiary band went from the active to non-activated state when the light intensity was reduced from 1.5 to $1.3Wm^{-2}$. It is suggested

that the observed rise in activity of primary and sub-primary bands, when the light intensity was reduced, may reflect the transfer of OH^- efflux function on the deactivation of a subsidiary band.

Analysis of the Lag in Activation of the Primary OH^- Band

The OH^- lag periods of four primary bands, in response to a range of light intensities, are presented in Table 5.2. (These experiments were conducted in bathing solution which contained 0.1mM $NaHCO_3$ (pH 6.9)). These data are plotted as a graph of the reciprocal of the lag period against light intensity (Figure 5.6). This form of analysis indicated that the results, for a particular cell, formed two linear regions. It appeared that light intensities greater than $5Wm^{-2}$ (approximately) did not cause a further increase in the reciprocal of the primary OH^- lag period. The lag period appeared to have attained a minimum value determined by factors other than light intensity. The linear region observed for light intensities generally less than $4Wm^{-2}$ was more informative. It implied that a substrate, which was essential for the activation of the OH^- efflux system, was being produced at a rate which was proportional to the light intensity. It suggested that this substrate was required at a specific level before the primary OH^- band could activate. The intercept, of this linear section of the graph on the ordinate axis, was interpreted as the light intensity which would take an infinite time to establish the activating condition. This intercept value was termed the critical light intensity and values below it should not cause activation of the primary band.

The validity of this prediction was tested experimentally. For example, analysis during Exp. No. 9 (Table 5.2 and Figure 5.6) gave a critical value of $0.9 \pm 0.5Wm^{-2}$. Hence a value of $0.8Wm^{-2}$ was

employed for a period of greater than 14h. The primary OH^- band did not activate (see Figure 5.4). In all experiments where subcritical illumination was employed, no alkaline bands formed. However, an interesting feature which has already been mentioned was that once the primary band was activated, a sub-critical light intensity would maintain it in the active state (see Figures 5.2D, 5.3 and 5.4).

Figure 5.7 is a reciprocal plot of OH^- lag period against light intensity for a series of experiments in which the chlorophyll concentration of the cell was determined at the conclusion of the experiment. The results expressed in Figure 5.7 suggest that higher chlorophyll concentrations correlate with a shorter OH^- lag period and a lower critical light intensity. Consequently part of the variation between cells (see Figure 5.6) may be due to the influence of different chlorophyll concentrations. This correlation between a shorter lag period and chlorophyll concentration was not expected, because the total carbon concentration in the bathing solution was rate limiting for photosynthesis, i.e. at these high light intensities the light reactions of photosynthesis would not be limiting CO_2 fixation. However, the correlation between the lower critical light intensity and higher chlorophyll concentration was expected. This was because in the presence of the higher chlorophyll concentration, more energy would be trapped in the lower light intensity range. Hence the actual $^{14}CO_2$ fixation rate would be higher (see Figure 3.3). It should be pointed out that this correlation held for cells cut from culture tanks XG-2 and delta, but not for the Mannum cells.

Deactivation of Primary OH^- Bands being Maintained by Sub-critical Light Intensities

Figure 5.8 presents the results of an experiment conducted on a cell whose critical light intensity value was $0.9Wm^{-2}$. The primary band was activated by 1.1 or $1.3Wm^{-2}$ and it was given a 1h treatment (in the activated state) at this light intensity before the commencement of the experimental treatments. The reduction from 1.3 or $1.1Wm^{-2}$ to $0.8Wm^{-2}$ caused the primary band to decrease its steady state band-centre pH value. During the establishment of this new steady state pH value, dark periods of up to 3 minutes duration did not cause the band to deactivate. Although during a 3 minute dark period the pH value dropped considerably, the band increased its efflux rate again at the conclusion of the dark period and the pH value was raised back up to the steady state level. A slightly longer dark period of 5 minutes, however, converted the band to the non-activated state. This was demonstrated by transferring the cell to the dark.

A similar experiment was conducted using a cell which had a lower critical illumination value of $0.5Wm^{-2}$. As would be expected the primary OH^- band was maintained by much lower light intensities. Figure 5.9 indicated that under the influence of dark periods of 5, 12.5, 15 and 25 minutes duration, the primary OH^- band always recovered its activity under the influence of a $4Wm^{-2}$ light intensity. However, when sub-critical intensities of 0.4 or $0.2Wm^{-2}$ were employed (Figure 5.10), a dark period of 0.5 minutes was sufficient to reduce the activity of the band to a very low level. In the case of the $0.4Wm^{-2}$ light intensity, further dark periods of 40, 60 and 120 seconds did not appear to influence the shape of the decaying trace. Nevertheless the band was still in the non-activated state as was shown by the dark response. The response

in the 0.2Wm^{-2} light intensity situation was very interesting. As shown in Figure 5.10, the change from an intensity of 0.6 to 0.4Wm^{-2} resulted in a slightly more stable response than the repeat experiment which went from 0.5 to 0.4Wm^{-2}. Upon reducing the intensity from 0.3 to 0.2Wm^{-2}, the band-centre pH value responded immediately and it began to fall at quite a steady rate. After 15 minutes the band was still active, so a 30 second dark period was applied. In response to this treatment, the band appeared to deactivate completely, as is evident from the close correlation with the dark OH^- band response (broken line). The transfer of the cell from the 0.2Wm^{-2} light intensity to the dark also had very little effect on the shape of the pH trace.

Discussion

Photosynthetic Induction in Relation to the OH^- Lag Period

Photosynthetic fixation of CO_2 often requires an induction period of between 1-2 minutes before a maximum rate, governed by the prevailing conditions, is attained (Osterhout and Haas, 1918; Rabinowitch, 1956; Heber and Willenbrink, 1964; and Walker, 1973). A deficiency in the level of ribulose-diphosphate, at the beginning of the light period, may explain this induction period. Wildner and Criddle (1969), however, suggested that the ribulose-diphosphate carboxylase requires photoactivation (see also Bassham, 1971). Further evidence of the involvement of light as a requirement for the activation of Calvin cycle enzymes was presented by Pedersen et al.(1966) and Buchanan et al.(1967).

Regardless of its actual mechanism, the induction period could account for at least part of the lag period associated with the OH^- bands. It is considered that the maximum time which could be accounted

for on the basis of this phenomenon, would be 2-3 minutes. Since the induction period does not increase with decreasing light intensity (Walker, 1973), it cannot account for the long OH^- lag periods observed under low light intensities. Walker (1973) also demonstrated that an increase in chlorophyll concentration did not result in a shortening of the induction period. This condition did not apply to the influence of chlorophyll concentration on the OH^- lag period; it was evident that under identical experimental conditions, the cell with a higher chlorophyll concentration had a shorter OH^- lag period (see Figure 5.7).

OH^- Diffusion: Theoretical Lag

Consideration should also be given to the natural diffusion process by which the OH^- ions are transferred from the Donnan free space, outside the plasmalemma, to the mean sensing height of the pH electrode (see Chapter 4), i.e. what is the diffusion time required for the establishment of the steady state OH^- concentration at this radial distance. The easiest method of determining this time was by the application of the instantaneous spherical surface source equations. By assuming that an instantaneous pulse of OH^-, of strength Q, was effluxed over the surface of a sphere of radius R_{Chara}, the time dependent change of OH^- concentration at any radial distance could be obtained, using the following equation (Carslaw and Jaeger, 1959 p. 259 (6)).

$$C_{OH^-}(R) = \frac{Q}{8\Pi R.R_{Chara}(\Pi Dt)^{\frac{1}{2}}} \left[e^{-(R-R_{Chara})^2/4Dt} - e^{-(R+R_{Chara})^2/4Dt} \right] \quad .....(5.1)$$

where the symbols have their previously assigned meanings. Hence, for a fixed value of R, namely the radial distance to the mean sensing height of the electrode (R_{Chara} + 0.03cm, see Chapter 4),

using R_{Chara} = 0.045cm and the previously assigned value of $D_{OH^-} = 2.129 \times 10^{-5} cm^2 s^{-1}$ the value of C_{OH^-} was calculated as a function of time. The resultant theoretical concentration profile is presented in Figure 5.11A; this profile was calculated using the normal diffusion coefficient for OH^- ions. The diffusion time required to establish the steady state at this radial distance is clearly of the order of 20 seconds.

Because the OH^- ions would be forced to diffuse out through the cell wall, the diffusion coefficient in this region may in fact be smaller than the value for diffusion in a free solution. However, Spanswick (1964) has shown that the Characean cell wall is a very permeable structure. He concluded that the movement of K^+ and Cl^- was probably limited by the rate of diffusion in the unstirred region between the plasmalemma and the bulk solution. Consequently the correction for the lower diffusion coefficient may not significantly alter the time required to establish the steady state. The influence of reducing the diffusion coefficient from 2.129×10^{-5} to $2.129 \times 10^{-6} cm^2 s^{-1}$ and applying this value over the entire diffusion path is shown in Figure 5.11B. The steady state time was still only three minutes. Since this correction would be far in excess of that caused by the experimental system (Nobel, 1970 p. 27), it is obvious that the steady state time (pH electrode located at $R = R_{Chara} + 0.03$) of the true diffusion system is probably between 20 - 40 seconds. Consequently this physical system cannot account for the long OH^- lag period; the pH electrode trace will be an extremely close reflection of the cellular response at the plasmalemma.

The Relationship between Cytoplasmic CO_2 and HCO_3^- and the OH^- Efflux System

An obvious factor, which would influence the length of the OH^- lag period, is the CO_2 concentration of the cytoplasm. The equilibria, diffusion and transport processes which would be involved in determining cytoplasmic CO_2 concentration, are outlined in Figure 5.12. After the induction phase, when light is non-limiting, the value of R_5 will be governed primarily by the concentration of CO_2 in the cytoplasm. If the combined rates of R_1 and R_2 balance R_5, OH^- ions would not be generated and also under such a system there would not be any requirement for an operational HCO_3^- transport system. Similarly the OH^- efflux system would not operate. As demonstrated in Chapter 3, an experimental system of this nature would require an exogenous CO_2 concentration of approximately 1.0mM and the pH value of the bathing solution would have to be in the region 5.3 to 5.6. However, when $R_2 + R_1 < R_5$, a situation which would occur either when the bathing solution had a low exogenous carbon level, or it contained HCO_3^- rather than CO_2, fixation of CO_2 from the cytoplasmic pool would cause the equilibria, illustrated in Figure 5.12, to move to the left, i.e. OH^- ions would be generated by the removal of HCO_3^- from the cytoplasmic pool. This rate of OH^- generation, at a fixed value of $(R_1 + R_2)$, will depend on the cellular level of HCO_3^-, the absolute fixation rate (R_5) and the endogenous H^+-buffering capacity of these cells.

If the activation of the OH^- and/or HCO_3^- system(s) required a specific cytoplasmic substrate level (e.g. this may be reflected in a particular pH value) this would provide a link between the photosynthetic fixation process, the external conditions and the observed OH^- lag period. The existence of a critical

cytoplasmic substrate level is inferred from the lag periods of OH^- activation greater than required for the induction of photosynthesis. The existence of a critical substrate level is also supported by the form of the OH^- band response to low levels of illumination, i.e. the non-activated state exists during the lag period and then at a predictable time, the band activates with a rate of approach towards the steady state which is equivalent to the band's response at higher light intensities (see Figures 5.3 and 5.4).

Total OH^- Efflux Activation Under High Light Intensities

At least two sequences of activation are possible based on the scheme presented in Figure 5.12. In the first the following may occur: $R_5 > (R_1 + R_2)$ which results in a lowering of the $[HCO_3^-]_{cyt.}$ and an increase in $[OH^-]_{cytoplasm}$; when a critical activation level is reached for either $[HCO_3]_{cytoplasm}$ or $[OH^-]_{cytoplasm}$, the coupled HCO_3^-/OH^- transport system is activated. The second possibility is that the HCO_3^- and OH^- ion movement is not coupled in the manner proposed by Lucas and Smith (1973). Hence the following sequence may occur: $R_5 > (R_1 + R_2)$ results in a lowering of $[HCO_3^-]_{cyt.}$ and this increases $[OH^-]_{cyt.}$, R_3 operates because of the reduction in $[HCO_3^-]_{cyt.}$, when $[OH^-]_{cyt.}$ reaches a critical level R_4 is activated allowing R_3 to increase; the steady state value of R_4 is expected to equal R_3 (based on the results presented in Chapter 4). It is obvious that if this second sequence does occur, the transport of HCO_3^- must be restricted during the non-activated OH^- efflux period. If this condition did not hold, the resultant HCO_3^- influx would cause the generation of very negative membrance potentials. Experimental evidence in support of this second sequence will be presented in Chapter 7. Consequently the discussion relating to the interactions between these transport systems and the electrical

properties of the plasmalemma will be deferred until Chapter 7.

The involvement of the H^+ transport system is difficult to assess since the nature of "S" is not known, i.e. just how "S" transfers (H^+) and to what extent this results in an adjustment of cytoplasmic pH is completely unknown. What has been found is that, in bathing solutions which have pH values of 7 or more, the net H^+ efflux does not appear to be very large (Chapter 4). If this is in fact true, then at these pH values R_{H^+e} must equal R_{H^+i} (Figure 5.12), and so the H^+ transport system would have very little influence on the pH value of the cytoplasm.

At this point it is worth re-examining the $H^{14}CO_3^-$ time-course results which were presented in Chapter 3, Figure 3.1. It will be recalled that no apparent lag in $H^{14}CO_3^-$ influx occurred under the existing experimental conditons. On the basis of the results presented in this chapter a lag may have been anticipated. However, the main point to note is that in the $H^{14}CO_3^-$ time-course experiments, the cells were bathed in normal solutions (no added $NaHCO_3$) during their 1h dark pretreatment, and so the CO_2 generated by respiration would have diffused out of the cell into the bathing solution. When the cells were transferred to the exogenous $H^{14}CO_3^-$ conditions (pH 8.6, light intensity 2 or $3Wm^{-2}$), R_5 would have been supplied mainly via R_1 and R_3; R_2 wouldhave been small due to the low exogenous CO_2 level. Provided the cytoplasmic pool of HCO_3^- was not large in the dark state, the activating conditions may have been quickly established. As a result the $H^{14}CO_3^-$ influx would have commenced almost immediately the cells were illuminated. In contrast, if the cells had been treated in 0.2mM $NaHCO_3$ (pH 7.2) during their 1h dark treatment, there may have been a detectable lag in $H^{14}CO_3^-$ influx due to the equilibration of the CO_2 and

HCO_3^- levels of the bathing solution and cytoplasm, i.e. a 'pool' of total carbon would have been established within the cytoplasm and R_3 would not activate immediately.

The Primary, Sub-primary and Subsidiary OH^- Band Hypothesis

In the previous section a sequence was proposed to account for the activation of the OH^- efflux system. It is proposed that the following properties and conditions operate within the total cell OH^- efflux system:

(i) There exists a set of OH^- carriers (which constitutes one OH^- band) whose critical activation level is lower than all of the other carriers. These carriers have a greater affinity for OH^- than the other carriers; i.e. the Michaelis-Menton K_m is much lower for this set of carriers. This set of carriers constitutes what has and will be termed a primary OH^- band.

(ii) A second set of carriers exists which has a slightly higher substrate level required for activation and whose affinity for OH^- is slightly lower than (i), i.e. the K_m for this system is greater than that proposed for (i). This constitutes a sub-primary OH^- band.

(iii) Numerous sets of carriers exist which have a substrate level required for activation which is greater than is required for (i) or (ii) and similarly they have lower affinities for OH^- and higher K_m values. These constitute subsidiary OH^- bands.

Although the basic carriers are likely to have the same molecular form, there is considered to exist, within the transport sites, particular functional groups which impart to the OH^- carriers this observed range of affinities, activation levels etc. An hypothetical time-course, which embodies the above proposals, is

presented in Figure 5.13. The change in cytoplasmic substrate (which may be OH^- or some more complex compound) produced by illumination is considered with respect to the activation of the various OH^- efflux systems. Under $10Wm^{-2}$ illumination, the increase in $[OH^-]$ is such that the primary and sub-primary bands activate at the 6.0 and 8.0 minute marks respectively. However, the efflux rates do not become maximal until a period of 15-20 minutes has elapsed (see Figure 5.1), hence $[OH^-]$ continues to rise and once it reaches the subsidiary level, these bands become activated. The total OH^- efflux load governs the number of subsidiary bands which remain active. Under the $1.0Wm^{-2}$ light intensity, the rate of $[OH^-]$ increase is proportionately lower and hence the time required before the activating condition is established was 21 minutes. The rate of $[OH^-]$ increase was equalled by this activated primary OH^- efflux band at the 30 minute mark and in fact the efflux rate through this system was sufficient to prevent the $[OH^-]$ level from being raised to the sub-primary activation level, ie. under these conditions only one OH^- efflux system became operational.

When sub-critical illumination is employed, it is proposed that the $[OH^-]$ increases for some time and then, as a result of the low intensity other cellular processes influence the cytoplasmic pH value or perhaps its buffering capacity. As a result, the $[OH^-]$ does not continue to increase but may appear to fall as the result of processes which may utilize the OH^- ions in a reaction. This form of sub-critical illumination response was proposed to account for the experimental results which indicated that this treatment modified the cellular response (see for example Figure 5.3). Hence the application of light intensities above the critical intensity, following a sub-critical treatment, would have to restore the

cytoplasmic "state" before the "normal" [OH] increase occurred. From the experimental results it was obvious that light intensities just above the critical value were slow in effecting this reversal, but that higher intensities could rapidly accomplish the readjustment.

Experimental support for a light-induced increase in $[OH^-]_{cyt.}$ has been provided by the work of Walker and Smith (1974). These workers used the equilibrium distribution of [^{14}C] DMD* between the bathing solution, cytoplasm and vacuole, to determine the average pH values of these cellular compartments. Their preliminary results indicated that when the bathing solution was buffered at pH 7.1, the cytoplasmic pH value rose from approximately 7.6 to 7.8 following illumination. When the bathing solution was buffered at pH 7.8 and the cell illuminated, the cytoplasmic pH value was estimated to be 8.3. Unfortunately the dark value under these conditions was not measured.

Subsidiary Band Deactivation as Light Intensity is Reduced

It was demonstrated in Figure 5.5 that, for a particular subsidiary band, there exists a light intensity below which its activity is reduced before finally becoming inactive. This suggests that not only is there a critical "substrate" level for activation, but that there is also a substrate level at which this band deactivates. Loss of activity of this subsidiary band would result in a slight rise in substrate level and the operational primary and sub-primary systems would respond by slightly increasing their efflux rates (see Figures 5.2, 5.3 and 5.4).

---

* 5,5-dimethyl 2,4-oxazolidinedione is a lipid soluble weak acid; its lipid solubility applies only to the undissociated acid.

Further Evidence for Critical Activating and Deactivating Substrate levels

Strong support is obtained for the existence of a critical activating substrate level, from the results which show that the primary OH^- band, once activated, can be maintained in an active form, in the presence of sub-critical light intensities.

The deactivation of the subsidiary bands has already been discussed, however it would appear that a situation of this nature also exists for the primary band. When a dark period was given it had to be of a certain duration before it caused band deactivation (see Figures 5.8 and 5.9). In the initial phase of the dark period, it is possible that CO_2 was still being fixed (see Gaffron and Fager, 1951; and Togasaki and Gibbs, 1967); $t_{\frac{1}{2}}$ for this fixation can vary from 15 to 120 seconds. Hence the duration of the deactivating period would be determined by the characteristics of this dark fixation as well as the amount by which the $[OH^-]$ level had to be reduced for it to fall below the deactivating value. It is considered that the reduction of OH^- during this dark period occurs by HCO_3^- formation via R_1 and R_2. It is also possible that OH^- still effluxes in the dark and that these two processes reduce the $[OH^-]$ level below the activating substrate level. Once this occurs, OH^- efflux stops and only HCO_3^- formation via R_1 and R_2 continues.

Deactivation would not be due to a reintroduction of a photosynthetic induction lag (Walker, 1973). Hence, the fact that the primary OH^- band cannot regain activity following this dark period, must be taken as conclusive evidence for the existence of a critical substrate level below which the band cannot function. A further property must therefore be added to (i), (ii) and (iii) above. This property would be:

(iv) Each specific OH^- carrier system has a critical level of substrate, which will result in deactivation. The levels being in the order, subsidiary > sub-primary > the primary system.

Spatial Distribution of OH^- bands

If the HCO_3^- and OH^- systems can function independently, the HCO_3^- carriers within the plasmalemma may be distributed uniformly over the cell surface. This would mean that the cytoplasmic diffusion path to the chloroplasts would have a maximum value of 4-6μm (Costerton and MacRobbie,1970). Consequently the time associated with the diffusion of HCO_3^- from the carrier to the chloroplasts would be extremely short.

The OH^- situation is more complex. Hydroxyl ions would be generated at, or very near, the outer limiting chloroplast membrane as a result of CO_2 diffusion into the stromal matrix. (If carbonic anhydrase is involved in this equilibration, then it is assumed to be located in this region). This production of OH^- ions at the surface of the chloroplast layer would mean that a concentration gradient, with respect to cytoplasmic OH^- along the length of the cell, would not be generated until the OH^- efflux systems were activated. Under high light intensities several OH^- efflux sites are usually activated. Consequently the lateral diffusion path from the site of OH^- generation to the closest operational OH^- effluxing system would usually be approximately 0.5cm. However, under conditions when the primary OH^- band is the only active OH^- efflux site, lateral diffusion paths of up to 3cm may exist (see Figure 5.2C).

The time associated with free diffusion of OH^- over these lateral distances will be considerable, especially for path lengths of 2-3cm. As a first approximation this lateral diffusion system

can be equated to the movement of OH^- in the direction parallel to the x axis; the OH^- being generated by a planar surface source parallel to the y axis (i.e. the longitudinal axis of the *Chara* cell is considered to lie parallel to the x axis). The diffusion time for the OH^- ions to reach a maximum concentration at any point from the planar surface source is related to the diffusion coefficient and path length by the expression;

$$t = \frac{(\text{diffusion path})^2}{2\, D_{OH^-}} \quad \text{(after Moore, 1958)} \quad \ldots\ldots (5.2)$$

Consequently t under high light intensities when the lateral diffusion path would be approximately 0.5cm, would be 5.9×10^3s or 1.63h. The low light intensity situation where the lateral diffusion path could be as long as 2-3cm, t would be 9.4×10^4s or 26.1h (for 2cm) and 2.1×10^5s or 58.7h (3cm).

It should be emphasized that this treatment is indeed a very crude approximation to the actual cytoplasmic situation, nevertheless it does give an indication of the order of magnitude of the diffusion times. These long diffusion times suggest that OH^- ions are not moved exclusively by free diffusion. The simplest and most rapid transport of OH^- ions would occur if the ions diffused from the chloroplasts into the streaming cytoplasm. Assuing a streaming rate of 60µm s^{-1}, the ions would cover the 0.5 or 2cm distances in approximately 1.4 and 5.6 min respectively. The diffusion time associated with the movement of OH^- from the boundary of the streaming cytoplasm to the plasmalemma would be short. Applying (5.2) and assuming this path length is equal to 6µm, the estimated time would be 0.14s.

It is therefore proposed that following illumination of the cell, OH^- are generated in the chloroplast layer and from here they diffuse into the cortical (gel) and streaming cytoplasm. The streaming cytoplasm and the short diffusion time between this phase and the cortical cytoplasm results in a uniform concentration of OH^- throughout the entire cytoplasm. Once the OH^- efflux activating conditions are established, the various OH^- efflux systems begin their transport of OH^- across the plasmalemma. The localized decrease in OH^- concentration will be relatively small because of the coupling between this region and the "larger" pool of OH^- in the streaming cytoplasm. The existence of an OH^- "pool" of this form would account for the slow readjustment in efflux activity observed for subsidiary OH^- bands (see Figure 5.5). The proposed system would also explain the spatial distribution of the OH^- efflux bands in that the interaction between OH^- efflux activity at the plasmalemma and the entire cytoplasm would result in an excellent feedback system. If under a particular light intensity insufficient OH^- efflux bands activated to cope with the OH^- production, the OH^- level within the cytoplasm would rise slowly. This rise would be slightly greater in the cortical cytoplasmic region having the greatest distance separating consecutive active OH^- efflux sites; this would ensure that the next OH^- site to activate would be in this region. As a consequence, the OH^- efflux bands appear to operate at almost regular intervals along the length of the cell.

Summary of OH^- Efflux Characteristics

Finally Table 5.3 presents the basic OH^- efflux characteristics presented in this Chapter and reference is made to the respective experimental evidence upon which these characteristics were formulated.

TABLE 5.1

The Number of Activated OH^- Bands at a Particular Light Intensity

Experimental Number	Cell Length (cm)	Light Intensity (Wm^{-2})	Number* of Alkaline Bands Activated
A	3.1	10.0	4
		2.1	2
		1.2	1
B	4.2	9.5	6
		3.0	4
		2.0	2
		1.6	1
C	4.6	9.5	6
		4.0	5
		2.7	3
		2.0	1
D	3.0	10.0	3
		1.7	1
E	3.9	9.5	5
		3.1	3
		1.2	2
		0.9	1
F	3.6	8.0	5
		4.0	4
		2.0	2
		1.8	1
G	3.4	10.0	4
		6.6	4
		2.0	2
		1.0	1
H	2.6	9.7	2
		1.4	1
I	3.5	8.0	5
		3.5	2
		1.5	1

* Number of alkaline bands activated at a particular intensity was determined by conducting pH scans along the cell wall after a 2h illumination period.

TABLE 5.2

Lag period for primary hydroxyl bands in response to different light intensities

Experiment Number											
5			7			9			10		
LI*	AT+	AT^{-1} ‡	LI*	AT+	AT^{-1} ‡	LI*	AT+	AT^{-1} ‡	LI*	AT+	AT^{-1} ‡
2.3	> 300	—				0.8	> 14h	—	0.6	> 205	—
2.5	90	0.011	2.5	70	0.014	1.1	71.5	0.014	0.8	56.5	0.018
2.9	26	0.038	3.0	23	0.043	1.3	35.5	0.029	1.1	20.5	0.049
3.2	25	0.040	4.0	11.5	0.087	1.5	24.0	0.042	3.0	6.5	0.154
4.0	13.5	0.074	5.0	9.7	0.103	1.7	15.5	0.065	5.0	4.0	0.250
6.7	9.0	0.111	6.7	9.0	0.111	2.0	12.0	0.083	10.0	4.0	0.250
9.5	9.0	0.111	9.5	8.8	0.114	2.5	8.5	0.118			
11.2	7.0	0.143	11.2	9.5	0.105	3.6	7.0	0.143			
14.5	8.5	0.118	14.5	9.2	0.109	5.3	6.7	0.149			
17.0	8.0	0.125				8.3	6.5	0.154			
						10.0	6.5	0.154			

* LI is the light intensity in Wm^{-2}

\+ AT is the lag period (see Fig. 1) in minutes

‡ AT^{-1} is the reciprocal of the lag period in min^{-1}.

TABLE 5.3

Summary of the OH^- Efflux System Characteristics

Hydroxyl System Characteristic	Illustrative Experimental Evidence
A lag period exists prior to activation of OH^- efflux	Figures 5.1, 5.3 and 5.4
Hierarchical OH^- band status; primary, sub-primary and subsidiary bands	Figure 5.2 and Table 5.1
Critical activating "substrate" levels	Figures 5.3, 5.4, 5.5, 5.6 and 5.7 and Table 5.2
Critical deactivating "substrate" levels	Figures 5.5, 5.8 and 5.10
Critical and sub-critical light intensities	Figures 5.3, 5.4, 5.8 and 5.10
"Substrate pool" in relation to critical deactivating "substrate" levels	Figures 5.5, 5.8 and 5.10.

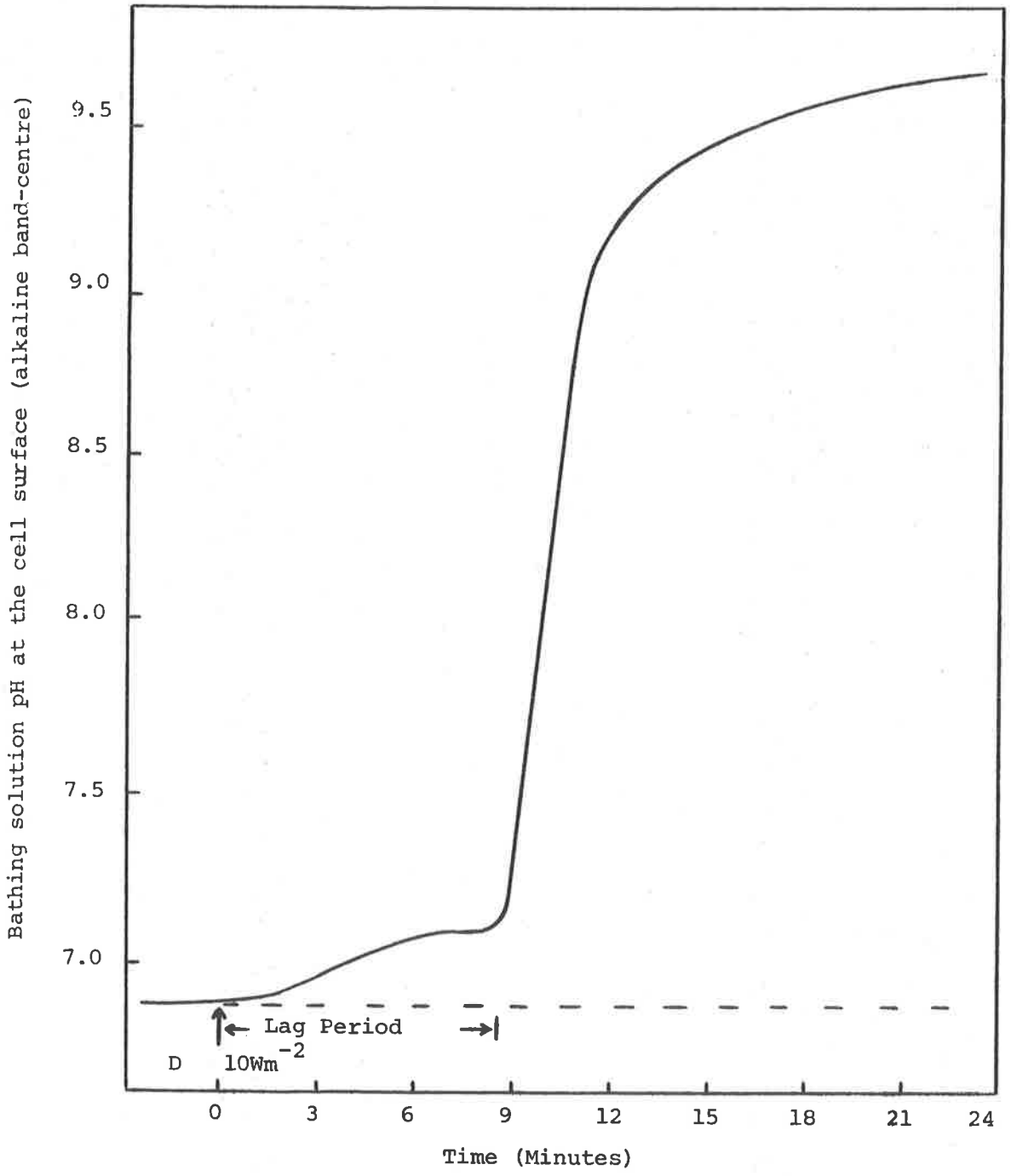

Figure 5.1. An alkaline band response to $10Wm^{-2}$ illumination following a 1h dark pretreatment. The bathing solution contained 0.1mM $NaHCO_3$; the pH value was 6.90. The hydroxyl lag period for this experiment was 8.6 min.

Figure 2.5. Cell wall pH scans conducted after 2h illumination at the specified light intensity. (A 1h dark pretreatment was employed before each illumination period). The actual light intensity employed for each scan is indicated on the figure.

The alkaline bands are labelled A to F, and their band-centres are indicated by vertical arrows. The broken line represents the pH value of the bathing solution, which contained 0.1mM $NaHCO_3$.

The results in this figure form part of Expt. No. 10 (see Table 5.2). In Figure 5.2D, (○) represents the cell response to a light intensity of 0.6Wm^{-2}. The actual time-course of this response is shown in Figure 5.3. The symbol (●) represents the cell response after 2h at 0.6Wm^{-2} following activation of this band by 3Wm^{-2}. This activating sequence is also shown in Figure 5.3.

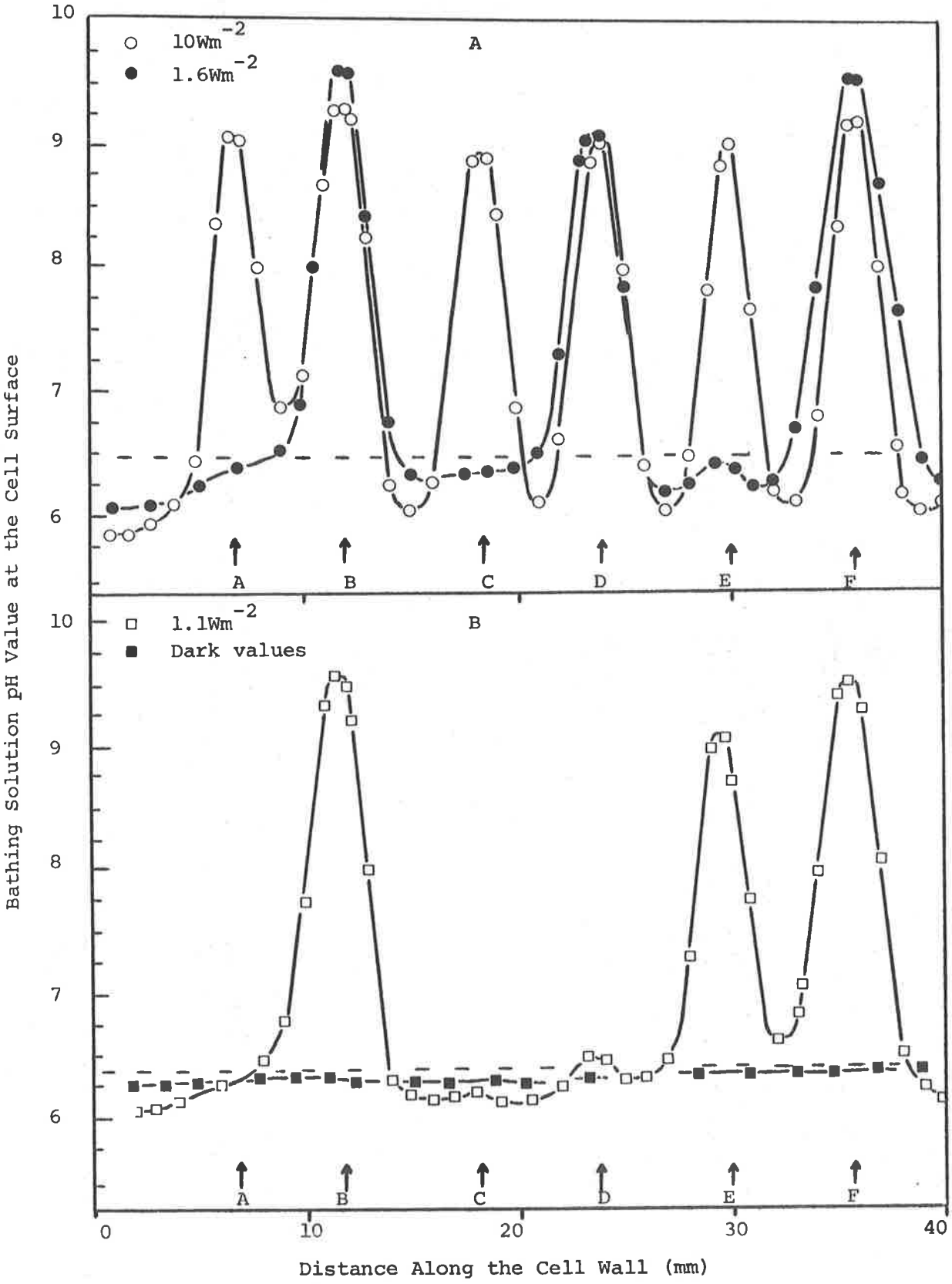
10
9
8
7
6
10Wm^{-2}
1.6Wm^{-2}
A
A
B
C
D
E
F
10
9
8
7
6
1.1Wm^{-2}
Dark values
B
A
B
C
D
E
F
0
10
20
30
40
Bathing Solution pH Value at the Cell Surface
Distance Along the Cell Wall (mm)

Figure 5.2 (A & B)

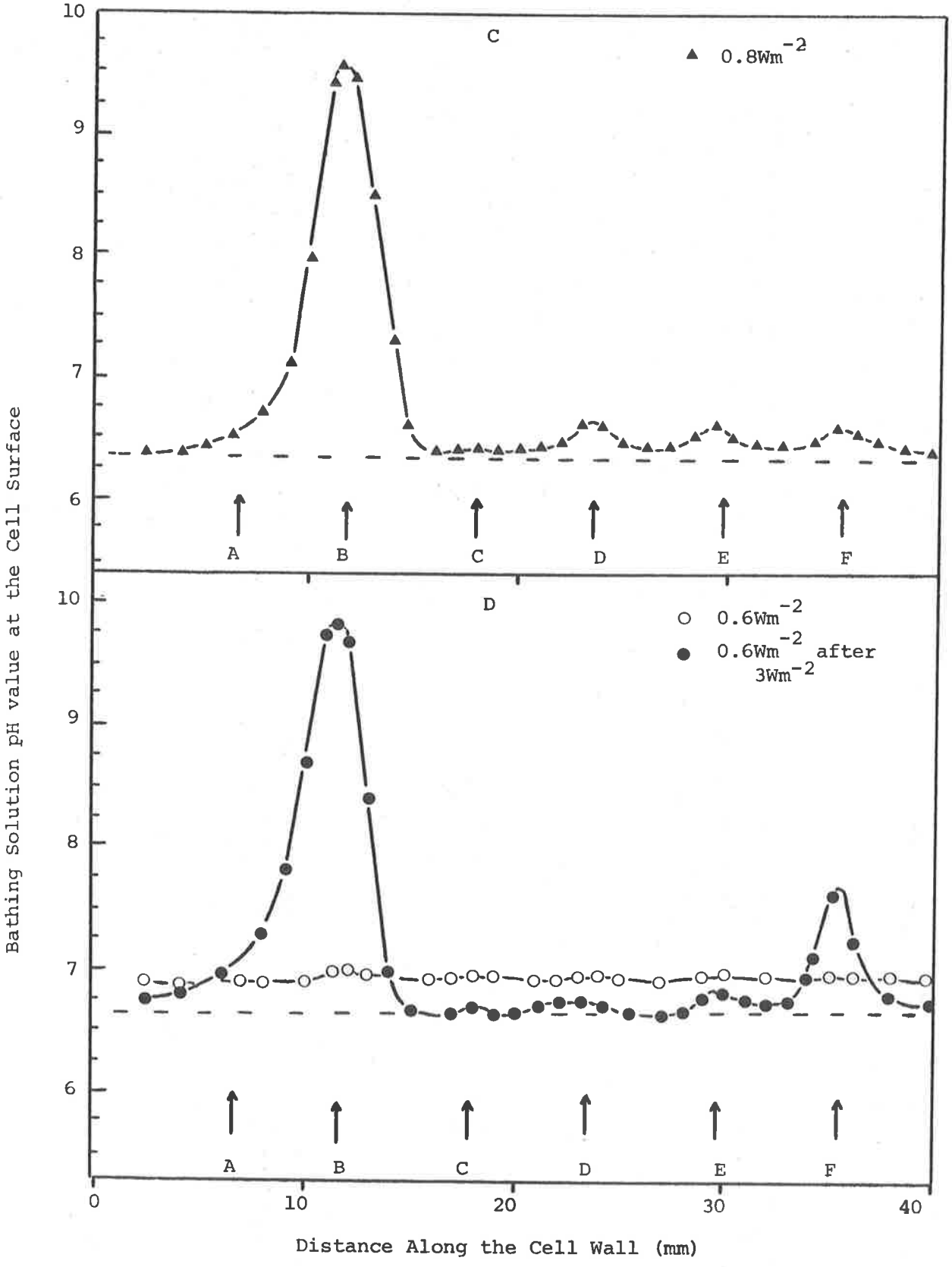
C
▲ 0.8Wm^{-2}
D
○ 0.6Wm^{-2}
● 0.6Wm^{-2} after 3Wm^{-2}
A
B
C
D
E
F
10
9
8
7
6
0
10
20
30
40
Bathing Solution pH value at the Cell Surface
Distance Along the Cell Wall (mm)

Figure 5.2 (C & D)

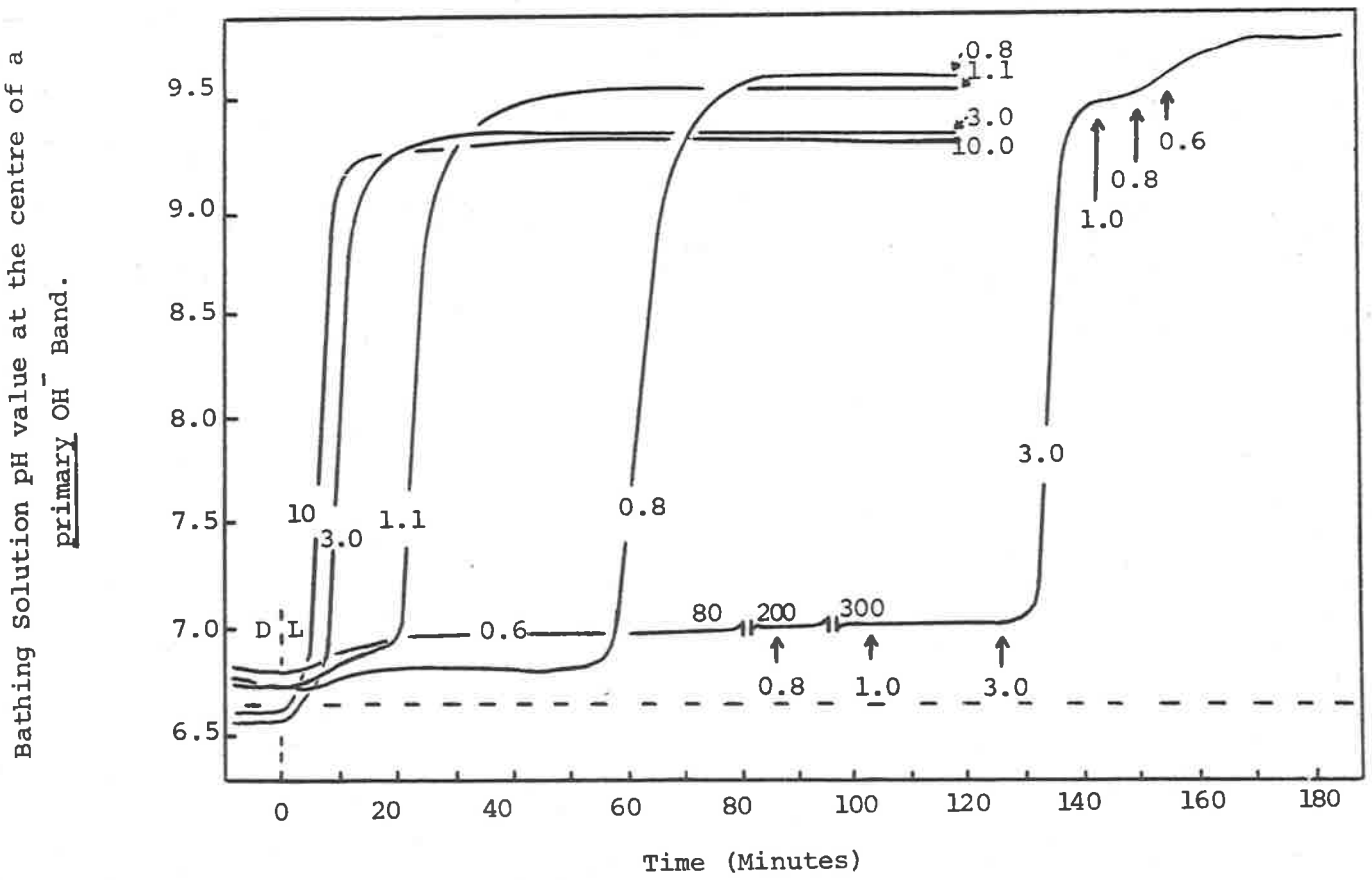

Figure 5.3. Primary OH^- band response to various light intensities. Each trace is the cell response to illumination, following a 1h dark treatment; the respective light intensities are indicated on the traces (values in Wm^{-2}). The vertical broken line and the symbols D and L indicate the transition from dark to light. The $0.6Wm^{-2}$ light intensity did not cause the primary band to activate. Intensities of 0.8 and 1.0 did not cause the expected activation: an intensity of $3Wm^{-2}$ was used to activate the band. (See text for full details).

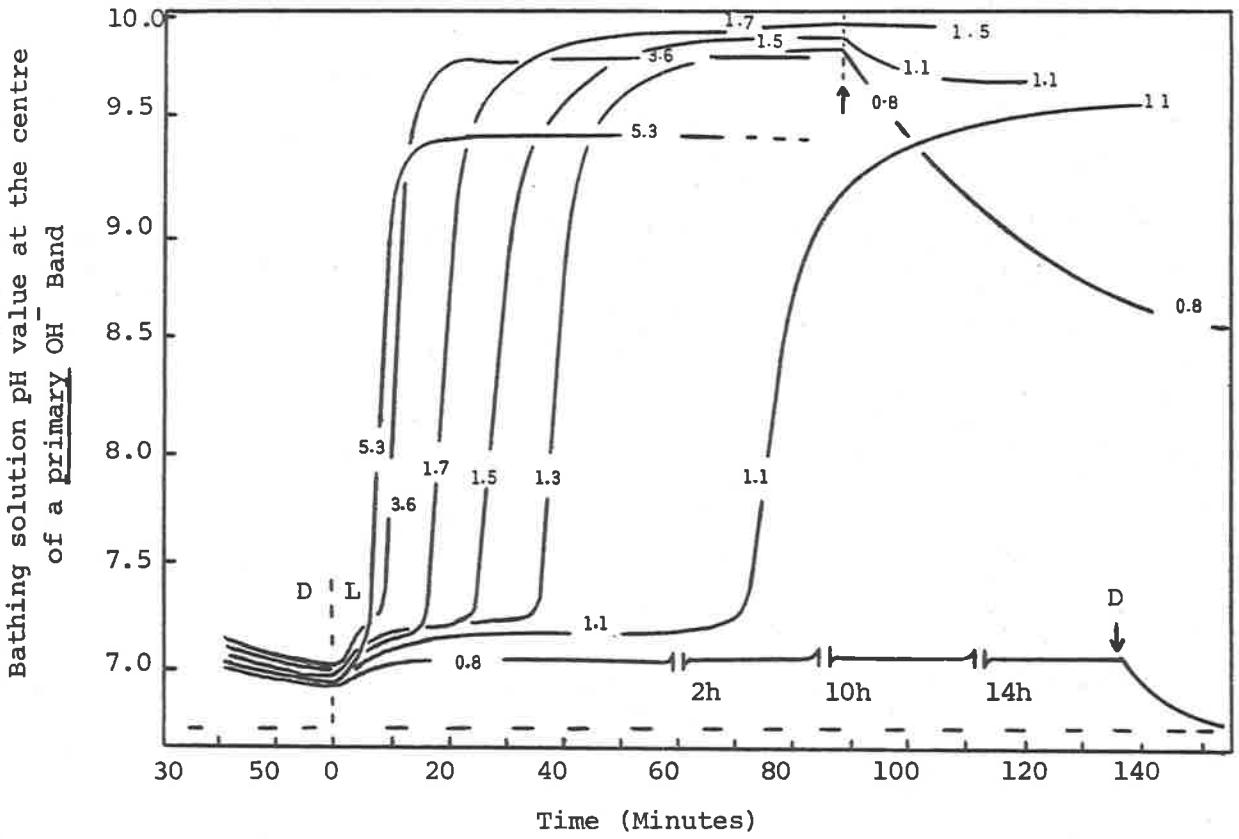

Figure 5.4. Primary OH^- band response to various light intensities. The explanation of the figure is the same as for Figure 5.4. For this cell $0.8Wm^{-2}$ would not activate the primary OH^- band, even after 14h illumination. The arrowed vertical broken line indicates the change to a lower light intensity. The change from 1.3 to $0.8Wm^{-2}$ is important, for it demonstrates that once the primary band is activated, it can remain active at intensities below which it could not be activated from the dark condition. The D on the $0.8Wm^{-2}$ response indicates the position where the light was switched off.

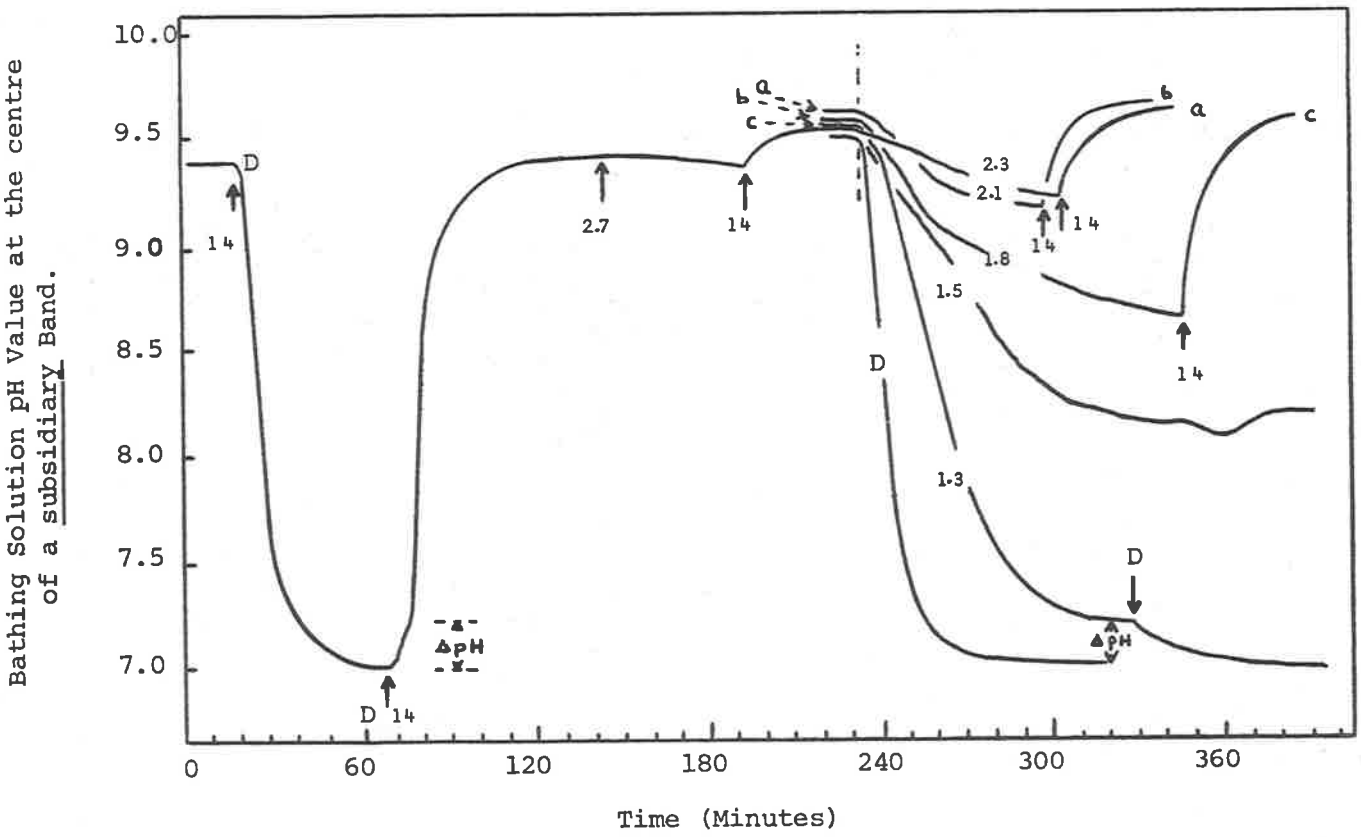

Figure 5.5. Subsidiary OH^- band response to decreasing light intensity. Arrows and vertical broken lines indicate changes in light intensities; the actual intensities are indicated on each trace (Wm^{-2}). D, represents a dark treatment. At the conclusion of each low light intensity treatment, the cell was given a 40 minute treatment under a $14Wm^{-2}$ light intensity. The letters a to c represent the sequence in which the treatments were performed, c is associated with the $1.3Wm^{-2}$ condition. The band had to be reactivated for the $1.5Wm^{-2}$ and dark treatments. ΔpH is the amount by which the $1.3Wm^{-2}$ light intensity raised the cell wall pH above the bathing solution.

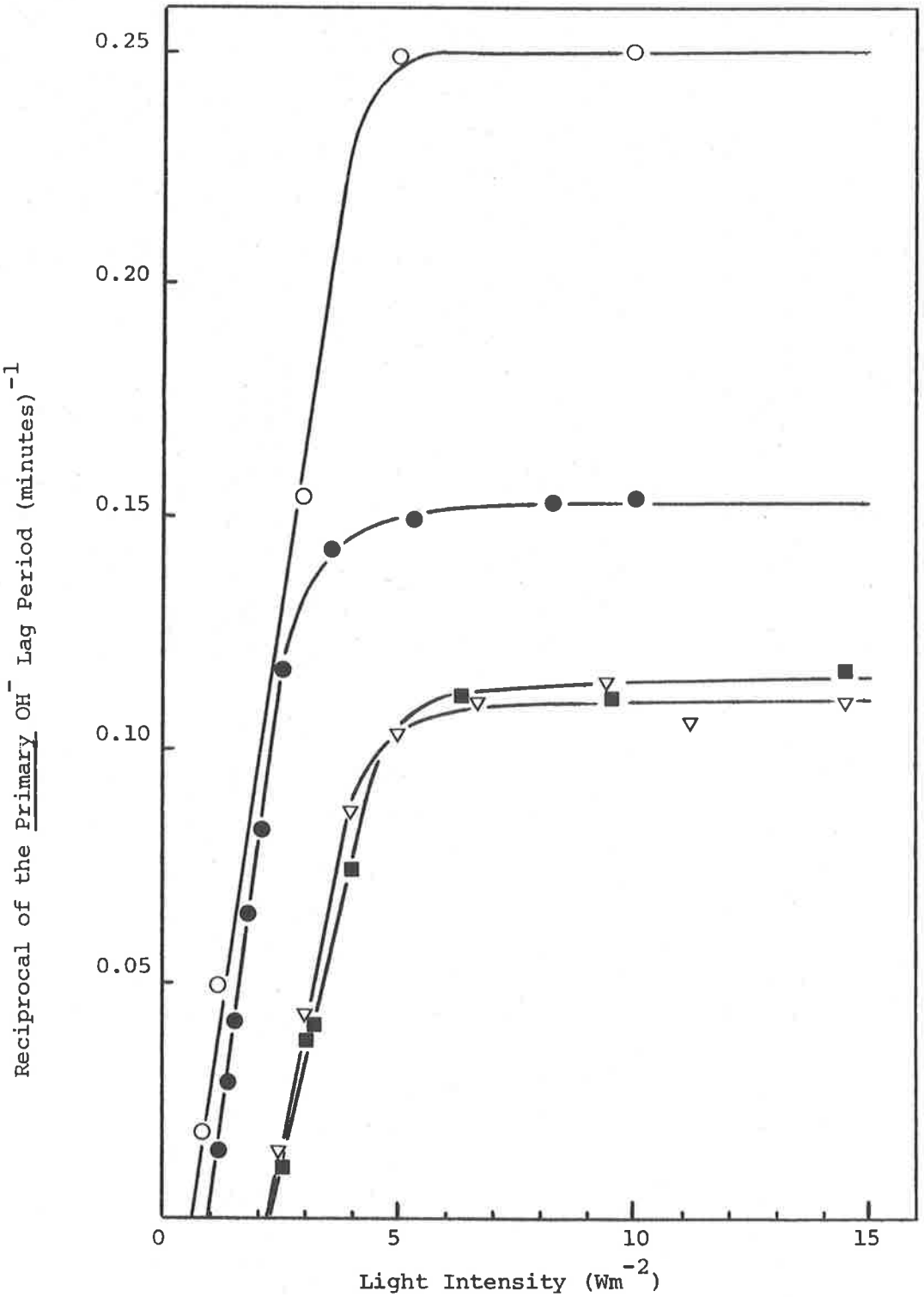

Figure 5.6. Reciprocal plot of primary OH^- lag period against light intensity; actual experimental values are presented in Table 5.2, and the symbols correlate as follows; (■), Exp. 5; (▽), Exp. 7; (●), Exp. 9; and (○), Exp. 10. The critical activation light intensities obtained from this analysis were 2.3 ± 0.5, 2.2 ± 0.5, 0.9 ± 0.5 and 0.7 ± 0.5 Wm^{-2} for experiments 5, 7, 9 and 10 respectively.

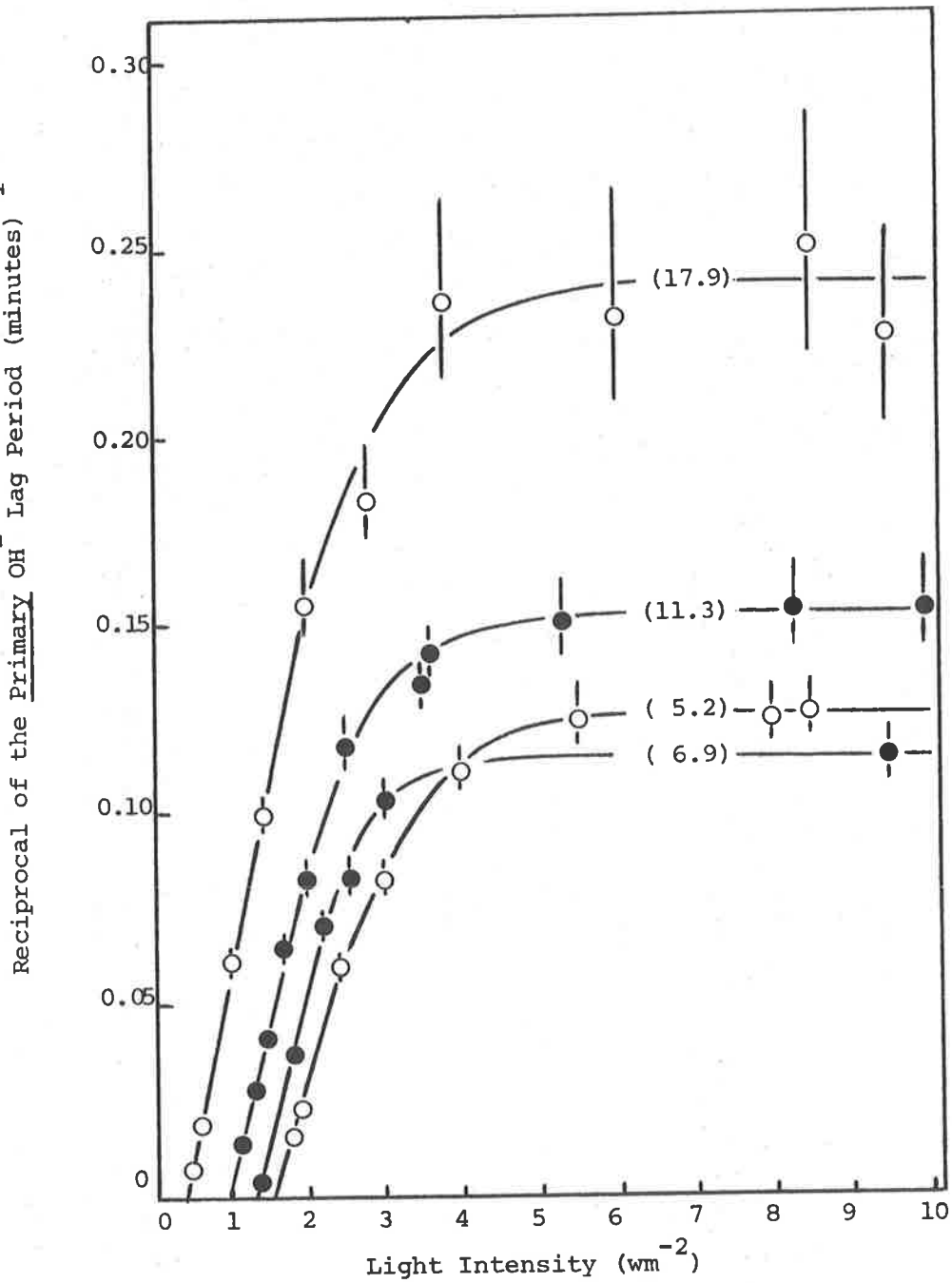

Figure 5.7. Reciprocal plot of primary OH^- lag period against light intensity. The values in parentheses are the chlorophyll concentrations of the cell in μg chl. cm^{-2} (see Appendix B). The bars represent ±0.5 minute on the experimentally determined lag periods.

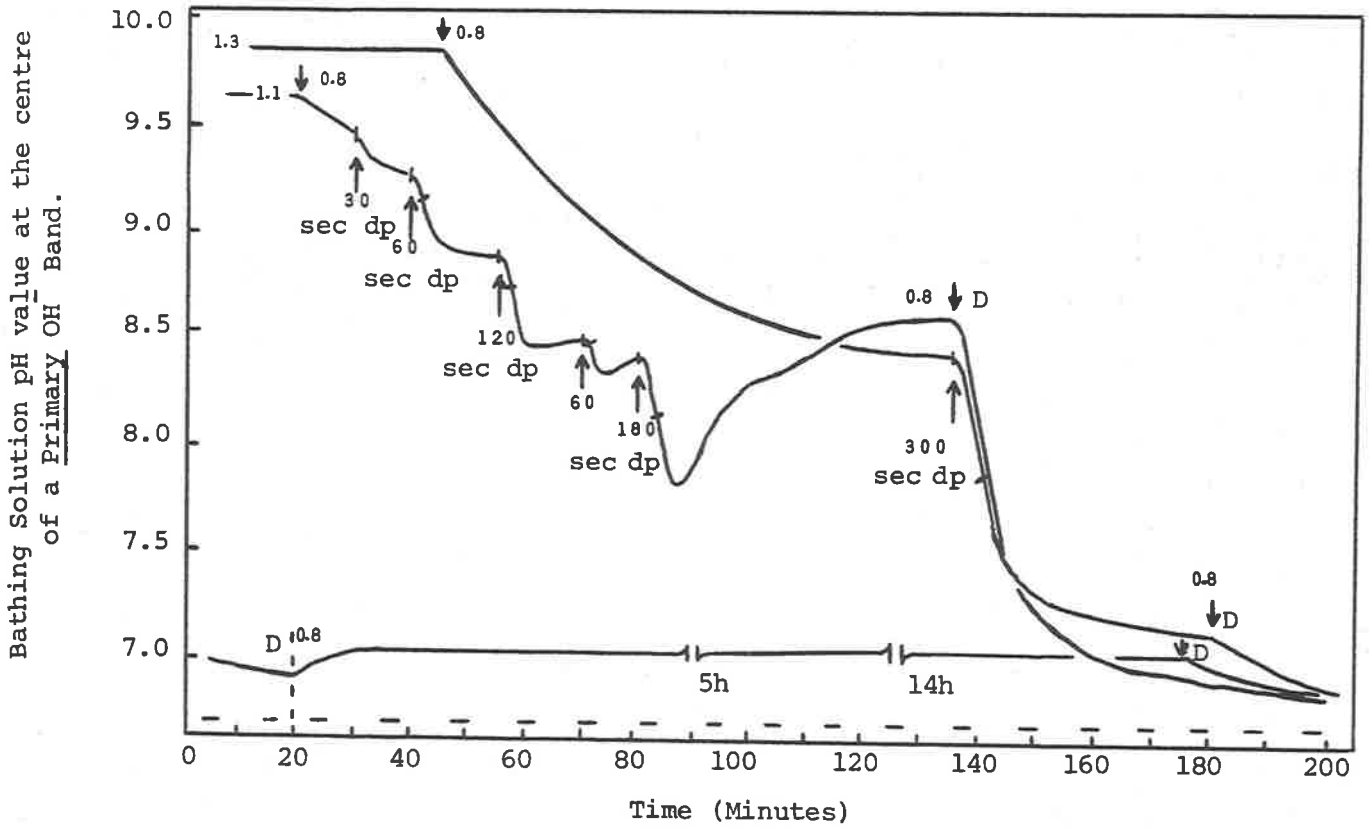

Figure 5.8. Deactivation of a primary OH^- band being maintained by sub-critical light intensities. The critical light intensity for this cell was $0.9 Wm^{-2}$. The band was active for 1h (at the intensity indicated on the individual traces) prior to the commencement of the experiment. The abbreviation, 30 sec dp, represents a 30 second dark period.

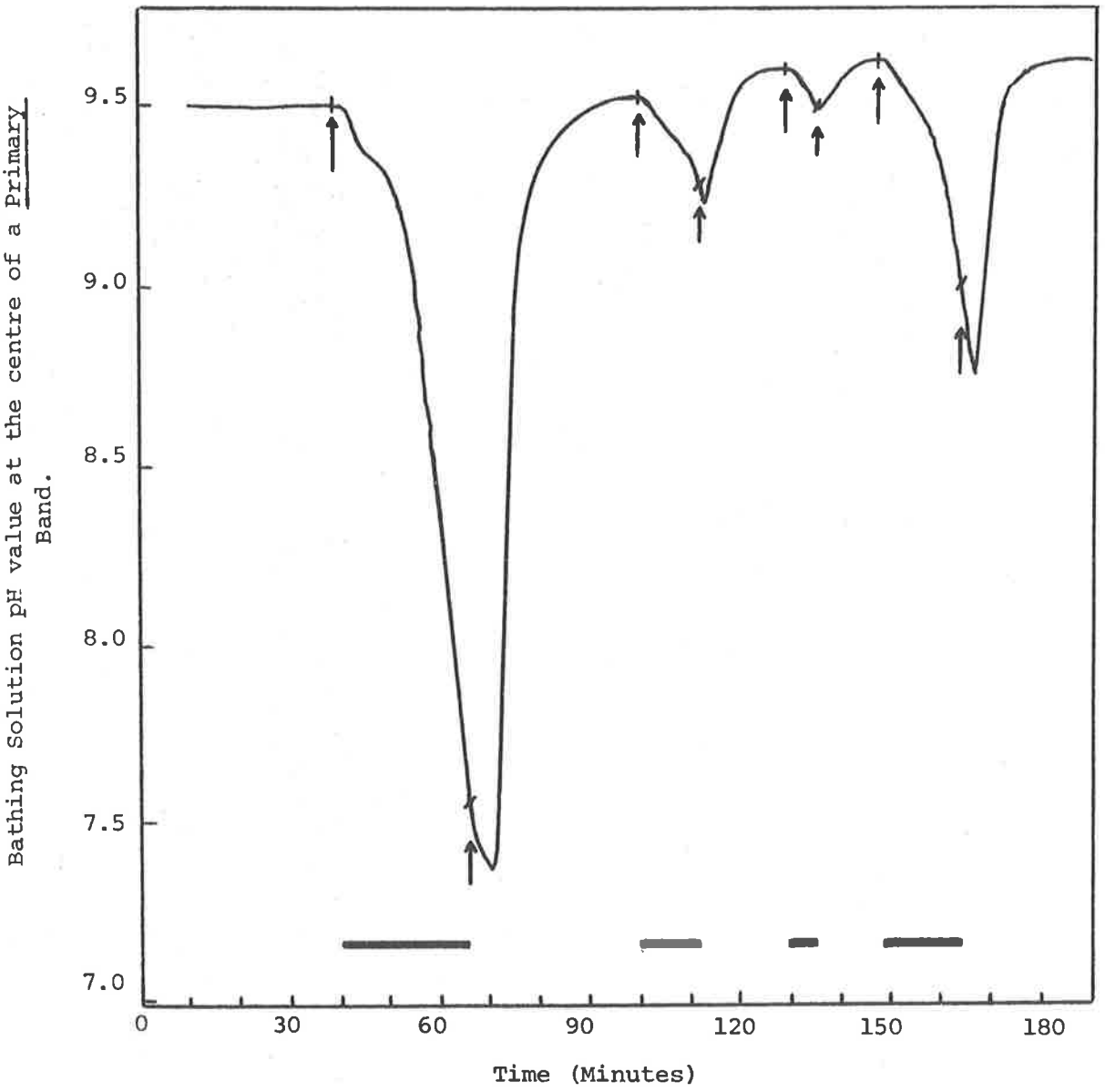

Figure 5.9. Activation of a primary OH^- band following dark periods of 25, 12.5, 5 and 15 minutes (from left to right). This cell had a critical light intensity of $0.5Wm^{-2}$. The light intensity used to activate the band was $4Wm^{-2}$ throughout. The arrows and black horizontal lines indicate the duration of the dark periods. Further results using this cell are presented in Figure 5.10.

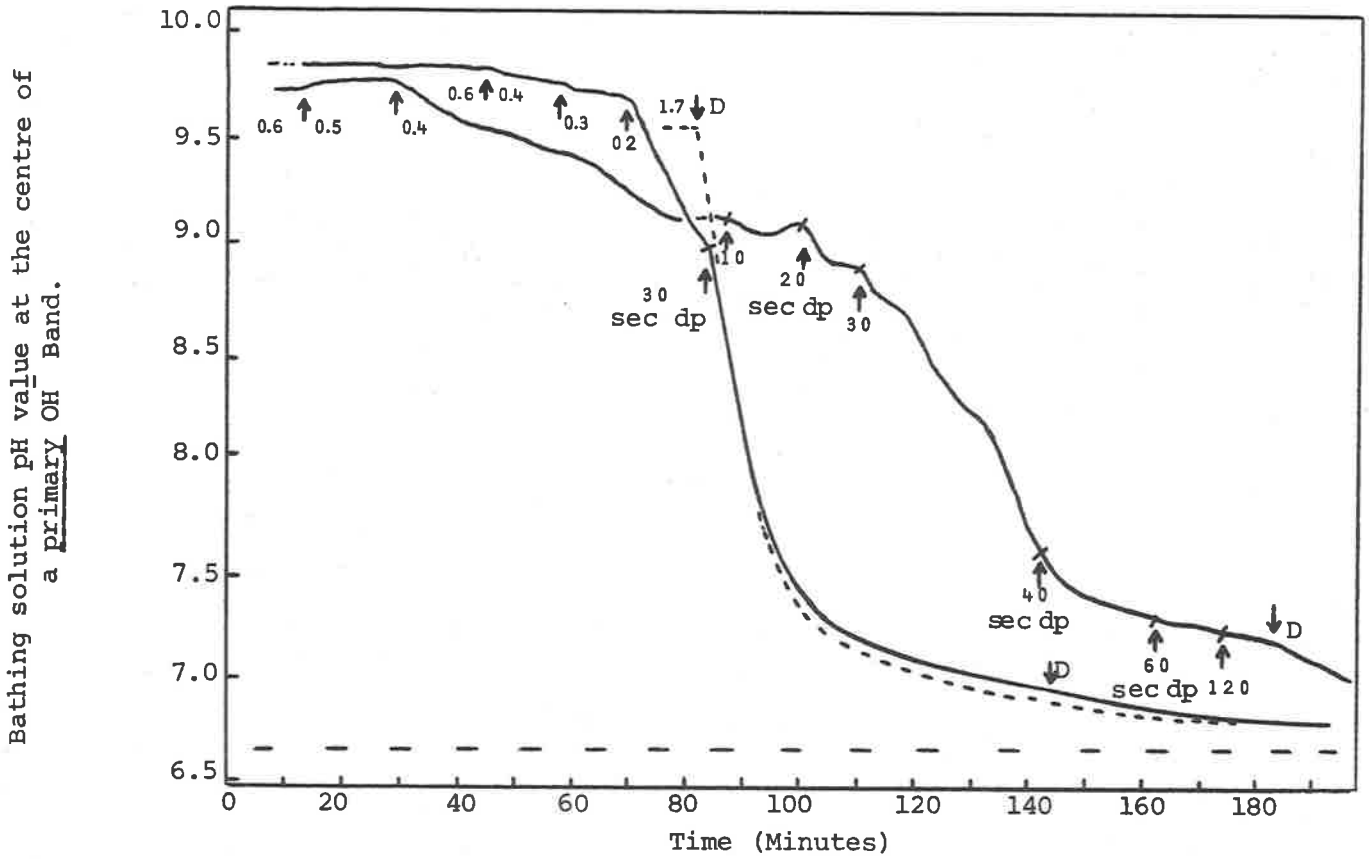

Figure 5.10. Deactivation of a primary OH^- band being maintained by sub-critical light intensities. The critical light intensity for this cell was $0.5 Wm^{-2}$. The band was active for 1h (at the intensity indicated on the individual traces) prior to the commencement of the experiment. The abbreviation, 30 sec dp, represents a 30 second dark period.

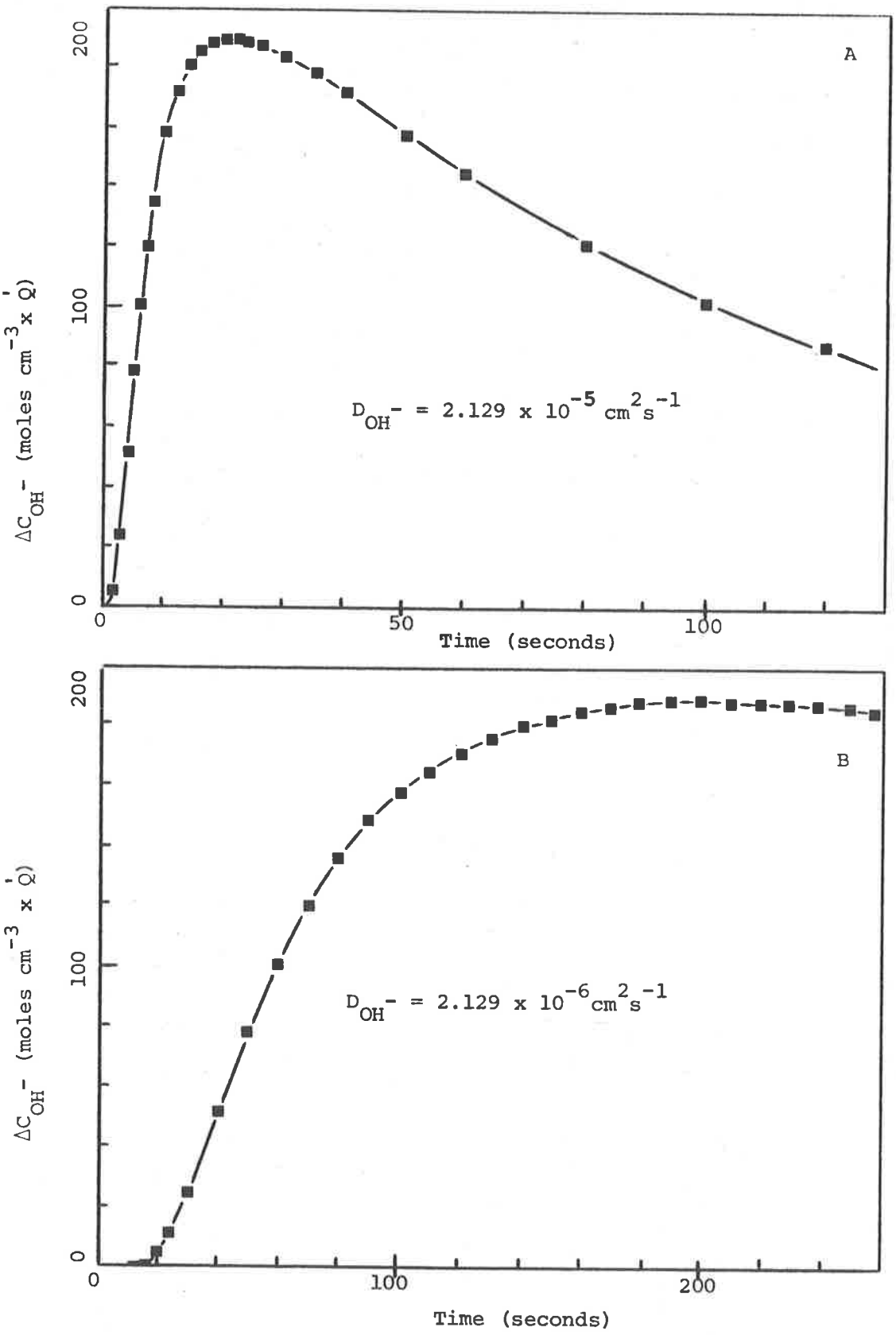

Figure 5.11. Concentration (OH^-) profiles at the mean sensing distance of the pH electrode. See Text for full details. ΔC_{OH^-} is the increase in OH^- concentration above the background, due to the diffusion of OH^- ions from the hypothetical instantaneous spherical surface source.

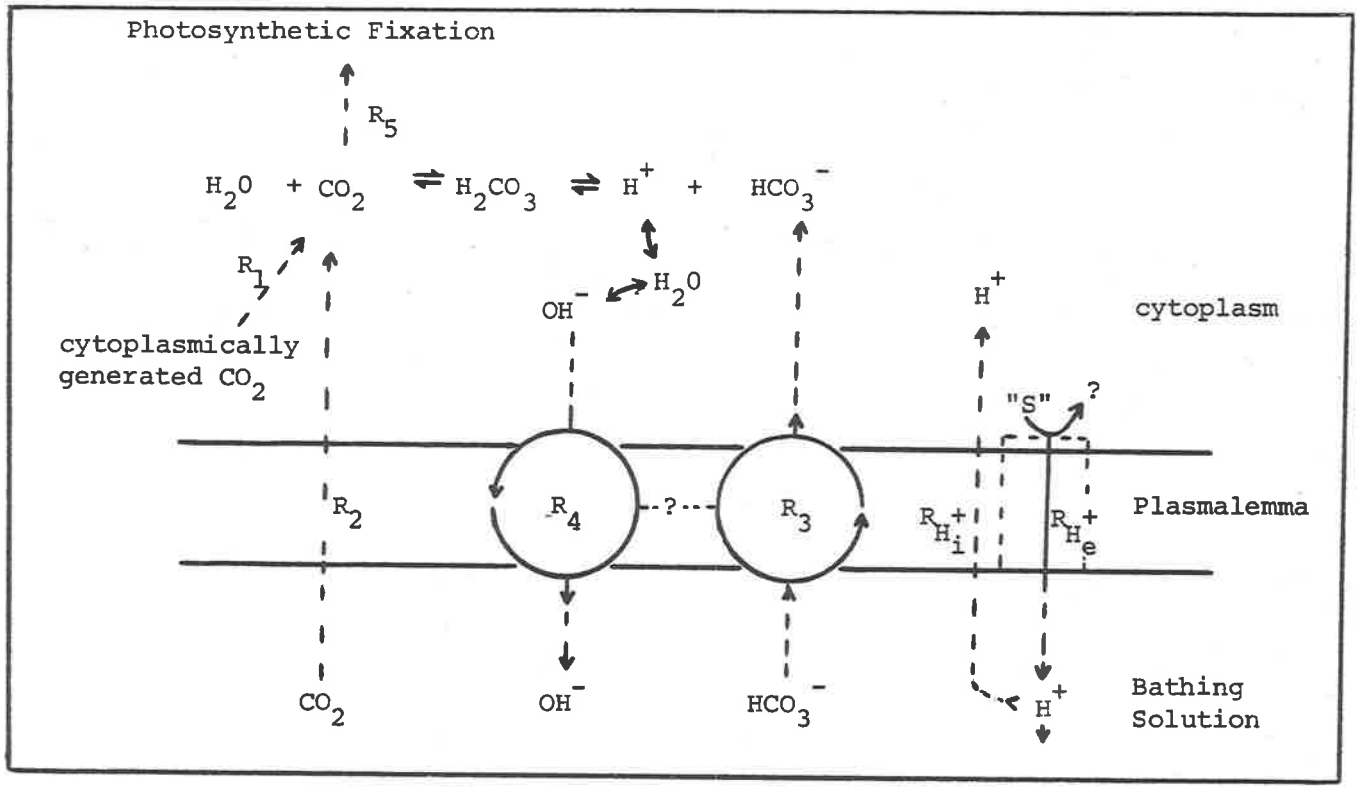

Figure 5.12. Schematic representation of the equilibria, diffusion processes and carrier systems associated with the photosynthetic supply of CO_2 and HCO_3^- in an internodal cell of *Chara corallina*. R_1 is the rate at which CO_2 is supplied, via respiration and photorespiration, to the cytoplasmic pool of CO_2; R_2 is the rate of diffusion of CO_2 from the bathing solution; R_3 is the rate of supply of HCO_3^-, via a plasmalemma carrier system, from the bathing solution to the cytoplasm; R_4 is the rate of OH^- efflux, via plasmalemma carriers, from the cytoplasm to the bathing solution; R_5 is the rate of CO_2 fixation in the chloroplasts. The coupling between HCO_3^- and OH^- carriers is doubtful. R_{H^+} is the rate of efflux of H^+, and R_{H^+} is the rate of passive influx of H^+ ions. The nature of "S", the substrate for this "H^+ system" is not known.

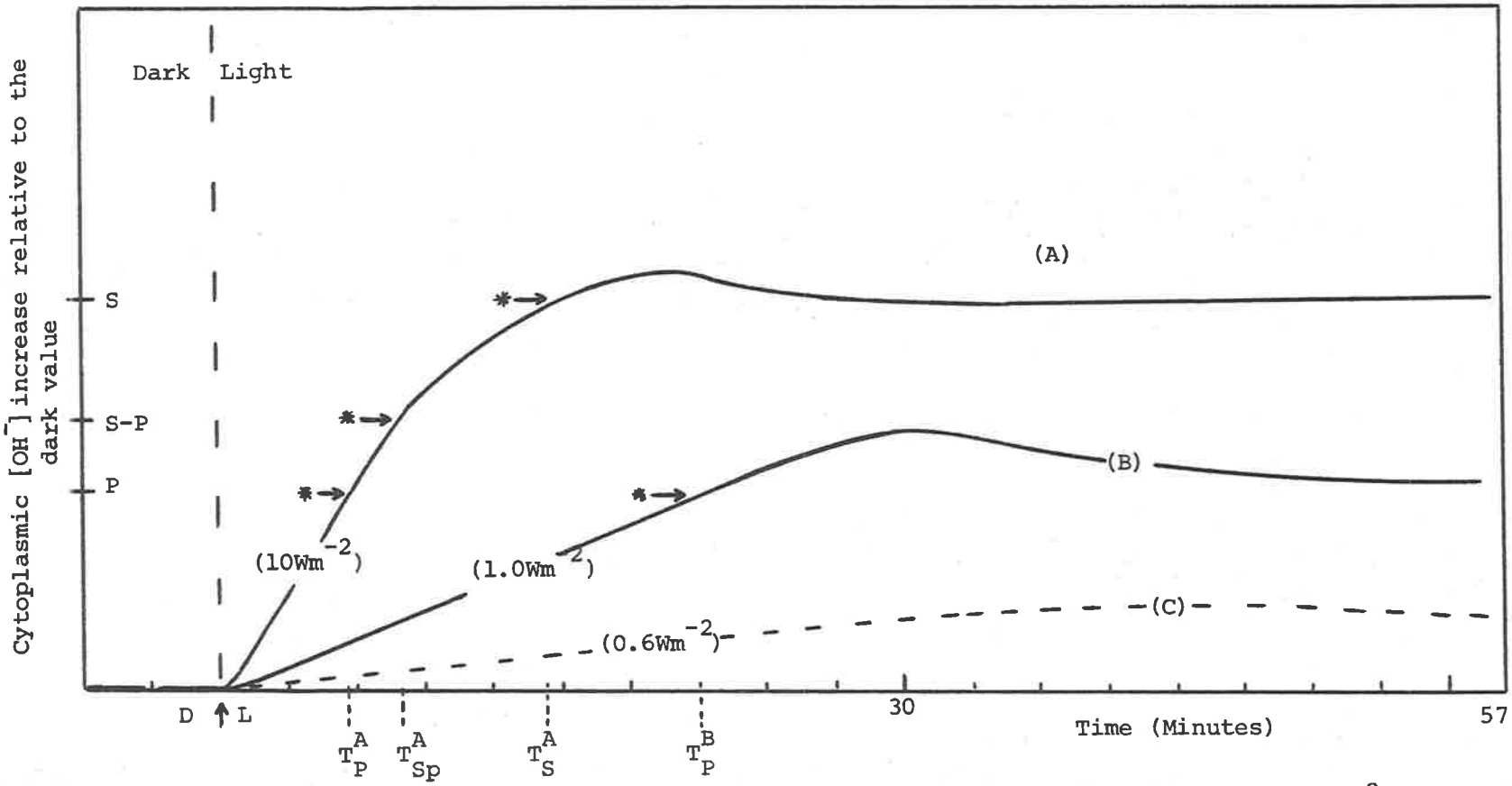

Figure 5.13. Hypothetical response of the cytoplasmic [OH^-] to illumination using high ($10Wm^{-2}$), low (1.0 WM^{-2}) and sub-critical ($0.6Wm^{-2}$) light intensities. The activating substrate levels are marked as P, S-P and S for the primary, sub-primary and subsidiary sets of OH^- carriers respectively. The abbreviations are as follows, (✱→), activation substrate level attained; T^A_P, primary OH^- Lag period associated with response A; T^A_{Sp}, as before but the lag associated with the sub-primary OH^- band; T^A_S, subsidiary OH^- lag periods. Response (A) was considered to have activated a primary, sub-primary and several subsidiary bands, response (B) only a primary OH^- band, and for response (C) no bands activated. (The experimental solution contained 0.1mM $NaHCO_3$, pH 7.0).

CHAPTER SIX

THE INFLUENCE OF LIGHT INTENSITY ON THE H^+ EFFLUX SYSTEM: AN INVESTIGATION AIMED AT TESTING THE Cl^- TRANSPORT MODELS

Introduction

Spear et al. (1969) demonstrated that Cl^- uptake into *Nitella clavata* was restricted primarily to the acidic surfaces of the cell. Since the acidification phenomenon and the major portion of the Cl^- influx were light dependent, these workers proposed that Cl^- influx might be "mechanistically" linked to H^+ efflux. (The dark or light-insensitive component of Cl^- influx, which is usually 0.2 - 0.5 pmol $cm^{-2}s^{-1}$, was considered by these workers to result from exchange diffusion (see also Hope, Simpson and Walker, 1966, for *Chara corallina*). Unfortunately Spear et al. misinterpreted the alkaline regions as resulting from passive H^+ entry at these regions, rather than the site of OH^- efflux resulting from HCO_3^- uptake. Consequently they rejected the possibility of a coupled Cl^-/OH^- transport system. What they failed to realize was that for a Cl^-/OH^- system the most favourable site, on an energetic basis, would be within the acid regions (Smith, 1970).

These workers did, however, propose three possible mechanisms by which Cl^- could be accumulated; the main hypothesis concerned the selective movement of Cl^-, via a Cl^- specific channel, into an intramembrane region where H^+ was being formed. Molecular HCl was considered to partition into the lipid phase of the membrane, and preferential inward diffusion of HCl to the cytoplasm was proposed. For diffusion to be restricted to this direction, it was necessary for these workers to postulate that the outer portion of the membrane functions as a barrier to the diffusion of HCl. Similarly to account for the observed net H^+ efflux, they were forced to include a specific channel for H^+ movement between the intramembrane

space and the external solution. Conceptually it is difficult to envisage these Cl^- and H^+ channels as "pores" (MacRobbie, 1970). This difficulty stems from the required selective movement of Cl^- or H^+ with the complete exclusion of HCl, for if this ion-pair could enter the channels it could escape to the external medium. The other weakness in this model is the partitioning into, and preferential movement of HCl through the "lipid phase" of the membrane. It is considered inexpedient to extrapolate the results of organic solvent studies to biological membranes. This becomes particularly so when it is realized that the conceptual model of biological membranes is in a dynamic state (see Capaldi, 1974).

The only other model which has been proposed specifically for Cl^- transport in *Chara* cells, is that developed by Smith (1970). His model was aimed specifically at Cl^- influx into *Chara corallina* and was based on the earlier ion exchange systems proposed to account for observed cation and anion imbalances in roots (Jacobson, Overstreet, King and Handley, 1950; Jackson and Adams, 1963; Hendricks, 1966; and Van Steveninck, 1964, 1966). Smith suggested that the active process was a Mitchell-type charge separation of H^+ and OH^- at the plasmalemma. (Supporting evidence for the existence of this transport system was claimed from the acid regions on this cell and the electrical studies of Kitasato, (1968)). The secondary transport processes of Na^+ and K^+ influx, both of which are passive in this species, were considered to result from the electrogenic nature of this H^+/OH^- separation. It was suggested that the pump increased the negative potential on the membrane such that the electrochemical potential driving force for these ions increased, in the direction which stimulated the influx of cations. The more important secondary process was the passive exchange of Cl^- for OH^-. Smith proposed that this exchange

process was driven by the OH^- concentration gradient across the plasmalemma. It was considered that Cl^- uptake would be limited by the rate of H^+ extrusion.

The common feature of the models proposed by Spear et al. (1969) and Smith (1970) is that the transport of Cl^- should be related to the observed H^+ efflux at the cell surface. Hence, both models suggest that activation of the Cl^- transport system should follow closely the activation response of the acid bands. Both models are similarly based on the electrogenic movement of H^+, so there should also be a correlation between the light stimulated time-courses of acid efflux, membrane potential hyperpolarization and Cl^- influx.

These Cl^- transport models can therefore be tested by measuring the time-course of net acid efflux and Cl^- uptake over a range of light intensities. If the net acid efflux exhibits long lag periods at low light intensities (i.e. similar to those observed for the OH^- bands), the time-course of Cl^-uptake should also have a response of this form if its transport is linked to H^+ generation.

Results.

Time-Course of H^+ efflux

H^+ efflux experiments were conducted along the same lines as the OH^- experiments described in Chapter Five. Acidification time-courses, obtained when a particular cell was transferred from the dark to four different light intensities, are presented in Figure 6.1. The dark period in each case was 1h, and because the acid bands required a considerable time to return to the steady dark value, the dark section of the pH traces in Figure 6.1 are in fact still rising towards the steady state. This equilibration

period was always a problem when studying the acid regions. At each intensity, following a 90 minute illumination period, a pH scan was performed along the cell wall. Figures 6.1 and 6.2 represent a complete acid band time-course and cell surface steady state analysis for a particular cell. These results were typical of the responses obtained when cells were illuminated over a range of light intensities.

On the day after an acid band experiment had been conducted, the primary OH^- band system was investigated so that the lag periods prior to activation of the acid and alkaline bands could be compared. Table 6.1 contains experimental data for two such consecutive acid and primary OH^- band studies (Experiment A refers to the results presented in Figures 6.1 and 6.2). This comparison revealed that although the acid and alkaline bands had comparable lag periods under high light intensities, the similarity did not extend to the situation where very low light intensities were employed. As the intensity was reduced, both the H^+ and OH^- efflux lag periods increased, however under low light intensities of 0.8 - 1.2 Wm^{-2} the acid efflux system did not appear to activate at all (see also Figures 6.3 and 6.4). Under the same conditions the primary OH^- efflux system did activate after a prolonged lag period.

A second distinguishing feature between the activity of these bands was that each of the acid bands, comprising the total acid efflux system, appeared equivalent in efflux status. Thus the acid bands did not follow the primary, sub-primary and subsidiary band status of the alkaline bands. This can be seen by examining the pH values of the respective acid band-centres of Figure 6.2. Each of the four acid bands active on this cell, depressed the bathing solution pH value to approximately the same value under the respective light intensity. The slightly lower pH values observed for

the two outer bands (at $10Wm^{-2}$) resulted from the fact that these acid bands had only one neighbouring OH^- band. Note also that under $0.8Wm^{-2}$, when no net acid activity could be detected, the primary OH^- band remained operational.

Figures 6.1 and 6.2 also demonstrated that the actual depression of the bathing solution pH value increased in a regular manner once the light intensity was raised above a certain intensity. Further experimental support for this correlation between the light intensity and the activity of the acid bands, is presented in Figure 6.3. Here the results of four experiments have been summarized by presenting the response of a single acid band from each cell. (For each band, the acid band-centre was indicated by an arrow). These results were included not only to illustrate the regular progression of the acid levels, but also to give some indication of the variability in acid efflux observed between different cells. The range of activity expressed between Figures 6.3A, B and D was frequently observed. It was also found that the acid activity did not depend to any significant extent on the pH value of the bathing solution, provided this value was not higher than pH 6.8 - 7.0. The apparent reduction in H^+ efflux activity above this pH value was discussed in Chapter 4. It is also worth stressing at this point that, on the basis of the diffusion analysis which was applied to the acid bands in Chapter 4, the net H^+ efflux rates observed during the time-course studies would have had a maximum value of approximately 1 pmol $cm^{-2}s^{-1}$, under $10Wm^{-2}$ illumination. The value associated with the type of response illustrated in Figure 6.3D would have been extremely small.

For most cells the acid efflux activity appeared to saturate under a light regime of approximately 3-4 Wm^{-2} (Figure 6.3). However, in some cells the acid efflux appeared to saturate at

lower intensities. A set of results for a cell of this type are presented in Figures 6.4 and 6.5. The dark induced acid band deactivation was also illustrated in Figure 6.4. Diffusion of H^+ away from the acid band required periods of greater than 1h before the pH value approached that of the bathing solution. Figure 6.5 also demonstrated that the primary OH^- band remained active under light intensities which would not elicit net H^+ efflux from the cell.

Influence of Light Intensity Reduction on H^+ Efflux Activity.

Having established a steady state pH value using a light intensity of 2.1 Wm^{-2} (see Figure 6.6), the intensity was increased to 10 Wm^{-2}. The cell responded immediately (within 30 seconds) to this higher light intensity, however a period of in excess of 40 minutes was required before the system approached a new steady state pH value. When the light regime was returned to the previous intensity of 2.1 Wm^{-2}, the pH value at the band-centre remained constant for some 5-10 minutes, it then slowly began to rise. The slow response was considered to be due to a readjustment of some cellular function rather than the diffusion characteristics of the physical system. As in the alkaline band studies (see Chapter 5), this conclusion was based on the considerable difference between the cellular responses elicited by transfer to the dark, as opposed to a lower intensity (see Figure 6.6). After 20 minutes the light intensity was reduced from 2.1 to 1.2 Wm^{-2}. This caused an acceleration of the upward drift in the pH value; even so it took 80 minutes to establish a new steady state under this low light regime. This final pH value was very close to the steady state pH value established when this cell was transferred from the dark to a light intensity of 1.2 Wm^{-2}.

There was a distinct similarity between these results and those obtained for subsidiary OH^- bands (see Figure 5.5). Hence it appeared that under a high light intensity a "pool" of "H^+-substrate" was developed, and it existed for some time after the cell was transferred to a much lower light intensity. The acid efflux system (net) was further investigated by illuminating ($10Wm^{-2}$) cells for 2h and then observing the acid band response when the light regime was reduced over a range of intensities. The type of response obtained,using this sequence, is demonstrated by the results presented in Figure 6.7. A slow readjustment of the acid band pH value was again observed. From the results associated with Figure 6.7, it was found that although an intensity of 0.8 Wm^{-2} could not, in itself, elicit cellular H^+ efflux activity, once the "H^+-substrate pool" had been established this intensity permitted H^+ efflux to continue. Unfortunately the $0.8Wm^{-2}$ treatment was not followed for more than 30 minutes; it would have been interesting to see whether the trace converged on the dark response after the cytoplasmic "H^+-substrate pool" was exhausted.

The slowly increasing pH value could be arrested simply by returning the cell to a higher light intensity (10 Wm^{-2} in Figure 6.7). Within 2 minutes of this readjustment in intensity, the acid band-centre pH value was being depressed towards the previously established steady state value.

$^{36}Cl^-$ Uptake Time-Course in Relation to the Measured H^+ Efflux Lag Period

The results presented in Figures 6.1, 6.4 and also 4.3 indicated that after an initial rise in the pH value at the acid band-centre, it was possible to discern net acid efflux activity within 8-10 minutes after the dark-to-light transition. This lag period was

for a light intensity of $10 Wm^{-2}$, but the results presented in Figure 6.1 and Table 6.1 indicated that this lag period did not increase significantly under lower light intensities. Hence, if the transport of Cl^- was coupled to the H^+ efflux process, the time-course for the light promoted uptake of this ion should exhibit a lag of approximately 10-20 minutes.

Preliminary $^{36}Cl^-$ experiments, conducted to determine whether a lag of this nature existed, were performed using unbuffered bathing solutions. A 1h dark period was employed so that the conditions would be consistent with those of the H^+ efflux experiments, and $^{36}Cl^-$ was substituted immediately before the commencement of the light period. Results obtained using this experimental sequence are presented in Figure 6.8A. A lag in $^{36}Cl^-$ uptake was in fact observed. Uptake did not attain a steady state value until the cells had been illuminated for a period greater than 40 minutes.

This lag in $^{36}Cl^-$ uptake may have been a reflection of cellular disturbance caused by solution substitution just prior to illuminating the cells. This possibility was tested by substituting the radio-active solutions 30 minutes before the cells were illuminated. (Figure 6.8B; $10.0 Wm^{-2}$). Again it was found that $^{36}Cl^-$ uptake was only slightly stimulated above the dark level for the first 30 - 40 minutes of the illumination period. At the end of this period the uptake increased significantly. This procedure was repeated using solutions which were buffered at pH 5.8 by 5mM HEPES buffer. (Smith (1970) showed that HEPES buffer did not affect $^{36}Cl^-$ uptake). The results were identical to the unbuffered treatments (see Figure 6.8B, $14.4 Wm^{-2}$).

$^{36}Cl^-$ Uptake: The Influence of Light Intensity

Experiments at different light intensities were conducted in an identical manner to that employed in Figure 6.8B. The solutions were buffered at pH 5.8 (5mM HEPES) to reduce the influence of the OH^- efflux system associated with the cellular assimilation of HCO_3^-, which would have become troublesome after prolonged illumination periods. It was argued that since similar results were obtained in the presence or absence of this buffer, it could not be having an effect on the functioning of the $^{36}Cl^-$ uptake system. The results obtained using cells from culture tanks Δ and E' are presented in Figures 6.9 and 6.10 respectively. In Figure 6.9 the $^{36}Cl^-$ uptake values have not been corrected for dark $^{36}Cl^-$ uptake. Since the experiments were conducted over several days, at least one dark uptake treatment was included in each light intensity series. Following the completion of the series, an average dark $^{36}Cl^-$ influx value of 0.261 ± 0.03 pmol $cm^{-2}s^{-1}$ was computed from the collective results. This value was then used to construct the "mean averaged" dark uptake line marked on Figure 6.9. The same procedure was employed for the results presented in Figure 6.10, except that the $^{36}Cl^-$ uptake values were corrected for this dark uptake component.

The results from these experiments were used to calculate $^{36}Cl^-$ influx values present under the respective light intensities; the values are presented in Figure 6.11. Some influx values included in this figure were determined by pre-illuminating the cells for 2h, under the specified light intensity, before substituting radioactive solutions. The $^{36}Cl^-$ uptake and hence influx values were determined over a 1h experimental period. The shape of these $^{36}Cl^-$ versus light intensity graphs (Figure 6.11) are interesting in two respects. Firstly, they show that the maximum $^{36}Cl^-$ influx rate

of 4 pmol $cm^{-2}s^{-1}$ was obtained under light intensities in excess of 6-7 Wm^{-2}. This influx value is equal to or greater than the maximum stimulation of $^{36}Cl^-$ influx reported by Smith (1970, e.g. Figure 1a). Secondly, they indicate that experiments conducted in the light intensity region of 2-5 Wm^{-2} could give variable influx results if a stable light system was not employed.

Discussion

The Cl^- Hypothesis Proposed by Spear et al. (1969)

On the basis of the Cl^- transport hypothesis proposed by Spear et al., the uptake of this ion should commence at least as soon as, and possibly before, net H^+ efflux was discernable at the cell surface. This follows as a direct property of their model. However, the observed lag in Cl^- uptake (see Figures 6.9 and 6.10) was greater than the lag associated with net H^+ efflux appearance (Figure 6.1). Consequently the hypothesis proposed by these workers has been invalidated, at least for *Chara corallina*.

The Cl^-/OH^- Hypothesis Proposed by Smith (1970)

During the lag in $^{36}Cl^-$ uptake, the actual uptake of $^{36}Cl^-$ was only just stimulated above the dark value. This was particularly so for tank delta cells (Figure 6.9). The duration of this lag was approximately 40-50 minutes for tank delta cells and 20-30 minutes for tank E' cells. For cells from either culture, under a particular light intensity the $^{36}Cl^-$ influx did not attain the steady state until a period of greater than 50-60 minutes had elapsed. These lags are similar in magnitude to those reported for $^{36}Cl^-$ influx into *Griffithsia flabelliformis* (Lilley and Hope, 1971) and slightly longer than the lag these workers reported for *Griffithsia monile*.

Hence, there does appear to be a degree of correlation between the lags observed in $^{36}Cl^-$ uptake and net H^+ efflux. (The H^+ efflux experiments were conducted using cells cut from culture tank E'). It would appear that the true light stimulation of the $^{36}Cl^-$ uptake began approximately 20 minutes after the cells were illuminated by a light intensity of 10.2 Wm^{-2}. The same cells would have commenced net H^+ efflux at approximately 6-10 minutes after the onset of illumination (see Figure 6.1). The delay in attaining the maximum rate of uptake may have been related to the establishment of a particular energy situation across the plasmalemma. Figures 6.1 and 6.4 demonstrated that the pH traces approached the steady state value only after prolonged illumination periods of at least 60 minutes. If the "activating energy" situation was not established for 20-30 minutes, it would account for this net H^+ efflux response. Once the activating condition for Cl^- uptake had been established across the plasmalemma, the Cl^-/OH^- exchange system would have limited further acidification of these regions.

The strongest experimental evidence against this activating condition being associated with the magnitude of the external acid concentration was obtained from the $^{36}Cl^-$ uptake experiments in which the solutions were buffered. The presence of 5mM HEPES buffer did not appear to influence the length of the lag period (see Figure 6.8B). This buffering capacity would certainly have prevented the development of acidic regions on the cell surface; the situation at the plasmalemma may not have been buffered to quite the same extent as the bating solution. Nevertheless the development of the acidity in this Donnan free space would certainly have been retarded, relative to the unbuffered situation. This suggests that the activating condition for Cl^- uptake is controlled by the development of an energy substrate (perhaps an OH^- gradient)

located in the cytoplasm.

Further experimental evidence which similarly does not support the concept of a critical external H^+ value, as the factor which determines the stimulation of the light induced Cl^- uptake, is the fact that the lag period appears to be of almost the same duration for each light intensity studied. Since most of the cells employed would have had light intensity acid-time-course responses similar to those presented in Figure 6.1, the time to establish a particular acidic pH value would have increased as the intensity was reduced.

The results suggest, therefore, that the cytoplasm is the most likely site for the development of the activating condition. Smith (1970) proposed that a Mitchell-type H^+-OH^- separating mechanism created the energetic situation by which Cl^- was transported into the cell. Hence the H^+-OH^- may establish a critical OH^- concentration at the plasmalemma. There appears to be some degree of conflict between this interpretation and the biophysical results obtained during studies on the time-course of the light induced hyperpolarization of the plasmalemma. The pertinent results of some of these biophysical studies are presented in Table 6.2. The experimental times listed in this table relate to the time required for the cell to establish a new steady state membrane potential following illumination. This period seems to lie between 10 and 30 minutes, i.e. the membrane potential would have stabilized before the $^{36}Cl^-$ uptake was stimulated. If the light induced hyperpolarization of the plasmalemma, in this pH region, is due to the operation of an electrogenic H^+ pump (Kitasato, 1968; and Spanswick, 1972), the steady state membrane potential would indicate that a balance had been achieved between the H^+ efflux and influx rates. Influx of Cl^- should also be correlated with the attainment of the steady

state hyperpolarization. Why then does the $^{36}Cl^-$ influx rate attain the steady state only after a period of approximately twice this duration?

Energetics of the Cl^-/OH^- Transport Process

The Gibbs free energy involved in the coupled transfer of a mole of Cl^- from the bathing solution to the cytoplasm, in exchange for a mole of OH^- being transferred in the opposite direction, can be calculated. Assuming conditions of constant temperature and pressure the expression for the change in Gibbs free energy is:

$$\Delta G_{\substack{Cl^o \rightarrow Cl^i \\ OH^o \leftarrow OH^i}} = (\mu^i_{Cl} - \mu^o_{Cl}) + (\mu^o_{OH} - \mu^i_{OH}) \quad \ldots\ldots \quad (6.1)$$

where μ is the electrochemical potential of the respective species and the superscripts i and o refer to the cytoplasm and the bathing solution respectively. Substituting $\mu_j = \mu^\circ_j + RT \ell n\, a_j + z_j F\Psi$ in (6.1), where μ°_j is the chemical potential of the j^{th} species in its standard state, a_j is the activity of the j^{th} species, z_j is the algebraic valency of the charge on the j^{th} ion and Ψ is the electric potential, gives:

$$\begin{aligned}\Delta G_{\substack{Cl^o \rightarrow Cl^i \\ OH^o \leftarrow OH^i}} = \Big\{ & (\mu^{\circ i}_{Cl^-} + RT \ell n\, a^i_{Cl^-} + Z_{Cl^-} F\Psi^i - \mu^{\circ o}_{Cl^-} - \\ & RT \ell n\, a^o_{Cl^-} - Z_{Cl} F\Psi^o) \\ & + (\mu^{\circ o}_{OH^-} + RT \ell n\, a^o_{OH^-} + Z_{OH^-} F\Psi^o - \mu^{\circ i}_{OH^-} - \\ & RT \ell n\, a^i_{OH^-} - Z_{OH} F\Psi^i)\Big\} \quad \ldots\ldots \quad (6.2)\end{aligned}$$

This equation simplifies to:

$$\Delta G_{\substack{Cl^o \rightarrow Cl^i \\ OH^o \leftarrow OH^i}} = \left\{\left[RT \ln \frac{a^i_{Cl^-}}{a^o_{Cl^-}} + Z_{Cl^-} F(\psi^i - \psi^o)\right] + \left[RT \ln \frac{a^o_{OH^-}}{a^i_{OH^-}} + Z_{OH^-} \cdot F(\psi^o - \psi^i)\right]\right\} \quad ..(6.3)$$

Since $Z_{Cl^-}F(\psi^i - \psi^o)$ will always be positive and equal to $F\Delta\psi$, and $Z_{OH^-}F(\psi^o - \psi^i)$ will always be negative and equal to $F\Delta\psi$, (6.3) reduces to:

$$\Delta G_{\substack{Cl^o \rightarrow Cl^i \\ OH^o \leftarrow OH^i}} = RT \left[\ln \frac{a^i_{Cl^-}}{a^o_{Cl^-}} + \ln \frac{a^o_{OH^-}}{a^i_{OH^-}}\right]$$

$$= RT \ln \left[\frac{a^i_{Cl^-} . a^o_{OH^-}}{a^o_{Cl^-} . a^i_{OH^-}}\right] \quad .....(6.4)$$

Using equation (6.4), it is possible to determine whether the OH^- gradient would provide sufficient energy for the coupled transport process to move spontaneously in the direction stipulated, i.e. ΔG must be ≤ 0. The values of $a^o_{Cl^-}$ and $a^o_{OH^-}$ were taken as 1.2×10^{-3} mol l^{-1} and 6.309×10^{-9} mol l^{-1} (pH 5.8) respectively. Unfortunately $a^i_{Cl^-}$ and $a^i_{OH^-}$ are not known with the same degree of certainty. Coster (1966) measured the Cl^- activity of the cytoplasm of *Chara corallina* to be 1×10^{-2} mol l^{-1}. This value will be used in the calculations, but it should be pointed out that $a^i_{Cl^-}$ will vary as a result of the different culture techniques employed in different laboratories. (Unfortunately it is also difficult to estimate a^i_{Cl} due to the problems involved in separating the large apparent Cl^- activity associated with the chloroplasts). The recent value of $a^i_{OH^-} = 5.07 \times 10^{-7}$ mol l^{-1} (external pH 5.8), obtained by Walker and Smith (1974) will be used in these calculations.

Substituting these values into equation (6.4) gave a value of $\Delta G = -1.34$ k cal mol^{-1}. The influence of using a slightly higher value of $a^{i}_{Cl^-} = 4 \times 10^{-2}$ mol l^{-1} can be seen in that ΔG is reduced to -0.52 k cal mol^{-1}. It would appear that the Cl^-/OH^- system could function spontaneously in the direction in which Cl^- would be transported to the cytoplasm, provided the cytoplasmic Cl^- level is less than 96mM. Also by holding $a^{o}_{OH^-}$, $a^{o}_{Cl^-}$ and $a^{i}_{Cl^-}$ constant, the value of $a^{i}_{OH^-}$ for the situation where $\Delta G = 0$, can be evaluated. A value of 5.25×10^{-8} ($pH_{cyt.}$ 6.72) was obtained assuming a value of 10mM for $a^{i}_{Cl^-}$. Substituting $a^{i}_{Cl^-}$ = 40mM gave a value of 2.09×10^{-7} or a $pH_{cyt.}$ of 7.32.

In relation to the present studies, these calculations show that by holding $a^{o}_{OH^-}$ constant, using buffers, would not prevent the establishment of a favourable energy transporting gradient. However, Walker and Smith (1974) showed that in the dark, when the bathing solution was buffered at pH 5.8, the cytoplasmic pH value would be approximately 7.5. Consequently the energetic gradient in terms of the Cl^-/OH^- system would be present even before the cells were illuminated. If only the activity of OH^- in the cytoplasm was involved, the Cl^-/OH^- system would activate almost immediately the cell was illuminated. (The specific involvement of light could have been related to a conformational requirement which was light dependent as could have been the supply of substrate which maintained the cytoplasmic level of OH^-).

Since immediate activation was not observed, it would appear that the uptake of Cl^- is not coupled to the net H^+ efflux process in as simple a manner as originally proposed by Smith (1970). The delay in Cl^- uptake cannot be due to the time required to establish the energetic levels of $a^{i}_{OH^-}$ required to permit the transfer

process to operate. It is considered that the lag is more likely to be due to the slow build-up, in the cytoplasm, of an energy substrate produced by the chloroplasts, such as $NADPH_2$ and/or ATP (Lilley and Hope, 1971; and Smith and Raven, 1974). This substrate may mediate in the binding of the ions to the carrier, or it may be required in the actual transport process. For example, it may enable the activation of the carriers over a large energy of activation barrier.

TABLE 6.1

Acid and Alkaline Band Lag periods Prior to Activation

Expt. No.	Light Intensity (Wm^{-2})	Primary OH^- Lag Period (minutes)	Acid Band Lag Period (minutes)
A	10	4.5	6
	8	4.5	6
	2.1	6.5	10
	1.6	12.5	n.m.**
	1.2	20.0	12
	0.8	44.5	n.a.+
	0.6*		
B	9.5	6.3	8.5
	5.0	8.4	n.m.**
	3.0	9.8	11.0
	1.9	13.0	14.0
	1.2	53.0	n.a.+
	1.0*		

* The critical light intensity value determined by the graphical analysis of the reciprocal of the OH^- lag period against light intensity.

** An acid time-course was not conducted at this light intensity.

\+ The acid efflux system remained inactive at this light intensity.

TABLE 6.2

Time Required to Establish the Steady State Membrane Potential Following a Dark-to-Light Transition

Required Time (Minutes)	Experimental Conditions		Species	Reference
	Solution	Light Regime		
15-30	u/b*, 0.1mM KCl	1hD: $5Wm^{-2}$	*N. flexilis*	Nagai and Tazawa (1962)
10-20	0.1mM $NaHCO_3$ (pH 7.1)	1hD: ? Wm^{-2} ‡	*C. corallina*	Hope (1965)
8	u/b, 0.1mM KCl	D**: $10Wm^{-2}$	*N. flexilis*	Andrianov et al. (1968)
20	u/b, 0.5mM KCl, 0.2mM NaCl, 0.5mM $CaSO_4$	24hD: $10Wm^{-2}$	*C. braunii*	Nishizaki (1968)
≃ 30	pH 6.0, 1mM MES buffer, 0.5mM K^+, 0.1mM Ca^{++}, 0.1mM Mg^{++}, 1.4mM Cl^-, 1.0-1.3mM Na^+	1hD: $10Wm^{-2}$	*N. translucens*	Spanswick (1972)
5-20	u/s‡	D‡: $10-2Wm^{-2}$	*N. flexilis*	Volkov (1973)

* Bathing solutions unbuffered and hence the pH value would have been close to 5.75.

** These workers did not specify the exact duration of the dark treatment, but it would have been approximately 4-5 minutes.

‡ Unspecified by the author.

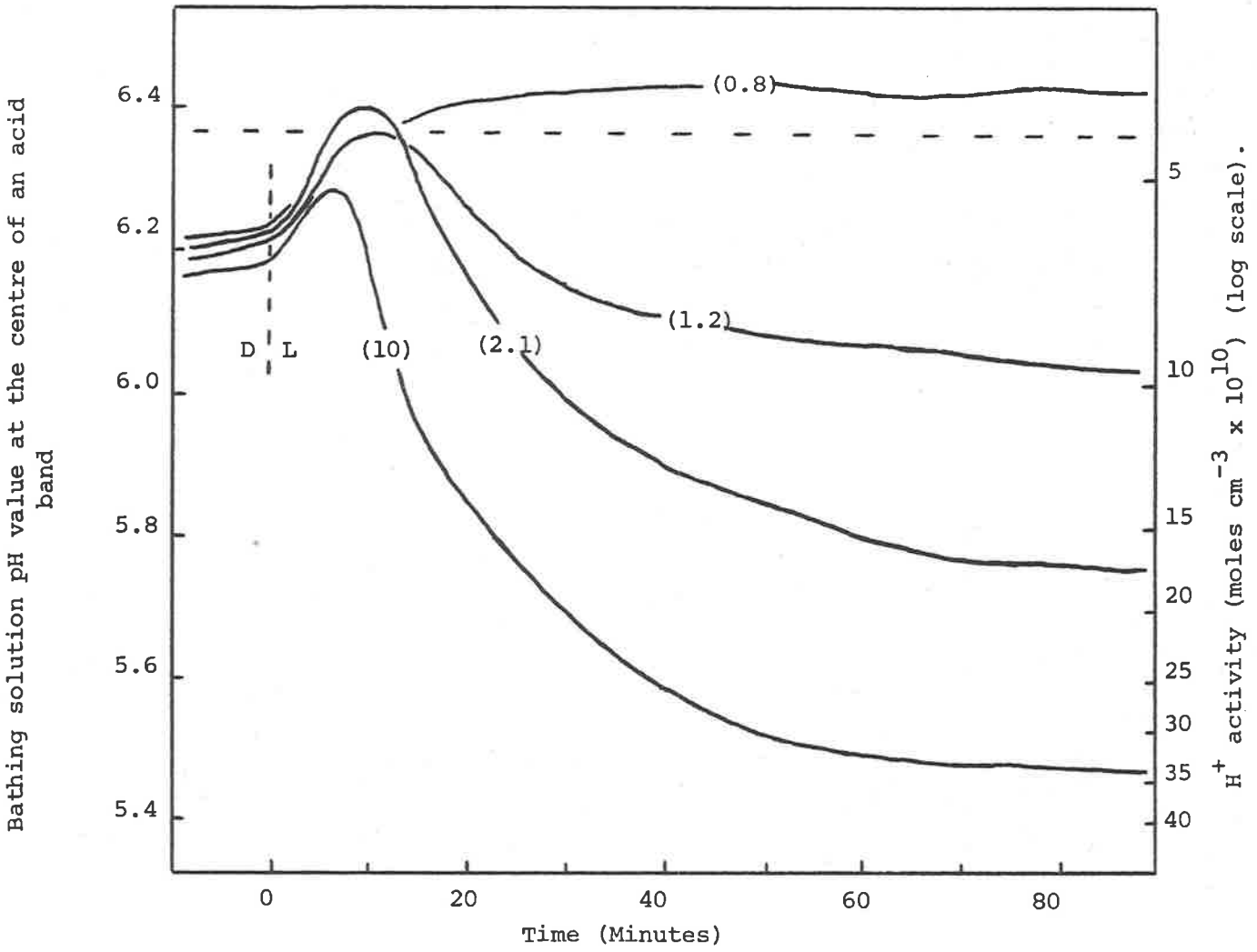

Figure 6.1. Acidification time-courses obtained under a range of light intensities. The cell was given a 1h dark treatment before each light intensity; actual values are indicated on the respective traces (Wm^{-2}). The broken line represents the pH value of the bathing solution and the symbols D and L indicate the transition from dark to light.

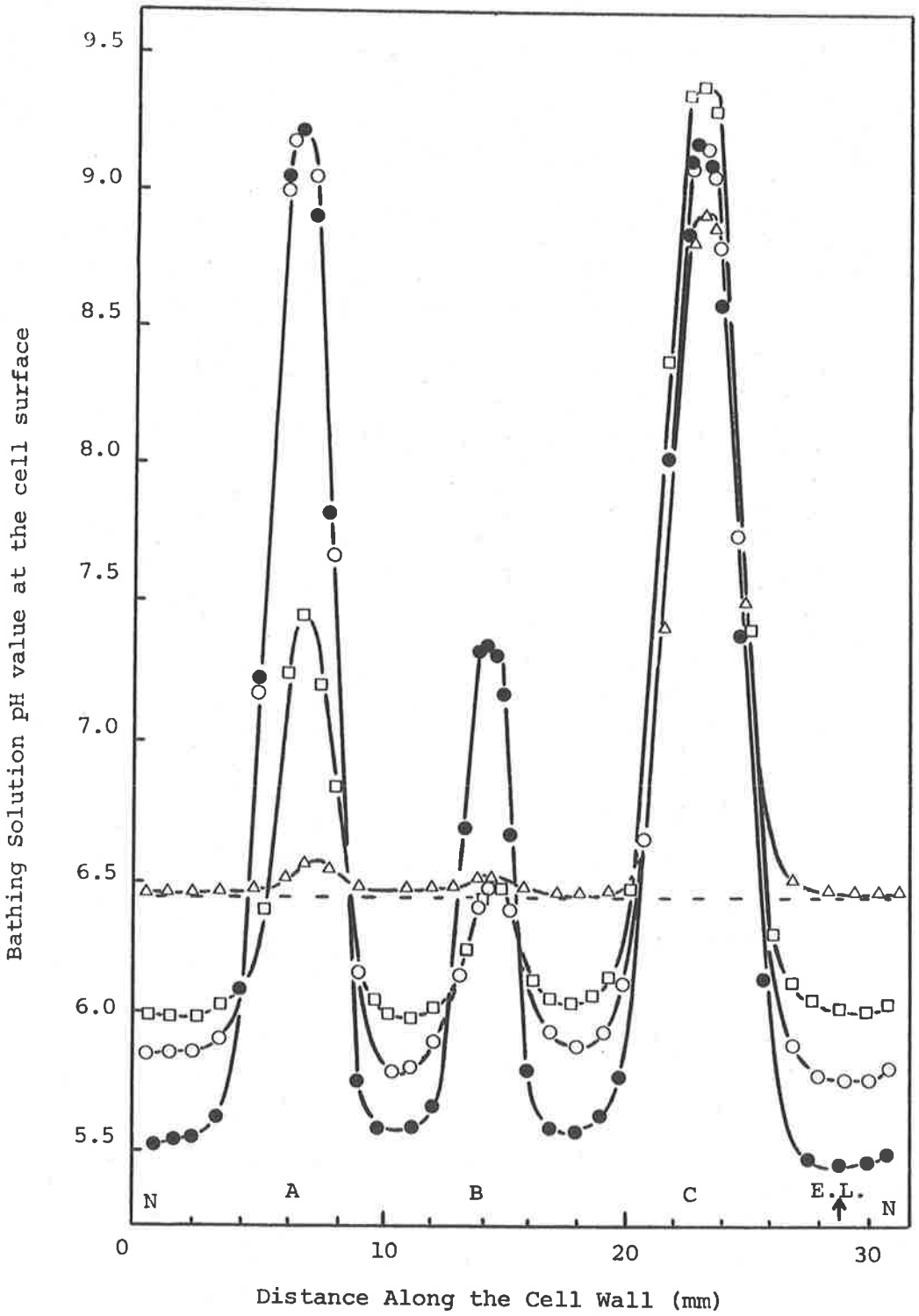

Figure 6.2. pH values established at the surface of the cell following a 90 minute illumination period. The symbols (●), (○), (□) and ($\triangle$) represent the values obtained under 10, 2.1, 1.2 and 0.8Wm^{-2} respectively. The nodal bcations are indicated by the symbol N, and E.L. represents the electrode location and acid band studied in the results presented in Figure 6.1. Alkaline bands C, A and D were the primary, sub-primary and subsidiary bands respectively. Note that the acid bands approach the same pH value under the respective light intensity.

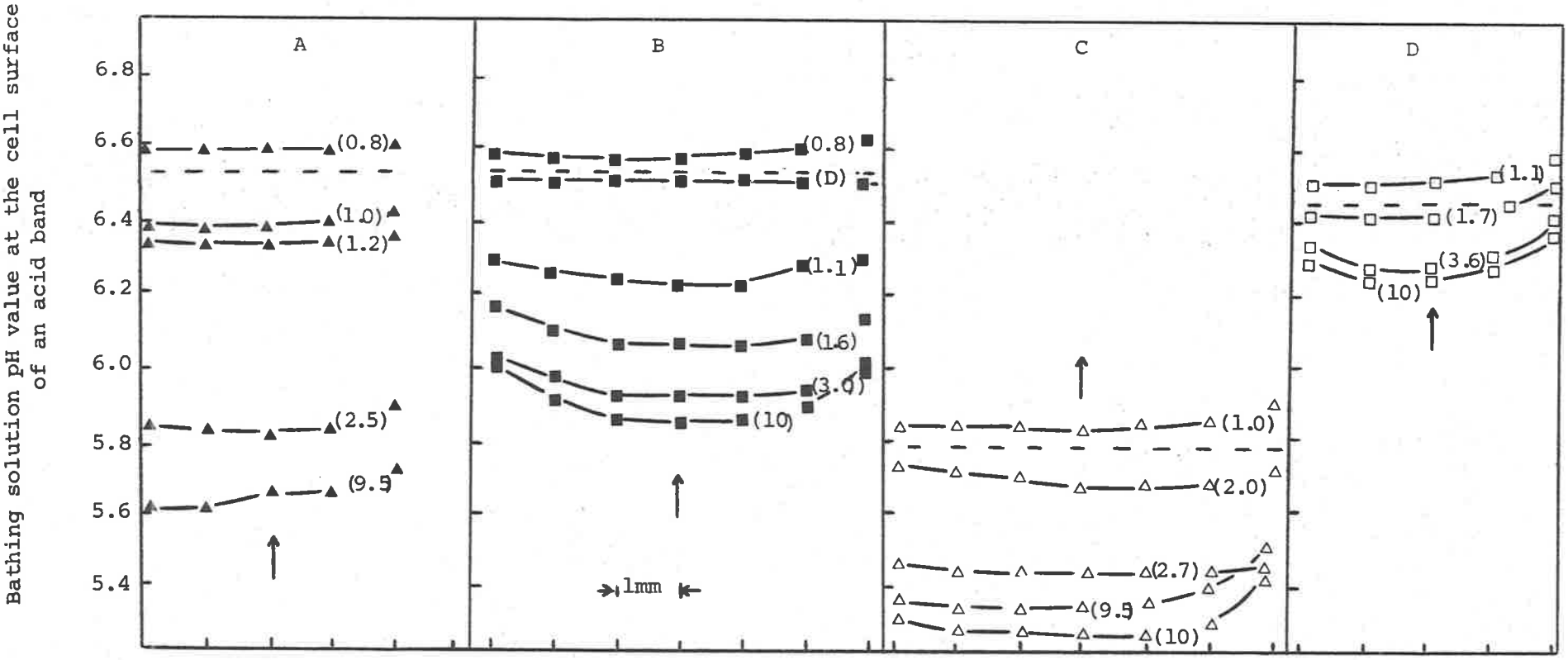

Figure 6.3. Approximate steady state acid values obtained under a range of light intensities. A, B, C and D represent the responses of four different cells and the values were recorded in the same manner as was employed for Figures 6.1 and 6.2. The broken lines represent the pH values of the bathing solutions A, B and D values were raised above 5.75 by using freshly prepared NaOH; C is the normal unaltered pH value. The values in parentheses are the respective light intensities in Wm^{-2} and the arrows indicate the location of the acid band-centres.

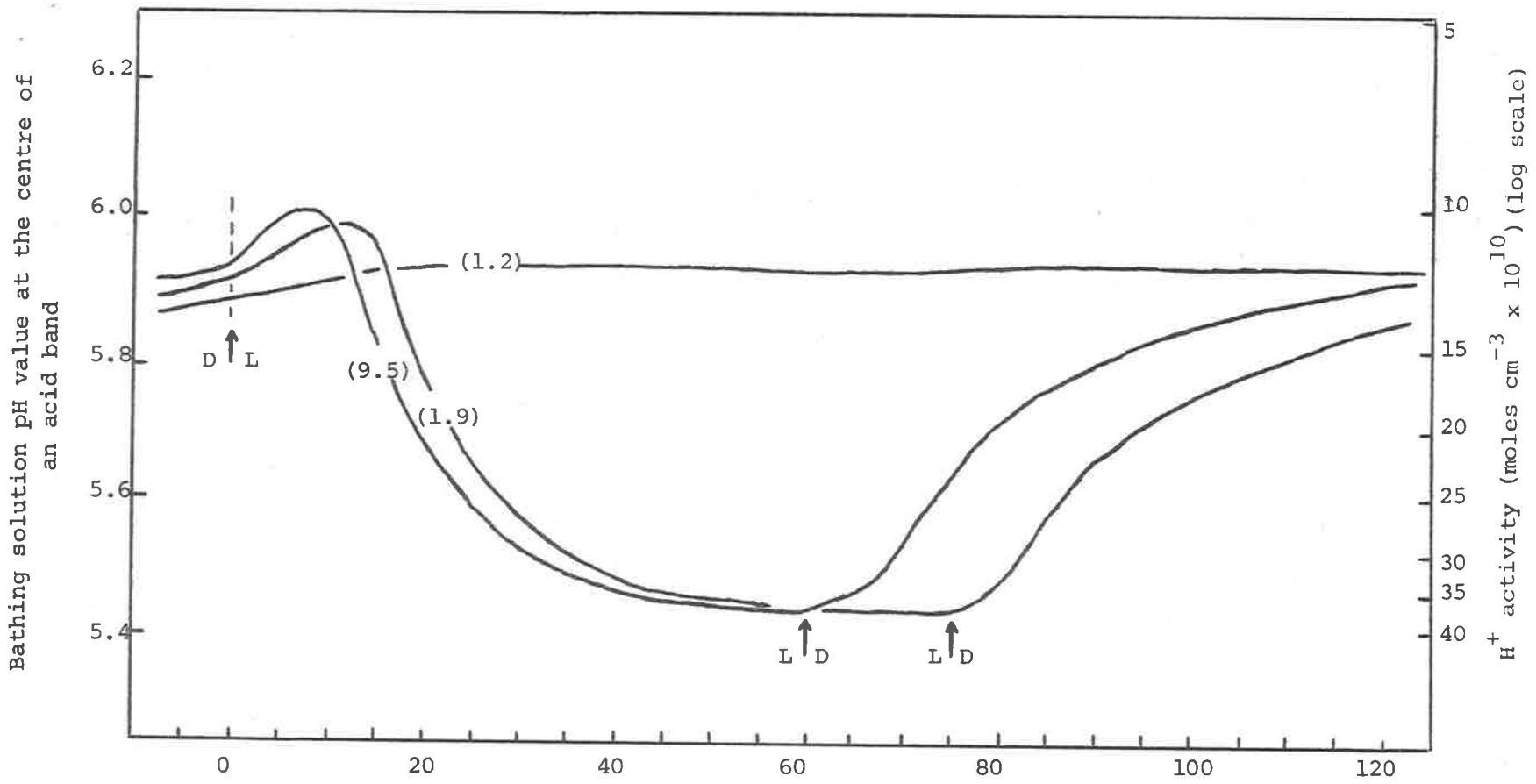

Figure 6.4. Acidification time-courses obtained under different light intensities. The experimental details are the same as for Figure 6.1. The arrowed symbols D↑ L and L ↑D represent the transition from dark-to-light and light-to-dark respectively.

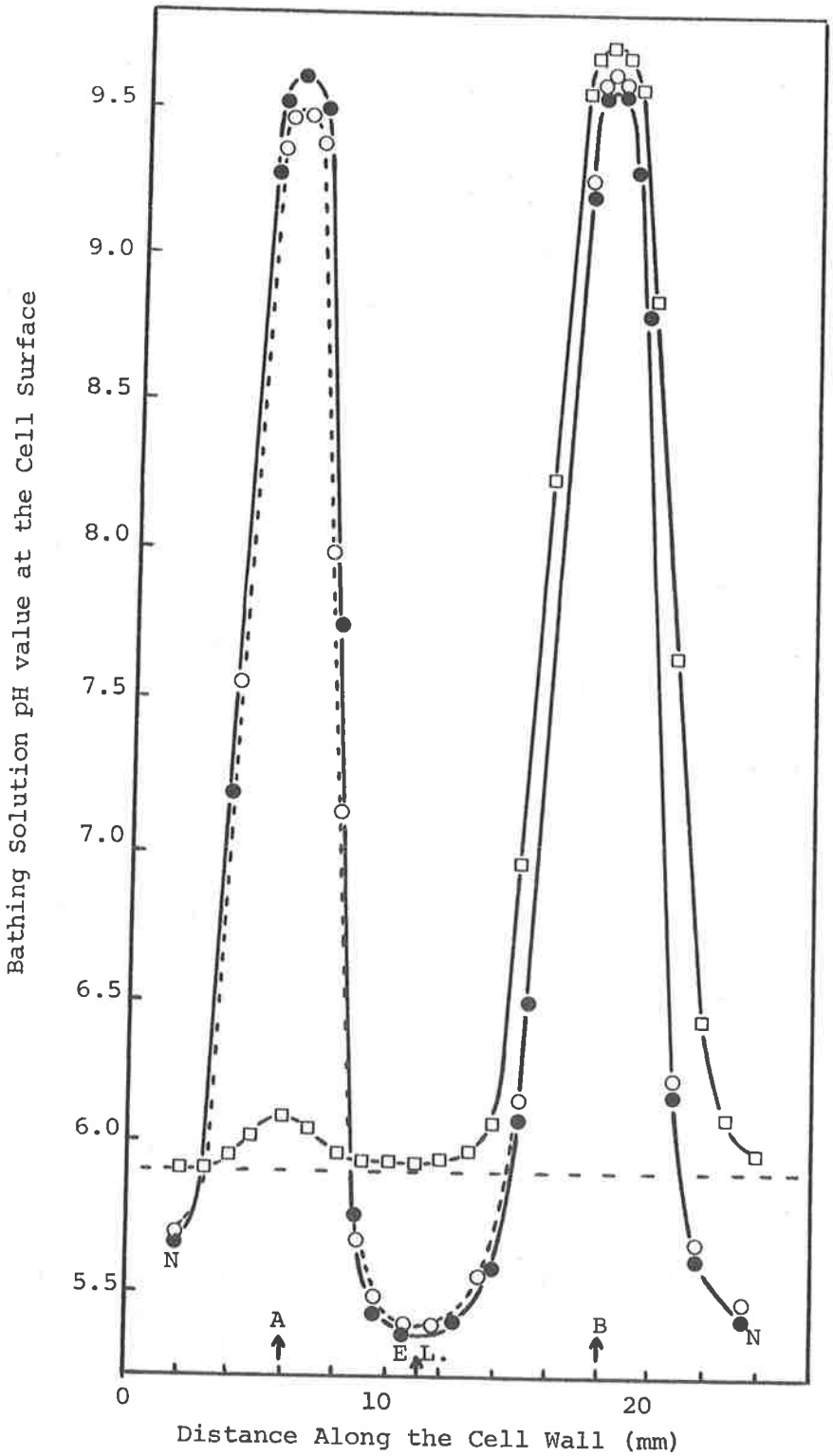

Figure 6.5. Bathing solution pH values established under three different light intensities; (●),(○) and (□) which were 9.5, 1.9 and 1.2Wm^{-2} respectively. These experiments were repeated after those presented in Figure 6.4. A 1h. dark period followed by a 90 minute illumination period was employed prior to the conducting of the cell wall pH scans. Band B was the primary OH band, and E.L. indicates that position of the pH electrode during the performance of the acidification time-course experiments of Figure 6.4.

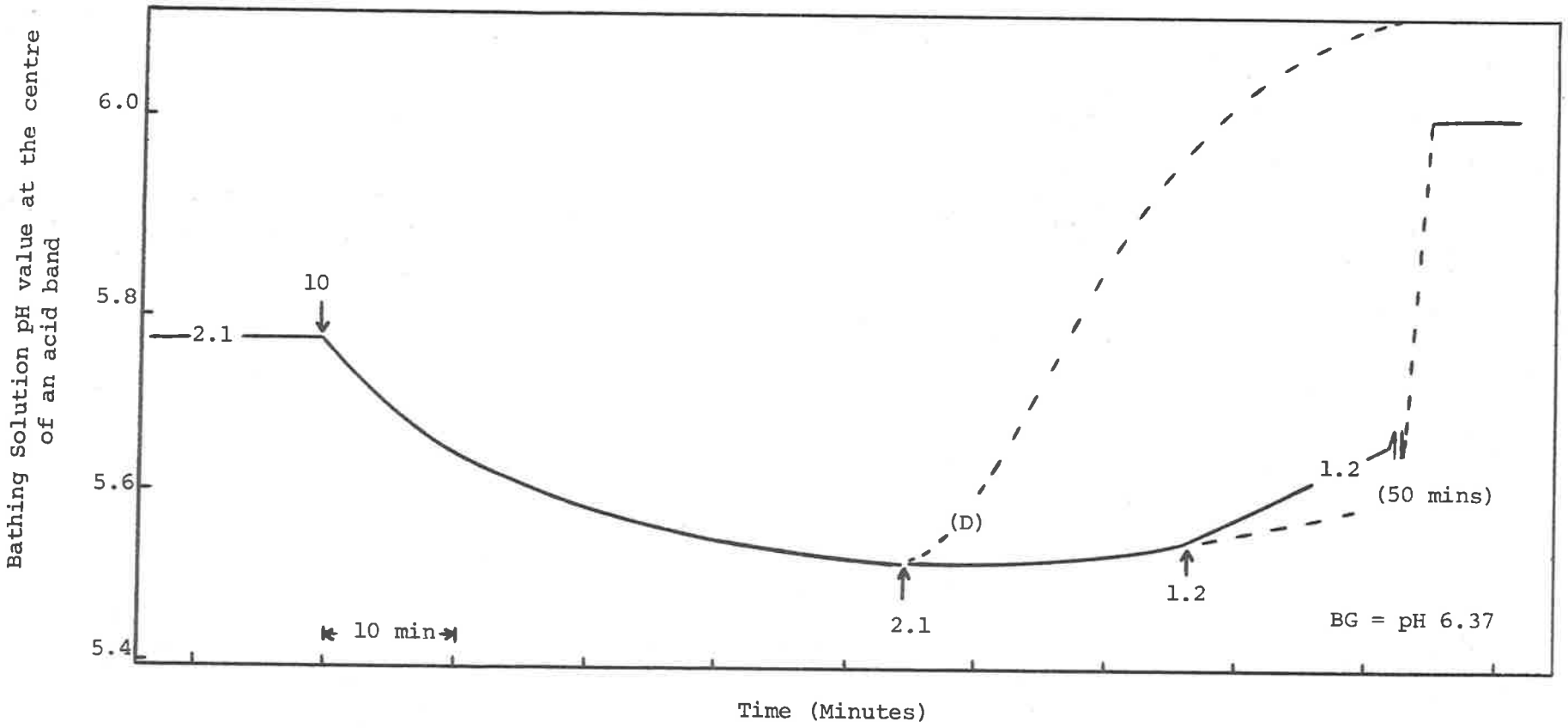

Figure 6.6. The influence of an abrupt change in light intensity on the steady state pH value at the centre of an acid band. An intensity of 2.1Wm^{-2} was employed for 90 minutes before the light regime was changed to 10Wm^{-2}. The cellular response to a change from this 10Wm^{-2} intensity to 2.1Wm^{-2} or darkness (D) was investigated.

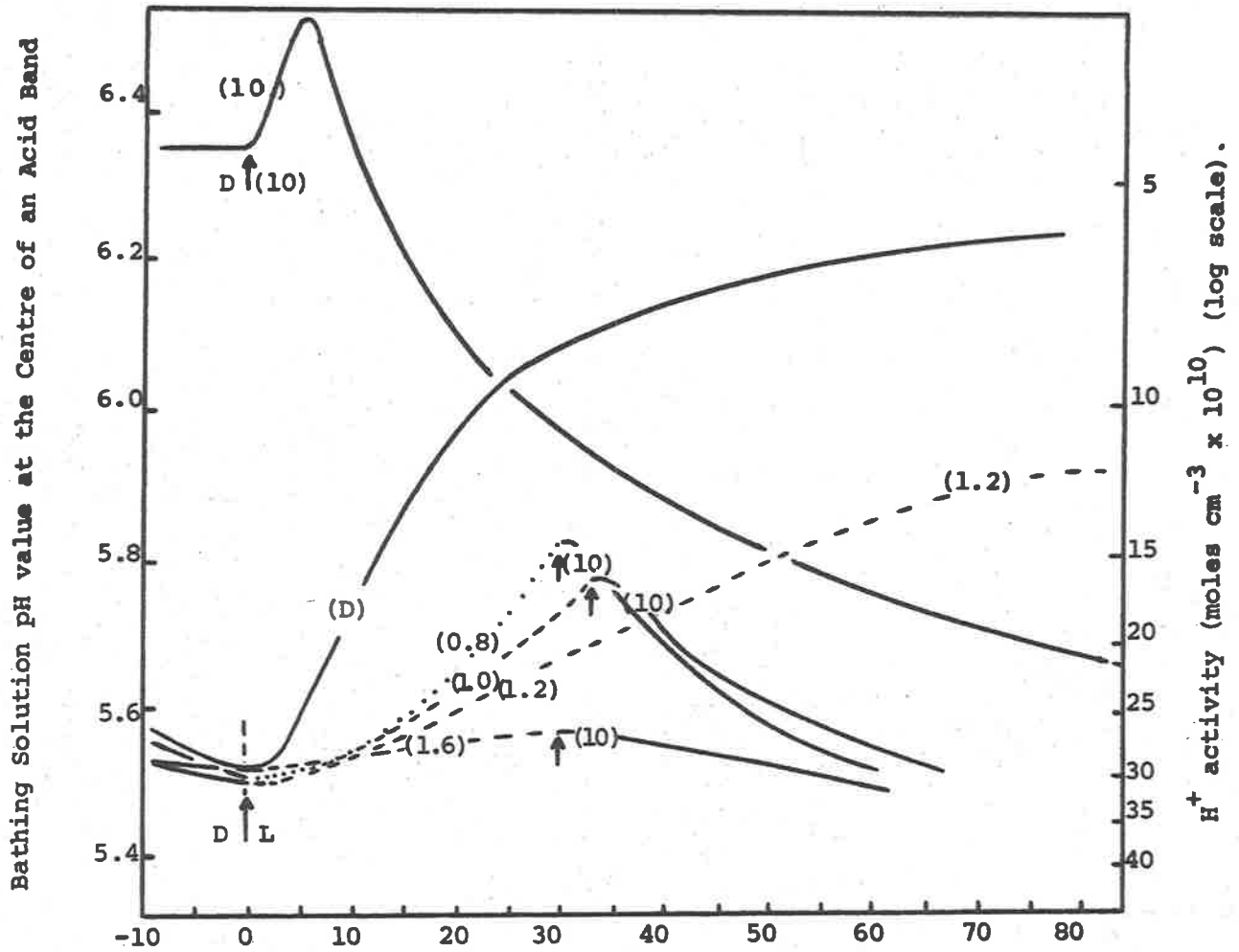

Figure 6.7. Acid band response to illumination: the influence of changing to lower light intensities. The cell was illuminated ($10 Wm^{-2}$) for 2h and then the cellular response to lower intensities of 0.8, 1.0, 1.2 and $1.6 Wm^{-2}$ were investigated. At the conclusion of the experiment the dark response was obtained. The values in parentheses are the actual intensities employed during the recording of the respective pH trace.

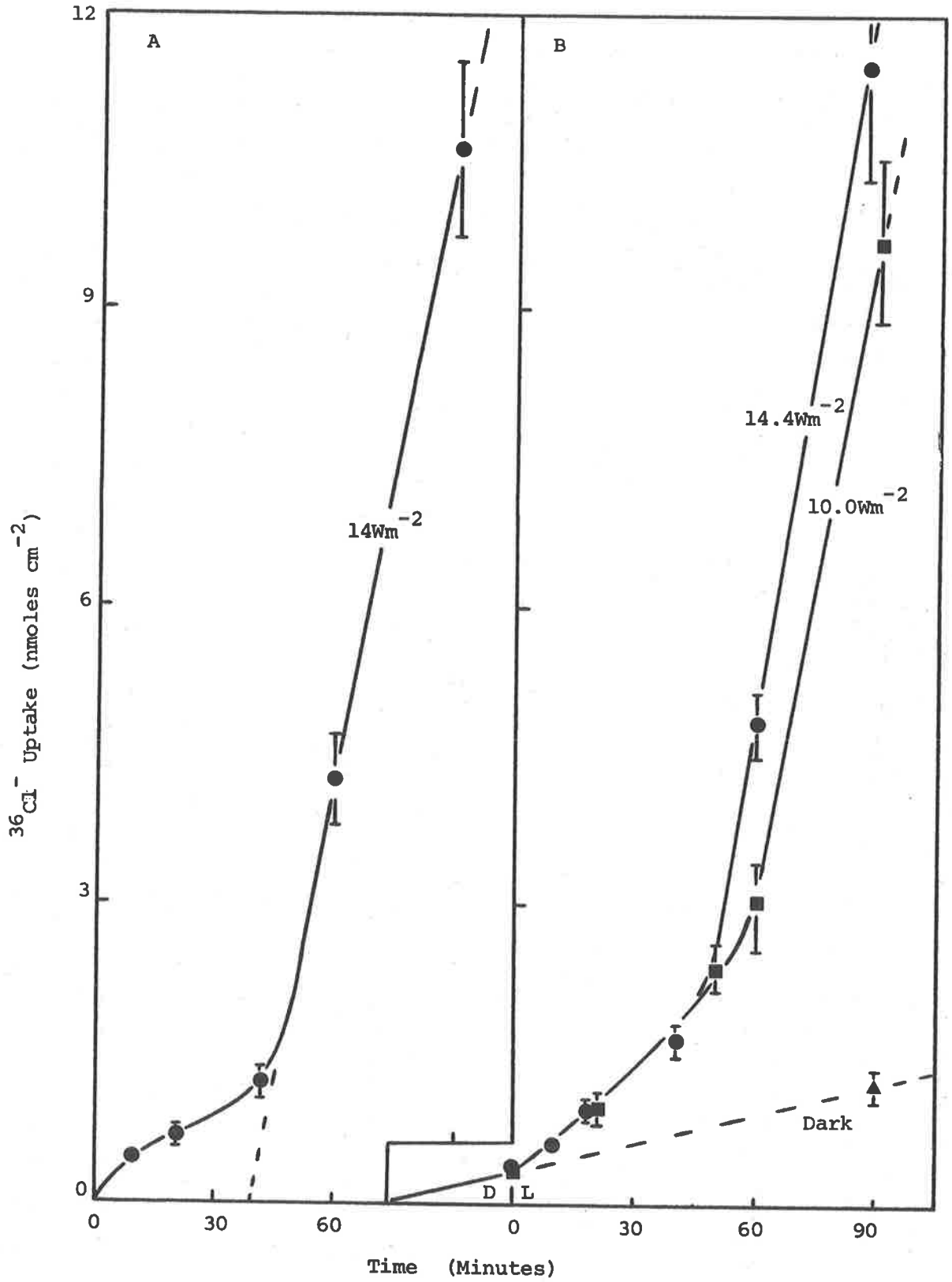

Figure 6.8. Time-course of $^{36}Cl^-$ uptake into culture tank Δ *Chara corallina* cells. A: Experiments conducted in unbuffered bathing solution, pH value 5.8. B: 10.0Wm^{-2} time-course as in A, except that the radioactive $^{36}Cl^-$ was substituted 30 minutes before the light treatment was commenced. The 14.4Wm^{-2} treatments were buffered by 5mM HEPES buffer, pH 5.8, and also included a 30 minute dark treatment in $^{36}Cl^-$ solutions.

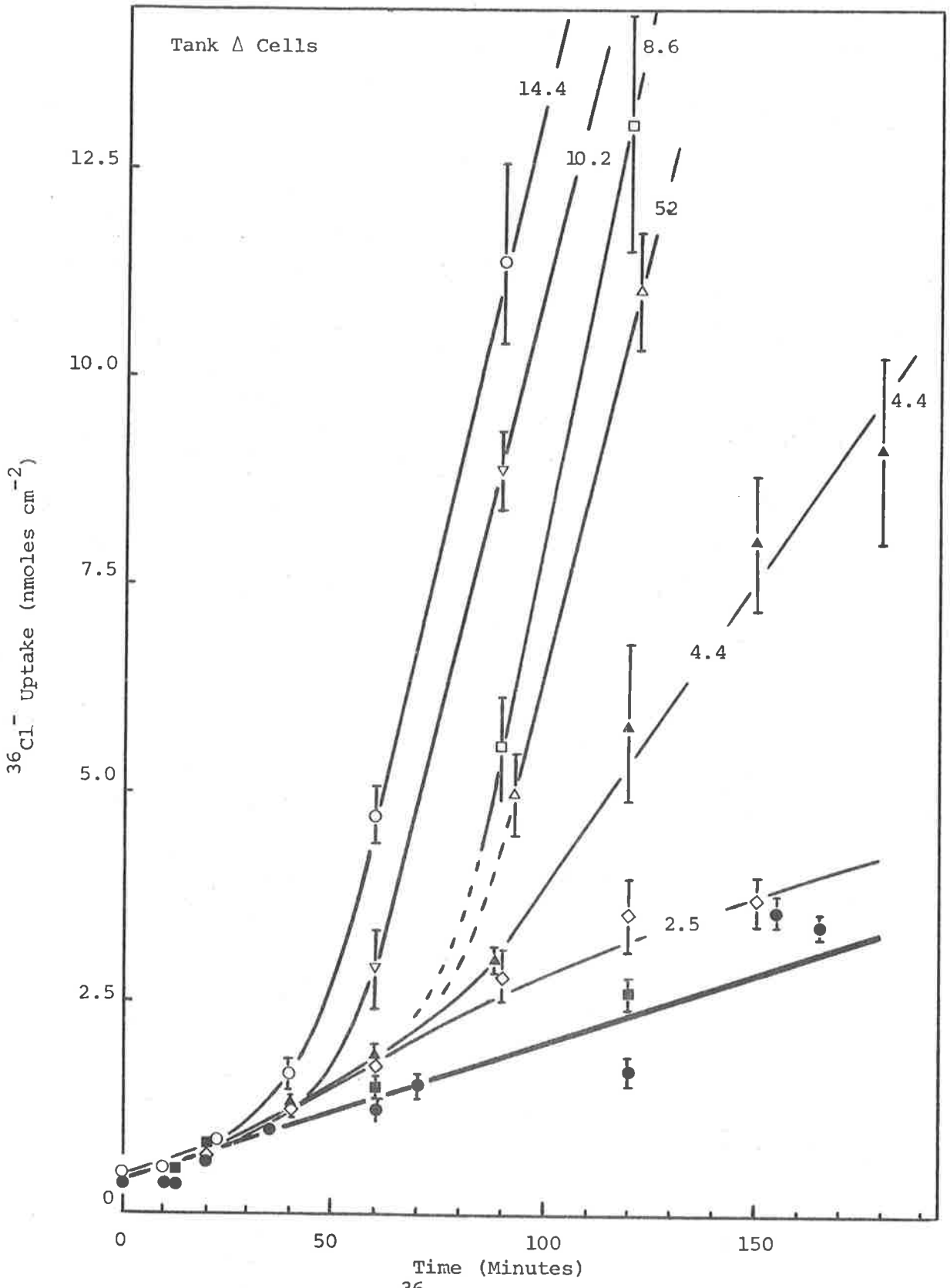

Figure 6.9. Time-course of $^{36}Cl^-$ uptake. Cells were given a 1h dark pre-treatment, 30 minutes of which was in normal solutions and an equal period in radioactive $^{36}Cl^-$. All solutions were buffered at pH 5.8 using 5mM HEPES buffer. The thick line (——) represents the mean averaged dark uptake rate and the symbols, (■) and (●) represent the uptake values measured under 1.4$Wm^{-2}$and dark conditions respectively. (Not all experimental points in the region 0-50 mins. have been included).

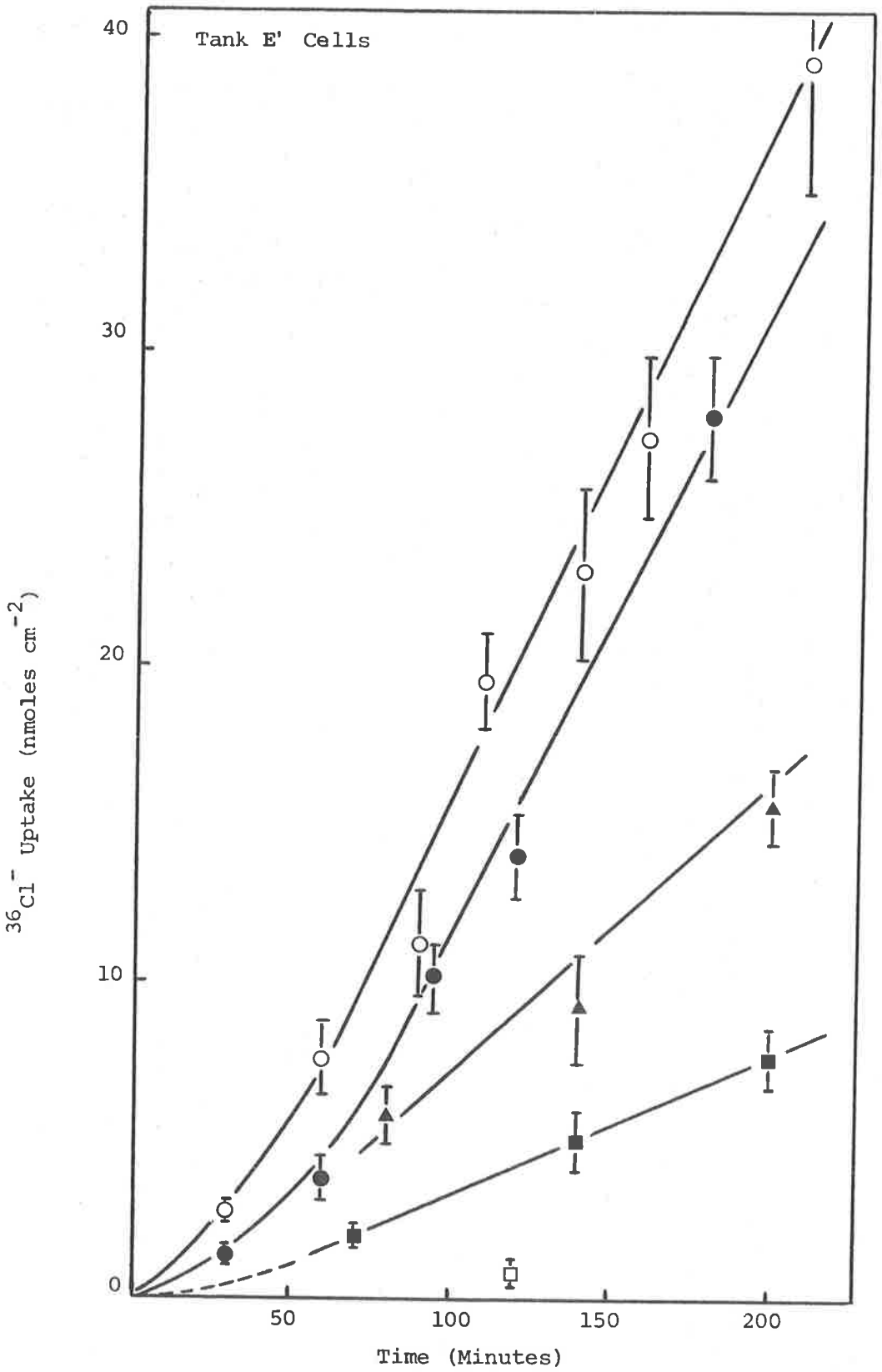

Figure 6.10. Time-course of $^{36}Cl^-$ uptake. Experimental solutions and treatments as in Figure 6.9. The symbols (□), (■), (▲), (●) and (○) represent the uptake values measured under 1.0, 2.0, 3.0, 6.0 and 10.2Wm^{-2} light intensities, respectively.

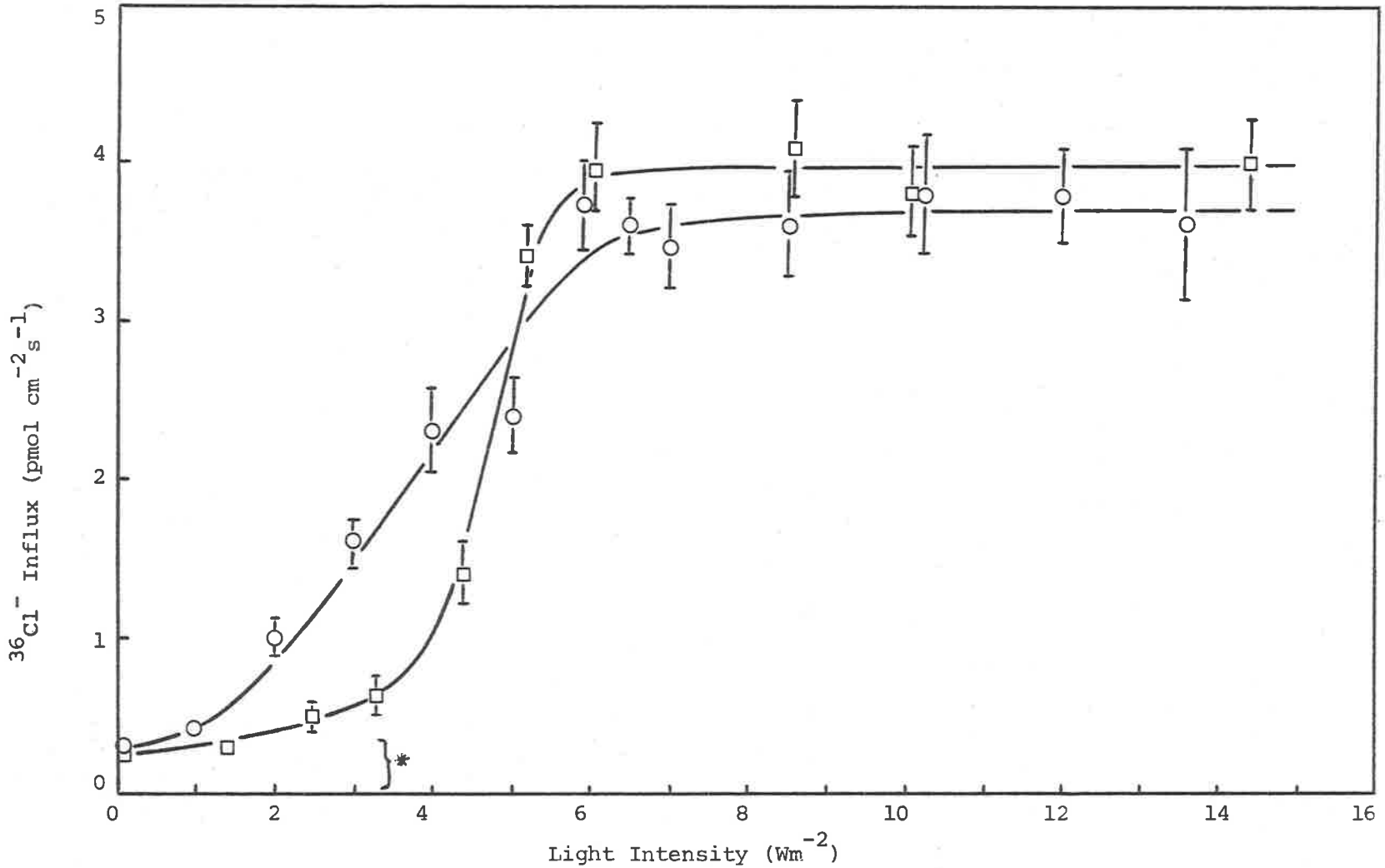

Figure 6.11. $^{36}Cl^-$ Influx as a function of light intensity. The influx values were determined from the results used to construct Figures 6.9 and 6.10. Additional values were measured over a 1h radioactive contact time, following a pre-illumination period of 2h. The symbols, (□) and (○) represent influx values for culture tanks Δ and E' respectively, and(*) represents the component of the influx which is considered to be due to exchange diffusion.

CHAPTER SEVEN

NON-OBLIGATE OPERATION OF THE HCO_3^- AND OH^- TRANSPORT SYSTEMS

Introduction

The obligate coupling of the HCO_3^-/OH^- (at the same site) transport system proposed by Lucas and Smith (1973) was tested by isolating the cell primary OH^- band within a special chamber (see Figure 2.6). (The primary band was selected since it would always be the last OH^- efflux site to deactivate). On the basis of the above hypothesis, cessation of OH^- efflux would be expected when the isolating chamber is flushed with a solution totally free of inorganic carbon (this solution will be called CO_2-free).

The cells used in individual experiments were pretreated for 6h in a bathing solution which contained 10mM MES-buffer, pH 5.0, to remove all deposits of $CaCO_3$. The location of the primary band was determined using the technique described in Chapter 5. Details of the experimental procedures associated with the use of the isolating chamber are given in Chapter 2,VII , (i)-(vi).

Results

The Influence of CO_2-Free Solutions

A typical result obtained using the isolating chamber technique is presented in Figure 7.1; a light intensity of $10Wm^{-2}$ was used throughout these experiments. The syringe-flushing system changed the solution within the isolating system four times a minute, and the normal flushing period was 5min. At the end of each flushing sequence the surface of the isolating chamber was resealed, to a depth of 6mm, with liquid paraffin. Figure 7.1 shows that removing

HCO_3^- from the isolated OH^- band had no effect on its efflux activity. This efflux activity could be maintained over prolonged periods of time, provided the outer cell segment was in contact with exogenous HCO_3^-. When the outer cell segment was immersed in liquid paraffin (following irrigation with CO_2-free solution) the OH^- efflux activity was influenced immediately, and the primary band deactivated eventually (see Figure 7.1). These results demonstrate that the OH^- transport system can operate in the absence of exogenous HCO_3^- at the actual effluxing site.

When HCO_3^- was returned to the outer chamber, the primary OH^- band was re-established (Figure 7.2). To demonstrate that deactivation of OH^- efflux was not caused by the effect of paraffin, per se, the reverse experimental sequence was investigated. (Figure 7.3 shows that sealing the outer cell segment in liquid paraffin whilst the inner chamber still contained HCO_3^-, did not result in deactivation of the isolated OH^- band. However, as soon as the HCO_3^- within the isolating chamber was replaced by a CO_2-free solution, the OH^- efflux activity was affected. Immediate deactivation did not occur; rather a gradual decline in OH^- efflux activity was observed which suggested that the OH^- system was operating on a cytoplasmic "pool". (Evidence for a pool of OH^--substrate was also presented in Chapter Five). Figure 7.3 also shows that when the OH^- efflux system had become inactive, the influence of the net H^+ efflux system could be discerned, i.e. the OH^- and H^+ systems emanate from entirely different cellular processes (cf. Spear et al. 1969).

The relationship between the deactivation of the OH^- site and the pH value of the cell surface within the isolating chamber was obtained to ensure that the actual OH^- band-centre remained stationary during the deactivation process. A typical result is presented

in Figure 7.4, and it is clear that the actual OH^- efflux centre remained at a constant location during the entire experimental period. Figure 7.4 also shows that the initial decline in OH^- efflux activity, which resulted when the outer cell segment was immersed in liquid paraffin, was similar in form to that obtained by transferring the cell from light to dark.

The influence of 0.2mM CO_2 (pH 5.0), in the outer chamber bathing solution, on the activity of the primary OH^- system was investigated to determine whether OH^- efflux would cease when the isolating chamber was flushed with CO_2-free solution. The results (see Figure 7.5) demonstrated that exogenous CO_2 could not support the isolated OH^- efflux activity under these conditions. For these particular experiments the solutions in the outer chamber also contained 0.1mM phenol red. In this way it was possible to ascertain whether OH^- bands were present on the outer cell segment; it was found that no alkaline bands developed when 0.2mM CO_2 (pH 5.0) was employed.

Dark Treatments: Their Influence on the OH^- Efflux Activity

When the isolating chamber and outer chambers contained 0.2mM $NaHCO_3$, simultaneous dark and flushing treatments of 2-5min duration did not cause the isolated OH^- site to deactivate when the cell was re-illuminated. A similar procedure in which the outer chamber contained 0.2mM $NaHCO_3$ while the isolating chamber contained (and was flushed with), CO_2-free solution is presented in Figure 7.6. In this figure the primary band response to dark periods of 2 and 3 min are compared; the difference was striking. This type of response demonstrated that under these particular conditions the OH^- efflux system is very labile. Apparently the longer dark period caused the isolated OH^- band to lose its primary status, otherwise it would have been the first OH^- efflux system to reactivate

following re-illumination. The slow recovery of OH^- efflux activity (see Figure 7.6) was noteworthy. (Scans conducted along the cell segment within the isolating chamber revealed that the pH trace was still being recorded at the true band-centre.

Transfer of OH^- Efflux Function

The influence, on the isolated OH^- efflux activity, of transferring the outer cell segment to the dark was examined. For these experiments the cells were placed in the apparatus in such a way that approximately half the cell surface was projecting into the outer chamber; the other half was sealed within the isolating chamber system. For cells whose total length was greater than 3.0cm, part of the isolating chamber cell segment projected into the outer chamber. This segment was sealed in liquid paraffin, to isolate it from the solution in the outer chamber. Darkening of the outer cell segment was achieved by slipping a black polythene sleeve (filled with outer chamber solution) over this half of the cell. The type of response recorded when the outer cell segment was darkened and re-illuminated in this manner is shown in Figure 7.7. Re-illumination of the darkened cell surface caused a decline in the primary OH^- peak height. This was interpreted as resulting from reactivation of OH^- efflux sites located on the outer cell segment, and the subsequent transfer of OH^- efflux function to these particular sites. Support for this interpretation was acquired by the primary band response to darkening and reilluminating the outer cell segment when the outer bathing solution contained 0.2mM CO_2 (pH 5.0). A slight drop in the steady state peak height when the cell was darkened, implied that the chloroplasts in this region were fixing a small component of the HCO_3^- being influxed from the solution within the isolating chamber.

Figure 7.8 illustrated the response observed when the above sequence was repeated using firstly, 0.2mM HCO_3^- within the isolating chamber, and then CO_2-free solutions; the outer chamber contained 0.2mM HCO_3^- throughout. The OH^- efflux activity still remained when the outer cell segment was darkened and the inner chamber contained CO_2-free solution. If the continued OH^- efflux had been due to a cytoplasmic "pool" of OH^- (or HCO_3^-), the peak height should have decayed within 1-2h. Over a prolonged dark period (outer cell segment only) a fall in OH^- peak height to a new steady state was observed (see Figure 7.8A), but activity was still retained over these long dark periods. This suggested that HCO_3^- could be supplied by the dark cell segment. However, almost immediately the entire cell surface was darkened, the primary OH^- site deactivated (Figure 7.8B).

An accurate estimate of the actual OH^- efflux through the primary band, under these prolonged dark periods to the outer cell segment, could not be obtained because the cell was resting directly on the perspex. Hence the OH^- effluxed over the band surface which was in contact with the perspex would be reflected back over the cell, in order for it to diffuse into the bathing solution of the isolating chamber. However, based on knowledge gained during the diffusion analysis experiments (Chapter Four), it was considered that the steady state OH^- efflux rate established in Figure 7.8A would be in the order of 0.6pmol s^{-1}. Assuming that this was the only active OH^- efflux site, the HCO_3^- influx across the darkened cell surface would be 0.75 pmol $cm^{-2}s^{-1}$ for this particular cell (cell surface area in the outer chamber was approximately $0.8cm^2$). Estimates of the rates obtained during other experiments gave dark HCO_3^- influx rates of between 0.4 and 1.0 pmol $cm^{-2}s^{-1}$.

Measurement of Dark $H^{14}CO_3^-$ Transport

An experimental system was constructed which simulated the conditions used to obtain results typified by Figure 7.8. A perspex holder (width 10cm x length 11cm x depth 2cm) was used in which cells could be partitioned into two equal halves such that each half was located in a separate chamber. (Each chamber was 4.7 x 11 x 2cm). The partition between the chambers was constructed of black perspex (0.6 x 11 x 2cm) and consisted of two sections each 1cm in depth. The basal section was a permanent fixture whilst the upper half was held in position by self-locating pins. Ten holes were evenly spaced along the central interface of this partition. Each hole consisted of a pair of matched hemi-cylinders of diameter 1mm and length 6mm. The experimental cells were located in these holes and silicon grease was used to isolate the two chambers. The sides of the holder were constructed of black perspex and hence one or both chambers could be darkened or illuminated simply by employing black or clear perspex tops and bottoms to the respective chamber.

Using this perspex holder, experiments were performed to investigate the magnitude of the dark, $H^{14}CO_3^-$ influx when one half of the cell was located in the dark and the other in the light. The results obtained using cells cut from culture tanks E' and XG-2 are presented in Table 7.1. Experiment numbers 1 and 4 indicated that holding the cells in the stocks did not interfere with the process of $H^{14}CO_3^-$ influx and its subsequent assimilation. (In terms of $H^{14}CO_4^-$ influx rates, these experiments revealed that tank E' cells were particularly active). Bicarbonate influx rates equivalent to control rates were obtained when $H^{14}CO_3^-$ was supplied to only one half of the cell surface and

the other half was darkened (see Expt. no. 2). At the conclusion of the experiment the ^{14}C. fixation products were distributed between the light and dark regions of the cells in approximate proportions of 2:1 respectively. (The mobility of these products is in agreement with observations of Smith, 1965; see also Heber, 1974).

The dark $H^{14}CO_3^-$ results presented in Table 7.1 (Expt. Nos. 3, 5 and 6) support the estimated values obtained using the small isolating chamber apparatus. For tank E' cells, the average dark $H^{14}CO_3^-$ influx, associated with the cells partitioned into dark and light segments was approximately four times higher than the value obtained for cells which were darkened along their entire length (i.e. 0.50 ± 0.07 cf. 0.11 ± 0.01 pmol $cm^{-2}s^{-1}$). Results obtained using tank XG-2 cells indicated that the dark $H^{14}CO_3^-$ influx for the partitioned cells was also higher than the control cells which were completely darkened. However, it appeared that bathing the illuminated cell segments in normal bathing solution (pH 5.75) was not as effective in facilitating this stimulated dark influx (cf. Experiment nos. 5 and 6). The difference in levels of total carbon present under the two conditions may account for this result; the level in the normal bathing solution would have been approximately 12μM whereas the bathing solution titrated to pH 9.2 would have gained CO_2 from the atmosphere.

Discussion

The Coupled HCO_3^-/OH^- Transport Hypothesis

The results presented in this chapter demonstrate categorically that the OH^- efflux process can function in the absence of exogenous HCO_3^- at the actual OH^- efflux site. Collectively they invalidate the obligate HCO_3^-/OH^- transport hypothesis proposed by Lucas and Smith (1973). It must therefore be assumed that the transport of HCO_3^- and OH^- are independent, insofar as the two processes can be spatially separated. It is also probable that quite distinct carriers are involved in therespective transport of HCO_3^- and OH^- across the plasmalemma.

Another interesting feature of these results was that although HCO_3^- could be transported across the membrane in the dark cell segment, this influx value was always much lower compared with the rate obtained when the $H^{14}CO_3^-$ was added to the illuminated chamber. This low value may indicate that photosynthetic "energy" cannot be transported effectively over the distances which are involved. This seems unlikely, especially since the results of Experiment no. 2 (of Table 7.1) indicated that the products of photosynthesis could be distributed in the streaming cytoplasm. Hence it may have been that the energy required for the HCO_3^- transport system was present, but that other properties of the darkened cytoplasm prevented the "effective" operation of this system. Net production of CO_2 within this region via respiration may have prevented the establishment of a "critical" HCO_3^- concentration gradient across the plasmalemma. It may in fact be necessary to develop this "critical" HCO_3^- concentration at the interface between the plasmalemma carrier site and the cytoplasm.

Electrical Implications

The spatially separate and "independent" operation of the HCO_3^- and OH^- transport systems means that during the initial stages following illumination of the cell, any imbalance between R_3 and R_4 (of Figure 5.12) would cause fluctuations in the membrane potential. This is of course provided the movement of HCO_3^- and OH^- are not coupled to the movement of cations. (The extremely large fluxes involved suggest that this is not so). The form of the membrane potential response will be dependent upon the relative values of R_3 and R_4, and also upon the exogenous HCO_3^- conditions. To produce an hyperpolarization R_3 (HCO_3^-) would have to exceed $R_{4(OH^-)}$.

The main electrical influence of the fluxes through these particular carriers is likely to be via their contribution to the electrical conductance of the membrane. This will be particularly so at pH values where a supply of exogenous HCO_3^- exists. It is possible that the HCO_3^- and OH^- fluxes could account for a large proportion of the observed rise in conductance which occurs when the pH of the bathing solution is increased (see for example Spanswick, 1972, Figure 3).

TABLE 7.1

Investigation of $H^{14}CO_3^-$ Influx Using a Cell Partitioning Apparatus.

Tank	Expt. No.	Experimental Conditions: Chamber A Soln.	Chamber A Treatment	Chamber B Soln.	Chamber B Treatment	Duration of Pretreatment (h)	$H^{14}CO_3^-$ Influx (pmol $cm^{-2}s^{-1}$): Based on partitioned cell surface area exposed to radioisotope — Chamber A	Chamber B	Control* Cells
E'	1	$NaH^{14}CO_3$ +	L**	$NaH^{14}CO_3$	L	2	32.9 ± 1.7	33.0 ± 2.1	38.2 ± 3.1
E'	2	$NaH^{14}CO_3$	L	BS++	D**	2	32.2 ± 2.1	—	33.7 ± 0.5
E'	3	BS	L	$NaH^{14}CO_3$	D	2	—	0.50 ± 0.07	0.11 ± 0.01
XG-2	4	$NaH^{14}CO_3$	L	$NaH^{14}CO_3$	L	1	17.7 ± 2.2	18.3 ± 1.6	19.1 ± 1.8
XG-2	5	BS	L	$NaH^{14}CO_3$	D	1	—	1.12 ± 0.04	0.49 ± 0.02
XG-2	6	NBS++	L	$NaH^{14}CO_3$	D	1		0.62 ± 0.04	0.412 ± 0.01

* Cells placed free in chamber containing the radioactive HCO_3^-

** Symbol L represents a light treatment of $10 Wm^{-2}$, while the symbol D represents a dark treatment.

\+ The $NaHCO_3$ solutions were at a concentration of 0.5mM and the pH value was 9.2.

++ The symbol BS represented bathing solution titrated to pH 9.2 using freshly prepared NaOH, and NBS indicates normal bathing solution, pH value 5.75.

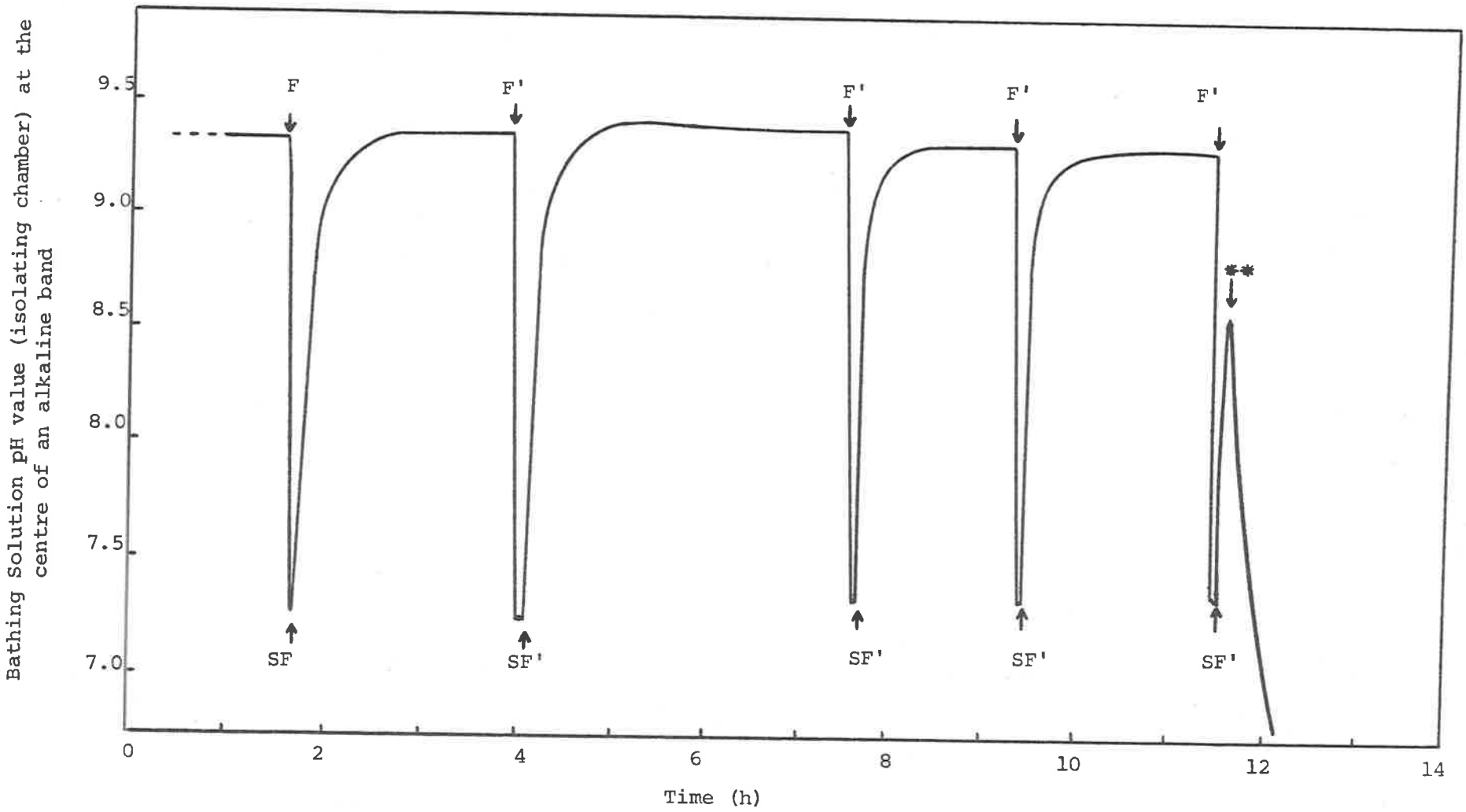

Figure 7.1. Hydroxyl band activity in the presence of CO_2-free bathing solution. A primary OH^- band was located in the isolating chamber (see Figure 2.6) and the chamber flushed with normal solution containing 0.2mM $NaHCO_3$ (F) or CO_2-free solution (F'). The symbols SF and SF' indicate when the flushing with the $NaHCO_3$ and CO_2-free solution respectively, was stopped; ** indicates when the outer cell segment was sealed in liquid paraffin.

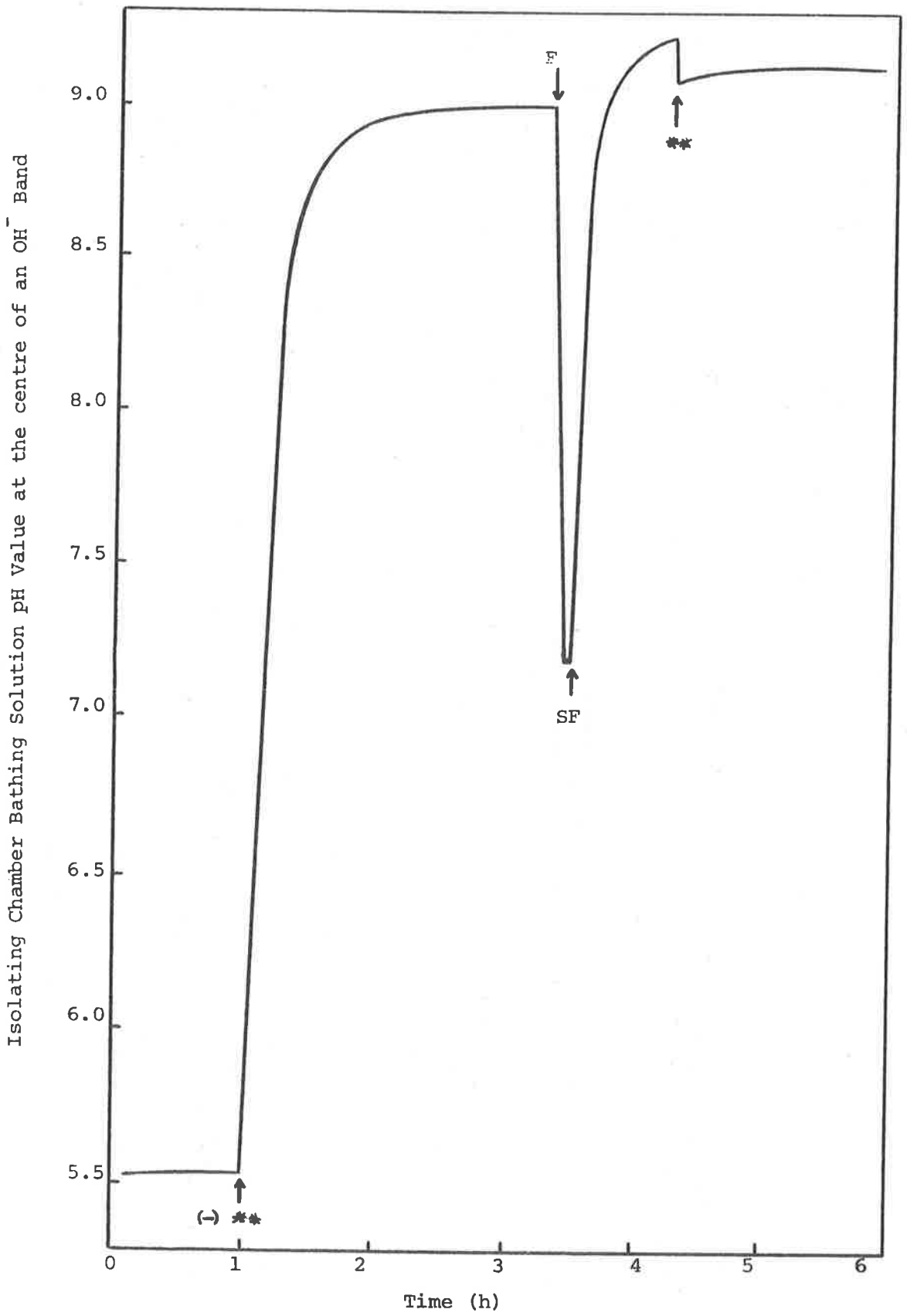

Figure 7.2. Reactivation of the isolated primary OH^- band. This trace is a continuation of Figure 7.1, the symbol (→)** indicates the removal of the liquid paraffin seal from the outer cell segment.

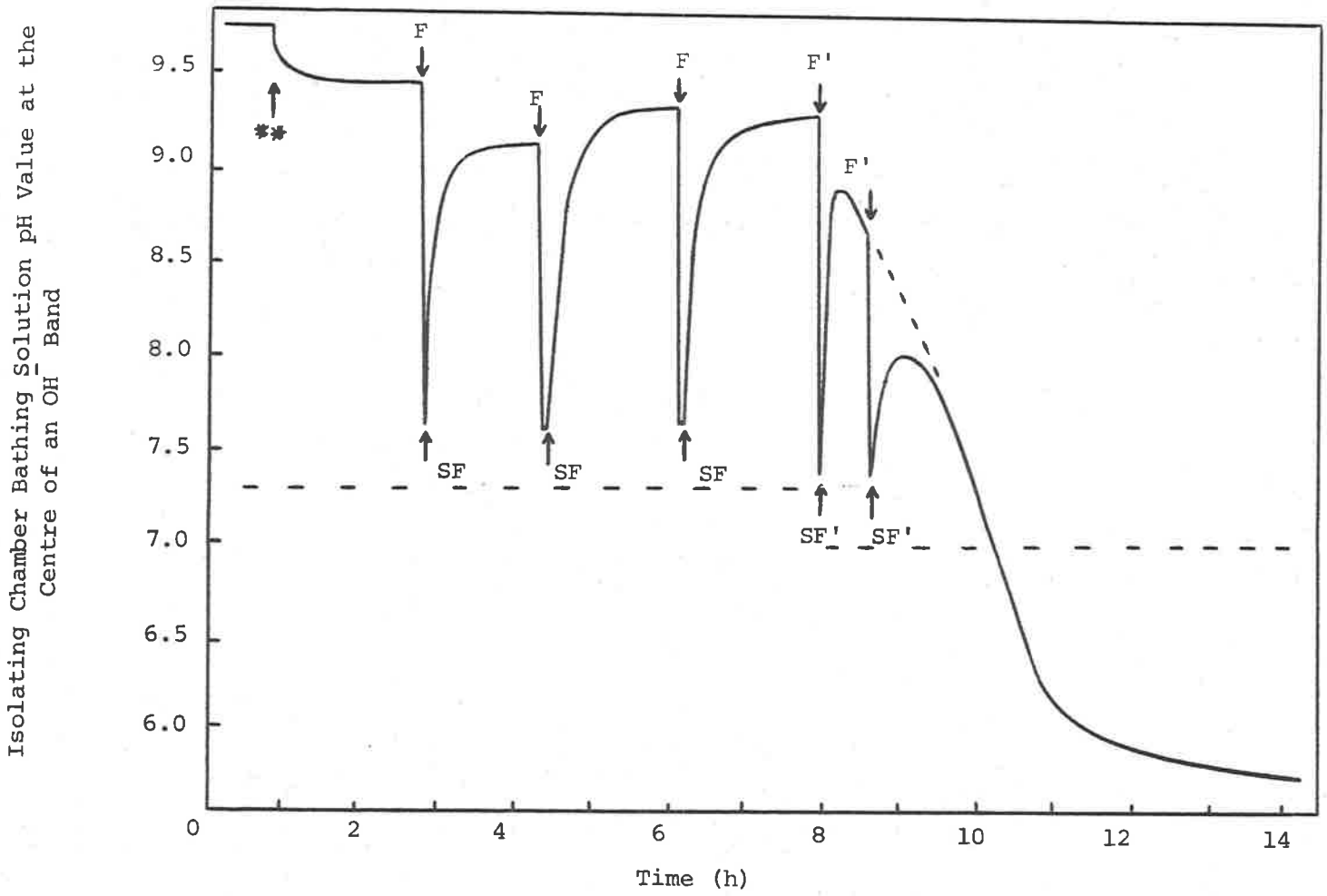

Figure 7.3. Hydroxyl band activity in the presence of CO_2-free bathing solution. The sequence was reversed in this experiment, the outer cell segment was sealed in liquid paraffin (**) before the isolating chamber was flushed with CO_2-free solution (F'). The symbols F, SF and SF' are as in Figure 7.1, and the horizontal broken line represents the background pH value.

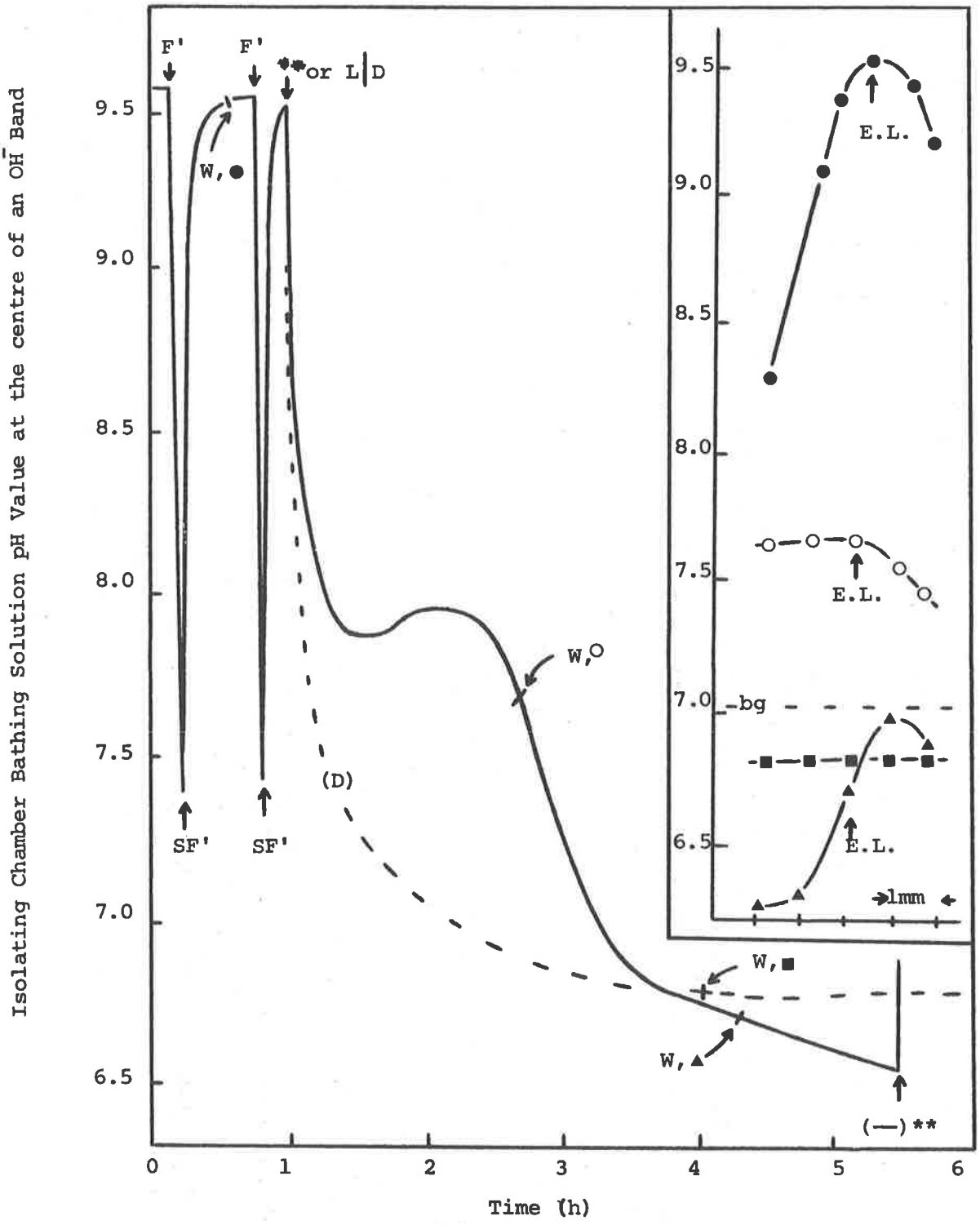

Figure 7.4. Relationship between OH^- band deactivation and the cell segment within the isolating chamber. Both chambers contained 0.2mM $NaHCO_3$ for 30 min prior to the first F', at the indicated points the cell wall within the isolating chamber was scanned, namely, W,● ; W,○ ; W,▲ ; and W,■ ; the latter being conducted during the dark response (D). The symbols are as defined in Figures 7.1 and 7.2, except that E.L. represents the electrode location during the experiment, and L|D indicates the transfer of the cell from $10 Wm^{-2}$ to the dark. The background value of the CO_2-free solution in the isolating chamber is represented by bg.

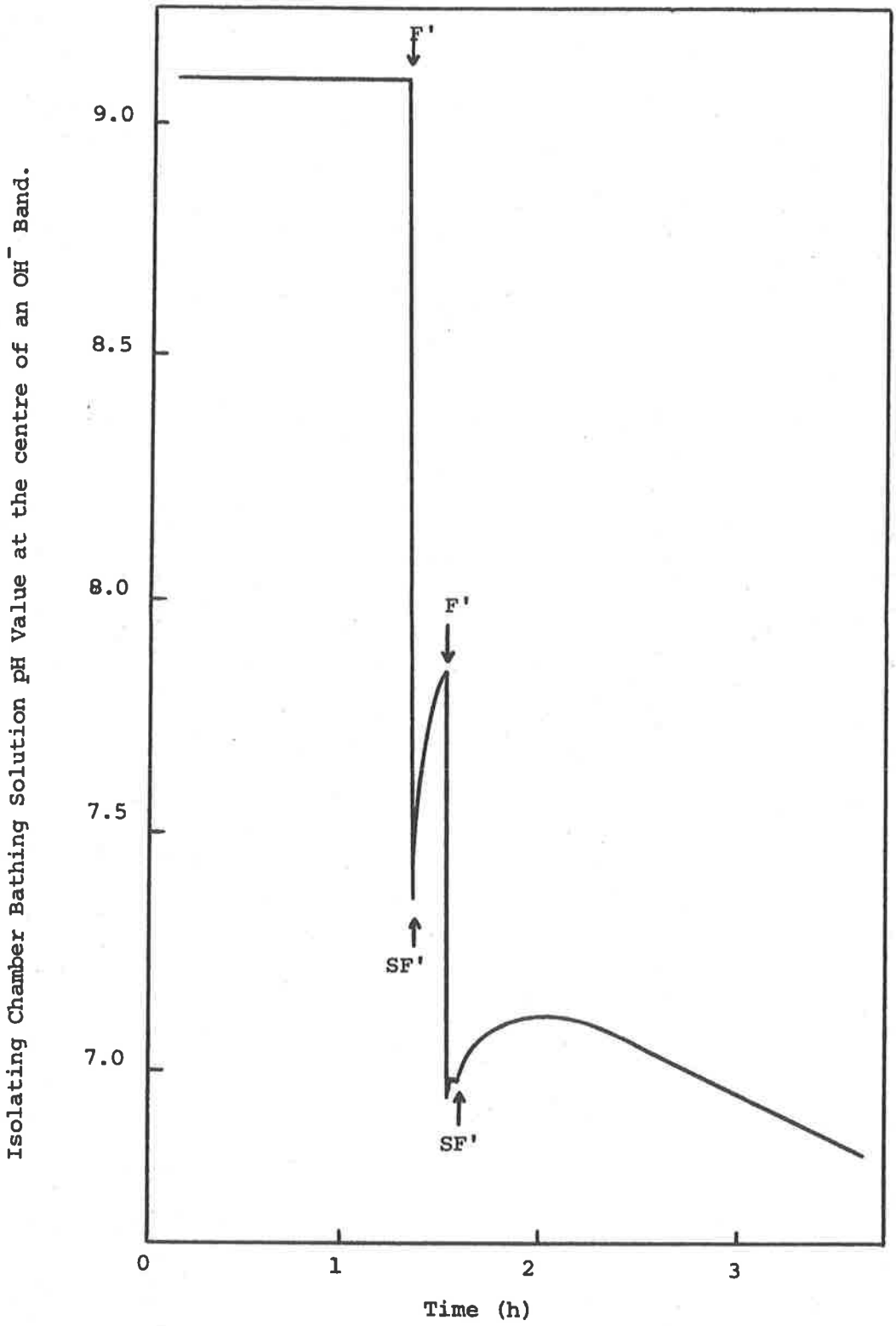

Figure 7.5. Influence of CO_2 in the outer chamber. The cell was treated with 0.2mM CO_2, pH 5.0 in the outer chamber and a solution containing 0.2mM $NaHCO_3$ in the isolating chamber for 1½h prior to flushing the inner chamber with CO_2-free solution. The outer chamber contained 0.2mM CO_2 (pH 5.0) for the entire experiment.

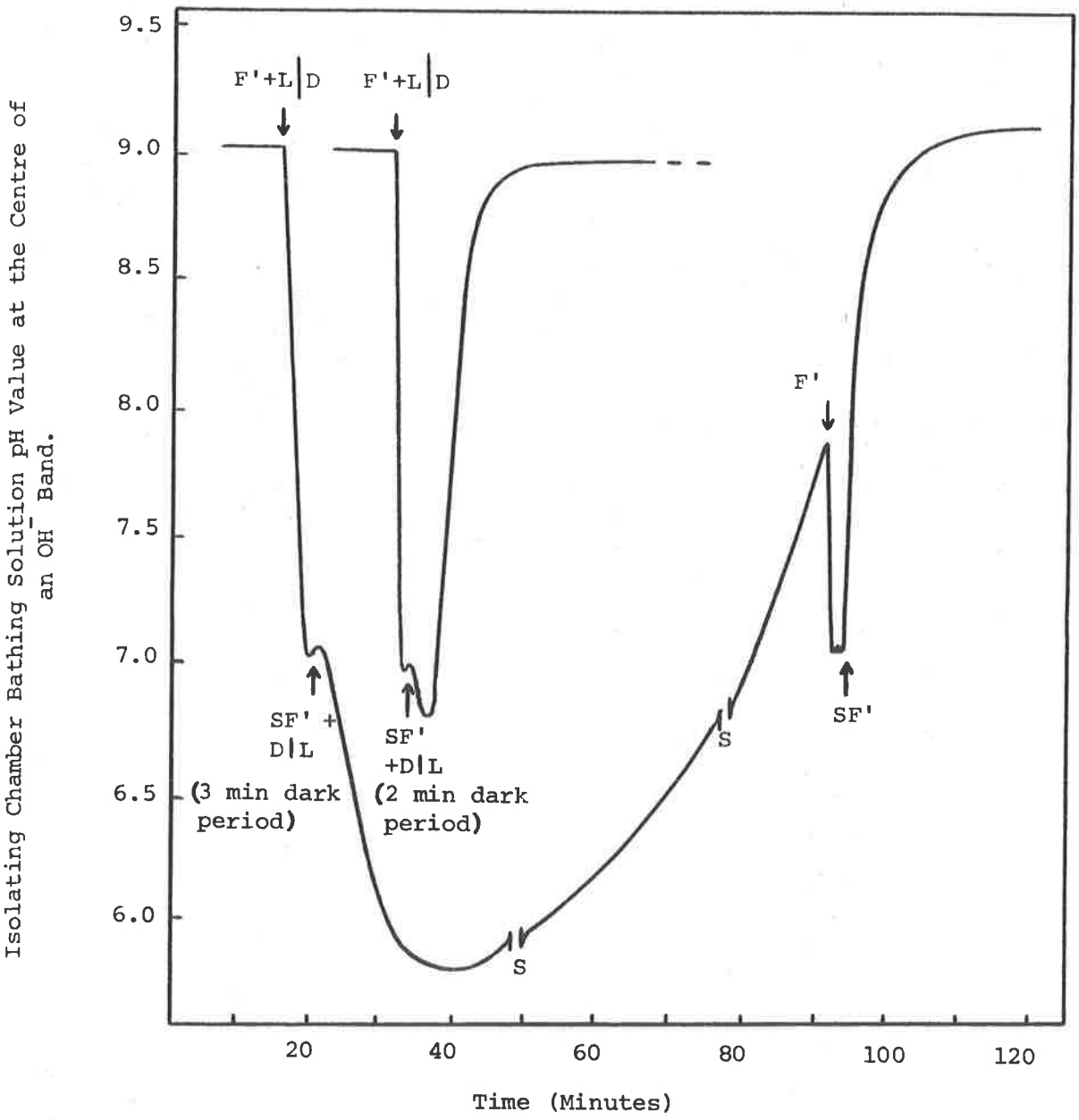

Figure 7.6. The influence of short dark periods on OH^- efflux activity when the isolating chamber contained CO_2-free solution. The symbols F' + L|D, indicate the commencement of a dark period during which the isolating chamber was flushed with CO_2-free solution, and SF' + D|L indicates the end of both the dark period and flushing procedure. The symbol S represents the point where a scan of the inner cell wall was conducted.

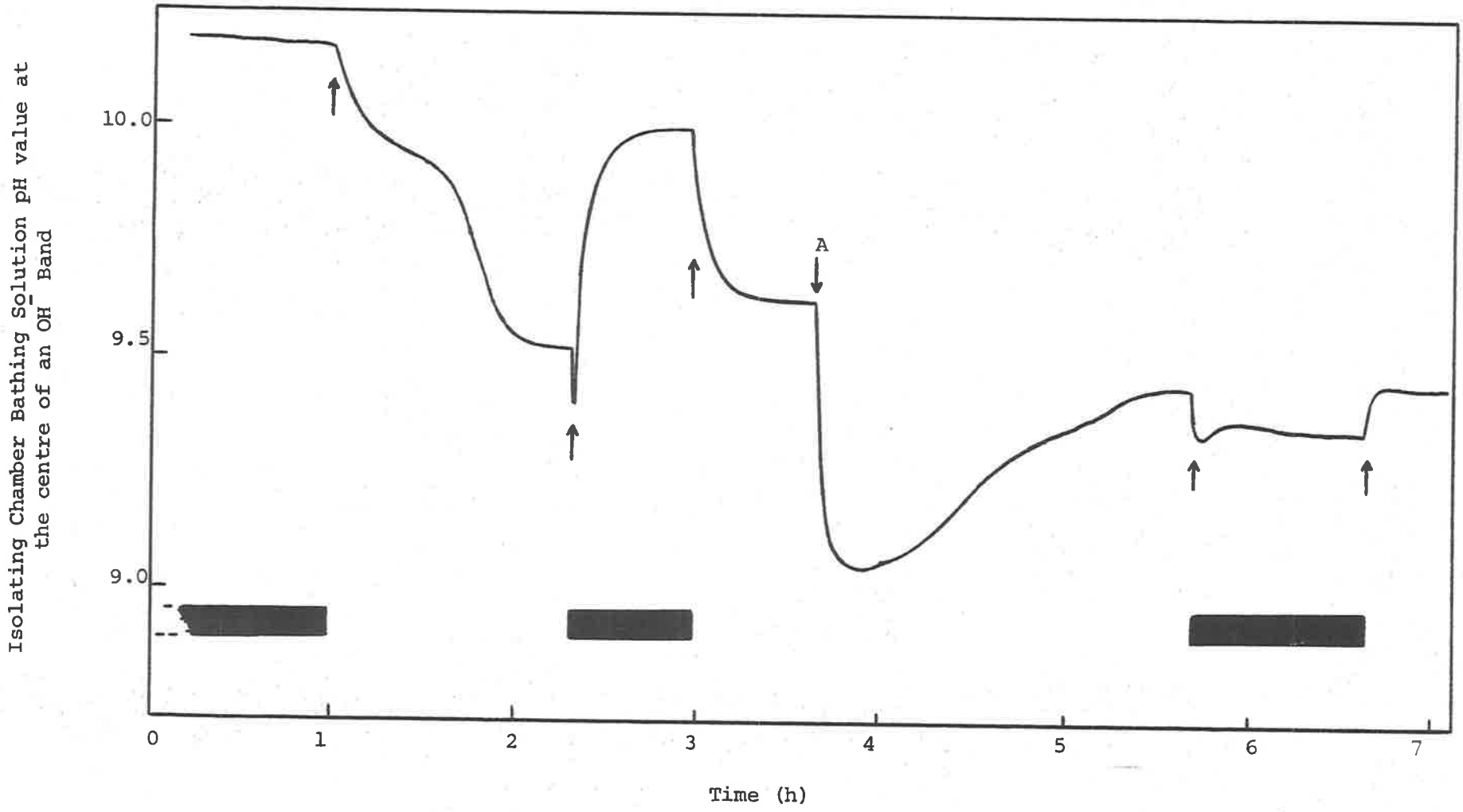

Figure 7.7. Dark treatments on the outer cell segment and their influence on the OH^- efflux activity within the isolating chamber. Both chambers contained 0.2mM $NaHCO_3$ solutions initially, the outer chamber was changed to 0.2mM CO_2, pH 5. 0 at A. The dark bars and arrows indicate dark treatments applied to the outer chamber only.

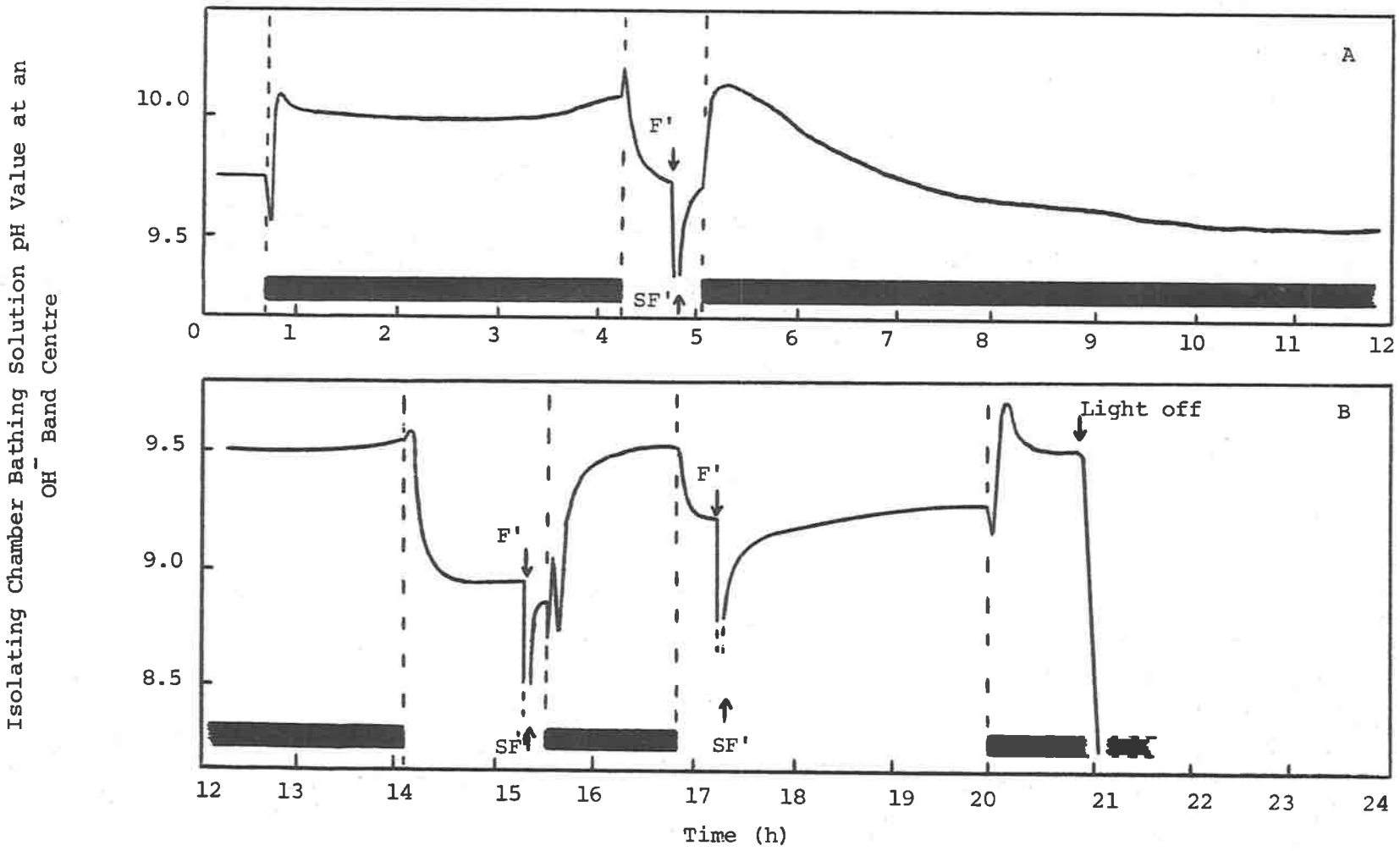

Figure 7.8. Dark treatments on the outer cell segment and their influence on the OH^- efflux activity within the isolating chamber. The outer chamber contained a 0.2mM $NaHCO_3$ solution throughout, and the inner chamber the same until it was flushed with CO_2-free solution. Figure B is a continuation of A; the experimental features are as previously described.

CHAPTER EIGHT

HCO_3^-, OH^- AND H^+ ACTIVITY IN THE PRESENCE OF $(NH_4)_2SO_4$.

Introduction

MacRobbie (1965, 1966) observed that Cl^- transport in *N. translucens* remained unaffected or was stimulated by the presence of imidazole or $(NH_4)_2SO_4$ (at or near neutral pH), while K^+ was severely inhibited. On the basis of the studies in vitro reported by Krogmann, Jagendorf and Avron (1959), Good (1960) and Hind and Whittingham (1963), MacRobbie suggested that these amino-compounds were uncoupling photophosphorylation in vivo. Smith (1965) also showed that these amino-compounds inhibited the influx of both phosphate and D-glucose. However, support for MacRobbie's suggestion that photophosphorylation was being uncoupled was not obtained from the results reported by Smith (1967a). Here it was shown that neither imidazole (5mM, pH 7.1) nor $(NH_4)_2SO_4$ (0.02 - 0.04mM, pH 6.5) affected in vivo $^{14}CO_2$ fixation at the specified pH range. This work was supported by the parallel studies, in vivo and in vitro, on the effect of these compounds conducted (using *Chara corallina*) by Smith and West (1969). They found that imidazole stimulated the light promoted influx of Cl^- (see also Coster and Hope, 1968), but that it had no effect on $^{14}CO_2$ fixation in vivo. In the situation in vitro, imidazole was in fact found to act as an uncoupler of photophosphorylation. A similar uncoupling in vitro was found using high concentrations of $(NH_4)_2SO_4$ (4mM).

Smith (1970) suggested that the stimulatory influence of imidazole, $(NH_4)_2SO_4$ and also tris, on the influx of Cl^- into *C. corallina* may be caused by their influence on cytoplasmic pH (see also Smith, 1971 and 1972). These amino-compounds were considered

to penetrate the plasmalemma either as neutral molecules which then reacted with H^+ in the cytoplasm to form the cationic species, or as the cation, in exchange for H^+. In either case, the net result would be an increase in the pH value of the cytoplasm. Experimental confirmation of this proposal was not obtained by Walker and Smith (1974), who determined cytoplasmic pH values under both dark and light conditions, in the presence and absence of 2mM $(NH_4)_2SO_4$ (bathing solution pH 6.9 - 7.0). They concluded that their results offered little support for the Cl^-/OH^- exchange hypothesis or the proposal that $(NH_4)_2SO_4$ increases the cytoplasmic pH value (see Smith, 1970).

An alternative mechanism by which these amino-compounds could act to stimulate Cl^- transport may be via their removal of the competitive inhibition of Cl^- which is observed in the presence of HCO_3^- (see for example Van Lookeren Campagne, 1957; Smith, 1965; Raven, 1968a). This would result if, for example, $(NH_4)_2SO_4$ inhibited the transport of HCO_3^- and/or OH^-, thereby making available more energy for the transport of Cl^-. If the increase in available energy was expressed as an increase in the rate of H^+ efflux and hence OH^- generation in the cytoplasm, the effect would only be observed, in terms of a rise in cytoplasmic pH, if the Cl^-/OH^- system did not follow a similar time-course of stimulation. The results of Walker and Smith (1974) therefore apparently invalidate the neutral $NH_3 \rightleftharpoons NH_4^+ + OH^-$ hypothesis but not necessarily the Cl^-/OH^- transport hypothesis (but see Chapter 6).

The effect of $(NH_4)_2SO_4$ on the light dependent formation of the acid and alkaline bands in *C. corallina* was investigated by Lucas (1971). This study showed that $(NH_4)_2SO_4$ (0.2 - 0.4mM pH 6.0 - 7.0) inhibited the development of both the H^+ and OH^- bands. The inhibition of the H^+ efflux system was also observed

in Cl^--free solutions. Hence a stimulated H^+ efflux rate was not being masked by a paralleled increase in the operational rate of the Cl^-/OH^- system. Ammonium sulphate thus appeared to influence the HCO_3^-, OH^- and H^+ systems but its mode of action remained obscure.

The experiments reported in this chapter were conducted in an attempt to elucidate the site(s) and mode(s) of action of $(NH_4)_2SO_4$ on these transport processes.

Results

The influence of 0.1 - 0.375mM $(NH_4)_2SO_4$ on the ability of these cells to raise the pH of the bathing solution was investigated. Typical results are expressed in Figure 8.1, and it can be seen that when $(NH_4)_2SO_4$ was present at a concentration of 0.375mM, no change in the external pH value was observed. However, at lower concentrations of NH_4^+ the pH value was raised after the cells had been in contact with the NH_4^+ solutions for several hours. These results are in accord with those obtained by Lucas (1971), and demonstrate that at neutral pH values and in the presence of low exogenous HCO_3^-, $(NH_4)_2SO_4$ does inhibit the efflux of OH^- and H^+. (The fall in pH when the treatments were transferred to the dark (see Figure 8.1) was considered to result from the influence of respiratory CO_2). At this pH range the cytoplasmic streaming rate was not influenced by these levels of $(NH_4)_2SO_4$. The streaming rate for the control cells was 76 ± 2.1μm s^{-1} and the ammonium treatments were 74 ± 4.3, 75.8 ± 1.4 and 74.8 ± 2.7 μm s^{-1} for the respective 0.125, 0.25 and 0.375mM concentrations.

Influence of $(NH_4)_2SO_4$ on $H^{14}CO_3^-$ Assimilation

The effect of various concentrations of $(NH_4)_2SO_4$ on $H^{14}CO_3^-$ assimilation was investigated. Experiments were conducted at pH 9.1 and all bathing solutions contained 3mM total carbon. The results (see Table 8.1) indicated that ^{14}C. assimilation was inhibited even at the lowest $(NH_4)_2SO_4$ concentration employed. This inhibition was expected on the basis of Figure 8.1 (and also Lucas, 1971) for it was argued that since the alkaline bands are related to, and dependent upon, HCO_3^- assimilation (see Lucas and Smith, 1973), inhibition of their development must imply that the particular treatment interferes with cellular assimilation of exogenous HCO_3^-. However, the $(NH_4)_2SO_4$ concentration required to give a 95% inhibition of the ^{14}C fixation rate was considerably higher than that required to prevent the formation of OH^- bands at pH 7.0 (cf. Figure 8.1).

Experiments were also conducted over the pH range 6.2 - 9.6. In these the concentrations of total carbon and $(NH_4)_2SO_4$ were held constant at 3.0mM and 1.25mM respectively. The results are presented in Table 8.2. The complete absence of an inhibitory effect of $(NH_4)_2SO_4$ on ^{14}C. fixation at pH 6.2 was in agreement with the earlier reports (Smith, 1967a; Smith and West, 1969), since at this pH value exogenous $^{14}CO_2$ was present at saturating concentrations. Based on the results presented in Chapter Three (see in particular Figures 3.6 and 3.7) and Figure 8.1, a much greater inhibition was expected than was indeed observed over the pH range 7.0 - 7.7. These results suggested that the effect of $(NH_4)_2SO_4$ within this pH range, may be sensitive to the exogenous HCO_3^- concentration, i.e. high concentrations of HCO_3^- may partially relieve this inhibition.

Analysis of the results presented in Tables 8.1 and 8.2, in terms of the percentage inhibition observed in the presence of a particular concentration of NH_4^+ compared with NH_3, revealed a positive correlation between the inhibition of ^{14}C. and the concentration of NH_3 in the exogenous solution (see Figure 8.2). This implied that either the HCO_3^- or OH^- transport systems were inhibited, or the chloroplasts were being uncoupled, in vivo, by NH_3. The observed pH-dependence of ^{14}C. inhibition may have been due to the influence of pH on the equilibrium level of exogenous NH_3. However, it could also have been that NH_4^+ penetrated to the cytoplasm and NH_3 which was formed in the cytoplasm by the reaction $NH_4^+ + OH^- \rightleftharpoons H_2O + NH_3$, may then have escaped from the cytoplasm under the influence of an external concentration gradient. In either case, the exogenous and cytoplasmic NH_3 levels would have been determined indirectly by the pH values of the bathing solution. Similarly both processes would influence the cytoplasmic pH and a response of this nature is as yet unsupported by experimental results (cf. Walker and Smith, 1974).

Cytoplasmic Streaming in the Presence of $(NH_4)_2SO_4$

It was demonstrated that at pH 6.9 - 7.0 the presence of $(NH_4)_2SO_4$ did not reduce the cytoplasmic streaming rate. Unfortunately cyclosis was not investigated during the ^{14}C. results presented in Tables 8.1 and 8.2. Experiments were therefore conducted to ensure that cyclosis remained unaffected at higher pH values. It was found that this was not so. The responses on transferring cells from control solutions to solutions containing 0.15, 0.25 and 0.4mM $(NH_4)_2SO_4$ are illustrated in Figures 8.3A, B and C respectively. At $(NH_4)_2SO_4$ concentrations of $\geq$0.4mM the initial response was similar to that observed using lower concentrations,

but cyclosis did not recover. Within 4h all cells used at concentrations ≥0.4mM were dead. These results demonstrated that at high pH values this amino-compound should not be employed at concentrations greater than 0.25 - 0.3mM. These results implied that the inhibition of ^{14}C. fixation observed at the higher concentrations of $(NH_4)_2SO_4$ were due to general metabolic uncoupling.

The reversibility of a potentially lethal $(NH_4)_2SO_4$ concentration (1.25mM) is shown in Figure 8.4. Following a 10 min exposure in this solution, one treatment was transferred back to the control solution (3mM $NaHCO_3$, pH 9.2). At the end of a 4h experimental period the latter cells had recovered whereas all cells bathed in the 1.25mM $(NH_4)_2SO_4$ had died. Figure 8.4 also demonstrated that this same concentration of $(NH_4)_2SO_4$ did not have any effect on the streaming rate when the bathing solution pH value was 7.0.

Isolating Chamber $(NH_4)_2SO_4$ experiments

The experimental apparatus (isolating chamber) and procedures detailed in Chapter Seven were employed to determine the site of inhibition of $(NH_4)_2SO_4$ with respect to HCO_3^- assimilation and also H^+ efflux. The only modification to the technique was that 0.1mM phenol red was included in the outer chamber bathing solutions. This made it possible to observe the OH^- banding patterns on the outer cell segment.

Figure 8.5 indicated that when $(NH_4)_2SO_4$ was present in the outer chamber, the activity of the isolated OH^- band decreased slightly and then recovered. The OH^- bands on the outer cell segment disappeared. The reverse situation, namely control solution in the outer and test solution in the inner chambers (see caption to Figure 8.5), resulted in an apparently instantaneous deactivation of the efflux activity of the isolated OH^- band

(cf. results presented in Chapter 7). The OH^- bands on the outer cell segment appeared to be unaffected by the $(NH_4)_2SO_4$ in the isolating chamber. Figure 8.5 also demonstrated that after a 10-40 min exposure to 0.2 $(NH_4)_2SO_4$, the inhibition of OH^- efflux activity could be reversed simply by flushing the isolating chamber with control solution. These results suggested, at least at this pH value, that the immediate site of $(NH_4)_2SO_4$ inhibition of OH^- efflux activity (and possibly HCO_3^- influx) was located at or within the plasmalemma. (The inhibition of HCO_3^- assimilation and the lethal nature of this compound observed at higher pH values was considered due to its effect(s) on cellular metabolism).

Similar experiments were conducted using CO_2-free solutions in the isolating chamber (see Figures 8.6 and 8.7). It was found that deactivation still resulted when CO_2-free solutions containing $(NH_4)_2SO_4$ were employed, but H^+ efflux appeared to be stimulated (cf. Figures 8.5, 8.6 and 8.7). (The generation of H^+ via the equilibrium reaction involving NH_4^+ and NH_3, i.e. assuming NH_3 penetrated to the cytoplasm, would not result in acidification to this level because the reaction is itself extremely pH dependent). More importantly the results presented in Figures 8.6 and 8.7 demonstrated that OH^- efflux activity, within the isolating chamber, remained even when this chamber contained CO_2-free solution and the outer chamber contained 0.2mM $(NH_4)_2SO_4$. (In this situation there were no active OH^- bands on the outer cell segment), i.e. $(NH_4)_2SO_4$ did not appear to inhibit the influx of HCO_3^-, for if it had, the isolated OH^- efflux site would have deactivated. In fact the activity of the isolated OH^- efflux site was found to increase under these conditions. Deactivation could, however, be obtained by sealing the outer segment in liquid paraffin (see Figure 8.7) which completely removed HCO_3^- from the cell.

Effect of HCO_3^- concentration on $(NH_4)_2SO_4$ Inhibition of ^{14}C. Assimilation

The results presented in Table 8.2 suggested that the inhibition of ^{14}C by $(NH_4)_2SO_4$ may be partially relieved by increasing HCO_3^- concentrations. Experiments were conducted in which an $(NH_4)_2SO_4$ concentration of 0.3mM was employed in the presence of 0.1, 0.2, 0.4 and 0.6mM total carbon. These experiments were conducted at pH 7.5 and 9.2 and in order that the results be comparable with the responses presented in Figure 8.1, "artificial" buffering capacity was not employed. The results obtained under these conditions are presented in Table 8.3. Experiments numbered 1-4 were conducted at an initial pH value of 7.5 and it was found that under these conditions, as the total carbon level was increased, the apparent inhibition of ^{14}C fixation decreased from 50 to 30% (approximately). However, using the Null Hypothesis and the Student t test, it was found that the changes in the values of percentage inhibition were not significant at the 95% confidence limit. It was therefore assumed that at pH 7.5, an increase in the concentration of HCO_3^- did not partially relieve the inhibitory effect of $(NH_4)_2SO_4$. A similar result was obtained at pH 9.2.

Discussion.

The results presented in this chapter demonstrate that $(NH_4)_2SO_4$ interferes with the normal operation of the OH^- efflux system. However, it should be emphasized that the actual mechanism by which this inhibition occurs is unresolved. It has also been shown that $(NH_4)_2SO_4$ can influence total cellular metabolism and under certain conditions this influence can be deleterious.

One mode of interaction between NH_4^+ ions and the OH^- efflux system could be that NH_4^+ is titrated to NH_3 within the immediate vicinity of the OH^- efflux site by the released OH^- ions. This titration could also be performed artificially by raising the pH value of the bathing solution. The actual inhibition of OH^- efflux may be caused by the resultant molecules of NH_3 acting as weakly bound allosteric inhibitors of the OH^- carriers. This would explain both the pH dependence of the inhibition of $H^{14}CO_3^-$ assimilation and the rapid recovery of OH^- efflux function after removal of $(NH_4)_2SO_4$.

The decreased alkalinization of the external solution, in the presence of $(NH_4)_2SO_4$ (see Figure 8.1 and Table 8.3), is in agreement with the results obtained by Lucas (1971). However, the most interesting and yet perplexing feature of these results is that the pH rise in the solutions which contained $(NH_4)_2SO_4$ was almost constant, irrespective of the exogenous ^{14}C. level (see Table 8.3). This discrepancy can be quite simply explained by assuming that the major part of the ^{14}C. fixation, observed at pH 7.5, is due to exogenous $^{14}CO_2$. It was found that this was not so (see Chapter 9, Figure 9.6) and added to this, actual removal of CO_2 via photosynthetic fixation should in itself have raised the pH value of the bathing solution. Hence an alternative explanation is necessary to account for these results. This proposal must explain the apparent influx of HCO_3^- in the absence of OH^- efflux. Similarly it must account for the observation of Walker and Smith (1974) that the cytoplasmic pH value did not rise in the presence of $(NH_4)_2SO_4$.

It is clear that further research is required in this area to elucidate the relationship between HCO_3^- influx and the involvement of exogenous NH_4^+/NH_3. At this stage it would appear that $(NH_4)_2SO_4$ is capable of affecting several cellular processes located within the plasmalemma and cytoplasmic phases of the cell.

Stimulation of Cl^- Influx by Amino-Compounds

The results presented in Tables 8.1, 8.2 and 8.3 demonstrate that $(NH_4)_2SO_4$ reduces $H^{14}CO_3^-$ influx at pH values $\geq$7.0. Hence, if the apparent HCO_3^- inhibition of Cl^- influx is due to competition for an energy substrate between the Cl^- and HCO_3^- influx systems, these results offer an explanation of the apparent stimulation of the light promoted Cl^- influx observed in the presence of certain amino-type compounds. At pH values above 7.0 the influx of Cl^- is small (Smith, 1970) when compared with the influx of HCO_3^-. Consequently any process which reduces the influx of HCO_3^- may in effect stimulate Cl^- influx. An interactive response of this nature is in accord with the results presented in Chapter 6, where it was shown that a lag in $^{36}Cl^-$ influx existed prior to the establishment of a steady state rate. It was considered that this lag represented the time required to develop the Cl^- influx activating condition(s) within the cytoplasm. However, since $H^{14}CO_3^-$ influx in the dark is apparently quite low (see Chapter Seven), this proposal does not explain the dark stimulation of Cl^- influx reported by Smith (1970, 1971, 1972; see also Smith and Lucas, 1973).

Net H^+ Efflux

In the presence of $(NH_4)_2SO_4$ net H^+ efflux was almost always completely inhibited (this was also found by Lucas, 1971). Similar results were obtained using the isolating chamber, i.e. when the solution contained 0.2mM $(NH_4)_2SO_4$ and 0.2mM $NaHCO_3$, the isolated OH^- site deactivated and the pH value of the bathing solution was not depressed much below the background value (see for example Figure 8.5). This was in marked contrast to the net H^+ efflux response observed when CO_2-free solutions containing $(NH_4)_2SO_4$ were employed. Under these conditions the OH^- efflux system deactivated

and the pH value of the bathing solution was depressed very rapidly towards pH 5.5.

The simplest explanation for this difference in responses is that the buffering capacity of the 0.2mM $NaHCO_3$ masked the true H^+ efflux rate, which could be observed most effectively in CO_2-free conditions where the buffering effect would be minimal. It is felt that this is not in fact the case, for acidification was not observed in experiments in which the effect of $(NH_4)_2SO_4$ was investigated under conditions of low exogenous HCO_3^- (see Figure 8.1). It may have been that exposure of the isolated cell segment to carbon free solutions (i.e. CO_2 and HCO_3^-) affected the passive permeability properties of the plasmalemma (Sears and Eisenberg, 1961; Glinka and Reinhold, 1964), i.e. the passive permeability to H^+ may have been reduced.

Spanswick (1974) demonstrated that in *N. translucens* the resistance of the plasmalemma was lower under CO_2-free conditions when compared with solution conditions of 1mM total carbon. This situation was observed for both dark and light conditions. Spanswick also found that the membrane potential could be returned to its maximum hyperpolarized level by substituting the 1mM total carbon solution with a CO_2-free solution. To account for these results he proposed that the H^+ efflux system and the dark photosynthetic reactions compete for a common energy substrate (ATP).

It may be that a similar situation also exists in *C. corallina*. However, it is not clear what role $(NH_4)_2SO_4$ would play in the stimulation of the rate of H^+ efflux. Unfortunately parallel biophysical studies of the type conducted by Spanswick (1974) have not been conducted on cells of *C. corallina*.

TABLE 8.1.

Influence of $(NH_4)_2SO_4$ on $H^{14}CO_3^-$ Assimilation.

Experimental Solutions (3mM Total Carbon, pH 9.1 +)		Photosynthetic ^{14}C. Fixation* (pmol $cm^{-2} s^{-1}$)	Percentage Inhibition
$(NH_4)_2SO_4$ (mM)	NH_3 (mM)		
—	—	60.7 ± 3.0	—
0.05	0.041	44.9 ± 3.6	26.0
0.10	0.082	20.5 ± 2.9	66.2
0.25	0.206	11.4 ± 0.5	81.2
0.50	0.412	9.0 ± 0.4	85.2
0.50	0.412	12.4 ± 0.6	79.6
0.75	0.617	7.7 ± 0.6	87.3
1.25	1.029	3.5 ± 0.2	94.3

* Cells were cut from culture tank E', and a light intensity of $25 Wm^{-2}$ was used throughout.

TABLE 8.2.

Influence of $(NH_4)_2SO_4$ on ^{14}C. Assimilation over a Range of pH Values

Experimental Conditions			Photosynthetic ^{14}C. Fixation** $(NH_4)_2SO_4$		
Solution pH	NH_3^+ (mm)	Buffer and Concentration (mm)	(-)	(+)	Percent Inhibition.
6.2	0.002	MES, 5 + C_T*	127.1 ± 4.4	128.9 ± 4.0	0
7.0	0.014	TES, 5 + C_T	130.2 ± 5.1	109.6 ± 4.2	15.8
7.3	0.027	TES, 5 + C_T	98.5 ± 5.9	85.4 ± 4.5	13.3
7.7	0.068	TES, 5 + C_T	96.4 ± 2.4	61.6 ± 1.6	36.1
8.3	0.249	TES, 5 + C_T	50.7 ± 2.7	20.4 ± 2.1	59.8
8.4	0.306	C_T	64.5 ± 5.3	20.7 ± 0.8 16.6 ± 0.9	67.9
9.0	0.893	C_T	61.3 ± 4.8	3.5 ± 0.05	94.6
9.6	1.722	C_T	39.4 ± 3.3	1.6 ± 0.04	95.9

\+ 1.25mM $(NH_4)_2SO_4$ was added to each experimental solution under the heading (+), the actual equilibrium concentration of NH_3 was calculated using the equilibrium reaction $NH_3 + H_2O \rightleftharpoons NH_4^+ + OH^-$ and $K_b = 1.77 \times 10^{-5}$ (Bates and Pinching, 1949).

* C_T represents total added carbon and was 3.0mM throughout.

** As in Table 8.1, except that shaded tank delta cells were employed for these experiments.

TABLE 8.3.

Influence of a Constant [$(NH_4)_2SO_4$] on ^{14}C. Fixation in the Presence of Increasing [HCO_3^-]

Expt. No.	$NaHCO_3$ Concentration (mM)	0.3mM $(NH_4)_2SO_4$ ^{14}C. Fixation (pmol $cm^{-2}s^{-1}$) (-)	(+)	Solution pH (-) Initial	(-) Final	(+) Initial	(+) Final	% Inhibition* A	B
1	0.1	8.97 ± 0.57	5.67 ± 0.32	7.50	8.30	7.45	7.64	36.8	46.8
2	0.2	16.96 ± 1.11	9.90 ± 0.89	7.48	8.56	7.53	7.75	41.6	48.6
3	0.4	22.05 ± 1.51	16.62 ± 1.06	7.50	8.52	7.52	7.75	24.6	29.2
4	0.6	28.23 ± 2.2	20.74 ± 1.59	7.50	8.20	7.50	7.70	36.5	33.6
5	0.1	7.59 ± 0.68	0.42 ± 0.02	9.15	9.20	9.20	9.15	94.5	**
6	0.2	14.14 ± 0.32	0.86 ± 0.05	9.15	9.25	9.18	9.15	94.0	
7	0.4	22.01 ± 2.0	1.21 ± 0.06	9.15	9.20	9.20	9.22	94.5	
8	0.6	27.6 ± 1.65	2.06 ± 0.12	9.15	9.29	9.20	9.12	92.5	

* % Inhibition; A, values obtained using ^{14}C rates uncorrected for $^{14}CO_2$ fixation; B, values corrected for $^{14}CO_2$ contribution using the results presented in Chapter Three.

** Correction due to $^{14}CO_2$ insignificant at this pH value.

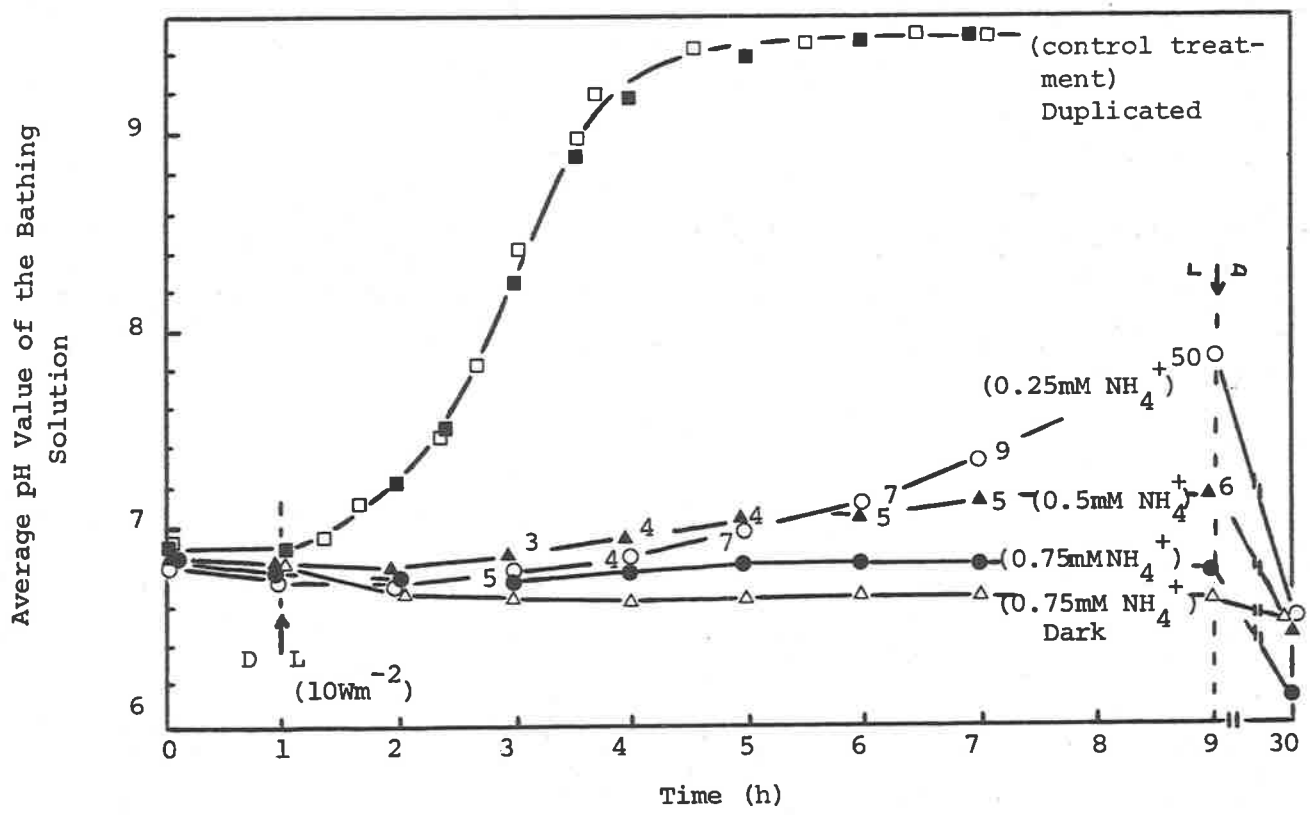

Figure 8.1. Ability of *Chara* cells to influence the pH of the bathing solution in the presence and absence of $(NH_4)_2SO_4$. Experiments were conducted in sealed test tubes and the ^{14}C. experimental system was employed. Cells were bathed in normal solution, containing 0.1mM phenol red, and were titrated to pH 6.9 - 7.0 using 100mM NaOH. The pH values were measured by carefully mixing the solution and then inserting a small combination pH electrode. Ten cells, having an approximate total surface area of 13.0cm^2, were used per treatment. The concentration of NH_4^+ (added as $(NH_4)_2SO_4$) present in each treatment is indicated on the figure. Numerals next to the symbols (○) and (▲) indicate the number of OH^- bands developed.

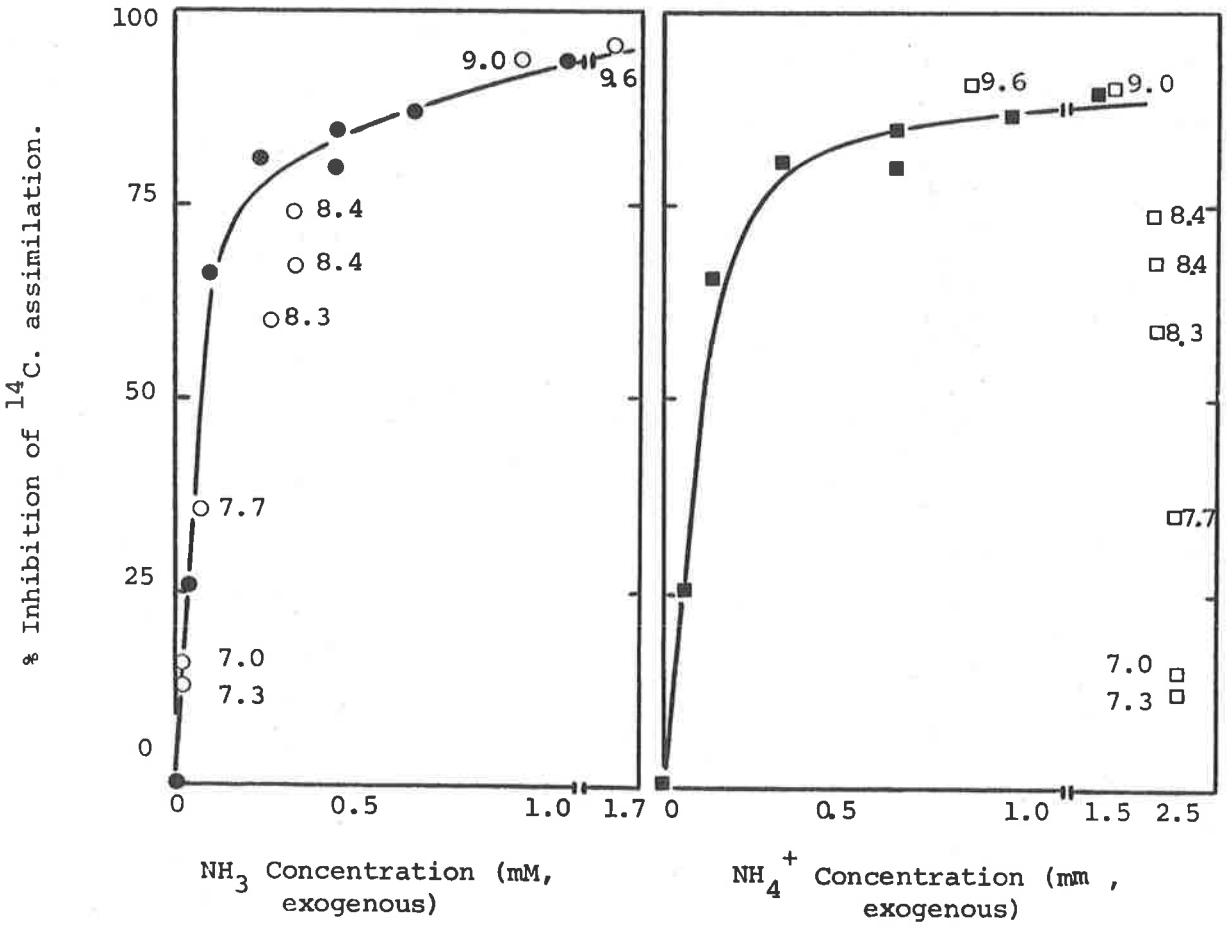

Figure 8.2. Relationship between percentage inhibition of ^{14}C assimilation and the exogenous concentration of NH_3 and NH_4^+. The results presented in Table 8.1 are represented by (●) and (■), whereas the values obtained at the various pH values (see Table 8.2) are represented by (○) and (□) respectively. For the latter the actual experimental pH values are indicated next to the actual experimental point.

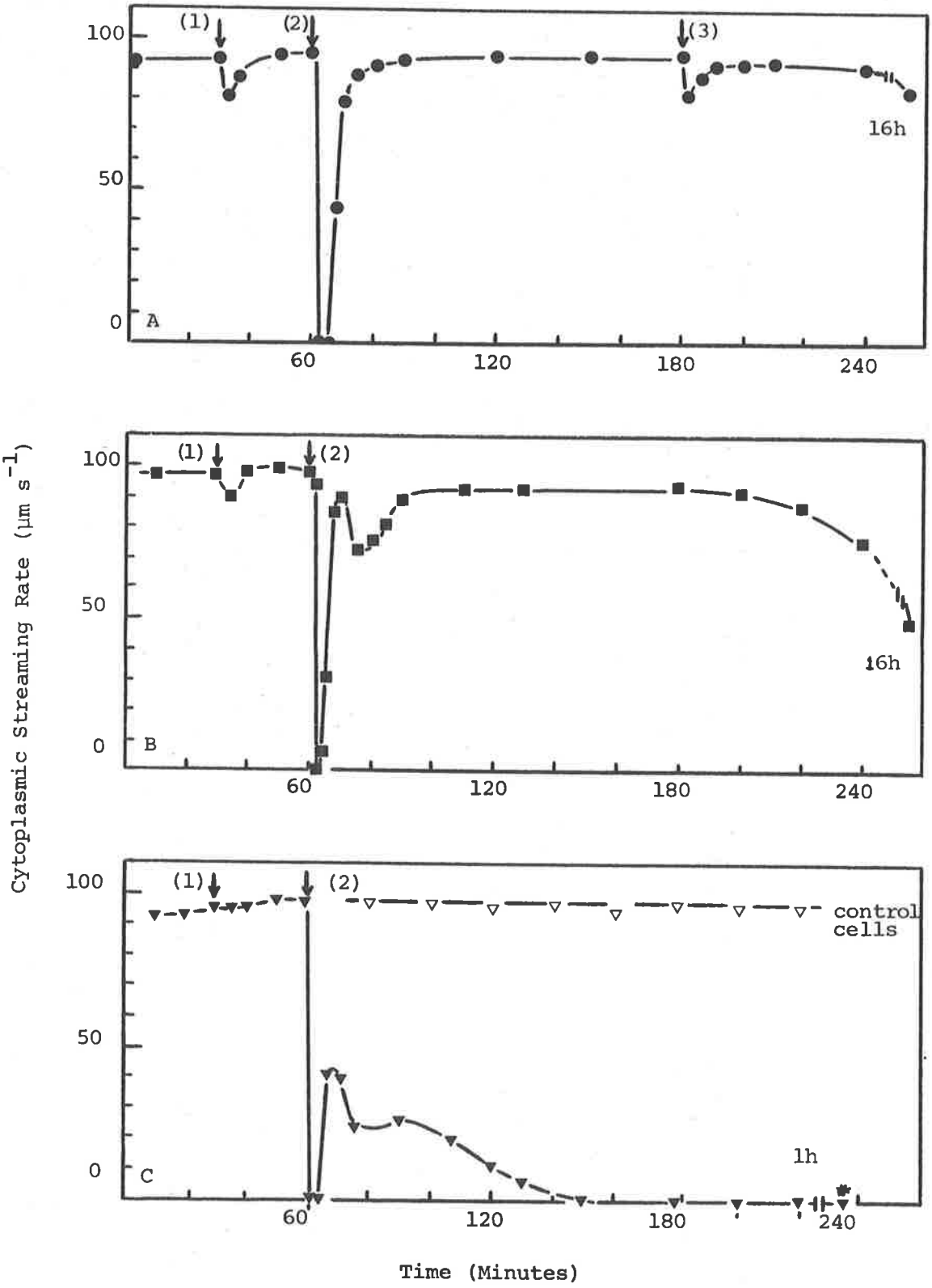

Figure 8.3. Effect of $(NH_4)_2SO_4$ on Cytoplasmic Streaming. The numerals (1), (2), and (3) represent respectively the transfer of the cells (10 per treatment) from normal bathing solution, pH 5.8 to 3.0mM $NaHCO_3$, pH 9.1; 3.0mM $NaHCO_3$ + x mM $(NH_4)_2SO_4$; as (2) but increasing x to y. The $(NH_4)_2SO_4$ concentration in A was 0.15 and 0.25mM for x and y; in B, x = 0.25mM; and for C, x = 0.4mM). (* indicates all cells dead).

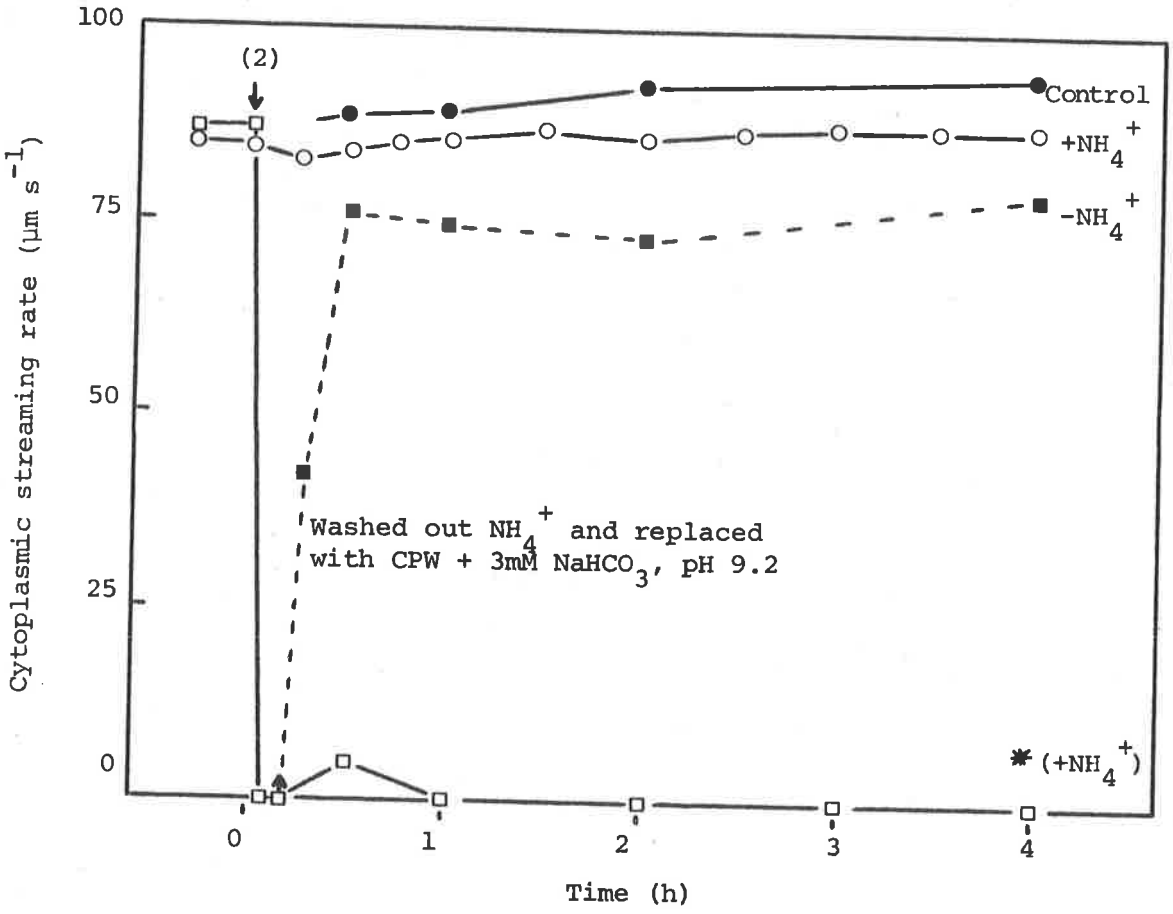

Figure 8.4. Reversible Effect of $(NH_4)_2SO_4$. Details are as for Figure 8.3 except that the $(NH_4)_2SO_4$ concentration was increased to 1.25mM. The symbol (■) represents the cytoplasmic streaming response of cells exposed to $(NH_4)_2SO_4$ for 10 min. and then returned to the control solution (3mM $NaHCO_3$, pH 9.2); (○) represents the response of a treatment whose pH value was adjusted to 7.0.

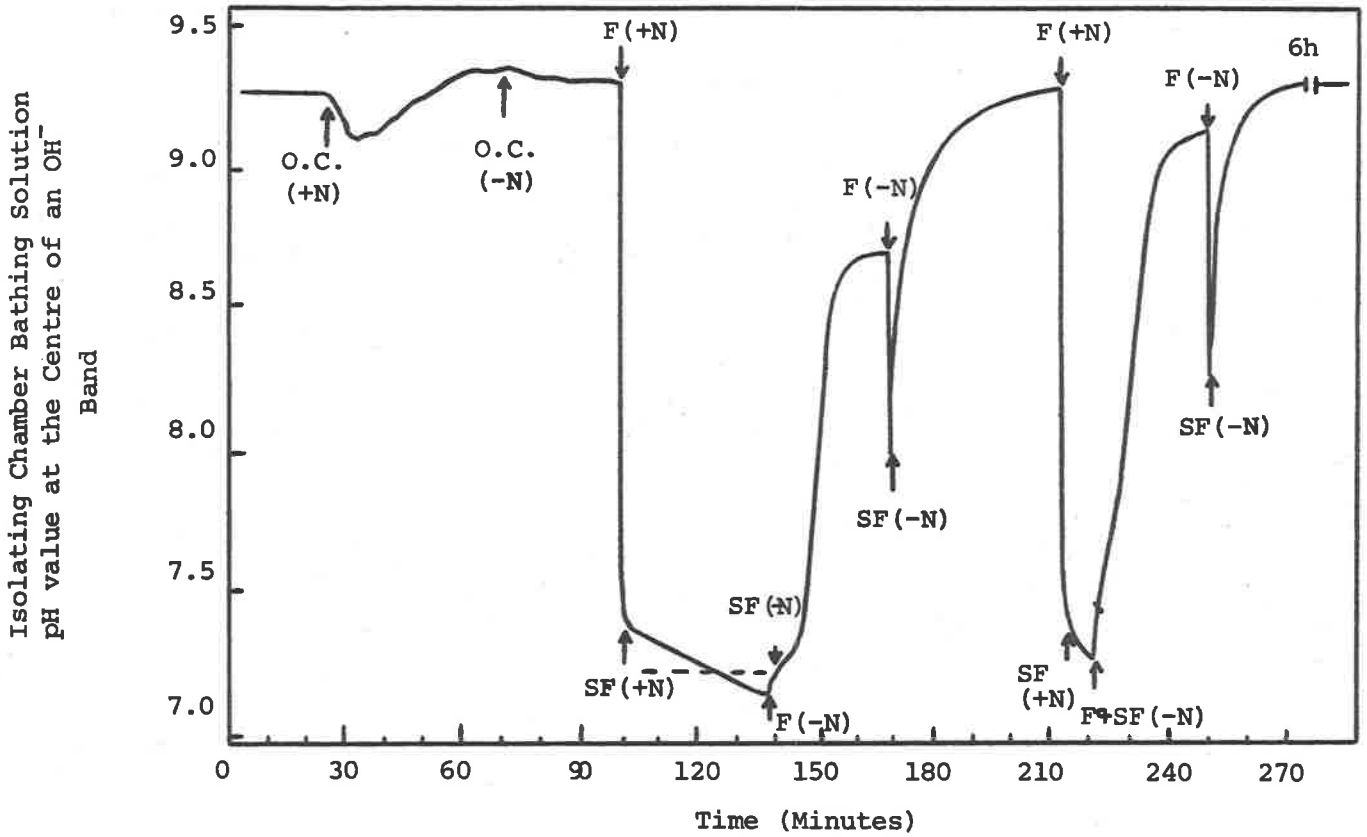

Figure 8.5. Inhibition of OH^- efflux by $(NH_4)_2SO_4$. The control bathing solution contained 0.2mM $NaHCO_3$, pH 7.2; and the test solution 0.2mM $NaHCO_3$ + 0.2mM $(NH_4)_2SO_4$, pH 7.2. The symbols are as follows: O.C. (+N), introduced test solution to the outer chamber; O.C. (-N), replaced outer chamber solution by control solution; F(+N), flushed inner chamber with test solution; SF(+N), stopped flushing inner chamber with test solution; F(-N) and SF(-N), flushed and stopped flushing inner chamber with control solution.

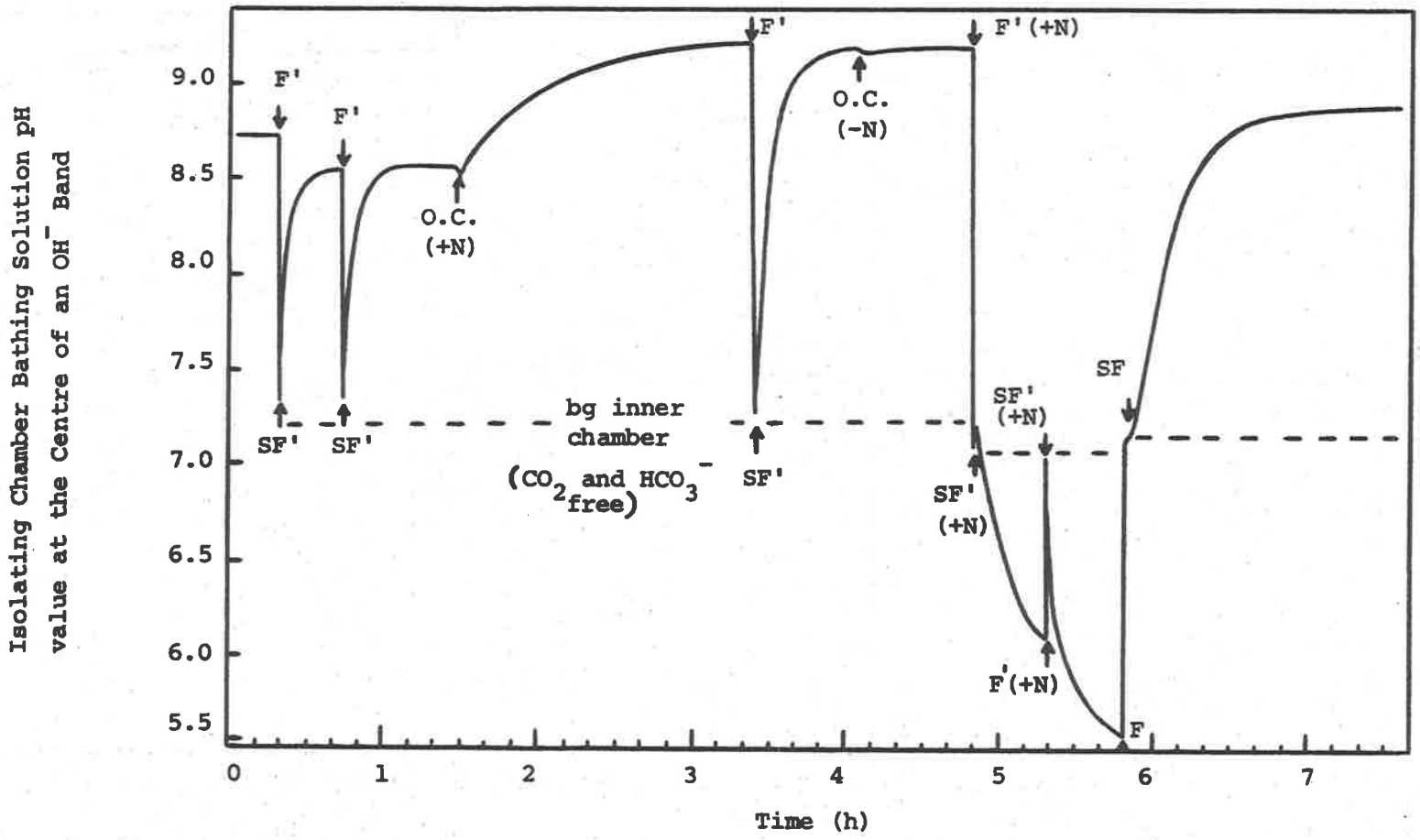

Figure 8.6. Inhibition of OH^- Efflux by $(NH_4)_2SO_4$ in the presence of CO_2-free solutions. Experimental details and symbols as in Figure 8.5, except that F' refers to CO_2-free solutions.

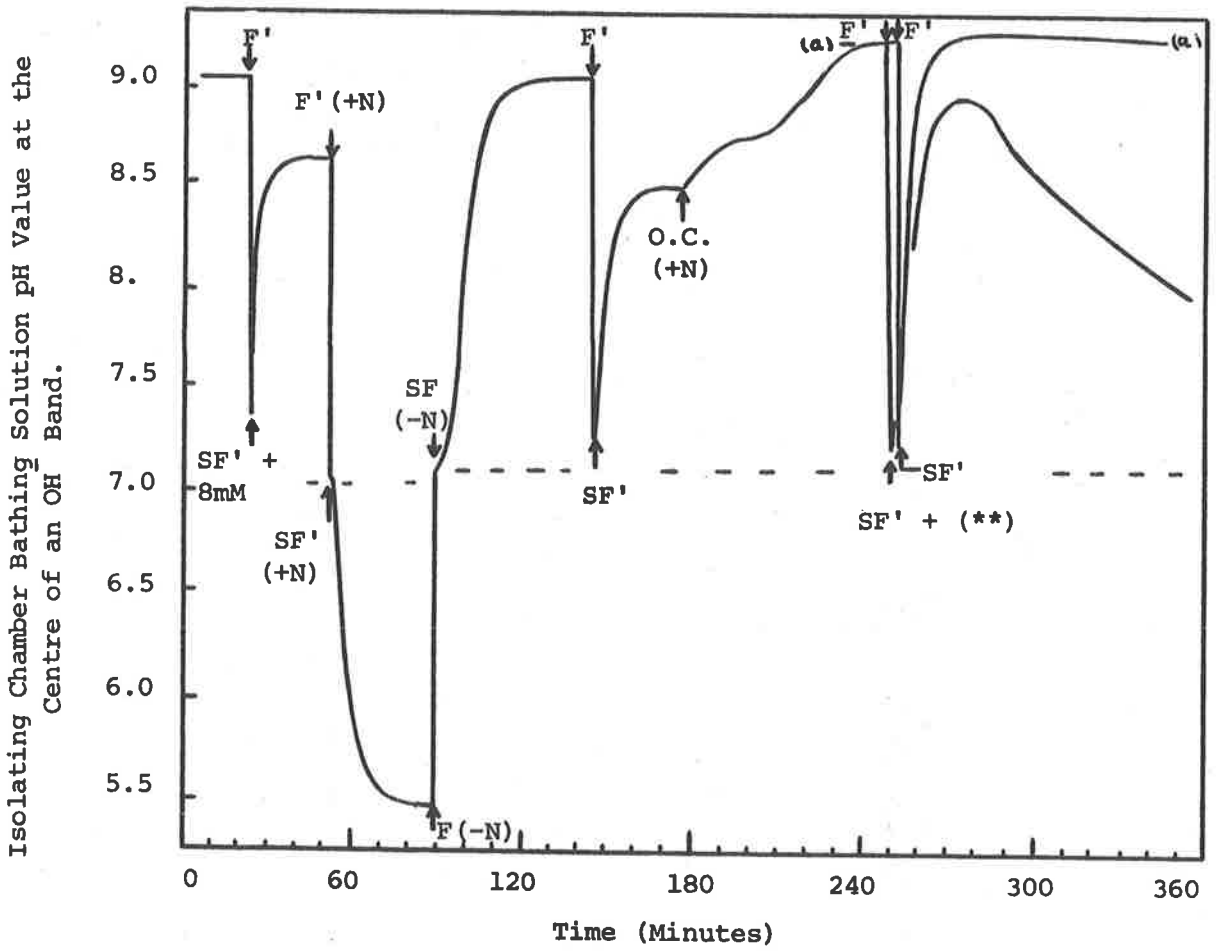

Figure 8.7. HCO_3^- INflux in the presence of $(NH_4)_2SO_4$. Experimental details and symbols as in Figure 8.6 except that (**) refers to the sealing of the outer cell segment in liquid paraffin (for full details see Chapter 7).

CHAPTER NINE

INFLUENCE OF $[Ca^{++}]$ AND $[K^+]$ ON THE INFLUX OF $H^{14}CO_3^-$

Introduction

The membrane potential of Characean cells can be partially described by equation (1.3) after cells have been exposed to Ca^{++}-free solutions (Osterhout,1949; Kishimoto, 1959; Hope and Walker, 1961; Spanswick, Stolarek and Williams, 1967; Kitasato, 1968). It has also been shown that in the presence of Ca^{++} ions, once the concentration of K^+ in the bathing solution has been raised above a certain value, the membrane appears to function as a "K^+ electrode" system (Kishimoto, 1959; Kishimoto, Nagai and Tazawa, 1965; Kitasato, 1968; Spanswick, 1972; Saito and Senda, 1973a; Volkov, 1973).

Kitasato (1968) and Richards and Hope (1974) also demonstrated that the "K^+ sensitivity" of the membrane was influenced by the pH value of the bathing solution. These results implied that the removal of Ca^{++}, or alternatively an increase in the K^+ concentration affected the electrogenic component of the membrane potential, i.e. the electrogenic system either becomes inoperative or is in some way short-circuited by these treatments.

Since it has been proposed that at or above bathing solution pH values of 6.0 the influx of HCO_3^- and efflux of OH^- may contribute towards determining the membrane potential and resistance (see Chapters 3, 5 and 7), it was of interest to determine the effect of these cationic treatments on the influx of $H^{14}CO_3^-$.

Results

The Effect of Removing Ca^{++} from the Bathing Solution

In Figure 4.11 it was shown that prolonged (10h) exposure to low Ca^{++} solutions (0.02mM) did not cause a decrease in $H^{14}CO_3^-$ influx. However, a decrease in $H^{14}CO_3^-$ influx was observed when Ca^{++}-free solutions were employed. The time-course of the decay in $H^{14}CO_3^-$ influx capacity which resulted following the exclusion of Ca^{++} from the bathing solution, is shown in Figures 9.1 and 9.2. Cells used for these experiments were pretreated for 2h in normal bathing solution which contained 10mM MES-buffer (pH 5.0), to ensure that $CaCO_3$ deposits were removed from the cell wall. The decay curve for Figure 9.1 was obtained via the following experimental procedure; at the conclusion of a 12h dark recovery period, during which time the cells were bathed in normal solution which contained 0.5mM $NaHCO_3$ (pH 8.8) the cells were divided into two batches.

One batch was simultaneously illuminated ($15Wm^{-2}$) and transferred to a modified bathing solution which contained 5mM NaCl, 0.2mM KCl, 0.5mM $NaHCO_3$ and no Ca^{++} (pH 9.0). The second batch of cells was employed for control treatments; they were illuminated under the same light intensity, but the bathing solution contained 1.0mM NaCl, 0.2mM KCl, 0.25mM $CaSO_4$ and 0.5mM $NaHCO_3$ (pH 9.0). Solutions for both treatments were changed at 2 hourly intervals, and a normal $H^{14}CO_3^-$ exposure period of 1h was employed.

Under these conditions the $H^{14}CO_3^-$ influx appeared to decrease slowly until by the 10th hour of contact with Ca^{++}-free solution the rate had dropped to a new steady value. This value was approximately 38% of the control.

Figure 9.1 also shows the effect upon $H^{14}CO_3^-$ influx of returning Ca^{++} to the experimental solution. These cells were given a similar decalcification treatment, except that the recovery phase was reduced to a 2h dark period. A 12h dark treatment using the 5mM NaCl solution was then employed, the solutions being changed every 4h. It was found that the cellular recovery of $H^{14}CO_3^-$ transport capacity followed almost the mirror-image of its decline. Recovery appeared to follow the same time-course irrespective of whether dark or light treatments were employed during the recovery phase.

The influence of extremely long exposure periods of Ca^{++}-free solutions is shown in Figure 9.2. The initial decline in cellular $H^{14}CO_3^-$ transport capacity was identical to that observed in Figure 9.1. However, it was found that a further decrease was not observed until cells had been exposed to these solutions for approximately 127h. Cyclosis was also measured on each $H^{14}CO_3^-$ treatment. These results, which are included on Figure 9.2, showed that after the initial 24h exposure to Ca^{++}-free solutions the streaming rate began to decrease. It should be noted that the region in which cyclosis declined most rapidly also coincided with the second phase in the reduction of $H^{14}CO_3^-$ influx. These results indicated that prolonged exposure to Ca^{++}-free solutions eventually depressed both $H^{14}CO_3^-$, influx and cyclosis and this effect culminated in the death of the experimental cells.

Effect of De-Calcification Treatments on Fixation of Exogenous $^{14}CO_2$

Table 9.1 indicates that the 10mM MES-buffer treatment did not alter significantly the cellular ability to utilize exogenous carbon (either $^{14}CO_2$ or $H^{14}CO_3^-$). The $^{14}CO_2$ fixation rate actually appeared to increase above that of the control cells. Similarly exposure to Ca^{++}-free solutions did not reduce the ^{14}C. fixation

rate in the presence of exogenous $^{14}CO_2$. The exogenous $H^{14}CO_3^-$ treatment, however, resulted in a decrease in ^{14}C assimilation in accord with the results presented in Figure 9.1. These results were taken as supporting evidence that the reduction in cellular ability to assimilate $H^{14}CO_3^-$, under Ca^{++}-free conditions, was due to an effect at the plasmalemma rather than the chloroplasts.

Increasing K^+ Concentration: Its Influence on ^{14}C. Assimilation

Figure 9.3 shows that when the K^+ concentration was increased above 2.0mM, the $H^{14}CO_3^-$ influx rate was depressed from approximately 20 to 3.5pmol $cm^{-2}s^{-1}$. Further reduction in the $H^{14}CO_3^-$ influx rate was not observed when higher K^+ levels were employed. A paralleled reduction in ^{14}C. fixation in the presence of exogenous $^{14}CO_2$ was not observed. Inhibition of $^{14}CO_2$ fixation was only observed at K^+ concentrations approximately ten times higher than those required to affect $H^{14}CO_3^-$ influx. Even at this concentration, the reduction in fixation rate was quite small. It would seem, therefore, that the reduction in $H^{14}CO_3^-$ influx and $^{14}CO_2$ fixation, reflect two separate modes of action of the K^+ ion. The reduction in $H^{14}CO_3^-$ influx which was elicited by increasing the K^+ concentration, was considered to result from the effect of K^+ either on the general structure of the plasmalemma or directly upon the HCO_3^- carrier system.

Figure 9.3 shows that some cells did not show reduced $H^{14}CO_3^-$ influx when $[K^+]$ was greater than 2.0mM. This phenomenon was further investigated by conducting an experiment in which 50 cells were treated in 10mM K^+ solutions and 30 control cells were treated in 0.2mM K^+ solutions. Frequency histograms of the results obtained from this experiment are presented in Figure 9.4. From the distribution of the control $H^{14}CO_3^-$ influx values, it

was assumed that K^+ treated cells which had influx values $\geq$ 10pmol $cm^{-2}s^{-1}$ had not been affected by the high K^+ concentration. This was unquestionably so for the five cells having values $\geq$ 18pmol $cm^{-2}s^{-1}$, however one cannot be as certain of the three values in the influx range 10-12 pmol $cm^{-2}s^{-1}$. Collectively the results presented in Figures 9.3 and 9.4 suggest that the reduction in $H^{14}CO_3^-$ influx, in response to [K] $\geq$ 2.0mM, is an "all or none" phenomenon.

Experiments in which $[K^+]$ was held constant at 0.2mM and $[Na^+]$ increased revealed that the influx of $H^{14}CO_3^-$ remained unaffected even at a concentration of 10mM Na^+. (cf. 18.62 ± 1.47 pmol $cm^{-2}s^{-1}$ [1.0mM NaCl, 0.2mM KCl, 0.5mM $NaHCO_3$, 0.5mM $CaSO_4$, pH 9.0] with 20.59 ± 1.3 pmol $cm^{-2}s^{-1}$ [10mM KCl + control bathing solution]). The absence of an effect of Na^+ on the $H^{14}CO_3^-$ influx process is in agreement with the relative insensitivity of the membrane potential to changes in the concentration of this ion (see for example Spanswick, 1972, Table 1).

Effect of 10 and 20mM K^+ on Cyclosis

Streaming rates were measured during the $H^{14}CO_3^-$ experiments and it was found that K^+ concentration as high as 10mM did not affect cyclosis. This observation was supported by experiments which were conducted over prolonged periodsduring which time cells were exposed to 10 or 20mM K^+. Table 9.2 shows that although cyclosis was not affected at 10mM K^+, prolonged contact with 20mM K^+ resulted in the death of the experimental cells.

Increasing HCO_3^- Concentration in the Presence of 10mM K^+

Figure 9.5 indicated that increasing the HCO_3^- concentration in the presence of a fixed concentration of K^+ (10mM) did not result

in the recovery of normal $H^{14}CO_3^-$ influx capacity. The apparent linear response is suggestive of a passive diffusion process. Alternatively it could be that the 10mM K^+ treatment affected the binding properties of the HCO_3^- carrier such that its K_m was increased to a much larger value. This large K_m would give an approximately linear response between influx and substrate concentration. The effect of 0.3mM $(NH_4)_2SO_4$ was included to demonstrate that other inhibitory processes can depress the $H^{14}CO_3^-$ influx value even further. There also appeared to be a linear response to increasing HCO_3^- concentration in the presence of 10.3mM $(NH_4)_2SO_4$.

Influence of 10mM K^+ on ^{14}C. Fixation at pH 7.5.

In Chapter 8 it was found that the $(NH_4)_2SO_4$ inhibition of ^{14}C. fixation, in the pH region 7.0 - 7.7, was not as significant as was expected. There still remained the possibility that $^{14}CO_2$ was contributing more to the total ^{14}C. fixation than predicted from Figures 3.6 and 3.7.

Figure 9.6 demonstrates that when 10mM K^+ is employed the ^{14}C assimilation rate is considerably reduced, as would be expected if $H^{14}CO_3^-$ was contributing significantly to the total ^{14}C fixation rate. When the ^{14}C. fixation values, obtained in the presence of 10mM K^+, were corrected for the residual "concentration response" (using the data presented in Figure 9.5), the values were considered to represent the $^{14}CO_2$ component of fixation. It was calculated that at a total carbon concentration of 0.6mM, the level of CO_2 would have been 0.040mM. From Chapter 3 (Figure 3.2) it was estimated that this concentration (CO_2) would support a fixation rate of between 5.3 - 6.2pmol $cm^{-2}s^{-1}$. Assuming a linear relationship between $^{14}CO_2$ fixation and exogenous CO_2 over this concentration range, a straight line was constructed through the origin. The

agreement between the experimental values (i.e. 10mM K^+, subtracting the residual HCO_3^- influx) and this graph was taken as extremely strong support for the fact that these corrected values do represent the $^{14}CO_2$ contribution to fixation under these conditions. Hence the low inhibitory effect of $(NH_4)_2SO_4$ observed in the pH region 7.0 - 7.7 was not due to an unexpectedly high $^{14}CO_2$ contribution.

Discussion

The Influence of Ca^{++} on HCO_3^- Influx Activity

Dainty and Hope (1959b) reported that the removal of Ca^{++} from the ion exchange component of the cell wall of *C. corallina* could be separated into two fractions, one fast and the other slow. They found that the slow fraction had a $t_{\frac{1}{2}}$ of approximately 15 days! In the present series of experiments, the employment of a 5mM MES treatment and a 5mM Na^+ level, would be likely to produce a much faster elution of Ca^{++} from the cell wall and cytoplasmic phases.

The slow decrease in HCO_3^- influx capacity in response to cellular exposure to Ca^{++}-free solutions implies that either Ca^{++} is being eluted only slowly from the Donnan free space - plasmalemma system, or that the reduction in HCO_3^- influx involves several stages. Calcium may be required to maintain the integrity (or structural conformation) of the plasmalemma such that all membrane-bound processes can function normally. However, it may also be that Ca^{++} per se acts as an integral component of the functional HCO_3^- carrier. The almost identical "mirror-image" recovery phase of HCO_3^- influx capacity, following the re-introduction of Ca^{++}, did not help in distinguishing between these two possibilities. Further experiments, in which the influence of other divalent cations (e.g. Mg^{++}) on the recovery phase of HCO_3^--influx capacity, should demonstrate whether there is a specific require-

ment for Ca^{++} associated with the transport of HCO_3^-.

The second phase of the HCO_3^- influx decay curve (see Figure 9.2) may have been related to the depletion of Ca^{++} from the cytoplasmic phase. This process would certainly be extremely slow since the normal fluxes of Ca^{++} have been reported to be small (Spanswick and Williams, 1965).

The Influence of K^+ on HCO_3^- Influx Activity

The parallel between the effect of K^+ concentration on HCO_3^- influx capacity and the reported effects of this ion (K^+) on the membrane potential (see for example Spanswick, 1972; Saito and Senda, 1973a), indicates that the two phenomena must surely share some common feature. Support is given to this conclusion by the paralleled ineffectiveness of increasing Na^+ concentration on both the membrane potential (see Kitasato, 1968; Hope and Richards, 1971; Spanswick, 1972) and HCO_3^- influx capacity.

It is also important to note that the apparent insensitivity of the membrane potential,"when a large electrogenic component of potential is present" (Richards and Hope, 1974) may not have held, had the authors increased their K^+ concentration above 1mM. On the basis of the results presented in Figures 9.3 and 9.6, a K^+ concentration of 10mM should have given a response similar to that observed by Spanswick (1972).

The "all or none" effect of K^+ on HCO_3^- influx capacity which was demonstrated in Figure 9.4, also has a parallel in that similar effects have been observed during studies on the membrane potential (see Richards and Hope, 1974, Table 1). Hence, since both cationic treatments (Ca^{++} and K^+) influence the influx of HCO_3^- in a manner virtually identical to the electrical effects, this provides additional support to the possibility that HCO_3^- assimilation contributes to the electrical properties of the cell.

TABLE 9.1.

$^{14}CO_2$ and $H^{14}CO_3^-$ Assimilation Following MES-Buffer and Ca^{++}-free Solution treatments

Pretreatment	Experimental Treatment	$H^{14}CO_3^-$ Influx ($pmol\ cm^{-2}\ s^{-1}$)	$^{14}CO_2$ Fixation ($pmol\ cm^{-2}\ s^{-1}$)
10h in normal bathing solution which contained 0.5mM $NaHCO_3$, pH 8.8.	A*	25.35 ± 1.05	
	B*		58.37 ± 4.21
(i) 2h in normal bathing solution which contained 10mM MES-buffer, pH 5.0.	A*	25.13 ± 1.13	
(ii) 8h in normal bathing solution + 0.5mM $NaHCO_3$, pH 8.8.	B*		68.03 ± 4.29
(i) 2h in normal bathing solution + 10mM MES-buffer, pH 5.0	A+	7.01 ± 1.25	
(ii) 4h in 5.0mM NaCl + 0.2mM KCl, pH 5.75.			
(iii) 4h in 5.0mM NaCl + 0.2mM KCl + 0.5mM $NaHCO_3$, pH 8.8.	B+		64.28 ± 3.45

* A, represents the employment of normal bathing solution + 0.5mM $NaH^{14}CO_3$, pH 9.0;
B, normal bathing solution + 0.5mM $NaH^{14}CO_3$ + 5mM MES-buffer, pH 5.3.

\+ Both A and B as above except that the bathing solution did not contain Ca^{++}.

TABLE 9.2

Influence of 10 and 20mM K^+ on Cyclosis

K^+ Concentration (mM)*			
10		20	
Exposure time (h)	Streaming Rate** ($\mu m\ s^{-1}$)	Exposure time (h)	Streaming Rate ($\mu m\ s^{-1}$)
0	68.7 ± 1.13	0	68.2 ± 1.7
0.25	70.9 ± 1.1	-	
0.50	67.3 ± 1.0	-	
1.0	66.9 ± 2.3	1.0	59.5 ± 3.8
2.25	68.2 ± 1.7	2.25	46.3 ± 3.2
4.25	66.3 ± 2.8	-	
6.5	64.5 ± 2.9	-	
48	70.20± 7.8	48	(all cells dead)
72	64.10 ± 2.8		
140	70.62 ± 2.2 (1 cell dead)		

* The experimental solution contained, in addition to the 10 or 20mM KCl, 0.5mM $NaHCO_3$, pH 8.8. The solutions were prepared and changed twice daily.

** Ten cells were used per treatment.

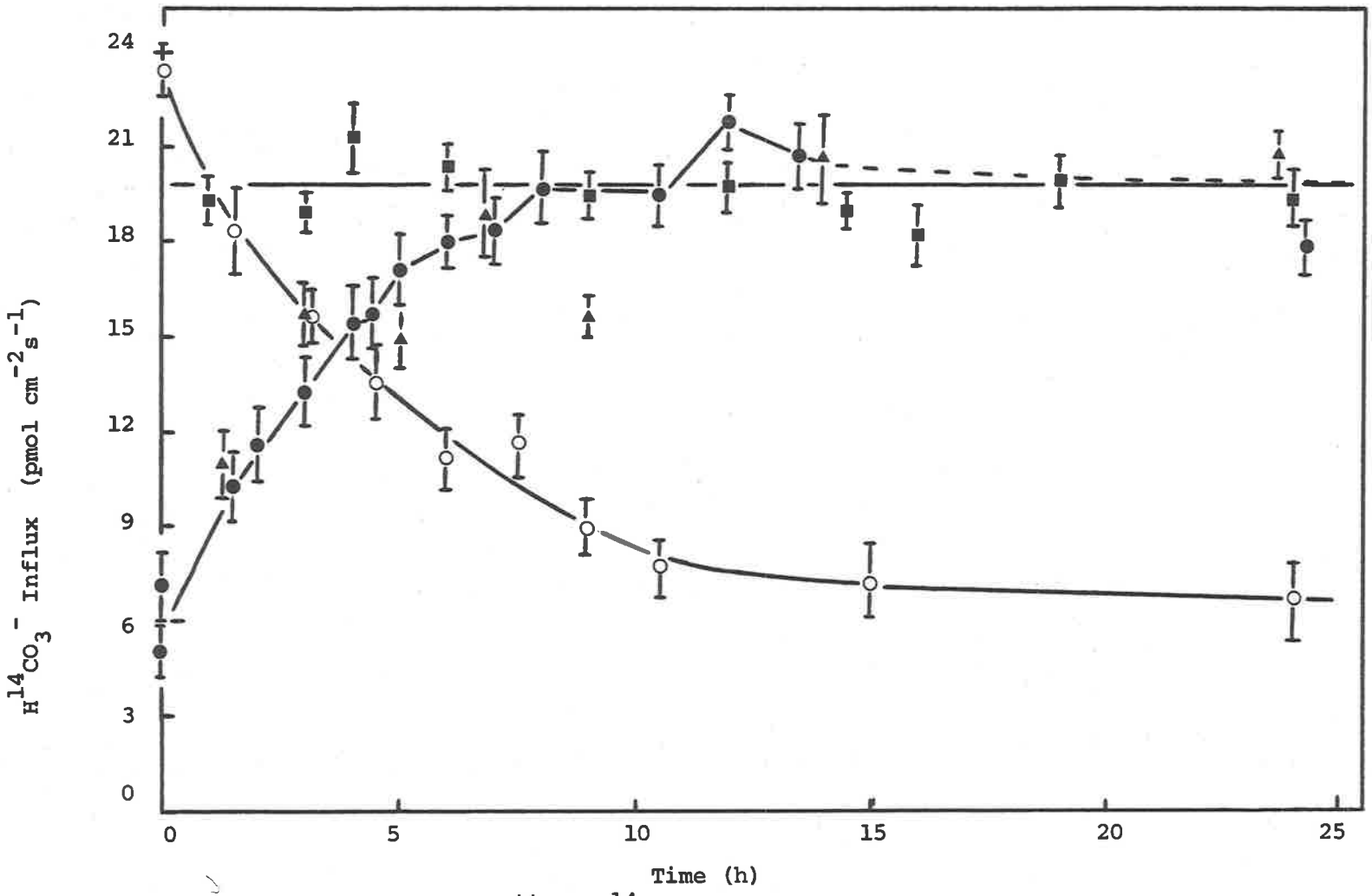

Figure 9.1. Influence of Ca^{++} on $H^{14}CO_3^-$ Influx. See text for full details of experimental treatments. The influence of exposure to Ca^{++}-free solutions is represented by the symbol (○); while (■) is the control treatment. The recovery of $H^{14}CO_3^-$ influx capacity following a 12h Ca^{++}-free exposure is shown by (●) (light) and (▲) (dark). The dark treatments were given a 30 min light pretreatment before exposure to $H^{14}CO_3^-$ solutions.

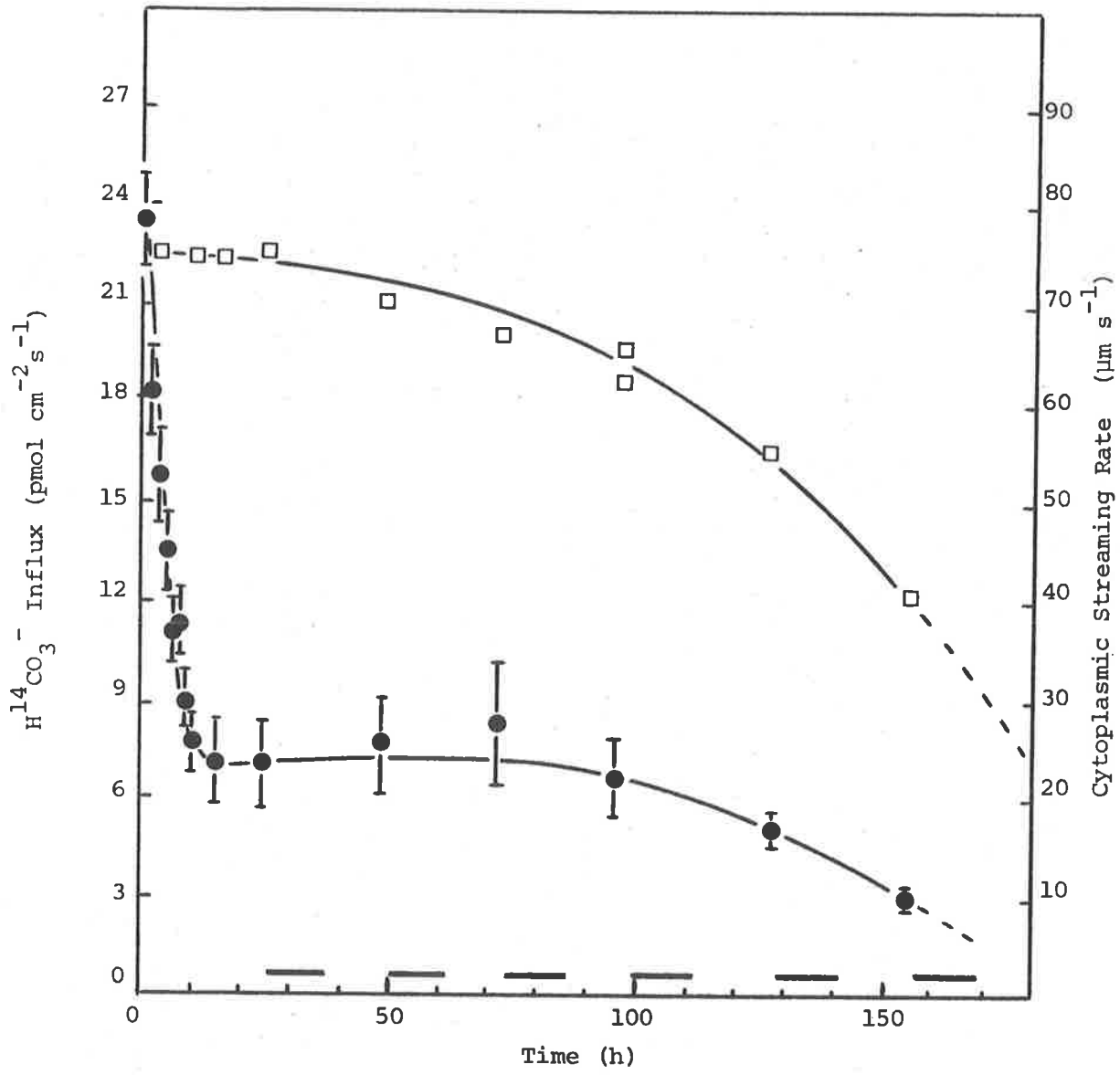

Figure 9.2. Effect on $H^{14}CO_3^-$ Influx and Cyclosis of Prolonged Exposure to Ca^{++}-free solutions. The experimental details are as for Figure 9.1, the solid bars along the abscissa indicate the employment of dark periods. The symbols are (●), $H^{14}CO_3^-$ influx; (□), cytoplasmic streaming rate. The S.E.M. for the cytoplasmic streaming rate was approximately ±1.5 µm s^{-1} for all treatments; this value was too small for inclusion on the individual experimental points.

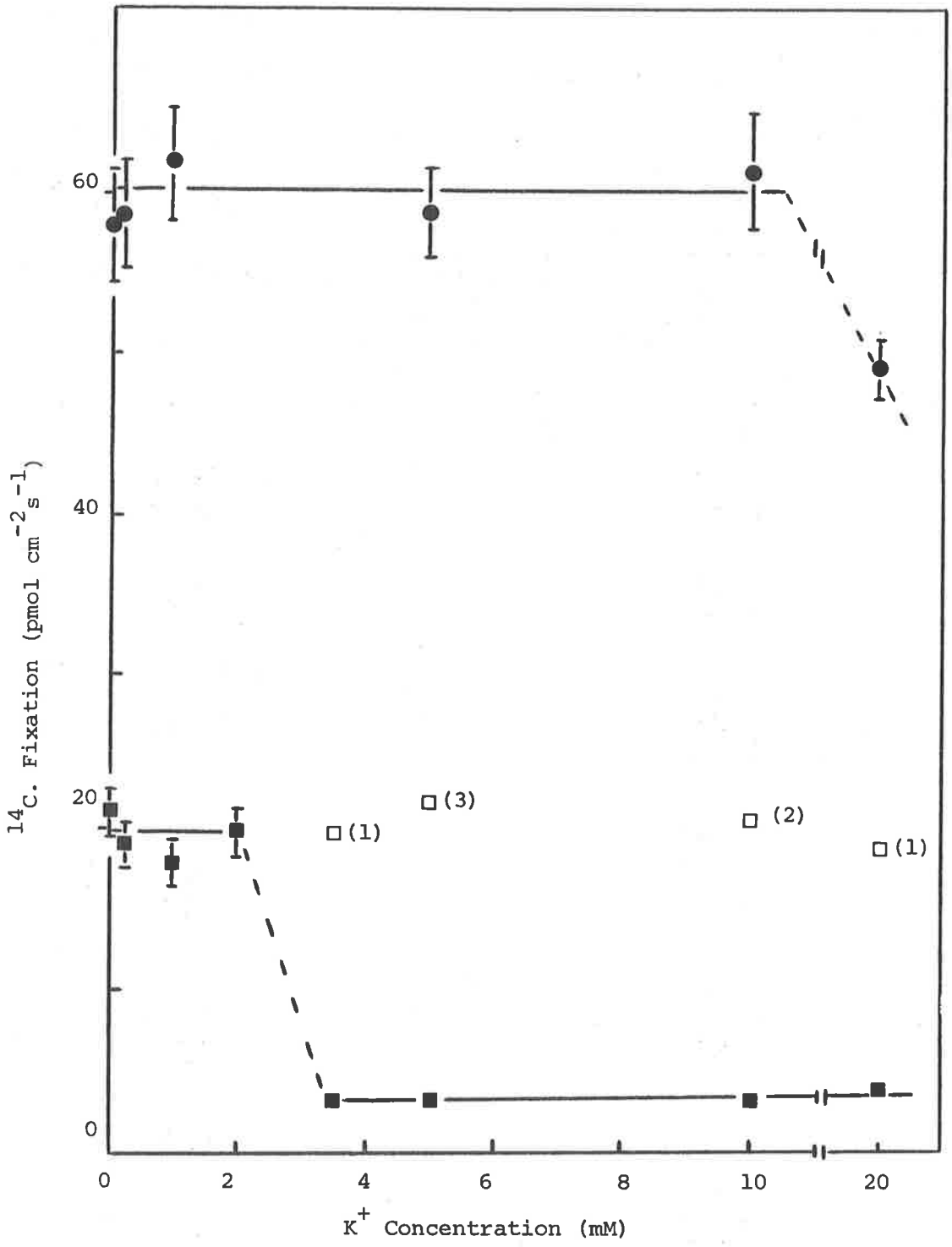

Figure 9.3. The Influence of K^+ concentration on ^{14}C. Fixation. The experimental solutions all contained 0.5mM $NaHCO_3$; (■) and (□) treatments were conducted at pH 9.0; (●), at pH 5.3 and at this pH value the solution was buffered by 5mM MES. The $[K^+]$ was increased by adding KCl to obtain the required concentration. The symbol (□) represents experimental values which deviated significantly from the mean obtained for the particular treatment and the value in parenthesis indicates the number of cells.

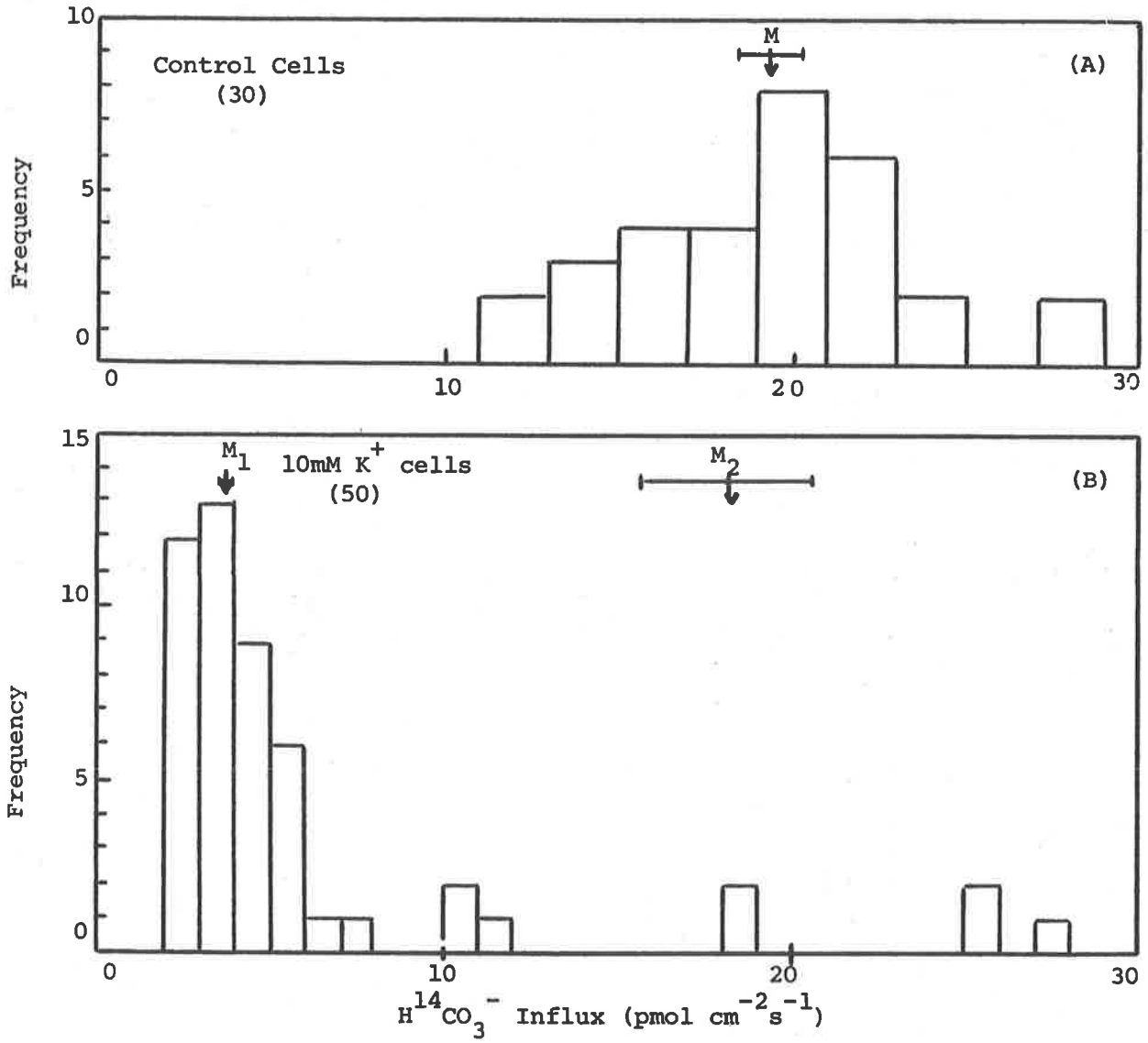

Figure 9.4. Histogram of the $H^{14}CO_3^-$ Influx Values obtained in the Presence and Absence of 10mM K^+. The control treatment (30 cells) was normal solution + 0.5mM $NaHCO_3$, pH 9.0; the 10mM K^+ cells were bathed in an identical solution except that it contained 10mM KCl. The symbol M and the accompanying arrow indicate the mean and the error bar is the associated S.E.M. In Fig. 2B, 4, M_1 is the mean calculated by including only values $\leq$ 8pmol $cm^{-2}s^{-1}$; and M_2 is the mean for $H^{14}CO_3^-$ influx values $\geq$ 8pmol $cm^{-2}s^{-1}$.

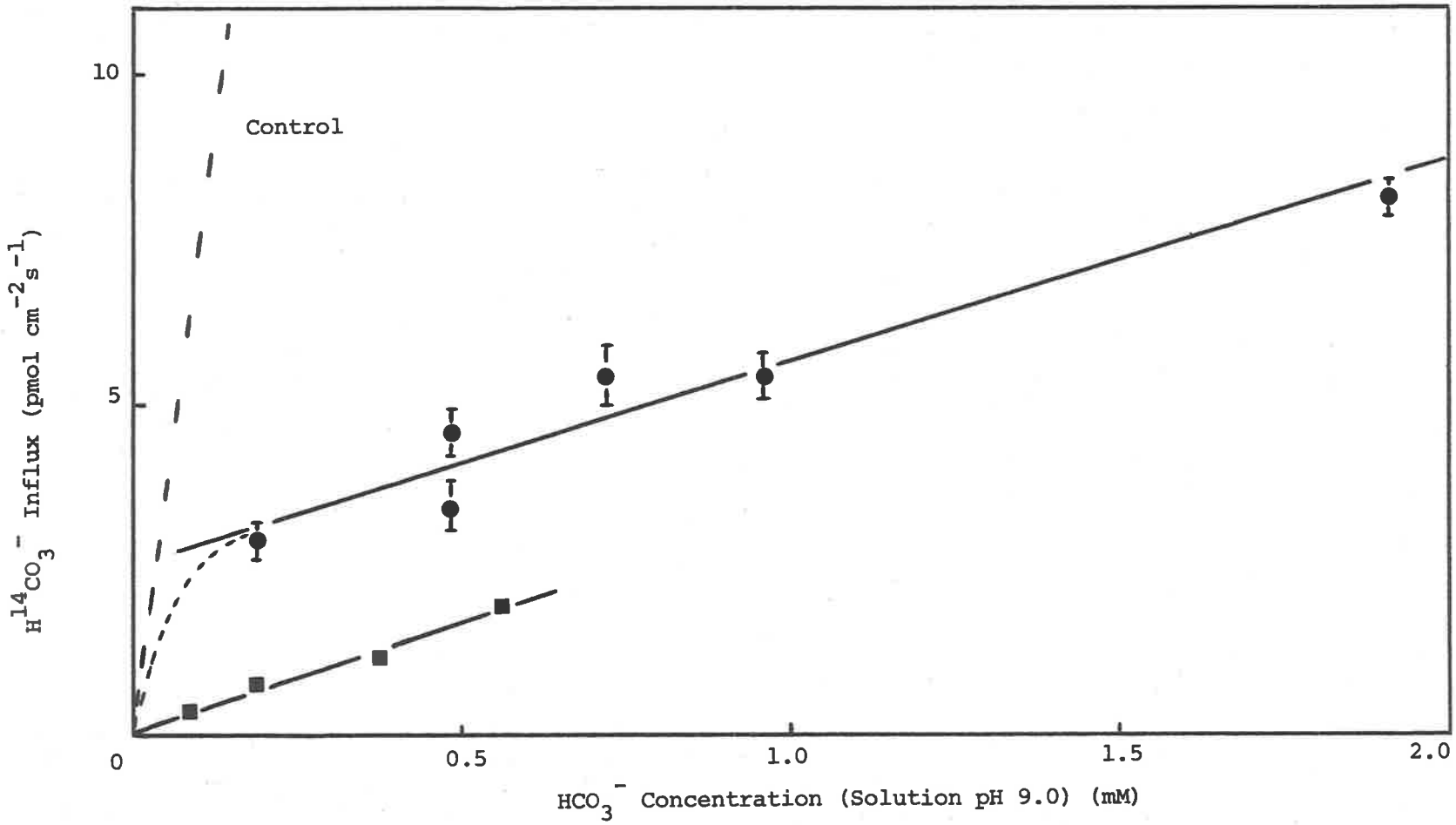

Figure 9.5. The Effect of Increasing $[HCO_3^-]$ in the Presence of 10mM K^+. Culture tank XG-2 cells were employed for these experiments and the normal $H^{14}CO_3^-$ procedures were followed; the initial pH value was 9.0. The symbol (●) represents the 10mM K^+ treatments, (■) represents $H^{14}CO_3^-$ influx in the presence of 0.3mM $(NH_4)_2SO_4$ and 0.2mM K^+.

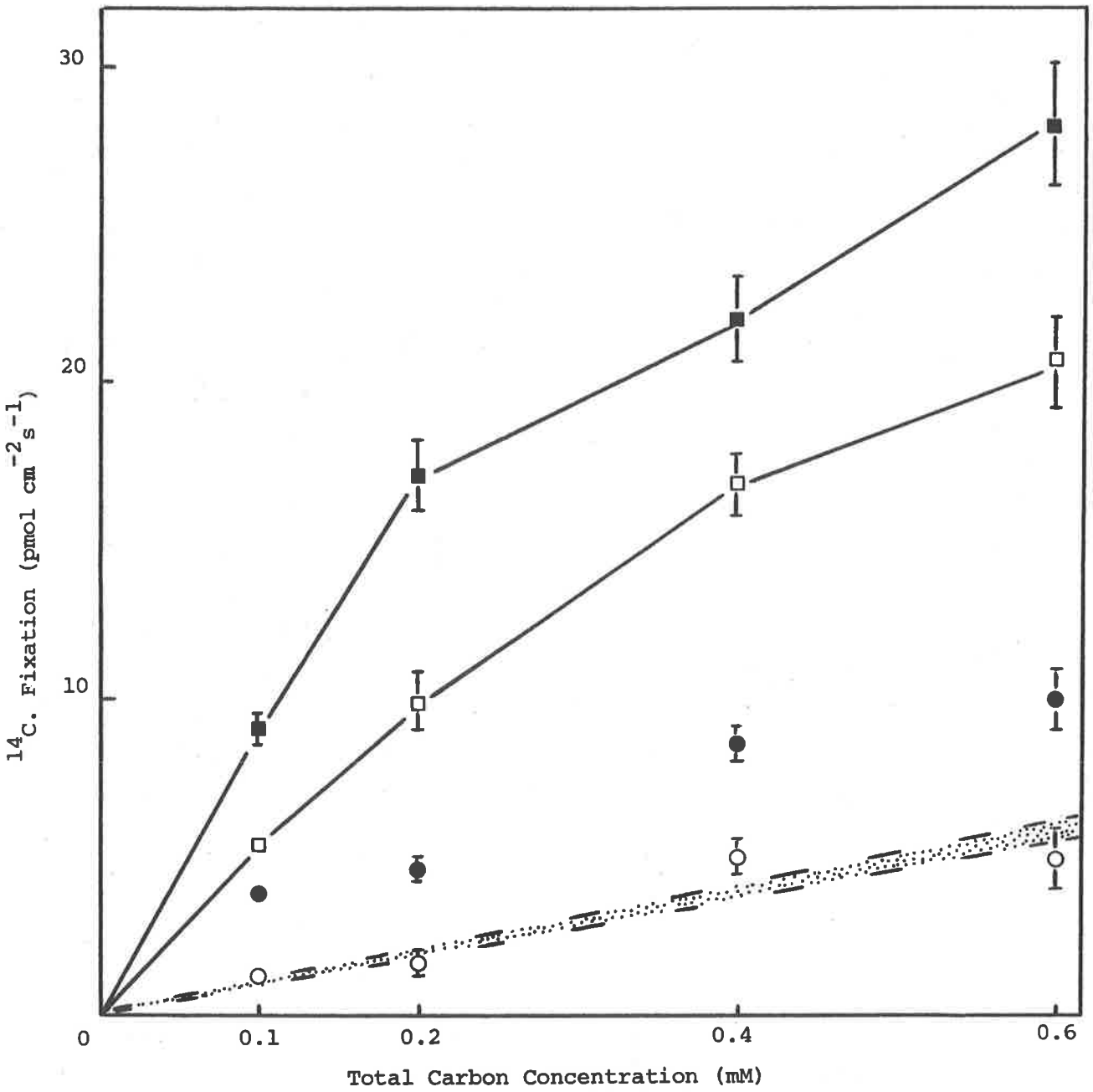

Figure 9.6. Influence of 10mM K^+ on ^{14}C. fixation at pH 7.5. Symbols are as follows: (■), control treatments; (●) ^{14}C. fixation in the presence of 10mM K^+; (○) values corrected for $H^{14}CO_3^-$ influence using data presented in Figure 9.5, (□), ^{14}C. fixation in the presence of 0.3mM $(NH_4)_2SO_4$. (These values are reproduced from Table 8.3). The stippled region represents the estimated $^{14}CO_2$ contribution at this pH value and was determined using Figure 3.2.

CHAPTER TEN

PRELIMINARY ELECTRICAL STUDIES.

Introduction

Most of the biophysical studies on the Characeae have been conducted on relatively young internodal cells. However, as noted in Chapter Two, mature internodal cells were employed for all experiments reported in this dissertation. A brief investigation of the electrical properties of these mature cells was conducted to determine whether both cell types respond similarly to pH changes in the external solution. Simultaneous measurements of membrane potential (Ψ_{vo}), membrane conductance(g_{vo}) and $H^{14}CO_3^-$ influx, at pH 9.2, were also made to ascertain whether the insertion of microelectrodes affected cellular assimilation of $H^{14}CO_3^-$.

Methods

The electrophysiological studies reported in this chapter were performed in the laboratory of Professor A.B. Hope (Flinders University, South Australia). The apparatus and techniques used for measuring Ψ_{vo} and g_{vo} were similar to those previously described by Findlay and Hope (1964) and Hogg, Williams and Johnston (1968).

During electrode insertion (tip diameter 0.5 - 0.8μm) cells were bathed in normal bathing solution (flowing) and a 30 min. recovery period was employed before making external pH changes. A 0.5mM concentration of $NaHCO_3$ was used both as a supply of exogenous carbon and as a buffer for the external solutions whose pH values ranged from 6.3 to 11.0. (Solutions were titrated to the required pH values using either 100mM NaOH or H_2SO_4). Following exposure to an external pH value within this range, cells were

always pretreated for 30 min in normal bathing solution (pH 5.75) prior to the investigation of a different pH value (see Spanswick, 1972).

Resistances were measured using a 3 second current pulse (0.1 - 0.4 μA) passed between a microelectrode inserted into the cell (at ℓ where 2ℓ is the length of the cell) and an external Ag - AgCl electrode. (The latter was positioned close to the cell surface and extended, in a parallel manner, along its entire length). The change in Ψ_{vo} caused by the current pulse was measured between a reference electrode in the bathing solution and a microelectrode which was inserted into the vacuole at a point 0.42ℓ from the centre of the cell. All potentials, and changes in potential elicited by current pulses, were recorded using a Rikadenki multi-pen recorder.

Results and Discussion

Effect of External pH on Ψ_{vo}

Typical responses of Ψ_{vo} to changes in the pH value of the external solution are shown in Figures 10.1 and 10.2. The results of these experiments are summarized in Figure 10.3, and for comparative purposes the steady Ψ_{vo} values obtained by Richards and Hope (1974) have been included. (The E_{K^+} value, i.e. the Nernst diffusion potential for K^+, was determined using the 10mM K^+ technique of Spanswick (1972)). The time-courses of Ψ_{vo} hyperpolarization in response to external pH changes were similar in form to those reported by Saito and Senda (1973a). However, these workers did not investigate the effect of external pH values above 9.0. Figure 10.2 shows that at pH values above 9.7 the membrane potential still hyperpolarized, but the decay in Ψ_{vo} following the attainment of the maximum hyperpolarization value was much more rapid. The potential appeared to return to a value close

to that which existed when the cell was bathed in normal solution, pH 5.75.

Reasonable agreement was also found between the Ψ_{vo} data of Richards and Hope (1974) and the results presented in Figure 10.3. This suggested that the plasmalemma of mature internodal cells and the cells used by Richards and Hope respond in a similar manner with respect to the response of Ψ_{vo} to external pH changes. A comparison with Kishimoto's (1959) earlier work on *C. corallina* indicated that the relationships between Ψ_{vo} and external pH were similar in form, but Kishimoto's data were displaced approximately one pH unit towards the lower end of the pH scale.

Differences appear to exist between cells of *C. corallina* and *N. translucens* in terms of the overall membrane potential response to external pH changes. It appeared that the maximum hyperpolarization value of Ψ_{vo}, for *C. corallina* cells, was always more negative at any particular pH value, compared with the value observed for *N. translucens* (cf. Spanswick, 1972, Fig. 2). A similar situation holds for the steady hyperpolarized value of Ψ_{vo}. It was also found that over the pH range investigated, Ψ_{vo} for *C. corallina* was always more negative than E_{K^+}. It would seem, therefore, that an electrogenic component of potential was present over this pH range 5.75 - 11.0 (cf. Spanswick, 1972, Figs. 2 and 6). These differences add weight to the earlier warning that *C. corallina* may differ from other Characean species in certain physiological aspects (see Chapter One, p. 16).

Simultaneous Measurement of Ψ_{vo}, g_{vo} and $H^{14}CO_3^-$ Influx

A series of experiments were performed in which Ψ_{vo}, g_{vo} and the influx of $H^{14}CO_3^-$ were determined simultaneously. During these experiments cells were given a 1h recovery period in normal bathing solution following electrode insertion. The membrane

potential was monitored continuously during this period, and at its conclusion membrane resistances were measured. A 30 min exposure period to non-radioactive bathing solution (0.5mM $NaHCO_3$, pH 9.2) was used to facilitate the establishment of steady hyperpolarized potentials prior to the commencement of $H^{14}CO_3^-$ experiments. (The electrical resistance was measured at 3 min intervals over both the 30 min pre-radioactive and 1h $H^{14}CO_3^-$ periods). Control $H^{14}CO_3^-$ influx values were obtained using the same experimental system except that cells did not have microelectrodes inserted.

The values of Ψ_{vo}, g_{vo} and $H^{14}CO_3^-$ influx obtained during these experiments are presented in Table 10.1. The most significant feature of these results was the identical $H^{14}CO_3^-$ influx values obtained for the control and electrode-inserted cells. It was assumed that this indicated cellular assimilation of $H^{14}CO_3^-$ was not affected by the insertion or presence of microelectrodes. The other point of interest was that the mean g_{vo} value of 106.3 ± 9.6 $\mu mho\ cm^{-2}$, obtained in unbuffered solutions (pH 5.75) was in accord with the g_{vo} value reported by Doughty and Hope (1973) and Richards and Hope (1974). However, the mean conductance value obtained at pH 9.2 appeared to be considerably higher than would have been predicted on the basis of the data presented by Richards and Hope (1974, Fig. 2). This higher g_{vo} value may have been associated with the observed influx of HCO_3^- and concomitant OH^- efflux. Since there was not a close correlation between individual g_{vo} and HCO_3^- influx values (for example compare the results of cell nos. 3, 4 and 5) further studies are required to test this relationship. Unfortunately there is not at present a satisfactory relationship between the theory of membrane permeability to ions and the experimentally measured conductance values.

Calculation of P_{OH^-}

Hydroxyl efflux appears to occur down its own electrochemical potential gradient, and it could be argued, therefore, that the efflux of this ion is passive. Although the Goldman (1943) flux equations and equation (1.3) do not express correctly the electrical properties of the plasmalemma, the efflux equation:

$$\overleftarrow{J_j} = Z_j P_j \frac{F\Psi_{co}}{RT} \frac{C^c_j \, e^{Z_j F \Psi_{co}/RT}}{e^{Z_j F \Psi_{co}/RT} - 1} \qquad \ldots.(10.1)$$

was used to calculate P_{OH^-}, so that its value could be compared with other permeability coefficients reported in the literature. The values of $J^{\leftarrow}_{OH^-}$ were calculated on the basis of the individual OH^- band efflux data presented in Table 4.5. The assumption was made that the value of Ψ_{co} obtained during the electrical studies could be extended to the diffusion analysis situation. The mean average pH value over the entire surface area was estimated to be 9.7 and using this figure, a value of -185mV for Ψ_{co} was estimated from Figure 10.3 ($\Psi_{co} = \Psi_{vo}$ - 10mV; see for example Findlay and Hope, 1964; or Doughty and Hope, 1973). The cytoplasmic pH value was assumed to be 8.4 on the basis of the results obtained by Walker and Smith (1974 and unpublished results).

The experimental OH^- efflux values and the individual computed P_{OH^-} values are given in Table 10.2. The average value of 1.44 x 10^{-2} cm s^{-1} obtained for P_{OH^-} is extremely large when compared with say the value of 1 x 10^{-9} - 1 x 10^{-14} cm s^{-1} obtained for P_{Cl^-} (Findlay and Hope, 1964; Hope, Simpson and Walker, 1966; Kitasato, 1968; Doughty and Hope, 1973; Richards and Hope, 1974).

Very little weight can be placed on this large value of P_{OH^-}, since the use of equation (10.1) is probably quite unjustified. However, the large P_{OH^-} value may imply that OH^- ions are effluxed via carriers and the possibility exists that these carriers require metabolic energy (see for example Dainty (1963), and also Raven (1968a) concerning his conclusions relating to his value of 1.0×10^{-4} cm s^{-1} for $P_{HCO_3^-}$ in *H. africanum*). The Characean permeability coefficient for water has been measured, and a value of 1.4×10^{-2} cm s^{-1} obtained (Dainty and Hope, 1959a; Dainty and Ginzburg, 1964). The similarity between the values of P_{OH^-} and P_{H_2O} is suggestive of a common pathway across the plasmalemma for OH^- (or $H_3O_2^-$) ions and H_2O molecules. However, it is more likely that the similarity is fortuitous. It would certainly be difficult to explain the localized nature of the OH^- efflux sites if a common pathway, via water filled pores, was proposed. There is one much more important property of the total OH^- efflux system which suggests that the efflux of OH^- ions occurs via a much more complex membrane carrier system, namely the observed hierarchy of OH^- efflux function (i.e. primary and subsidiary bands).

TABLE 10.1.

Simultaneous Measurement of Ψ_{vo}, g_{vo} and $H^{14}CO_3^-$ Influx

Cell No.	Ψ_{vo} (mV)			g_{vo} (μ mho cm^{-2})			$H^{14}CO_3^-$ Influx (pmol $cm^{-2}s^{-1}$)	Control $H^{14}CO_3^-$ Influx (pmol $cm^{-2}s^{-1}$)
	A	B	C	A	B	C		
1	-164	-173	-167	92.4	177.9	204.1	29.5	18.2
2	-170	-178	-164	102.7	128.4	177.6	17.9	24.0
3	-160	-170	-155	79.4	155.4	168.6	35.1	25.2
4	-174	-178	-165	75.2	135.1	165.8	12.7	24.6
5	-169	-175	-168	198.1	252.5	270.3	23.4	23.8
6	-170	-178	-178	152.7	175.1	186.3	24.0	19.9
7	-140	-175	-168	87.7	207.5	208.3	25.7	24.2
8	-174	-166	-165	88.0	263.2	277.8	24.0	20.9
9	-154	-180	-175	86.9	147.7	138.9	21.9	22.5
10	-160	-187	-182	65.4	149.3	149.0	15.8	
11	-162	-175	-174	70.9	179.5	172.1	15.4	
12	-160	-194	-189	126.9	250.0	250.0	22.8	
13	-173	-215	-208	90.4	110.9	116.9	15.7	
14	-144	-179	-176	139.3	223.2	222.2	29.2	
15	-145	-168	-169	139.1	190.1	185.2	28.5	
Mean ± S.E.M.	-161.3 ± 2.9	-179.4 ± 3.1	-173.3 ± 3.3	106.3 ± 9.6	183.1 ± 12.3	192.9 ± 12.0	22.8 ± 1.6	22.6 ± 0.8

A, steady value 1h after insertion of electrodes (normal bathing solution).

B, steady value after 30 min exposure to 0.5mM $NaHCO_3$, pH 9.2.

C, steady value at conclusion of 1h $H^{14}CO_3^-$ experiment.

TABLE 10.2.

P_{OH^-}: Calculated on the Basis of Individual OH^- Efflux Band Data

Expt.* No.	Band* No.	OH^--Band Width (cm)	OH^--Band Efflux Area ($cm^2 \times 10^2$)	Q_t* (pmol s^{-1})	Q_t/Efflux Area (pmol $cm^{-2} s^{-1}$)	P_{OH^-} (cm $s^{-1} \times 10^2$)
16	A	0.03	0.84	2.15	257.0	1.42
	B	0.05	1.39	4.54	325.7	1.79
	C	0.05	1.39	5.35	383.8	2.12
18	A	0.06	1.67	5.13	306.6	1.69
	B	0.03	0.84	1.39	166.2	0.92
	C	0.03	0.84	1.49	178.2	0.98
	D	0.03	0.84	1.92	229.5	1.27
	E	0.06	1.67	2.67	159.6	0.88
20	A	0.04	1.16	2.72	234.0	1.29
	B	0.06	1.74	5.95	341.3	1.88
	C	0.05	1.45	4.60	316.6	1.75
	D	0.06	1.74	3.99	228.8	1.26
						Av 1.44 ± 0.12

* Experimental values obtained from Table 4.5

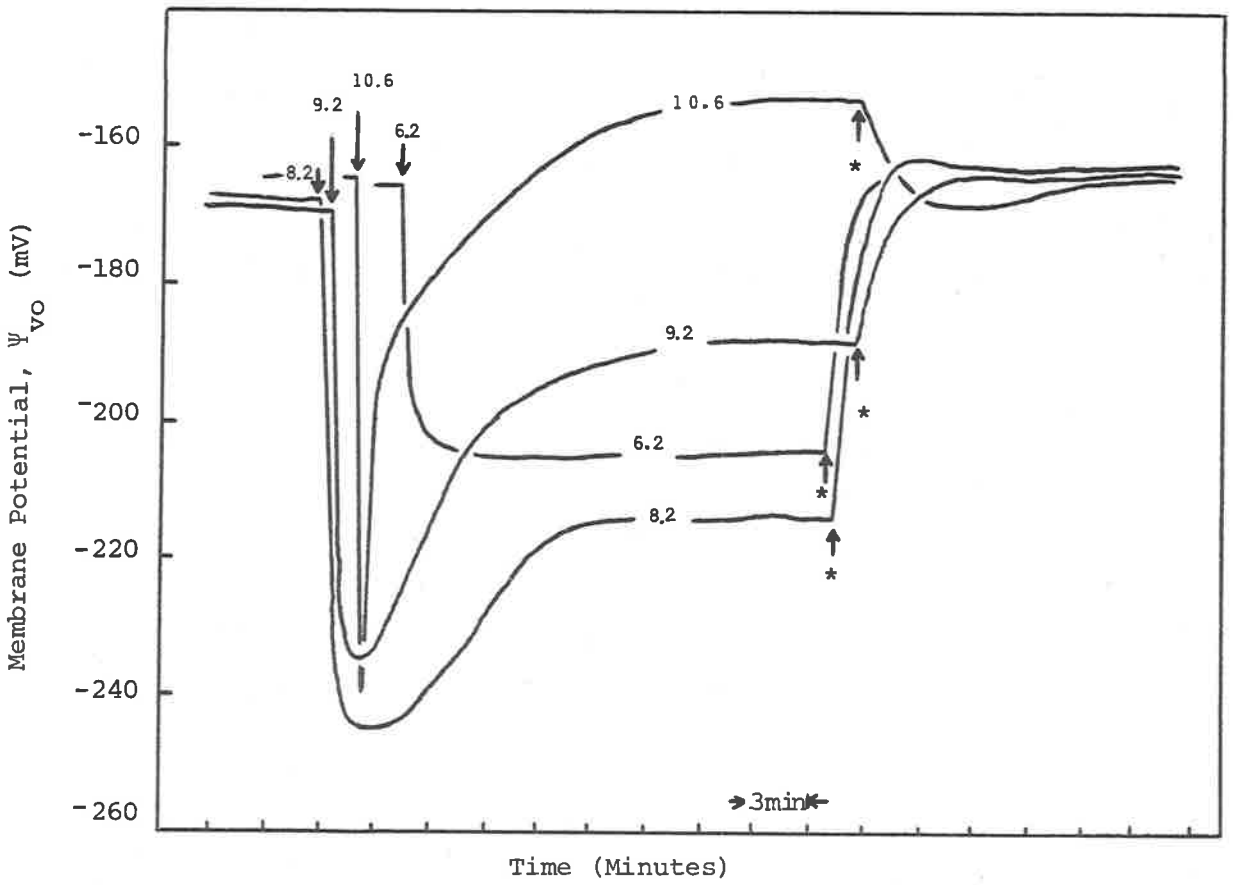

Figure 10.1. The effect on Ψ_{vo} of a change in external pH from normal bathing solution to a solution containing 0.5mM $NaHCO_3$, titrated to the specified pH value. The symbol (*), represents the return to normal bathing solution, pH 5.75. A light intensity of 14Wm^{-2} was employed for all experiments.

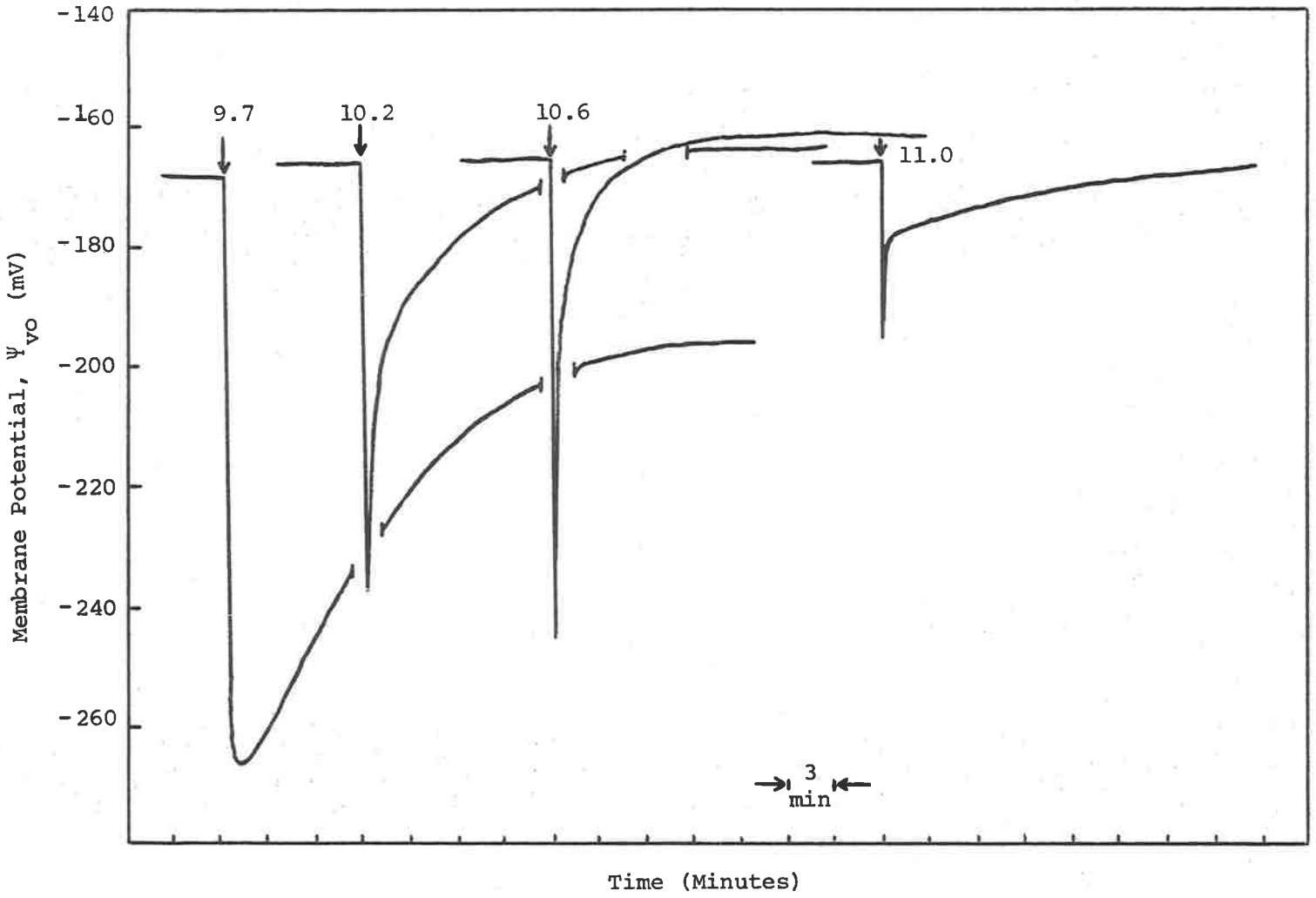

Figure 10.2. The effect on Ψ_{vo} of a change in external pH. Experimental details as for Figure 10.1.

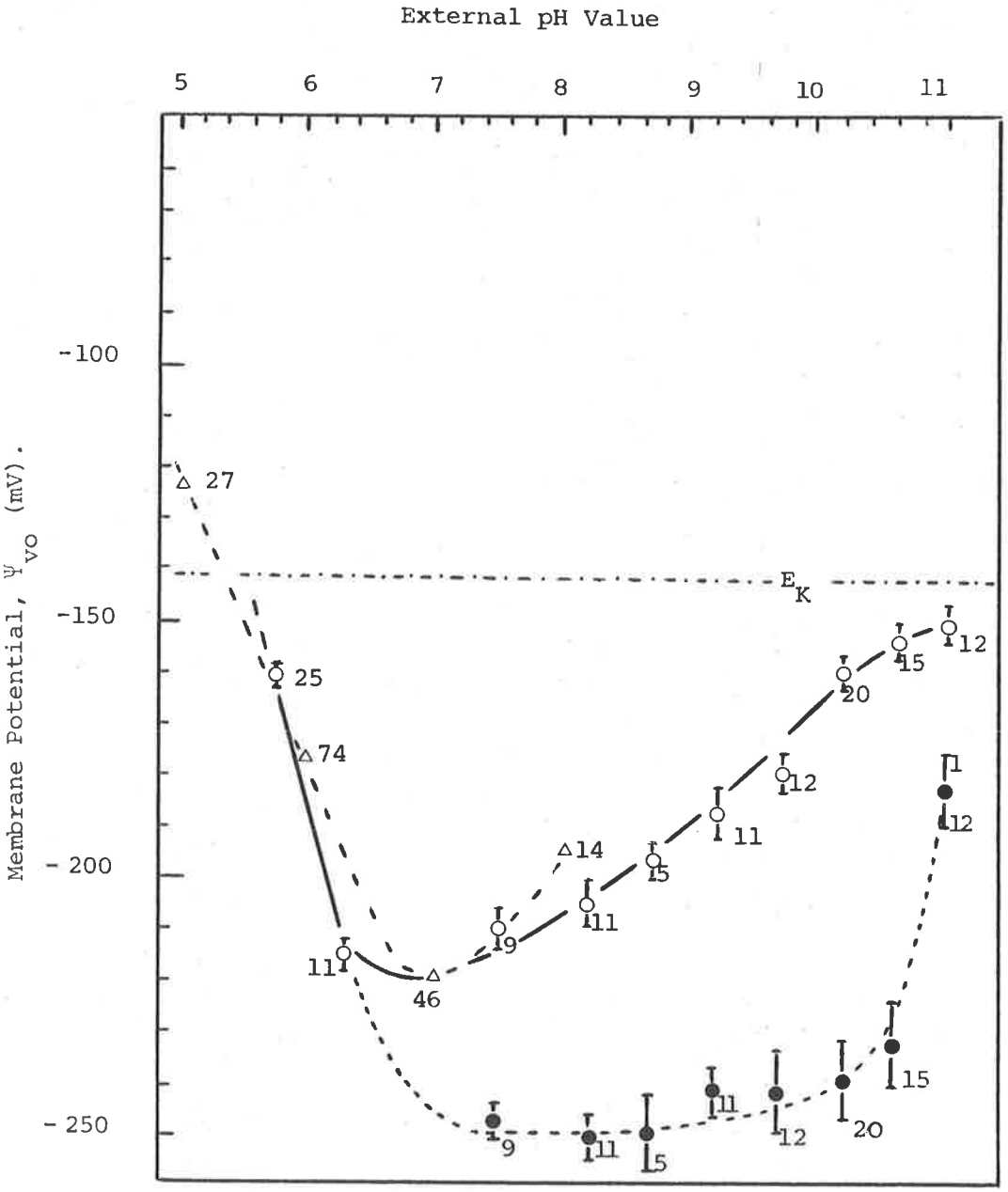

Figure 10.3. Ψ_{vo} as a function of the external pH value. The symbols are; (○); steady potential; (●), maximum hyperpolarized value, (△), steady potential values of Richards and Hope (1974); E_K, the Nernst diffusion potential for K^+; the numerals represent the number of cells used to obtain the mean ±S.E.M. at each pH value.

CHAPTER ELEVEN

CONCLUSIONS AND FUTURE WORK.

The properties of the plasmalemma bound HCO_3^-, OH^- and H^+ transport systems were studied using two different approaches. The activity of the HCO_3^- system was quantified using ^{14}C, while the net activity of the H^+ and OH^- systems were measured by analysing their diffusion profiles. These results indicated that, at pH values above 7.0, HCO_3^- influx and OH^- efflux rates were equivalent. Since it was shown that these two systems (i.e. the HCO_3^- and OH^-) can operate independently, in that they can function at spatially separate sites in the membrane, it follows that their rates need not always be equivalent. Under low external pH values (5.0 - 5.7) HCO_3^- influx and internal OH^- generation will be low (in the absence of added $NaHCO_3$). Under these conditions the efflux of OH^- ions may be less than the HCO_3^- influx value, because the majority of the OH^- ions may be neutralized by passive H^+ influx. In this case, the H^+ efflux system may serve as the main cytoplasmic pH regulating mechanism. However, it is likely that the H^+ fluxes are not as high as has been previously proposed.

When the bathing solution contains exogenous HCO_3^- and its pH value is at least one pH unit above the pKa of H_2CO_3 (i.e. 7.3), the role of cytoplasmic pH regulation may be transferred completely to the OH^- efflux system. This would mean that net H^+ efflux should decrease as the pH value is increased above pH 6.3; becoming extremely small (or zero) at pH 7.3 . The results presented in Chapter Four indicated that the net H^+ efflux rate appeared to decline over this same pH range.

At the higher external pH range of 9.5 - 11.0, where it was found that $H^{14}CO_3^-$ influx was inhibited, the OH^- efflux system may still be required to maintain the cytoplasmic pH value to within physiological limits. Thus, although HCO_3^- influx cannot occur at pH 10.5 - 11.0, there may be a small passive influx of OH^- ions which is balanced by the OH^- efflux system.

Assuming this proposal of a dual cytoplasmic pH regulating mechanism (i.e. H^+ and OH^-) to be valid, it is obvious that Spanswick's (1972) equivalent circuit needs to be expanded at least for *Chara corallina* cells. The following equivalent circuit may more accurately depict the situation for illuminated *C. corallina* cells:

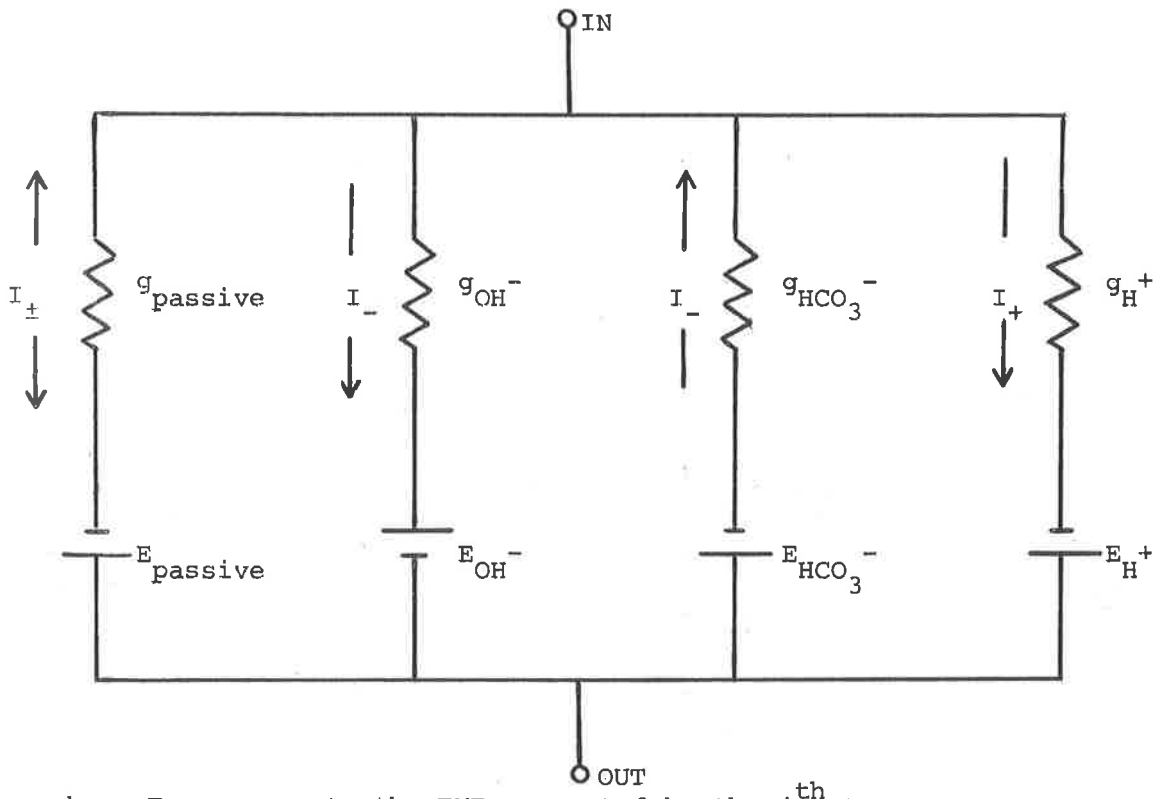

where E_j represents the EMF generated by the j^{th} transport system, and E passive is the passive diffusion potential given by equation (1.3), $I_\pm$ is the current passing through the respective system and g_j is the conductance of the j^{th} transport system. In this model it is assumed that HCO_3^- influx is active (see Chapter Three) and

that metabolic energy is required for the functioning of the carrier system. Efflux of OH^- is also considered to be mediated by carriers which are controlled by metabolism. (The P_{OH^-} value and the hierarchy of OH^- efflux bands suggests that this is the case, even though the OH^- ion is moving down its own electrochemical potential gradient).

When the membrane potential of the illuminated cell is in the steady state, at any particular external pH value, the total resistance of the mixed equivalent circuit can be expressed as:

$$\frac{1}{R_{Total}} = \sum_j \frac{1}{R_j} = \frac{1}{R_{H^+}} + \frac{1}{R_{HCO_3^-}} + \frac{1}{R_{OH^-}} + \frac{1}{R_{passive}} \quad ...(11.1)$$

Since conductance is defined as $\frac{1}{R_j}$, the total conductance can be expressed as:

$$g_{Total} = \sum_j g_j = g_{H^+} + g_{HCO_3^-} + g_{OH^-} + g_{passive} \quad ...(11.2)$$

For a steady state membrane potential, the net current movement across the membrane must be zero, but in contrast to Spanswick's model, an equivalent current does not have to pass through each component of the circuit, Thus,

$$I_{net\ (steady\ potential)} = \sum_j I_j = 0, \quad ...(11.3)$$

but it may be that

$$I_{H^+} \neq I_{HCO_3^-} \neq I_{OH^-} \neq I_{passive} \quad ...(11.4)$$

In the steady state, the following general condition should hold:

Measured potential difference =

$$E_{H^+} - \frac{I_{H^+}}{g_{H^+}} = E_{HCO_3^-} - \frac{I_{HCO_3^-}}{g_{HCO_3^-}} = E_{OH^-} + \frac{I_{OH^-}}{g_{OH^-}} = E_{passive} + \frac{I_{passive}}{g_{passive}} \quad ...(11.5)$$

From (11.5) it is clear that the characteristics of the individual components of the system must be known before the observed electrical properties of the plasmalemma can be accounted for on the basis of the contribution made by each component. On a speculative note, based on the hypothetical models propounded by Finkelstein (1964) and Rapoport (1970), it is possible that:

(a) The potential generated by each component may be a function of;

  (i) conductance of the system, particularly the model(s) by which charge is transported across the membrane,

  (ii) metabolic energy available to that particular transport system,

  (iii) the equilibrium constants of associated reactions and,

  (iv) the actual rate of the "electrogenic" driving reaction.

(b) The conductance of each component may be a function of:

  (i) the physio-chemical properties of the transport system, for example the mobility of the putative carriers etc,

  (ii) the concentration of functional carriers, which will probably be related to metabolism,

  (iii) the influence of the external solution on the functional properties of the transport system as a unit; it is likely that the pH value, and the K^{+} and Ca^{++} concentrations will be significant in this respect. (On an extremely speculative note, it could be that a certain set of external conditions results in the isolation of a particular transport system from the outer solution, i.e. in electrical circuit terminology, the component would become open-circuited).

On the basis of these suggestions, it is possible to propose a working hypothesis to account for the as yet unexplained, plasmalemma electrical response, observed at high pH values. The high conductivity, of *Chara corallina*, observed at pH 8.0 - 9.0 (Walker, 1962, 1963; Coster, 1969; Richards and Hope, 1974), may be associated with the HCO_3^- and OH^- systems. At this pH value (11.2) may reduce to:

$$g_{Total} = g_{HCO_3^-} + g_{OH^-} \qquad \ldots(11.6)$$

The reduction of g_{H^+} to zero may be related to (b) (ii) and / or (iii) in that competition for metabolic energy may exist between the H^+ and OH^- efflux systems. The actual balance between the competing species may be affected by the external pH value; this would, in essence, provide a "feed-back" system between the external solution and (a) (iv) above.

The hyperpolarization and subsequent depolarization of Ψ_{vo} observed when *Chara* cells, bathed in solutions of high pH, are illuminated, may also be due to the HCO_3^- and OH^- systems. If the HCO_3^- system begins operation, following illumination, in a shorter period than the OH^- system, the membrane potential will become hyperpolarized due to the net transport of negative charge (HCO_3^-) into the cell. (It should be stressed that the membrane potential will only hyperpolarize if $g_{passive}$ is small). Once the OH^- system becomes activated, the net transport of charge will be reduced and if the OH^- efflux rate exceeds the HCO_3^- influx rate, the membrane potential will depolarize. If the steady state potential at high pH values (7.0 - 10.0) is determined primarily by the HCO_3^- and OH^- systems, $I_{HCO_3^-}$ will have to be equal and opposite in sign to I_{OH^-}. Hence the actual value of the potential may be determined primarily by the values of $g_{HCO_3^-}$, and g_{OH^-}, which need not be equal.

Similarly the rapid hyperpolarization and subsequent depolarization of Ψ_{vo}, observed when the pH value of the bathing solution is changed from 5.8 to 7.5 - 10.6 may result as a consequence of differences in the time-course of approach towards the operational steady state of the HCO_3^- and OH^- systems (see for example Figures 10.1 and 10.2).

At this point it should be stressed that it is probable that not all Characean species can assimilate exogenous HCO_3^- at the rates observed for *Chara corallina*. Smith (1968a) showed that there was a significant difference between the $H^{14}CO_3^-$ assimilation rates of collected and cultured cells of *Nitella translucens*. There may therefore be cells, grown under a particular physiological set of conditions, whose membrane electrical properties are not significantly affected by exogenous HCO_3^-. It is important, therefore, to stress the point raised by Volkov (1973), namely that cultured cells be grown under uniform conditions. Other Characean species which can assimilate HCO_3^-, and form alkaline bands, may have different OH^- and HCO_3^- activation time-courses. As a result their respective responses to illumination may vary in form, but their overall steady state electrical properties should be similar to those of *Chara corallina*. Studies, similar to those presented in this thesis, on all the Characean cells used for biophysical research would provide an extremely valuable basis for inter-species comparisons.

Suggestions for Future Work

Testing the HCO_3^-, OH^- Proposal

(a) Light Stimulation of the HCO_3^- and OH^- Systems

At a particular external pH value, and in the presence of a certain level of exogenous HCO_3^-, the time-course of OH^- activation can be measured using the experimental techniques

described in this thesis. Simultaneous time-course measurements of potential and conductance can also be obtained on the same cell. Using the continuous spherical surface source equation, for the non-steady state (Carslaw and Jaeger, 1959), it should be possible to derive the time dependent efflux of OH^- for the cell under examination.

Unfortunately it is not possible to measure the time-course of HCO_3^- influx on a single cell. Thus a sub-sample from a population of cells must be used, and if it can be shown that the population of cells is sufficiently uniform, comparisons can be made between the $H^{14}CO_3^-$, OH^-, potential and conductance time-courses; all of which were obtained under identical experimental conditions. If OH^- and HCO_3^- are making a significant contribution there should be a close correlation between the respective time-courses (cf. Nishizaki, 1963, 1968).

(b) Light Intensity Experiments

The results presented in Chapter Five suggest that it should be possible to discern the influence of OH^-, on the basis of parallel light intensity studies. The predictive ability of the derived mathematical relationship between the OH^- lag period and the light intensity, for an individual cell, can be employed. Together with the non-steady state spherical surface source equation, the two relationships can be used to predict the time-course of the light stimulated conductance change for a particular light intensity. This prediction can then be tested experimentally.

(c) Analogue Inhibition of HCO_3^- Influx

It is considered that if a suitable analogue for HCO_3^- can be found, experiments conducted in the presence and absence of this compound, on the same cell, will provide valuable information concerning the electrical involvement of the HCO_3^- system. This should form an interesting avenue for further research.

Final Conclusions.

The basic aim of this work was achieved, in that some of the major operational characteristics of the HCO_3^-, OH^- and H^+ transport systems in *Chara corallina* have been resolved. However, it is felt that the present study has probably provided only a glimpse into the complex functioning of the plasmalemma-bound transport systems. As pointed out above, these newly-identified systems will need to be fully resolved before a comprehensive electrical model of this membrane can be propounded.

APPENDIX A

POTENTIOMETRIC (pH) DETERMINATION OF HCO_3^- CONCENTRATION IN THE *CHARA* CULTURE TANKS

The Gran (1952) potentiometric technique for determining total carbon was employed to obtain an estimate of the natural HCO_3^- concentration in the *Chara* culture tanks. The technique employed was based largely on the work of Edmond (1970), and was as follows:

(i) A 50ml aliquot was withdrawn from a depth of 20cm below the solution surface of the culture tank.

(ii) The aliquot of culture tank water was pipetted, under a 1cm liquid paraffin seal, into a titrating vessel. The pH and calomel electrodes were then inserted in the solution, through the paraffin seal.

(iii) A 50ml burette was used to deliver the standardized 3mM HCl, the tip of the burette was also inserted into the solution through the paraffin seal.

(iv) The sample was titrated, stepwise, from its initial pH value down to pH 3.3. A 1min equilibration period was employed following each acid addition. (A smooth stirring action was obtained using a magnetic "flea" system).

In the titrated solution, the total alkalinity can be expressed as:

$$\text{Total alkalinity} = [HCO_3^-] + 2[CO_3^{2-}] + [OH^-] - [H^+]$$

To obtain a value of total carbonate alkalinity, it was necessary to correct for the non-carbonate component. This was achieved using the mathematical procedure described by Talling (1973, steps (c) and (d), p 336). Since the initial pH values were generally in the region pH 8.3 - 9.3, it was assumed that the value of total carbon alkalinity obtained from these computations represented the level of HCO_3^- (see Figure 3.7).

APPENDIX B

DETERMINATION OF CHLOROPHYLL

The procedure outlined by Arnon (1949) was used to determine the chlorophyll concentration of the cells used in the various experiments. The following set of simultaneous equations were used, in which the specific absorption coefficients for chlorophyll a and b were those determined by MacKinney (1941).

$$OD_{663} = 82.04\,[Chl_a] + 9.27\,[Chl_b] \quad \ldots(B.1)$$

$$OD_{645} = 16.75\,[Chl_a] + 45.6\,[Chl_b] \quad \ldots(B.2)$$

where $[Chl_a]$, $[Chl_b]$ are the concentration of chlorophyll a and b respectively in grams per litre and OD is the optical density at the indicated wavelength. From (C.2):

$$[Chl_a] = \frac{OD_{645} - 45.6\,[Chl_a]}{16.75} \quad \ldots(B.3)$$

substituting (C.3) in (C.1) and solving for $[Chl_b]$ gives:

$$[Chl_b] = 0.02288\,OD_{645} - 0.00467\,D_{663} \quad \ldots(B.4)$$

Similarly substituting (C.4) in (C.2) and solving for $[Chl_a]$ gives:

$$[Chl_a] = 0.01271\,D_{663} - 0.00259\,D_{645} \quad \ldots(B.5)$$

Hence total chlorophyll (C_t) equals $[Chl_a]+[Chl_b]$, or

$$C_T = 0.02029\,D_{645} + 0.00804\,D_{663}$$

$$C_T = 20.29\,D_{645} + 8.04\,D_{663} \text{ (mg Chl. } \ell^{-1}) \quad \ldots(B.6)$$

To obtain a value of Chlorophyll concentration on a cell surface area basis, the value given by equation (C.6) was multiplied by:

$$\frac{\text{Total Volume of Chlorophyll Extract}}{1000 \times \text{(Total Cell Surface Area)}}$$

The chlorophyll determination using the specific absorption coefficient at 652nm was also used, and as shown by Arnon (1949):

$$C_{T\ 652} = \frac{OD_{652} \times 1000}{34.5} \quad \text{(mg Chl. per litre)} \qquad \ldots(B.7)$$

This value was multiplied by the same factor as was (C.6) to convert it to mg Chl cm^{-2}.

The mean chlorophyll concentration was obtained as:

$$(C_T + C_{T\ 652}) / 2 \qquad \ldots(B.8)$$

APPENDIX C

A CALCULATION OF THE MAXIMUM RATE AT WHICH CO_2 COULD BE SUPPLIED BY THE DEHYDRATION OF H_2CO_3

The supply of CO_2 by the uncatalyzed reactions (i.e. carbonic anhydrase assumed to be absent):

$$2H^+ + CO_3^{2-} \underset{(i)}{\rightleftharpoons} H^+ + HCO_3^- \underset{(ii)}{\rightleftharpoons} H_2CO_3 \underset{(iii)}{\rightleftharpoons} CO_2 + H_2O \qquad .(C.1)$$

would be limited by reaction (iii) since (i) and (ii) are ionic in nature and hence almost instantaneous (Sirs, 1958). The equilibrium constants for these reactions (25°C) are $K_{(i)} = 4.69 \times 10^{-11}$ (Harned and Scholes, 1941), $K = K_{(ii)}K_{(iii)} = 4.45 \times 10^{-7}$ (Harned and Davis, 1943) and $K_{(iii)} = 2.59 \times 10^{-3}$ (Wissburn, French and Patterson, 1954). The consequence of the almost instantaneous nature of (i) and (ii) is that H_2CO_3 can be considered to be in equilibrium with HCO_3^- and CO_3^{2-}. As a result, the formation of CO_2, from added $NaHCO_3$, can be obtained by solving the rate equation for the reaction:

$$H_2CO_3 \underset{k_b}{\overset{k_f}{\rightleftharpoons}} CO_2 + H_2O \qquad ..(C.2)$$

where k_f and k_b are the first order forward and backward rate coefficients respectively. It is important to note that reaction (C.2) would be catalyzed by OH^- ions at pH values above 8.0 (Faurholt, 1924; Brinkman, Margaria and Roughton, 1933; and Kiese and Hastings, 1940). To allow for this catalysis, Watt and Paasche (1963) employed a slightly higher value for the forward rate coefficient, namely $k_f = 24\ s^{-1}$ (25°C) (cf $k_f = 20\ s^{-1}$ quoted in the review by Kern, 1960). The higher k_f value of Watt and Paasche (1963) will be employed in the following calculations.

The rate equation for the production of CO_2 would be:

$$\frac{d\,[CO_2]}{dt} = k_b\,[CO_2] + k_f\,[H_2CO_3] \qquad \ldots(C.3)$$

To obtain an absolute maximum rate at which CO_2 could be supplied to the *Chara* cells, it was assumed that CO_2 tended to zero. This would not only provide a maximal rate, but also greatly simplifies the solution of the rate equation. Thus (C.3) becomes:

$$\frac{d\,[CO_2]}{dt} = k_f\,[H_2CO_3] \qquad \ldots\ (C.4)$$

Since H_2CO_3 is in equilibrium with HCO_3^- and CO_3^{2-}, its concentration can be expressed as:

$$[H_2CO_3] = \frac{[HCO_3^-]\,[H^+]}{K_{(ii)}} \qquad \ldots\ (C.5)$$

By substitution of $[HCO_3^-] = \dfrac{[\text{Total added carbon}]}{\left\{1 + \dfrac{[H^+]}{K} + \dfrac{K_{(i)}}{[H^+]}\right\}}$

(after Buch, 1960) into (C.5) and re-expressing (C.4) gives:

$$\frac{d\,[CO_2]}{dt} = k_f\,\frac{K_{(iii)}}{K}\cdot[H^+]\cdot\frac{[\text{Total added carbon}]}{\left\{1 + \dfrac{[H^+]}{K} + \dfrac{K_{(i)}}{[H^+]}\right\}} \qquad \ldots\ (C.6)$$

Under experimental conditions where the total added carbon existed almost entirely as exogenous $H^{14}CO_3^-$ (1mM $NaHCO_3$, pH 9.0), the observed ^{14}C assimilation rate was approximately 53 pmol $cm^{-2}s^{-1}$ (see Figure 3.4C). Substituting these values (1mM total carbon and $[H^+] = 10^{-9}$ mol l^{-1}) into equation (C.6) and solving gives:

$$\frac{d\,[CO_2]}{dt} = 1.331 \times 10^{-10}\ \text{mol cm}^{-3}\text{s}^{-1}.$$

To determine the contribution of this CO_2 supply in terms of the observed ^{14}C assimilation rate required that this value be converted to the same units employed to express the rate of carbon fixation in *Chara* cells. This necessitated several assumptions concerning the physical system in which the CO_2 was considered to be generated. The most simple assumption which could be applied was that the CO_2 was being formed in a cylindrical volume element. The length of this cylindrical volume element was equivalent to that of the *Chara* cell concerned and it was considered to extend from the plasmalemma into the bathing solution, by an amount dr. It was also assumed that within this volume element:

(a) HCO_3^- was supplied from the bathing solution such that $\frac{d[HCO_3^-]}{dt} = 0$,

(b) as soon as a molecule of CO_2 was formed, it was immediately transferred across the plasmalemma, i.e. $[CO_2]$ remained at or near zero. (This assumption greatly simplifies the physical diffusion system which would otherwise have had to have been solved, in order to obtain a value for $\frac{d[CO_2]}{dt}$. However, it is clear that this assumption will result in a rate much greater than that present during a ^{14}C assimilation experiment).

(c) For the purpose of calculating the volume element, $r_1 = R_{Chara}$ = 0.045cm and dr was increased from 20μm up to 1000μm. The cell surface area of a 1cm length of cylinder was equivalent to $0.2827cm^2$.

Hence the value of $\frac{d[CO_2]}{dt}$ could be converted from mol $cm^{-3}s^{-1}$ to mol $cm^{-2}s^{-1}$ by the following:

$$\frac{d[CO_2]}{dt} \times \frac{\Pi \ell (r_2^2 - r_1^2)}{\text{Surface area per unit length of cylinder}} \qquad \ldots(C.7)$$

where ℓ = unit length of cylinder in this case and $r_2 = r_1 + dr$.

Substituting the value of 1.331×10^{-10} mol $cm^{-3}s^{-1}$ into (C.7)

and solving for various values of $\pi\ell(r^2_2 - r^2_1)$ gives an indication of the relative order of magnitude of the maximal supply of CO_2 at the cell surface. The values obtained are listed below.

dr (μm)	Volume element = $\pi\ell(r^2_2 - r^2_1)$ (cm^3)	$\frac{d[CO_2]}{dt} \times \pi\ell(r^2_2 - r^2_1)$ / (surface area per unit length of cylinder) (pmol $cm^{-2}s^{-1}$)
20	5.78×10^{-4}	0.27
40	1.18×10^{-3}	0.56
100	3.14×10^{-3}	1.47
300	1.13×10^{-2}	5.33
1000	5.97×10^{-2}	28.11

It should be emphasized that all of the above assumptions were such that the value obtained was considerably higher than would be obtained in the true experimental situation. Even under the influence of these assumptions the calculated rate remained less than the observed ^{14}C value (50-60 pmol $cm^{-2}s^{-1}$) obtained using these cells. It can therefore be concluded that internodal cells of this species can assimilate exogenous HCO_3^-.

BIBLIOGRAPHY

ANDRIANOV, V.K., BULYCHEV, A.A., and KURELLA, G.A., 1970. Biophys. 15, 199-200.

ANDRIANOV, V.K., KURELLA, G.A., and LITVIN, F.F., 1968. Tsitologiya, 11, 1014-20.

ANDRIANOV, V.K., VOROB'EVA, I.A., and KURELLA, G.A., 1968. Biophys. 13, 396-98.

ARENS, K., 1930. Planta, 10, 814-16.

ARENS, K., 1933. Ibid. 20, 621-58.

ARENS, K., 1936a. Jahrb. wiss. Bot. 83, 513-60.

ARENS, K., 1936b. Ibid. 83, 561-66.

ARENS, K., 1939. Protoplasma, 33, 295-300.

ARNON, D.I., 1949. Pl. Physiol. 24, 1-15.

BARR, C.E., and BROYER, T.C. 1964. Ibid. 39, 48-52.

BASSHAM, J.A., 1971. Science, New York. 172, 526-34.

BATES, R.G., 1964. Determination of pH. Theory and Practice. New York, John Wiley & Sons.

BATES, R.G., and PINCHING, G.D., 1949. J. Res. natn. Bur. Stand. 42, 419-30.

BLINKS, L.R., 1963. Protoplasma, 57, 126-36.

BRINKMAN, R., MARGARIA, R., and ROUGHTON, F.J.W., 1933. Philos. Trans. (London) A 232, 65-97.

BROWN, D.F., RYAN, T.E., and BARR, C.E., 1973. In: Ion Transport in Plants. Ed. W.P. Anderson, New York, Academic Press, pp. 141-52.

BROWN, S.O., 1938. Pl. Physiol. 13, 713-36.

BUCH, K., 1960. In: Encyclopedia of Plant Physiology. Ed. W. Ruhland, Berlin, Springer, Vol. 5/1, pp. 1-11.

BUCHANAN, B.B., KALBERER, P.P., and ARNON, D.I., 1967. Biochem. Biophys. Res. Commun. 29, 74-79.

CAPALDI, R.A., 1974. Sci. Amer. 230, 26-33.

CARSLAW, H.S., and JAEGER, J.C., 1959. Conduction of Heat in Solids. Second Edition, Oxford, Clarendon Press.

CLELAND, W.W., 1963. Nature, 198, 463-5.

COHN, F., 1862. Abh. Schles. Ges. 2, 35-55.

COOPER, T.G., FILMER, D., WISHNICK, M., and LANE, M.D., 1969. J. Biol. Chem. 244, 1081-83.

COSTER, H.G.L., 1966. Aust. J. biol. Sci. 19, 545-54.

COSTER, H.G.L., 1969. Ibid. 22, 365-74.

COSTER, H.G.L., and HOPE, A.B., 1968. Ibid. 21, 243-54.

COSTERTON, J.W.F., and MACROBBIE, E.A.C., 1970. J. exp. Bot. 21, 535-42.

CRANK, J., 1956. The Mathematics of Diffusion, London, Oxford University Press.

DAHM, P., 1926. Jahrb. wiss. Bot. 65, 314-51.

DAINTY, J., 1962. Ann. Rev. Pl. Physiol. 13, 379-402.

DAINTY, J., 1963. In: Advances in Botanical Research. Ed. R.D. Preston, London, Academic Press, pp. 279-326.

DAINTY, J., and GINZBURG, B.Z., 1964. Biochim. biophys. Acta, 79, 102-111.

DAINTY, J., and HOPE, A.B., 1959a. Aust. J. biol. Sci. 12, 136-45.

DAINTY, J., and HOPE, A.B., 1959b. Ibid. 12, 395-411.

DOUGHTY, C.J., and HOPE, A.B., 1973. J. membrane Biol. 13, 185-98.

DRAPER, J.W., 1844. J. prakt. Chem. 31, 21-39.

EDMOND, J.M., 1970. Deep-Sea Res. 17, 737-50.

EDSALL, J.T ., and WYMAN, J., 1958. Biophysical Chemistry, New York, Academic Press.

FAURHOLT, C., 1924. J. Chim. phys. 21, 400-55.

FINDLAY, G.P., and HOPE, A.B., 1964. Aust. J. biol. Sci. 17, 62-77.

FINDLAY, G.P., HOPE, A.B., PITMAN, M.G., SMITH, F.A., and WALKER, N.A., 1969. Biochim. biophys. Acta, 183, 565-76.

FINKELSTEIN, A., 1964. Biophys. J. 4, 421-40.

FORSBERG, C., 1965. Physiologia Pl. 18, 275-90.

GAFFRON, H., and FAGER, E.W., 1951. Ann. Rev. Pl. Physiol. 2, 87-114.

GILLET, C., and LEFEBVRE, J., 1973. In: Ion Transport in Plants. Ed. W.P. Anderson, New York, Academic Press, pp. 101-12.

GLINKA, Z., and REINHOLD, L., 1964. Pl. Physiol. 36, 1043-50.

GOLDMAN, D.E., 1943. J. gen. Physiol. 27, 37-60.

GOLDSWORTHY, A., 1968. Nature (London), 217, 62.

GOOD, N.E., 1960. Biochim. biophys. Acta, 40, 502-17.

GRAN, G., 1952. Analyst (London), 77, 661-71.

GRISCHOW, C.C., 1845. J. prakt. Chem. 34, 163-72.

HANSTEIN, J., 1873. Bot. Ztg, 31, 694-97.

HARNED, H.S., and DAVIS, R., 1943. J. Amer. Chem. Soc. 65, 2030-37.

HARNED, H.S., and SCHOLES, S.R., 1941. Ibid. 63, 1706-9.

HASSACK, C., 1888. Unters. Bot. Inst. Tübingen, 2, 465-77.

HEBER, U., 1974. Ann. Rev. Pl. Physiol. 25, 393-421.

HEBER, U., and WILLENBRINK, J., 1964. Biochim. biophys. Acta, 82, 313-24.

HENDRICKS, S.B., 1966. Proc. Soil. Sci. Soc. Am. 30, 1-7.

HIGINBOTHAM, N., 1973. Ann. Rev. Pl. Physiol. 24, 25-46.

HIND, G., and WHITTINGHAM, C.P., 1963. Biochim. biophys. Acta, 75, 194-204.

HODGKIN, A.L., and KATZ, B.J., 1949. J. Physiol. (London) 108, 37-77.

HOGG, J., WILLIAMS, E.J., AND JOHNSTON, R.J., 1968. Biochim. biophys. Acta, 150, 518-20.

HOOD, D.W., and PARK, K., 1962. Physiologia Pl. 15, 273-82.

HOPE, A.B., 1962. Aust. J. biol. Sci. 16, 429-41.

HOPE, A.B., 1965. Ibid. 18, 789-801.

HOPE, A.B., and RICHARDS, J.L., 1971. In: Proceedings of the First European Biophysics Congress. Eds. E. Broda, A. Locker and H. Springer-Lederer, Wien, Verlang Wien Med. Akad. Vol. 3, pp. 105.

HOPE, A.B., SIMPSON, A., and WALKER, N.A., 1966. Aust. J. biol. Sci. 19, 355-62.

HOPE, A.B., and WALKER, N.A. 1961. Ibid. 14, 26-44.

JACKSON, P.G., and ADAMS, H.R., 1963. J. gen. Physiol. 46, 369-86.

JACOBSON, L., OVERSTREET, R., KING, H.M., and HANDLEY, R.A., 1950. Pl. Physiol. (Lancaster), 25, 639-47.

JENSEN, A., and FAURHOLT, C., 1952. Acta Chem. Scand. 6, 385-94.

KATCHALSKY, A., 1961. In: Membrane Transport and Metabolism. Ed. A. Kleinzeller and A. Kotyk. London and New York, Academic Press, pp. 69-86.

KEDEM, O., 1961. Ibid. pp. 87-93.

KERN, D.M., 1960. J. chem. Educ. 37, 14-23.

KIESE, M., and HASTINGS, A.B., 1940. J. Biol. Chem. 132, 267-80.

KISHIMOTO, U., 1959. Ann. Rep. Sci. Works., Faculty of Sci., Osaka Univ. 7, 115-30.

KISHIMOTO, U., NAGAI, R., and TAZAWA, M., 1965. Pl. Cell Physiol. 6, 519-27.

KITASATO, H., 1968. J. gen. Physiol. 52, 60-87.

KROGMANN, D.W., and JAGENDORF, A.T., 1959. Pl. Physiol. 34, 272-77.

LANNOYE, R.J., TARR, S.E., and DAINTY, J., 1970. J. exp. Bot. 21, 543-51.

LATZKO, E., and GIBBS, M., 1969. Pl. Physiol. (Lancaster), 44, 396-402.

LEWIN, J.C., 1962. In: Physiology and Biochemistry of Algae. Ed. R.A. Lewin, New York, Academic Press pp. 457-65.

LILLEY, R.McC., and HOPE, A.B., 1971. Biochim. biophys. Acta, 226, 161-71.

LINDAHL, P.E.B., 1963. Symb. bot. upsal. 17, 1-47.

LOWENHAUPT, B., 1956. Biol. Rev. 31, 371-95.

LOWENHAUPT, B., 1958. J. Cell. comp. Physiol. 51, 199-208.

LUCAS, W.J., 1971. pH Banding Along the Cell Wall of *Chara corallina*. B.Sc. Honours Thesis, University of Adelaide.

LUCAS, W.J., and SMITH, F.A., 1973. J. exp. Bot. 24, 1-14.

LUNDEGÅRDH, H., 1949. Ann. Agric. Coll. Sweden, 16, 372-403.

MACKINNEY, G., 1941. J. Biol. Chem. 140, 315-22.

MACROBBIE, E.A.C., 1962. J. gen. Physiol. 45, 861-78.

MACROBBIE, E.A.C., 1965. Biochim. biophys. Acta, 94, 64-73.

MACROBBIE, E.A.C., 1966. Aust. J. biol. Sci. 19, 363-70.

MACROBBIE, E.A.C., 1968. Abh. dt. Akad. Wiss. Berl. Kl. Med. Bd. 4a, 179-86.

MACROBBIE, E.A.C., 1970. Q. Rev. Biophys. 3, 251-94.

MOORE, B., WHITLEY, E., and WEBSTER, T.A., 1921. Proc. Roy. Soc. London, B, 92, 51-60.

MOORE, W.J., 1958. Physical Chemistry. Third Editon, London, Longmans.

NAGAI, R., and TAZAWA, M., 1962. Pl. Cell Physiol. 3, 323-39.

NISHIZAKI, Y., 1963. Pl. Cell Physiol. 4, 353-56.

NISHIZAKI, Y., 1968. Ibid. 9, 377-87.

NOBEL, P.S., 1970. Plant Cell Physiology, San Francisco, Freeman.

OSTERHOUT, W.J.V., 1949. Proc. Nat. Acad. Sci. Washington, 35, 548-58.

OSTERHOUT, W.J.V., and HAAS, A.R.C., 1918. J. gen. Physiol. 1, 1-16.

ÖSTERLIND, S., 1949. Symb. bot. upsal. 10, 1-137.

ÖSTERLIND, S., 1951. Physiologia Pl. 4, 514-27.

PAULSEN, J.M., and LANE, M.D., 1966. Biochemistry 5, 2350-57.

PEDERSEN, T.A., KIRK, M., and BASSHAM, J.A., 1966. Physiologia Pl. 19, 219-31.

PICKARD, W.F., 1973. Can. J. Bot. 51, 715-24.

PON, N.G., 1959. Studies on the Carboxydismutase System and Related Materials. Ph.D. Thesis, University of California, Berkeley.

RABINOWITCH, E.I., 1951. Photosynthesis and Related Processes, New York, Interscience, Vol. II, Pt. 1, pp 603- 1208.

RABINOWITCH, E.I., 1956. Ibid. Vol. II, Pt. 2, pp. 1211-2088.

RAPOPORT, S.I., 1970. Biophys. J. 10, 246-59.

RAVEN, J.A., 1967. J. gen. Physiol. 50, 1607-25.

RAVEN, J.A. 1968a. J. exp. Bot. 19, 193-206.

RAVEN, J.A., 1968b. Ibid. 19, 233-53.

RAVEN, J.A., 1969a. New Phytol. 68, 45-62.

RAVEN, J.A., 1969b. Ibid. 68, 1089-1113.

RAVEN, J.A., 1970. Biol. Rev. 45, 167-221.

RAVEN, J.A., and SMITH, F.A., 1974. Can. J. Bot. 52, 1035-48.

RENT, R.K., JOHNSON, R.K., and BARR, C.E., 1972. J. membrane Biol. 7, 231-44.

RICHARDS, J.L., and HOPE, A.B., 1974. Ibid. 16, 121-44.

ROBINSON, J.B., 1969. J. exp. Bot. 20, 212-20.

ROBINSON, R.A., and STOKES, R.H., 1965. Electrolyte Solutions, Second Edition, London, Butterworths.

RUTTNER, F., 1921. Sbor. Akad. Wiss. Wien. math-nat. Kl. I, 130, 71-108.

RUTTNER, F., 1947. Öst. bot. Z. 94, 265-94.

RUTTNER, F., 1948. Ibid. 95, 208-38.

RYBOVA, R., and SLAVIKOVA, M., 1974. Z. Pflanzenphysiol. 72, 287-96.

SAITO, K., and SENDA, M., 1973a. Pl. Cell Physiol. 14, 147-56.

SAITO, K., and SENDA, M., 1973b. Ibid. 14, 1045-52.

SCHUTOW, D.A., 1926. Planta, 2, 132-51.

SEARS, D.F., and EISENBERG, R.M., 1961. J. gen. Physiol. 44, 869-87.

SHIEH, Y.J., and BARBER, J., 1971. Biochim. biophys. Acta, 233, 594-604.

SIMONS, R., 1969. Ibid. 173, 34-50.

SIRS, J.A., 1958. Trans. Faraday Soc. 54, 207-12.

SLAYMAN, C.L., 1965. J. gen. Physiol. 49, 93-116.

SLAYMAN, C.L., 1970. Am. Zoologist, 10, 377-92.

SLAYMAN, C.L., LONG, W.S., and LU, C.Y-H., 1973. J. membrane Biol. 14, 305-38.

SMITH, E.L., 1936. Proc. Nat. Acad. Sci. Washington, 22, 504-11.

SMITH, F.A., 1965. Links between solute Uptake and Metabolism in Characean Cells. Ph.D. Thesis, University of Cambridge.

SMITH, F.A., 1967a. J. exp. Bot. 18, 509-17.

SMITH, F.A., 1967b. Ibid. 18, 716-31.

SMITH, F.A., 1968a. Ibid. 19, 207-17.

SMITH, F.A., 1968b. Ibid. 19, 442-51.

SMITH, F.A., 1970. New Phytol. 69, 903-17.

SMITH, F.A., 1971. In: Proceedings of the First European Bio-Physics Congress. Eds. E. Broda, A. Locker and H. Springer-Lederer, Wien, Verlang Wien. Med. Akad. Vol. 3, pp. 429-33.

SMITH, F.A., 1972. New Phytol. 71, 595-601.

SMITH, F.A., and LUCAS, W.J., 1973. In: Ion Transport In Plants. Ed. W.P. Anderson, New York, Academic Press, pp. 223-31.

SMITH, F.A., and RAVEN, J.A., 1974. New Phytol. 73, 1-12.

SMITH, F.A., and WEST, K.R., 1969. Aust. J. biol. Sci. 22, 351-63.

SPANSWICK, R.M., 1964. Ion Uptake and Electrical Potentials in Plants. Ph.D. Thesis, University of Edinburgh.

SPANSWICK, R.M., 1970a. J. membrane Biol. 2, 59-70.

SPANSWICK, R.M., 1970b. J. exp. Bot. 21, 617-27.

SPANSWICK, R.M., 1972. Biochim. biophys. Acta, 288, 73-89.

SPANSWICK, R.M., 1973. In: Ion Transport in Plants. Ed. W.P. Anderson, New York, Academic Press, pp. 113-28.

SPANSWICK, R.M., 1974. Biochim. biophys. Acta, 332, 387-98.

SPANSWICK, R.M., STOLAREK, J., and WILLIAMS, E.J., 1967. J. exp. Bot. 18, 1-16.

SPANSWICK, R.M., and WILLIAMS, E.J., 1965. Ibid. 16, 463-73.

SPEAR, D.G., BARR, J.K., and BARR, C.E., 1969. J. gen Physiol. 54, 397-414.

STEEMANN NIELSEN, E., 1946. Nature (London), 158, 594-96.

STEEMANN NIELSEN, E., 1947. Dansk Bot. Ark. 12, 1-71.

STEEMANN NIELSEN, E., 1951. Physiologia Pl. 4, 189-98.

STEEMANN NIELSEN, E., 1955. Ibid. 8, 317-35.

STEEMANN NIELSEN, E., 1960. In: Encyclopedia of Plant Physiology. Ed. W. Ruhland, Berlin, Springer, Vol. 5/1, pp. 70-84.

STEEMANN NIELSEN, E., 1963. Physiologia Pl. 16, 466-9.

TALLING, J.F., 1973. Freshwat. Biol. 3, 335-62.

TEORELL, T., 1949. Arch. Sci. Physiol. 3, 205-19.

THAIN, J.F., 1973. In: Ion Transport in Plants. Ed. W.P. Anderson, New York, Academic Press, pp. 77-94.

TOGASAKI, R.K., and GIBBS, M., 1967. Pl. Physiol. 42, 991-96.

USSING, H.H., 1949a. Physiol. Rev. 29, 127-55.

USSING, H.H., 1949b. Acta Physiol. Scand. 19, 43-56.

VAN LOOKEREN CAMPAGNE, R.N., 1957. Acta bot. neerl. 6, 543-82.

VAN STEVENINCK, R.F.M., 1964. Physiologia Pl. 17, 757-70.

VAN STEVENINCK, R.F.M., 1966. Aust. J. biol. Sci. 19, 271-81.

VERDUIN, J., 1954. Science, 120, 75-76.

VOLKOV, G.A., 1973. Biochim. biophys. Acta, 314, 83-92.

VOLKOV, G.A., and MISYUK, L.A., 1969. Tsitologiya 11, 998-1006.

VOLKOV, G.A., and PETRUSHENKO, V.V., 1969. Ibid. 11, 1007-13.

VREDENBERG, W.J., and TONK, W.J.M., 1973. Biochim. biophys. Acta, 298, 354-68.

WADDELL, W.J., and BATES, R.G., 1969. Physiol. Rev. 49, 285-329.

WALKER, D.A., 1973. New Phytol. 72, 209-35.

WALKER, N.A., 1962. Annu. Rep. Div. Plant Ind. C.S.I.R.O., p. 80.

WALKER, N.A. 1963. Ibid. p. 96.

WALKER, N.A., and HOPE, A.B., 1969. Aust. J. biol. Sci. 22, 1179-95.

WALKER, N.A., and SMITH, F.A., 1974. Intracellular pH in *Chara corallina* measured by DMO distribution. Plant Sci. Lett. In press.

WATT, W.D., and PAASCHE, E., 1963. Physiologia Pl. 16, 674-81.

WERDAN, K., and HELDT, H.W. 1972. Biochim. biophys. Acta, 283, 430-41.

WHITTINGHAM, C.P., 1952. Nature (London), 170, 1017-18.

WILDNER, G.F.,and CRIDDLE, R.S., 1969. Biochem. biophys. Res. Commun. 37, 952-60.

WILLIAMS, E.J., JOHNSTON, R.J., and DAINTY, J., 1964. J. exp. Bot. 15, 1-14.

WISSBURN, K.F., FRENCH, D.M., and PATTERSON, A., 1954. J. phys. Chem. 58, 693-5.

WOOD, R.D., and IMAHORI, K., 1965. A Revision of the Characeae. Weinheim, J. Cramer.